UNIVERSITY OF NEWCASTLE UPON TYNE
DEPARTMENT OF CIVIL ENGINEERING

THE ACTION OF GEOTEXTILES IN PROVIDING COMBINED DRAINAGE AND REINFORCEMENT TO COHESIVE SOIL

A Thesis submitted for the degree of Doctor of Philosophy

by

SOHRAB HESHMATI BSc., MSc.

December 1993

ABSTRACT

This thesis describes a study into the action of geotextiles in providing combined drainage and reinforcement to cohesive soil and the identification of the interaction of different geotextiles with a cohesive soil. The study involved both experimental and analytical investigations.

Fine grained cohesive soil is a complex material. The introduction of geosynthetics providing both drainage and a reinforcement function produce a marked increase in the shear strength characteristics of the clay material.

A number of consolidated undrained and consolidated drained triaxial compression tests and Rowe cell consolidation tests were conducted. The objective of the tests was to identify the separate effects (improvement) on the shear strength properties of the cohesive soil (kaolin) provided by the drainage function and separately that provided by the reinforcing function of a number of geotextiles. An Electron Scanning Microscope study was used to investigate the interaction between the cohesive soil and the geosynthetic materials.

The study provided qualitative information concerning the relative improvement of the physical properties of a fine grained cohesive soil when used in construction with range of geosynthetic materials. Analysis of the results of the research suggest that geotextile products could offer significant technical, practical and economic advantages when constructed with poor quality soils. The combined function of drainage and reinforcement which could be developed by some geosynthetic materials could be substantial.

Combining the functions of drainage and reinforcement in a single material requires the resulting geosynthetic to have special properties. The form of a geocomposite drainage and reinforcement material with these properties is proposed.

ACKNOWLEDGEMENTS

I wish to express my sincere gratitude for the help and companionship I received from members of the Geotechnical Group and the Department of Civil Engineering as a whole.

First and foremost I would like to express my deepest gratitude to my supervisor, Prof. Colin J.F.P. Jones, who was extremely patient and always willing to help, encourage and assist me in all my needs. His confident support of my work from the early stages and sharp perception for events of scientific significance were invaluable source of inspiration. Prof. Colin Jones was very kind to put his vast and valuable library at my disposal.

I would like to gratefully acknowledge to Dr. Barry G. Clarke for his laboratory supervision and help received from him.

I feel indebted to Dr. Evan K.S. Passaris, for his invaluable help and advice.

Thanks is also to Mr. A.I.B. Moffat, who was always kind to offer his assistance.

The assistance of all Geotechnical Division technical staff headed by Mr. J.T. Moore, Mr. M. Mckenna, Mr. J. Allen, Mr. C. Hunt is greatly acknowledged.

I would like to thank the Group's secretaries Mrs. S.L. Dodd and Mrs. A.E. Bridges for their cooperation and help.

Thanks is also due to Mr. H. Sargent of the University's Material Division who helped to perform the electron microscopy study.

I wish to acknowledge the support of Netlon Limited and Conwed Limited who provided the materials used in the tests.

Many thank to my friends and fellow research students, who had been very cooperative and helpful.

I would like to gratefully acknowledge my parents, parents in-law and friends specially Dr. A. Husseini and Mr. A. Ahmadi for their contribution and financially supports during my study.

No amount of words could be sufficient to express my gratitude to my family, especially to my wife Zahra, my son Saeed and my daughter Haniyhe, who with limitless patience offered me encouragement, help and support throughout this work special during the last absents of two years.

The thesis is also in remembrance of my mother who passed away suddenly during experimental work of the study.

Sohrab Heshmati
Newcastle upon Tyne
December 1993

TABLE OF CONTENTS

CHAPTER THREE: THE AIMS OF THE RESEARCH

CHAPTER FOUR: CONSIDERATION OF COHESIVE FILL

CHAPTER FIVE: IMPROVEMENT TO CONSTRUCTION USING GEOSYNTHETICS

CHAPTER SIX: TRIAXIAL TESTS, SAMPLE PREPARATION AND PROCEDURE

CHAPTER SEVEN: ROWE CELL TESTS, SAMPLE PREPARATION AND PROCEDURE

CHAPTER EIGHT: INTERACTION BETWEEN GEOTEXTILE AND SOIL, RESULTS AND DISCUSSION

CHAPTER NINE: ANALYSIS OF REINFORCED SOIL AND DISCUSSION

NOTATION

The following symbols have been used in the text. Deviations from the standard notations are defined locally.

Symbol	Definition
A	Bulk cross-sectional area emitting flow, e.g. m^2
A_0	Original area of triaxial sample, e.g. m^2
B	Width and length of transverse elements in a grid, e.g. m
c''	Apparent cohesion, e.g. kN/m^2
cv	Coefficient of Consolidation
E	Elastic (Young's) modulus
FOS_{ot}	Factor of Safety, Resisting Moment / Overturning Moment
FOS_{bc}	Factor of Safety, Bearing Capacity / Vertical Pressure
f_b	Bond coefficient is limited by the inequality
g	Acceleration due to gravity
H	Height of fill
h	Height, e.g. m
i	Hydraulic gradient
i_s	Hydraulic gradient in the adjacent soil
K	Coefficient of permeability
K_0	Coefficient of earth pressure at rest
K_a	Coefficient of active earth pressure
K_b	Coefficient of lateral earth pressure
K_m	Mobilised earth pressure coefficient
K_g	Permeability of geotextile
K_s	Permeability of the adjacent soil
K_{pg}	Flow of transmissivity of geotextile
L_b	Required bond development
L_r	Length of element of reinforcement
L_s	Required Sliding resistance length
Mv	Coefficient of compressibility
N	Number of the first layer of reinforcement
q_{pg}	Flow in the plane of the geotextile
S_v	Vertical spacing of reinforcements
S_h	Horizontal spacing of reinforcements
tf	Time to failure
$t100$	Time for 100% consolidation
T_i	Reinforcement tension due to fill above the reinforcement layer

T_{pi}	Reinforcement tension due to uniform surcharge
T_{si}	Reinforcement tension due to a concentrated load
T_{fi}	Reinforcement tension due to horizontal shear stress
T_{ci}	Reinforcement tension due to shear strength of the cohesive soil
U	Excess pore water pressure
u_a	Pore-air pressure
u_w	Pore-water pressure
W_r	Width of element of reinforcement
Z	Vertical height
α_0	Percent open area of a geogrid,
α_s	Percent solid area of a geogrid.
β'	Inclination of a potential failure plane to the vertical plane
γ	Unit weight of soil
δ	Direct shear friction angle between the soil and reinforcement
$\partial Q / \partial t$	The rate of water movement through soil
$\partial h/\partial l$	Hydraulic gradient
Δ	Change in particular parameter
ε	Axial strain
ε_f	Strain at failure
ε_v	Volumetric strain
μ	Coefficient of friction between the fill and reinforcement
ρ	Bulk density
ρ_d	Dry density
σ	Total stress
σ_1, σ_3	Principal Stresses
σ_n	Normal stress
$\sigma' n$	Effective normal stress
τ_f	Shear strength
τ'_f	Effective shear strength
ϕ'	Angle of internal friction
ϕ'_{cv}	Constant volume angle of friction
ϕ'_m	Mobilised soil friction angle
ψ_t	Total suction
ψ_m	Matrix suction component
ψ_s	Osmotic component
Φsg	Friction angle at the soil-geotextile interface
Φss	Friction angle at a soil-soil interface

CHAPTER ONE

INTRODUCTION

1.1 INTRODUCTION

Reinforced soil has been used extensively in geotechnical engineering design and construction. Its advantage are reduction in cost and ease of construction, coupled with a basic simplicity, Jones (1985).

The conventional method used to construct reinforced soil structures uses good quality frictional fill, DOT (1978). The cohesionless fills usually specified for reinforced soil structures are free draining and can be relied upon to provide stable conditions when reinforced. In many parts of the world frictional fills are difficult to obtain at economic rates and consequently the use of reinforced soil in the these areas is curtailed.

In many cases poor quality on-site soils are available. If these could be shown to be adequate for reinforced fill the requirement for expensive imported cohesionless soil could be eliminated.

Reinforced soil structures need not be restricted to frictional fills. Indeed the earliest examples of reinforced soil developed in Mesopotamia circa 2000 BC and including the Ziggurats were constructed using reinforced clay blocks , whilst parts of the Great wall of China contain examples of reinforced clay and gravel, Jones (1985). Recently, methods have been explored to design steep reinforced soil embankment structures using cohesive fill reinforced with geosynthetics, Tatsuoka et al (1990). Prototype structures constructed in Japan indicate that fine grained soils with water contents up to 130 per cent can be shown to be adequate as reinforced soil fill provided the correct type of reinforcement is selected, Tatsuoka (1992).

The reinforcements which offer the potential of being suitable for use with fine grained soils are geogrids and geotextiles. In the case of geotextiles a dual role is possible with composite geotextiles providing both drainage and reinforcement functions. The economics and cost benefits of using geosynthetic materials in reinforced soil structures have been discussed by Jones (1992) and Wu (1992).

There is a lack of information and understating concerning the relative improvement of the physical properties of a cohesive soil when used in construction with an appropriate geosynthetic used to provide drainage. Similarly there is a lack of information of the mechanisms of action of geosynthetic materials used as reinforcement for cohesive soils.

The combined function of drainage and reinforcement which could be offered by some geosynthetic materials has not been studied, although this combined function is a logical extension of the uses which currently could be made of geotextile materials.

Any study of the combined function of reinforcement / drainage geotextiles embedded in a cohesive soil would need to cover:

a. A study of the behaviour of the reinforcing function of the geosynthetic materials with the cohesive soil.

b. A study of the behaviour of the drainage function of the geosynthetics materials with the cohesive soil.

c. The mechanisms of interaction between the geotextiles used and the cohesive soil.

d. Measurement of the shear strength parameters, (angle of internal friction ϕ', cohesion c'), and coefficient of compressibility (m_v), and coefficient of consolidation (m_v) of the cohesive soil with and without geotextiles acting as reinforcement, drainage or as a combined function.

e. The development of suitable analytical or modelling procedures which could be used to accurately predict the behaviour of reinforced soil using cohesive fill and containing geosynthetics as reinforcement or as drainage or providing a combined function.

1.2 LAYOUT OF THESIS

This thesis is divided into ten chapters. The chapters are arranged as follows:

Chapter 1 provides an introduction and layout of the thesis.

Chapter 2 provides a brief literature review of reinforced soil, encompassing the various components of a reinforced soil structure together with the use of soil reinforcements

and their stress transfer mechanisms. A description of the various design methods proposed is given and an outline of the various construction procedures adopted is set out.

Chapter 3 defines the lack of information and knowledge concerning reinforced soil structures built using fine grained cohesive soil used as fill and identifies the aims and objectives of the research.

Chapter 4 considers the short term and long term stability of cohesive materials. The mineralogy and properties of clay are discussed. The shear strength of clay and stress - strain characteristics of clay are explained. The properties of the Kaolin used in this study are identified. Finally, the mechanisms of reinforced soil using the triaxial test are discussed.

Chapter 5 considers a brief history of the development of geotextiles and related products. The functions and the characteristics of geotextiles are described. The geotextiles used to provide reinforcement are discussed in terms of their characteristic strength, stiffness and bond. Geotextiles used to provide drainage are covered in respect of their permeability and compressibility, and the flow of water through the normal to the plane of the geotextile. Soil-geotextile in plane strain compression is also described.

Chapter 6 gives details of the experimental procedures used in the consolidated drained triaxial compression tests and the consolidated undrained triaxial compression tests which form the centre of the experimental research programme. Sample preparation and the apparatus used are described. The results of the experimental work are presented.

Chapter 7 details the experimental aim and procedure used with the Rowe cell consolidation tests. Sample preparation and the apparatus used are explained. The results of the experimental research are presented.

Chapter 8 gives details of the mechanisms of interaction between geotextiles and soil. A scanning electron microscopy study of the geotextiles used in this research is described. The test results of the experimental work are discussed.

Chapter 9 In this chapter the modelling and analysis of reinforced soil is briefly reviewed. The advantages of the use of the finite element method for reinforced soil are considered. The philosophy and finite element idealisation of reinforced soil is described, and the selection of appropriate material parameters used for analysis is discussed.

Chapter 10 contains the conclusions of the research and gives recommendations for future work.

Some of the relevant tables of results, figures and plates are included at the end of the appropriate chapters.

Appendix A contains the results of the experimental work.

Appendix B contains the relevant texts.

Appendix C contains sample calculations.

Appendix D contains copies of papers already published with the outline of other papers considered for publication.

CHAPTER TWO

LITERATURE REVIEW AND PRINCILES OF REINFORCED SOIL

2.1 INTRODUCTION

This chapter reviews briefly the history and development of soil reinforcement techniques, with special emphasis on the mechanism of reinforcement, the development of design theories and the reinforcing materials and fills used.

The use of fine grained (cohesive) soils in conjunction with geosynthetic reinforcement as is the growing practice in Japan is considered.

2.2 HISTORY AND DEVELOPMENT OF REINFORCED SOIL

There are many historical examples of constructions which use reinforcement elements strong in tension, to improve the strength and stability of soil. Some outstanding early structures are the Zigurrat of Agar-Quf in Iraq which is thought to be 3000 years old (Bagir, 1944) and the Great Wall of China.

An early application of soil reinforcement for military construction was introduced by Col. Pasley in 1822, Jones (1985). Pasley showed that the lateral pressure acting on a retaining wall could be reduced significantly by reinforcing the backfill with horizontal layers of brushwood, wooden planks or canvas.

A notable development to the modern concept of reinforced soil structures was made in the United States by Andreas Munster in 1925. The structure consisted of an array of wooden reinforcing members jointed to the a facing by using a sliding connection. In this way the problem associated with the settling of the backfill relative to the facing could be minimised.

In 1929, Andre Coyne patented in Paris a multi-anchorage system used for the construction of retaining walls, especially for the structures such as quaywalls and dykes. Coyne's system, known as "mur a echelle" (ladder wall), was made up of successive horizontal elements,

formed by a light facing element linked to either continuous or discrete anchors with ties.

It has only been comparatively recently, that Engineers have attempted to investigate and quantify the mechanics and processes behind earth reinforcement so that a more scientific basis can be applied to the design of such structures. The modern concept of reinforced soil was proposed by Casagrande, who idealised the problem in the form of a weak soil reinforced by high strength members laid horizontally in layers (Westergaard, 1938). The modern form of earth reinforcement was introduced and popularised by the French architect and engineer Henri Vidal in the 1960s. Vidal's original proposal was for a composite material to be formed from flat metal (galvanised or stainless steel) reinforcing strips laid horizontally in a frictional fill, the interaction between the soil and the reinforcement being generated solely by surface friction.

Vidal called this material "terre armee" and took out patents in many countries including America, Canada and France. The first major structures built using this concept were retaining walls constructed in the South of France in 1968. By the early 1970s reinforced soil walls had been constructed in both the United States and the United Kingdom. It soon became evident that this was a powerful new technique for the geotechnical engineer, and the 1970s and 1980s saw a rapid growth in interest in the method. Fundamental research work was sponsored by various national bodies, notably at the Laboratories des Ponts et Chaussees (LCPC) in France (Schlosser, and Vidal 1969), by the US. Department of Transport (Walkinshaw, 1975) and by the UK. Department of Transport (Murray, 1977), as well as work done by individual researchers in a number of countries including Japan. Most of the research has been associate with the use of good quality frictional fills.

Since then, many construction systems have evolved including the United Kingdom developments of the York Method, Jones (1978), the Transport and Road Research Laboratory (TRRL) anchored earth, Murray and Irwin (1981), the use of polymer anchors, Hassan (1992), and the Websol system, Kempton et al. (1985). The new systems utilise various different kinds of reinforcing materials including, geotextile nets, polymer strips anchors and grids and steel in the form of plates, bars, triangular anchors or grids. The facing units used are not restricted to reinforced concrete slabs, facing units made from other materials have been used, including glass-reinforced plastics (GRP), glass-reinforced cement (GRC), geotextiles, steel, timber, and masonry. This development work has led to a steady improvement in the technology and the economies of reinforced soil. Much of the development has been associated with the desire to improve long term durability.

2.3 APPLICATIONS OF REINFORCED SOIL

Reinforced soil structures can be shown to provide economic advantage over a wide range of conventional constructions, Jones (1990). An example of the scope for savings is shown in bridgeworks where overall savings of up to 50 percent are possible by selecting a reinforced soil option when constructing the abutments. A major advantage of reinforced soil is the improved idealisation which the concept permits, this results in structures, which would otherwise have been difficult or expensive to construct being considered. Because of its flexibility reinforced soil is particularly suited for use over compressible foundations or poor ground conditions.

Based on their applications, reinforced soil structures can be subdivided into three broad categories: (i) earth structures, (ii) load supporting structures and (iii) a combination of (i) and (ii).

(i) earth structures

Earth structures include slopes, walls, and embankments. Earth structures do not normally support significant external loads, and the primary design consideration is the stability of the structure under its own weight. In some cases facing is required especially for vertical or near vertical reinforced soil walls.

(ii) load supporting structures

Load supporting structures include building foundations, flexible pavements, unpaved roads, railroad track structures, and load supporting pads such as drilling pads, fabrication yards, and construction staging areas.

(iii) combination of (i) and (ii)

The combination of (i) and (ii) are exemplified by structures such as bridge abutments, piled embankments, walls supporting railroad tracks and earth works supporting structures. The design of these structures takes into account both dead and live loads.
Some examples of the applications of reinforced soil are illustrated in Fig. 2.1.

2.4 THE CONCEPT OF REINFORCED SOIL

Soils deform in shear before insatiably along a slip surface can occur. In common with other materials, shear deformation in soil causes compressive and tensile strains to develop.

Stability in soil is provided by frictional shearing resistance, derived from particle friction, particle shape, packing, and compressive stresses. The driving forces causing failure in a soil mass must overcome the frictional shearing resistance if a slip surface is to develop, Jewell (1987). Soil may be strengthened by reinforcement which exploits these features of soil behaviour making them work together. The reinforcement needs to be placed in the direction of tensile strain so that deformation in the soil generates tensile force in the reinforcement. The result of tension forces being developed in the reinforcement is to improve the soil.

This can be illustrated by a direct shear test on a frictional soil, Fig. 2.2. Compressive and tensile strains must occur for a shear surface to develop through the soil. In the shear tests the applied disturbing force, P_S, is resisted by the frictional resistance in the soil, $P_{resisting} = P_v \tan\phi$, Fig. 2.2a.

Shear deformation in the soil causes a tensile force, P_R, to develop in the reinforcement. The effect on the shear surface is twofold:

i) the component of the reinforcement force P_R, along the shear surface ($P_R \sin \phi$) directly reduces the disturbing force, and
ii) the component of the reinforcement forced, P_R, perpendicular to the shear surface ($P_R \cos \theta$) increases the compression in the soil across the shear surface and thereby increases the frictional shearing resistance.

Thus, the total shearing resistance in an unreinforced soil is;

$$P_{resisting} = P_v \tan \phi \qquad (2.1)$$

and this is increased in the reinforced soil to;

$$P_{resisting} = P_v \tan \phi + P_R(\sin \theta + \cos \theta \tan \phi) \qquad (2.2)$$

Other details concerning reinforced soils include;
(i) tensile strain typically develops in a horizontal direction in soil when the major loading is due to gravitational forces. Reinforcement is usually placed in horizontal layers because the reinforcement works best in tension.
(ii) the stiffness of the reinforcement, the relationship between the axial tensile load and the extension, determines how much deformation is needed in the soil to mobilise the required

reinforcement force.
(iii) the bond for the reinforcement governs whether the required reinforcement force can be held in equilibrium with the soil, or whether slip between the reinforcement and the soil will occur first.

2.4.1 Basic principles

The behaviour of reinforced soil is essentially a function of the stress distribution and interaction between the reinforcement and soil. There is some similarity to the principle of reinforced concrete, in that the reinforced mass may be considered as a composite material with improved properties, particularly in tension, compared with soil or concrete alone. However, the internal conditions are different, with reinforced concrete the reinforcement is designed usually to resist tension. In the case of soil it is likely that a completely compressive stress field will exist. The mode of action of reinforcement in soil is, therefore, not one of carrying developed tensile stresses but of the anisotropic reduction or suppression of one normal strain rate, Jones (1985).

Vidal (1969) demonstrated the increase of strength developed by soil reinforcement by considering two specimens, one (specimen A) formed with soil and the other (specimen B) with soil and a single horizontal layer of reinforcement placed at mid-height, Fig. 2.3a. Vidal demonstrated that due to the self-weight of the specimens, the vertical pressure is σ_v, and a minimum confining pressure of $K_a\sigma_v$ had to be applied to both the specimens to maintain equilibrium. An increase of $\delta\sigma_v$ to specimen A, without an increase in $Ka\sigma_v$ would cause a failure in the specimen. However, an equivalent increase of $\delta\sigma_v$ in specimen B, would induce tensile strains along the reinforcement through soil/reinforcement interfacial stresses. If the reinforcement is sufficiently rough and stiff as compared to the soil, movement would be restricted. This restriction of movement is analogous to an additional soil confining force $K_m\sigma_v$.

Another way of displaying the strength gain of reinforced soil samples is shown through Mohr-Coulomb circles in Fig. 2.3b. A sample of unreinforced soil under a vertical stress σ_1 and a horizontal stress of σ_3 would display a Mohr-Circle as shown in the Fig. 2.3b. Under the same horizontal forces σ_3, a reinforced sample would withstand a larger vertical stress σ_{1r} without causing any failure in the sample.

This demonstration of the reinforced soil mechanism encouraged researchers to investigate

the behaviour of reinforced soil using the triaxial and plane strain apparatuses which were considered to be representative of actual reinforced soil masses.

A very important theoretical contribution to the subject of reinforced soil is attributed to Basset and Last (1978). They pointed out that the mechanism of tensile reinforcement involves anisotropic restraint of the soil deformation in the direction of the reinforcements. Due to the soil-reinforcement interaction, which is discussed in detail in Chapter 8, the presence of reinforcement in a soil mass modifies the strain and stress patterns.

2.4.2 Strain Compatibility

To maintain strain compatibility between the soil and the reinforcement at all times, the reinforcement must strain the same amount as the soil under the influence of its self weight and externally imposed loads. The induced strains in the reinforcements develop forces which contribute to the equilibrium of the structure. This leads to the definitions of (i) Required Force and (ii) Available force.

(i) Required Forces:

These are the out of balance forces developed by the soil that need to be maintained by the reinforcement for equilibrium in the structure.

(ii) Available Forces:

These are the forces that are available from the reinforcement to maintain equilibrium in the structure.

For reinforced soil retaining structures, the required forced to be sustained by a strip reinforcement (T_{strip}) at an overburdened depth (h) and density (γ) is calculated as follows:

$$T_{strip} = k_m \gamma h S_v S_h \qquad (2.5)$$

where S_v and S_h are the vertical and horizontal spacing of the reinforcements and km is the mobilised earth pressure coefficient defined as:

$$k_m = \frac{1 - \sin \phi'_m}{1 + \sin \phi'_m} \qquad (2.6)$$

where ϕ'_m is the mobilised angle of friction.

The required force to be sustained by a sheet of reinforcement (T_{sheet}) at an overburdened depth (h) and density (γ) can be calculated as follows:

$$T_{sheet} = k_m \gamma h S_v \qquad (2.7)$$

For a particular layer of reinforcement, the only "variable" component in the equation is km, which is dependent on the mobilised soil friction angle (ϕ'_m). Thus for a given h and γ the required force vs lateral tension strain curve at an individual reinforcing strip or sheet layer can be drawn as shown in Fig. 2.4. This is basically a mirror image of the mobilised angle of friction (ϕ'_m) vs lateral tensile strain curve. As shown in Fig. 2.4, there is a decrease in the required force until the peak angle of internal friction of the soil is reached, followed by an increase in the required force until the strain at which the constant volume angle of friction (ϕ'_{cv}) is reached. Thereafter the required forces remains constant. The configuration of the curve, shows that required forces, other than that required at $\phi'_{p'}$ can be reached at two different strains, levels, one greater and one less than that at which peak angle of friction is reached.

The available force is that provided by the reinforcing material. For relatively inextensible reinforcements, such as steel, this can be estimated from short term constant rate of deformation or stress test data. However, due to the time and temperature dependency of most relatively extensible reinforcements, their available forces have to be estimated by using constant temperature long term sustained load (creep) test data at the operating temperature of the soil. These are presented as isochronous curves and typical data for a relatively extensible reinforcement and an inextensible reinforcement are shown in Fig. 2.4.

Strain compatibility and load equilibrium in the soil and the reinforcement occurs at the intersection of the required and available force curves, at which point the required force and the available force are in balance. A change in either would compel strains to develop thus allowing a new equilibrium point to be reached.

BS 8006; 1991, considers that reinforcement materials over a range between low extensibility (or high axial tensile stiffness) and high extensibility (or low axial tensile stiffness). Steel below the yield point and some geotextiles typically mobilise their design strength at a total axial strain of 1 per cent or less, whereas the majority of geotextiles mobilise their strength at substantially higher strains. The designer should be aware of the relation between strain in the soil/fill and the reinforcement, and the deformation of the

structure, Fig. 2.4. Fig. 2.4 shows the system compatibility of strains and forces for a reinforced soil structure represented by a retaining wall rotating ground about the toe, O'Rourke and Jones (1990).

2.5 THE DESIGN OF REINFORCED SOIL

The largest number of reinforced soil applications are related to vertical and near vertical walls. The design of the first wall by Vidal in the mid 1960's, was based on classical soil mechanics principles extended by the results of his research and development work. The principle of soil mechanics has been used in the limit equilibriume method of design for vertically faced structures.

Design of a vertically faced reinforced soil structure must satisfy two conditions covering external and internal stability, which have been described by O'Rourke and Jones (1990).

External stability is concerned with the basic stability of the reinforced structure considered as a unit. The structure is checked against forward sliding, tilt/bearing failure, and slip within the surrounding sub-soil or slips passing through the reinforced soil structure, Fig. 2.5, (c,d,and e).

Internal stability is concerned with the estimation of the numbers, size, strength, spacing and length of the reinforcing elements needed to ensure stability of the whole structure, together with the pressures exerted on the facing. A number of analytical approaches have been suggested including limit equilibrium, elastic analysis and the energy method. The limit equilibrium method, has been used extensively and forms the base of most national design Codes of practice.

Analysis covering internal stability is concerned with the ***adhesion*** and ***tension failure*** mechanisms, Fig. 2.5 (a) and (b). In the adhesion mode of failure, the structure will fail by the strips pulling out of the soil if sufficient bond does not occur between the strips and the soil to generate the force required. In the case of tension failure, the tensile force in the strips exceeds the breaking strength of the reinforcement.

2.5.1 External Stability

The analysis of the external stability of reinforced soil walls is similar to that used in traditional retaining wall design. Global factors of safety (FOS) are provided to prevent

sliding, bearing, overturning or overall slip failures. The checks and factors of safety recommended are as follows;

a) Sliding

The force acting at the wall may cause forward sidling at the reinforced soil and sub-soil interface. To prevent this, the resistance of the structure to movement is checked using the weaker properties of the two interacting soils;

$$Sliding\ Force = 1/2\ K_a\ \gamma H^2 \qquad (2.8)$$

and

$$Restraining\ Force = \gamma H L \tan\delta \qquad (2.9)$$

FOS_S = *Restraining Force/Sliding Force.*

A factor of safety between 1.5 and 2 is generally selected.

b) Overturning

Overturning occurs when the active forces behind the reinforced fill cause a moment greater than the resisting moment of the structure. In some cases, the flexibility of the wall does not allow this from of structural failure. The two moments occurring are as follows;

$$Overturning\ Moment = 1/6\ K_a\ \gamma H^3 \qquad (2.10)$$

and

$$Resisting\ Moment = 1/2\ \gamma H L^2 \qquad (2.11)$$

FOS_{ot} = *Resisting Moment / Overturning Moment.*

A factor of safety of 2 is generally selected.

c) Bearing Capacity

The safe bearing capacity of the sub-soil should not be exceeded. It is assumed that the base pressure is either a trapezoidal distribution, Schlosser and Vidal (1969) or the Meyerhof stress distribution. In the trapezoidal stress distribution from, the maximum and minimum pressures can be give as;

$$\sigma_{max} = \gamma H\left[1 + k_a\left(\frac{H}{L}\right)^2\right] \qquad (2.12)$$

$$\sigma_{min} = \gamma H\left[1 - k_a(\frac{H}{L})^2\right] \qquad (2.13)$$

for the Meyerhof stress distribution, Schlosser (1972), the spread of stress distribution is;

$$\sigma_v = \gamma H \frac{1}{1 - \frac{1}{3}k_a(\frac{H}{L})^2} \qquad (2.14)$$

FOS_{bc} = Bearing Capacity / Vertical Pressure.

Unlike concrete and stone structures, reinforced soil walls can withstand substantial settlements without damage. Foreword et. al. (1976) suggested a Factor of Safety of 2 instead of the usual factor of 3 used for rigid structures.

2.5.2 Internal Stability

The design methods for internal stability can be categorised largely into two groups. The first group consists of methods dealing with the Limiting Equilibrium condition of the reinforced structure while the second group consisders the Limit State methods which deal with the serviceability and ultimate conditions of the structure.

In the Limit Equilibrium methods, all the components are taken to be in a limiting failure condition simultaneously and the static equilibrium of the system is checked. Design under these condition only takes account of forces without considering strain compatibility. These methods are usually based on back analysis of laboratory models or field trials and are empirical or semi-empirical.

Within the Limit State methods, there are the Ultimate and Serviceability Limit States, McGown el. al. (1992), Yogarajah (1993). They involve the analysis of mechanisms of behaviour which take into account strain compatibility and any number of potencial failure mechanisms. Thus, they take into account the various behavioural complexities of the reinforced soil mass.

a) Serviceability Limit State

The Serviceability Limit State is defined as the condition when the maximum out of balance

forces generated by self-weight and imposed load, when transmitted from the soil to the reinforcements, generate limiting acceptable deformations of both the components (soil and reinforcement) and do not cause any other forms of distress which would render the structure unsightly, require unforeseen maintenance or shorten the expected life of the structure.

b) Ultimate Limit State

An Ultimate Limit State is defined as a condition under which condition the minimum out of balance forces generated by self-weight and imposed load, when transmitted from the soil to the reinforcing materials, would result in the structure developing one or a number of previously identified collapse conditions.

BS8006; 1991, recommends that at the ultimate limit state, the soil approaches it's residual shear strength, and the cohesive strength, (in a cohesive-frictional fill), tends to zero. The cohesive strength is thus ignored when calculating any resistancing forces.

The analytical techniques used to quantify the limiting conditions include Finite Element techniques, Romstad et. al. (1976), Al-Hussaini and Johnson (1978), Andrawes et. al. (1982), Gunn and Britto (1987), the Energy method, Osman (1977), Osman et. al. (1979), and the strain compatibility method McGown et. al. (1988, 1992), Jones (1988), and Yogarajah and Yeo (1993). Of the presently available methods, the Finite Element method seems to be the most versatile in developing the serviceability limit state conditions as unlike the other methods, internal stresses and strain in the soil, reinforcement and soil/reinforcement interface can be obtained fairly easily. The finite element method is not well suited to modelling the ultimate limit state.

2.5.3 Tension failures

(a) Coulomb wedge theory

In the Coulomb wedge theory, the reinforcement is assumed to be of sufficient length so as not to cause failure by lack of adherence. Assuming that the soil wedge is an active state condition and a linear distribution of tension in the layers of reinforcement, the maximum tension in the, i the layer of reinforcement, Ti is given by;

$$T_i = [n / (n+1)]\, k_a \times \gamma H \times \Delta H \qquad (2.15)$$

where n = number of effective layer of reinforcing elements,

k_a = coefficient of active earth pressure,

γ = unit weight of the fill in a structure,

H = height of fill,

ΔH = zone of action of an individual layer of reinforcement.

Alternatively, by assuming a Coulomb sliding wedge, the sum of the tension components of the reinforcement, ΣT, may be expressed as;

$$\Sigma T = \left\langle \frac{F - \tan\beta' \tan\phi'}{1 + \cot\beta' \tan\phi'} \right\rangle^{1/2} \times \gamma H^2 \qquad (2.16)$$

where F = factor of safety,

$\tan \beta' = \sqrt{(\tan^2\phi' + F\text{-}\tan\phi')}$

(b) Rankine theory

The Rankine theory was originally recommended by the Laboratoire de Central des Ponts et Chaussees for calculating the maximum tension in the reinforcement, T_{max}, which can be expressed as ;

$$T_{max} = K_a \times \gamma H \times \Delta H \qquad (2.17)$$

(C) Coulomb moment balance

In this approach the moment equilibrium due to the earth pressure and the reinforcement about the toe of a wall is used to arrive at the maximum tension in the bottom layer of reinforcement, Tmax, which given by;

$$T_{max} = [n^2 / (n^2\text{-}1)] \times K_a \times \gamma H \times \Delta H \qquad (2.18)$$

(d) Trapezoidal distribution

In the trapezoidal distribution method the analysis takes into account the backfill thrust, P which alters the state of stress within the block of reinforced soil and increases the vertical stress while increasing the tension in the reinforcement. By assuming a trapezoidal pressure distribution under the base, the maximum tension in the bottom layer of reinforcement, T_{max} is given by;

$$T_{max} = [1 + k_a(H / Lr)^2] \times K_a \times \gamma H \times \Delta H \qquad (2.19)$$

where L_r = length of the reinforcement.

(e) Meyerhof distribution

The Meyerhof distribution of earth pressure under the base of the structure has been suggested by Schlosser (1972) and is used in the French Code. In this approach the maximum tension, T_{max} is given by;

$$T_{max} = [\, K_a \times \gamma H \times \Delta H \,] / [1 - 0.3\, ka\, (H/LR)^2] \qquad (2.20)$$

(f) Elastic Analysis

Bannerjee (1975) used the finite element method for a simple elastic analysis and found that at a depth H, the maximum tension in a reinforcing element, T_{max} is given by;

$$T_{max} = 0.35\, \gamma H \times \Delta H \qquad (2.21)$$

It has been shown that the Coulomb wedge theory gives the minimum area of reinforcement and that the trapezoidal distribution gives the maximum.

BS 8006; 1991, recommended for local stability of a layer of reinforcing elements, the maximum ultimate limit state tensile, T_i, to be resisted by the, ith, layer of elements at a depth of h_i, below the top of the structure may be obtained from the summation of the appropriate forces for cohesive frictional fills as follows;

$$T_i = T_{pi} + T_{si} + T_{fi} - T_{ci} \qquad (2.22)$$

where;

T_i = reinforcement tension due to fill above the reinforcement layer,

T_{pi} = reinforcement tension due to uniform surcharge,

T_{si} = reinforcement tension due to a concentrated load,

T_{fi} = reinforcement tension due to horizontal shear stress applied to the structure,

T_{ci} = reinforcement tension due to shear strength of the cohesive soil.

A local stability check may be performed to ensure adequate provision of the reinforcement

area sustaining the tensile force to avoid tension failure. The maximum tensile force should not exceed the adhesion due to frictional resistance developed between the reinforcement and fill outside the failure plane. For longe term design c' = 0 except for PFA.

2.5.4 Adhesion failures

The development of adhesion due to friction relies upon the bond length or length of adherence. Several methods of analysis have been suggested to determine the required. adhesion resistance.

(a) Rankine theory

For a uniform normal stress, σv, the factor of safety, (FOS) against an adhesion failure is calculated from;

$$FOS = \frac{2(BL_R\mu)}{(K_a\Delta H)} \qquad (2.23)$$

where B = width of reinforcement element or length of transverse elements in a grid,

μ = coefficient of friction between the fill and reinforcement.

If the adhesion contributed by the reinforcement within the failure wedge is ignored, due to lack of adherence, equation 2.22 becomes;

$$FOS = \frac{2B\mu[L - H\tan(45° - \phi'/2)]}{K_a\Delta H} \qquad (2.24)$$

(b) Meyerhof distribution

Considering the Meyerhof distribution, the factor of safety, FS may be calculated from;

$$FOS = \frac{L}{\frac{H^2K_a}{3L} + [\frac{1}{1-1/3K_a}(\frac{H}{L})^2]\frac{K_a\Delta H}{2B\mu}} \qquad (2.25)$$

(c) Coulomb force balance

The overall factor of safety, FOS is calculated by equating the forces about the toe;

$$FOS = \frac{4B\mu\Delta H}{KaH^2}\sum_{i=N}^{n} i[L-(n-i)\Delta H\tan(45°-\phi'/2)] \qquad (2.26)$$

where N = the number of the first layer of reinforcement to cross the theoretical failure line,

(d) Coulomb moment balance

By taking moments, the Coulomb theory gives a factor of safety, (FOS) as;

$$FOS = \frac{2B\mu\gamma H^2}{KaH^3}\sum_{i=N}^{n} (n-i)i[L-(n-i)\Delta H\tan(45°-\phi'/2)] \qquad (2.27)$$

(e) Coulomb wedge

Resistance to the development of a Coulomb wedge failure using the adherence developed outside the wedge gives a factor of safety as;

$$FOS = \frac{2B\mu\gamma H[\frac{L}{2}(n+1)+H\tan\beta'(\frac{1-N^2}{6N})}{\frac{1}{2}\gamma H^2[\frac{FS-\tan\beta'\tan\phi'}{\cot\beta'+\tan\phi'+1}]} \qquad (2.28)$$

where β' = inclination of a potential failure plane to the vertical plane.

As the height of a structure or wall increases, the adherence developed between the soil and the reinforcement will increase. So for low walls at a limiting factor of safety, the adhesion criteria rather than the tension criteria will normally be critical. This observation has a significant influence on the economies of reinforced soil formed from polymeric anchors, Jones and Hassan (1992).

2.6 REINFORCING MATERIALS FOR SOIL STRUCTURES

Reinforcing elements may take a variety of forms, some of which are shown in Fig. 2.6 They fall into two broad categories; (i) Metallic reinforcement and (ii) Non-metallic reinforcements.

(i) Metallic reinforcement

The most common metallic reinforcement comes in the form of strips. Smooth and ribbed metallic strips have been used although the latter is an improvement of the former. Dimensions may vary with application and structure type, but are usually within the range of thickness 3-5 mm and width of 50-100 mm. Other forms of metallic reinforcement such as grids, perforated plates or round bars are also used.

The major concern with metallic reinforcement is corrosion. The presence of soluble salts in the reinforced soil fill has been shown to produce corrosive conditions, Blight and Dane (1989). The classic solution to potential corrosion problem is to provide additional sacrificial thickness over the thickness required by the analysis or / and to protect the reinforcement by galvanising or a protective coating and additionally to restrict the fill be good quality cohesionless material:

(ii) Non-metallic reinforcement

Manufacturing processes have evolved to a stage where strong and durable non-metallic reinforcing elements can be mass produced. The most familiar products used in earth retention systems are high density polyethylene (HDPE) and polyester, used as strips, grids or anchors. Other non-metallic reinforcements include glass fibre reinforced plastic strips (GRP), used rubber tyres, or concrete planks.

The development of geotextiles and geosynthetic fibres has raised interest in the three-dimensional reinforcement of soil fills, a process in which the soil is mixed with small inclusions of fibres or small plates or continuous elements.

Non-metallic reinforcement materials normally posses strong resistance to corrosion and are not sensitive to the presence of compounds such as soluble salts. Since corrosion is regarded as a problem for reinforced soil structures incorporating metallic reinforcements, the use of non-metallic reinforcing elements appears to be the best option.

An uncertainty regarding polymeric reinforcement is its long term behaviour associated with creep. The creep behaviour varies with the type of reinforcement, stress level and temperature. It is possible to achieve a safe design by giving allowance for creep in the design, McGown et al. (1984). It is noteworthy that the in-soil properties of fabric reinforcements can be different from in-air properties, McGown et al. (1982). In practice creep problems do not appear to be significant if high strength durable polymeric

reinforcement are used, Jones (1990).

2.7 FACTORS INFLUENCING REINFORCED SOIL

The design rules which are currently used in practice are largely based on empirical observations and measurements made on structures under working conditions. These rules have proved successful and have enabled stable reinforced soil structures to be built with confidence. Two shortcomings to the approach, however, are:

(i) the rules provide no information as to potential "weak links" in the structure, or how the design might be improved (in terms of the selection, spacing and orientation of the reinforcement for example), and

(ii) the simple extension of the existing empirical rules to different types of reinforcement in different soils, and different geometries is not always possible.

It would be more satisfactory if an assessment of the behaviour of a reinforced soil could be derived from consideration of the factors which influence its performance including:

a) the mechanical behaviour of the soil, described by standard parameters,
b) the material properties and geometry of the reinforcement,
c) an understanding of the mechanisms which operate when reinforcement is placed in soil (including the influence of the reinforcement properties, dimension, orientation and spacing in the soil),
d) the influence of construction.

A comprehensive list of the factors which influence a reinforced soil structure is given in Table 2.1.

(i) reinforcement

Reinforcement when introduced into soil and aligned with the tensile strain direction disrupts the uniform pattern of strain that would develop if the reinforcement did not exist. The reinforcement also inhibits the formation of continuous rupture surfaces through the soil, with the result that the soil exhibits an improved stiffness and shear strength.

Form, In order to improve the performance, the reinforcement must adhere to the soil or be

so shaped that deformation of the soil produces strain in the reinforcement. Reinforcement can take many forms depending largely upon the material employed. Common forms are sheets, bars, strips, grids and anchors are shown in Fig. 2.8. Some reinforcement such as plain strips, rely upon friction to develop bond between the soil and reinforcement; the grid and the anchor provide a more positive bond by developing an abutment effect or soil-reinforcement interlock. The performance of various forms of reinforcement in respect of bond has been studied by a number of researchers and performance criteria for frictional fill and established reinforcement have been developed by Schossler and Elias (1978) for strips, Milligan and Love (1989) for grids, Murray (1983) for triangular anchors, and Hassan (1992) for polymer anchors.

Stress distribution along reinforcement, In the case of grid reinforcement, the width of the reinforcement is not restricted by the actual material section of the reinforcement but by the dimensions of the traverse elements and the shear strength of the soil. The mechanism of action of a grid in providing resistance to slippage (pullout) is discussed by Milligan (1982). Among the mechanisms proposed is the passive resistance theory Chang et al (1977) and the bearing capacity theory Bishop et al (1982). The bearing capacity mechanism is a form of passive resistance with a limited failure plane; however, it has been concluded that the passive resistance mechanism may be true for a completed grid but does not hold for individual transverse members, Milligan and Love, (1985).

Surface properties, For sheets, bars and strips, the coefficient of friction between the reinforcement and soil is a critical property, the higher the friction the more efficient the reinforcement. Thus an ideally rough bar, strip or sheet is significantly better than a reinforcement with a smooth surface.

Dimensions, The dimension of the reinforcement must be compatible with the requirements of the structure. The theoretical dimensions of any reinforcement are likely to be modified to conform with the requirements of logistics, durability, and minimum specification requirements, BS 8006 (1991). In addition the form, strength, stiffness and spacing will all influence the dimensions chosen.

Strength, Reinforcement strength is synonymous with robustness; logic demands that any reinforcement be robust. Any sudden loss of strength could have catastrophic effects since the improvement in shear strength is directly dependent upon the magnitude of the maximum force generated in the reinforcement. Sudden loss of strength due to failure, would have the

effect of suddenly reducing the shear strength of the reinforced soil to the shear strength of the soil shown at an equivalent displacement.

Stiffness, Bending stiffness (EI/y), is the product of the elastic moulus, E, and the second moment of area, I, it has not been shown to have any significant effect on the performance of reinforced soils. Longitudinal stiffness is a critical parameter as this determines the stress state of the soil-reinforcement composite material, a point acknowledged in recent design Codes, BS8006 (1991), Jones (1992).

(ii) Reinforcement distribution

Location, In order to establish which is the logical area for the reinforcement, potential failure mechanisms and planes have to be established together with the associated strain fields. For optimum effect, reinforcement is positioned within the critical strain fields in the location of greatest tensile strains.

Orientation, General theories of the behaviour of reinforcement in the soil emphasise the importance of the reinforcement being placed along the principal tensile strain directions developed in the soil alone, under the same stress conditions. Changing the orientation of the reinforcement will reduce its effectiveness, and if orientated in the direction of the principal compressive strains, the action of reinforcement changes from that of tensile strain reinforcement to compressive strain reinforcement. If the reinforcement is orientated along the zero extension directions, an overall reduction in the strength of the reinforced soil may result, as the effect of the reinforcement can be to lubricate the failure plane, O'Rouke and Jones (1990).

Spacing, In laboratory tests, Smith (1977) and Jewell (1980) have established that the increase in strength of a reinforced soil is not always directly proportional to the number of reinforcing elements in the system (all other things being constant). The spacing between separate reinforcing elements affects the performance of individual reinforcing members, and in many cases the use of larger widely spaced reinforcement can be an improvement on the use of a multitude of closely spaced material.

Reinforcing Element, The type of materials used as reinforcing elements include steel, fiberglass and thermoplastics in the form of sheets, strips, or grids. The choice of material and the form in which it is used generally dictates the load transfer mechanism from the soil

to the reinforcement. It the case of strip and sheet reinforcement, the load transfer mechanism at the soil/reinforcement interface is principally frictional, while for grid reinforcements the principal mode of stress transfer is bearing stress developed at the junctions or protrusions, shown in Fig. 2.7.

When stressed, reinforcements have to be capable of sustaining the load without rupture and without reaching unacceptable strains during their lifetime. The wide variety of reinforcements and the variation in their behaviour has lead to the classification of reinforcements into two categories by Andrawes and McGown (1977);

(a) Relatively extensible reinforcement

Reinforcements that have rupture strains which are larger than the maximum tensile strain in the soil without reinforcement under the same operational conditions (e.g., some polymeric reinforcements),

(b) Relatively inextensible reinforcements

Reinforcements that have rupture strains which are less than the maximum tensile strains in soil without inclusions, under the same operational conditions (e.g., steel, some fibre reinforced plastics).

Embedding relatively inextensible reinforcements in soil, in the direction of the principal tensile strain results in a net increase in load carrying capacity of the soil or a reduction of boundary movements when compared to the soil alone. This continues to be effective until rupture of the reinforcement occurs, after which the composite reverts back to the properties of the soil alone. In the case of relatively extensible reinforcements, the extensibility of the reinforcement allows larger strains to occur without the reinforcement rupturing. In these circumstances, the benefit of the mobilised tensile strength of the reinforcement is available even after the peak strength of soil is reached, Fig. 2. 8.

Relatively inextensible metallic reinforcements, were the first form of reinforcing elements used, in modern times Vidal (1969). These reinforcements have two main inadequacies: they are susceptible to corrosion, Guilloux and Jailloux (1979) and Jewell and Jones (1981), and hinder the development of active soil pressures due to their inextensibility, Jones (1990), McGown et. al. (1988, 1992), and Yogarajah (1993). To overcome the corrosion aspect, certain building codes, recommend a sacrificial thickness. The lack of predictability of the extent of corrosion and the need to allow adequate soil movement for active pressure

development, have lead to these materials being in part replaced with materials made from synthetic polymers. The variety and availability of these relatively extensible polymeric materials have greatly increased in recent years, Jones (1985). Nevertheless, polymeric reinforcements have their own disadvantages such as being vulnerable in the long term to creep and stress relaxation. Additionally, degradation by ultraviolet light when exposed to the suns rays, together with thermal instability and decay caused by some biological agencies when they are embedded in the soil have to be considered.

(iii) Soil

Particle size, grading and index properties. Reinforced soil is essentially an earthworks structure and the constraints on the use of clay soils or poorly graded or drained materials in bulk earthworks are usually applied to fills used in reinforced soil construction. However, movements after construction may be more important in some reinforced soil applications such as faced structures so limiting the materials appropriate for use. Rapid construction, often an advantage of reinforced soil, may not be possible if fills with a high fines content are used, especially in wet weather.

(iv) soil state,

Density, the density of the reinforced soil has been shown to have a significant effect on the soil/reinforcement friction in granular soils, Schlosser and Elias (1978). The likely degree of construction control and compactibility of the soil should be taken into account when assessing design soil/reinforcement parameters lack of proper compaction can lead to structural instability, Ingold, (1979).

State of Stress, the state of stress at the level of the reinforcement element under consideration should be taken into account when the horizontal component of stress is considered. Field measurements have indicated that the upper levels of fill behind a reinforced soil wall, reinforced with axially stiff reinforcement, will exhibit a coefficient of lateral earth pressure equivalent to the at-rest pressure (K_0), Schlosser (1973), Sims and Jones (1974), Jones and Sims (1975), Ministere des Transports (1979), Ingold (1983), Jones (1990). This observation is reflected in the coherent gravity hypothesis method of design, BS8006 (1991) The use of less stiff reinforcement may result in yielding, where the strength of the soil is fully mobilised and stress conditions approximate to the active condition. In this case the use of the tie back method of analysis is appropriate, BS 8006, (1991).

Degree of Saturation. The Degree of Saturation is related to the particle size and grading of

the soil. A well graded granular soil will not hold water. However, if fine grained soils are used the effect of moisture content on the stress transfer should be considered, particularly where the construction rate is an important consideration.

2.7.1 Fill Materials for Reinforced Soil Structures

Fill forms the largest component of any reinforced soil structure. The choice of which soil or fill material to be used will depend upon the technical requirement of the structure in question and also upon the basic economics associated with the scheme. A large increase in cost of fill will lead to an overall increase in the total cost of the project.

The soil used in conventional reinforced soil structure is usually a well-graded cohesionless fill or, a good cohesive frictional fill. Purely cohesive soils are seldom used but offer potential major economic benefits, Tatsuoka, (1992). Cohesive frictional fill can be a convenient compromise between the technical benefits of cohesionless soil and the economic advantages of cohesive fill, Jones (1992) and Wu et. al. (1992).

(i) Cohesionless fill

Cohesionless fill, either frictional fill or granular backfill, is defined as good quality, well-graded non-cohesive materials usually possessing a good angle of internal friction. The advantages of cohesionless fills are that they are stable, free draining and not susceptible to frost. In the United Kingdom, frictional fill is defined as a material in which no more than 10 percent passes a 63μm BS. sieve, DOT (1987). The DOT (1987) further specifies that the effective angle of friction, ϕ' should be equal to or greater than 25°, with the coefficient of uniformity, $Cu \geq 5$. In France the term granular backfill is used to refer to the fill of reinforced soil structures in which no more than 15 percent (by weight) is smaller than 15μm. In this case, the angle of internal friction of saturated consolidated frictional fill must be greater than 25°.

(ii) Cohesive frictional fill

The main advantage of using cohesive frictional is its availability when compared with frictional fill. This may represent an economy.

In the United Kingdom cohesive frictional fill is defined as a material with more than 10 percent passing 63μm BS. sieve, DOT (1987). The effective angle of friction, ϕ' of the cohesive frictional fill must be equal to or greater than 20°. In addition, for material less than

52μm, the Liquid Limit, LL≤45 percent and the Plasticity Index, PI≤20 percent. The moisture content is an important criterion for easy handling of the material and the stability of the structure. Usually a minimum moisture content in the range 6-10 percent will be satisfactory. Alternatively, a value of 1.2-1.3 times the plastic limit of the soil may be used.

(iii) Cohesive fill

Cohesive fills are regarded as poor materials when used for reinforced soil and are not included in the British specification for vertical structures, DOT (1987). The main problem in using cohesive fills is in short-term stability resulting from the poor bond between the cohesive soil and reinforcement. Moreover, soil-reinforcement adhesion can be reduced if positive pore pressures develop. The durability of the reinforcing material can be impaired as some fine-grained cohesive soils are significantly more aggressive than cohesionless soil. It is known that same clay minerals such as illite accelerate corrosion.

Cohesive fills may be susceptible to frost and therefore additional earth pressures have to be accommodated by the reinforcement/facing connections. A proper drainage system should be provided when using cohesive soils.

Despite the above shortcomings, cohesive fills can be used beneficially with suitable reinforcements and appropriate construction techniques, particularly in areas where cohesionless fill is in short supply. Design methods can be modified to utilise the passive resistance developed in front of grid reinforcements or anchors instead of relying purely on frictional resistance.

(iv) Waste materials

The most commonly used waste materials are pulverised fuel ash (PFA) and minest ones. The use of these materials as fill for reinforced soil structures is attractive from an environmental as well as economic viewpoint.

(a) Pulverised fuel ash

The use of pulverised fuel ash as a lightweight fill in embankment construction is established practice. The material can equally be used as a lightweight fill, for long-term work in reinforced soil structures.

Pulverised fuel ash is relatively easy to place with compaction by vibrating rollers or footpath

compactors, giving an optimum moisture content varying in the range 19-26 percent, with 10 percent air voids. It provides an additional benefit in that the material can be self-hardening with a marked cohesion (c'), Clarke et al. (1990), Yang (1992) and Yang et. al. (1993). Although the cohesion of PFA is time dependent, the rate of development is compatible with the construction rate of reinforced soil structures and therefore can be relied upon. Even assuming conservative values for (c'), the implication of cohesion on reinforced soil design is significant. Because of its fine structure, grid reinforcement may prove the most satisfactory from of reinforcement, Jones (1990). However, PFA can be effectively reinforced with polymer reinforcing strips and anchors, Jones and Hassan (1992), Fig. 2.9. The classification of PFA as an engineering fill is shown in, Fig. 2.10.

Pulverised fuel ash is usually slightly aggressive to steel and even more aggressive to zinc so, in this case, the use of metallic reinforcements are not suitable. Other reinforcement materials resistant to corrosion are recommended and good drainage is necessary.

The implication of cohesion on the economics of the design of reinforced soil structures has been considered by Guler, (1990). Guler considered the effect of the addition of 5 to 10% lime to a cohesionless soil which is claimed to result in an increase in workability (easier compaction), increased permeability, and the development of cohesion of (150 to 180 kPa) in a material with an effective angle of friction, $\phi' = 19.5°$.

(b) Minestone

Minestones are the largest source of waste material in the United Kingdom. The range of particle size distribution of minestones is very variable and depends upon many factors, including the method of handling and placement. Typically the materials are predominantly fine-grained but include some sand and gravel-sized particles.

Minestones may be suitable when used with grid reinforcements to construct reinforced soil structures. When considering minestones as a backfill for reinforced soil, spontaneous combustion, chemical aggression and particle breakdown are factors which may affect its suitability, although investigations into minestones have shown that these problems can be solved with proper construction and the selection of an appropriate reinforcing material.
Due to the concern for the durability of the construction elements used with mine waste, reinforcing materials formed from materials which have high corrosion and degradation resistance are preferred, Jewell and Jones (1981).

2.7.2 Problems with fine grained and cohesive soils

The soil materials used in reinforced soil structures are dependent on the technical requirements of the structures and the basic economies associated with it. The main load transfer mechanism in reinforced soil structures is dependent on the shear forces developed at the soil-reinforcement interface. This major requirement of frictional force has lead to the use of cohesionless or cohesive frictional soils with high friction angles. Most codes of practice and most design methods are based on the use of a suitable frictional soil.

The main reasons why fine grained and cohesive soils are generally held to be unsuitable for reinforced soil construction have been discussed by a number of authors including Long (1977), Mckittrick (1978), and Jewell and Jones (1981). The main problems are;

(i) Short term stability;

The bond between cohesive soil and strip reinforcement is poor and subject to reduction if positive pore water pressures develop. It is unlikely that the current, largely empirical design methods for reinforced cohesionless soils may be satisfactorily applied to cohesive soils.

(ii) Corrosion;

Fine grained cohesive soils are significantly more aggressive than cohesionless soils.

(iii) Post-construction movements;

It is thought that long term creep deformations might occur when plastic soils are reinforced. Unacceptable creep strains have been known to occur, Elias and Swanson (1978).

2.8 RECENT PRACTICE ASSOCIATED WITH REINFORCED SOIL STRUCTURES USING FINE GRAINED (COHESIVE) SOIL

Cohesive reinforced soil structures are presently being constructed on an increasing scale especially in Japan, where there is a general shortage of good quality cohesionless fill, Tatsuoka et. al. (1983, 1985, 1986, 1987, 1990 and 1992) and Murata et. al. (1991). Recent studies in Japan indicate that fine grained soils with water contents up to 130 per cent can be shown to be adequate as reinforced soil fill provided the correct type of reinforcement is selected, Tatsuoka and Leshchinsky, (1992). These materials are outside the range and scope of the fill specification used in most International codes and specifications.

In the Japan, several tests of steep embankments formed of clay, reinforced either with a non-woven or a woven composite geotextile, have been constructed. The performance of

these test embankments, has shown that, other than reinforcing the embankment, the geotextiles also improved compaction by draining pore water from the interior of the embankments, Tatsuoka (1986, 1990 and1992).

The studies suggested that steep embankments can be safety constructed using clay / fine grain soil and that slopes can remain stable even during heavy rain, Tatsuoka, et al (1983) and Tatsuoka, et al (1985). Horizontal layers of non-woven geotextile sheets were used to provide;

(i) Compaction control; The degree of compaction of each layer thickness was controlled by the vertical spacing of the reinforcement. It was found that, heavy compaction machinery could be operated close to the shoulder of the embankment as the non-woven geotextiles effectively dissipated any pore water pressure generated within the soil during filling and compaction.

(ii) Drainage during heavy rain; the interior of the embankment even above the ground water level can be almost saturated, due to its original high degree of saturation, a low permeability after remoulding and the wet site condition. The pore water pressure is usually negative, resulting in an apparent cohesion. Non-woven geotextile sheets function as a drainage material during a heavy rain Tatsuoka et. al. (1986).

In the U.S.A., two tests walls, one with a cohesive backfill and the other with a granular backfill, have been constructed and tested at Denver, Colorado, Wu, (1991). The walls were constructed within a rigid loading facility in the laboratory. Extensive instrumentation was employed to monitor their behaviour at different surcharge pressures and at failure. From the results of the tests and the predication of the performance of the Denver walls it can be concluded that retaining walls can be constructed using cohesive soils and non-woven geosynthetic reinforcements.

2.9 CONSTRUCTION OF REINFORCED SOIL

The key aspects of a reinforced soil structure is its incremental form of construction and the interaction between the reinforcement and soil forming the structure. It is appreciated that construction technique is a dominant factor in the performance of reinforced soil. The method of construction and site practices can effect the performance of a reinforced soil structure in many ways, Jones (1990).

2.9.1 Methods of Construction

After the introduction of Vidal's (1969) incremental form of construction, various methods of construction have been developed. The methods of construction developed are based largely on the ability of the reinforcement to accommodate different amounts of settlements and distortion.

Construction methods commonly used at present are: (i) Concertina Method, (ii) Telescopic Method, (iii) Sliding (York) Method, (iv) Hybrid Methods are shown in Fig. 2.11.

(i) Concertina Method

Initially developed by Vidal (1969), the arrangement of this construction method is shown in Fig. 2.11 (i). The facing of the wall is usually made of thin aluminium or steel plating, and the reinforcement strips (usually steel) are connected to the facing. The flexibility of the facing, allows the lateral and horizontal deformations to occur, acting like a set of bellows. Structures built as wraparound structures formed from geotextiles or geogrids use this form of construction.

(ii) Telescopic Method

In the telescope method developed by LCPC and Vidal (1978), the facing of the wall is made up of elements usually fond in reinforced concrete with the reinforcement attached to the facing. The constructional arrangement is shown in Fig. 2.11 (ii). The vertical deformation of the soil is allowed by providing a discrete horizontal gap between adjacent facing panels. Compressible layers are usually used to form the gap and permit vertical settlement of the facing.

(iii) Sliding (York) Method

The sliding method of construction was invented by Jones (1978). In this method, instead of allowing the facing panels to move or distort, spacers, poles, grooves, slots or bolts are used at the reinforcement-facing connection, thus allowing the reinforcing elements to move relative to the facing. A typical Sliding method of construction is shown in Fig. 2.11 (iii).

(iv) Hybrid Method

The hybrid method, is a combination of the Sliding and Telescopic methods of construction. A growing example of this form of construction is the use of king posts and panels to form the facing. In this method, the reinforcement is attached to the king posts, and is allowed to move while the facing panels are slotted between the vertical king posts and allowed to act

in the Telescopic manner. Additionally, hybrid methods of construction include structures such as tailed gabions and tailed masonry O'Rourke and Jones (1990), is shown in Fig. 2.11(iv).

2.10 SUMMARY

The presence of an inclusion can favourably affect the behaviour of the soil-reinforcement composite. Various design approaches based on theoretical and experimental work have been suggested by a number of researchers. A comprehensive range of National structural codes have been devolved indicating that reinforced soil is an accept structural technique. All current codes suggest that good quality cohesionless soil is required to constructed permeable reinforced soil structures.

In some Countries good quality frictional fills are difficult to obtain at economic rates consequently the use of reinforced soil is limited. However, cohesive soils are available and soil structures could be built with these materials. Steep reinforced soil structures using cohesive fill reinforced with geotextiles have been constructed successfully.

There is a lack of information in respect of the theory concerning reinforcement of cohesive soils and the importance of drainage when using these materials.

The reinforcements which offer the potential of being suitable for use with fine grained soils are geogrids and geotextiles.

Table 2.1: Factors Influencing Reinforced Soil (After BS8006:1991)

FACTORS INFLUENCING REINFORCED SOIL				
REINFORCEMENT	**REINFORCEMENT DISTRIBUTION**	**SOIL**	**SOIL STATE**	**CONSTRUCTION**
from (bar, strip, grid or other) surface properties dimension strength stiffness	location orientation spacing	average particle size grading mineral content index properties	density state of stress degree of saturation	the influence of construction technique, (which will probably need to be coupled with the geometry of the structure and the soil type)

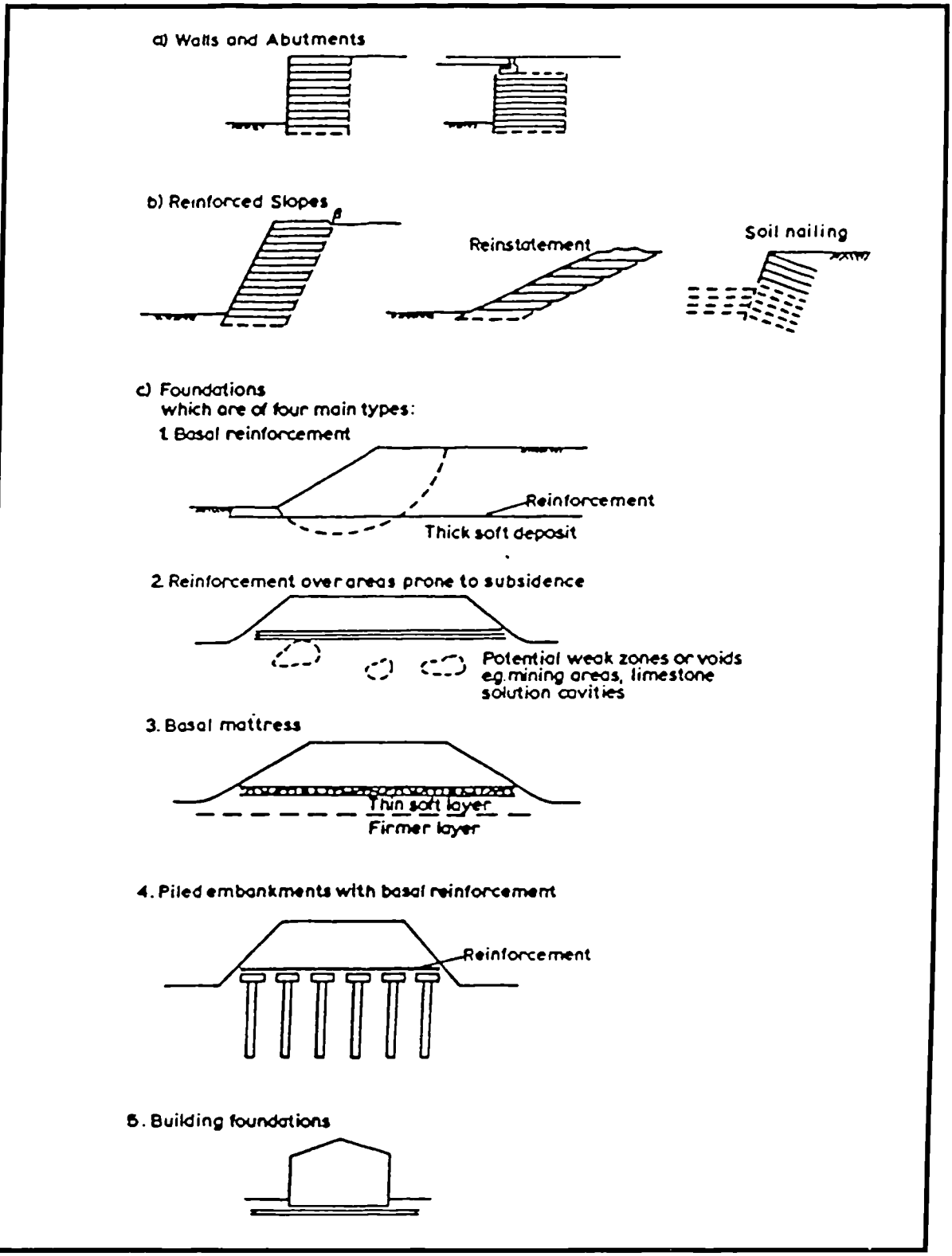

Fig. 2.1	Range of Application of Reinforced Soils (after BS: 8006, 1991)

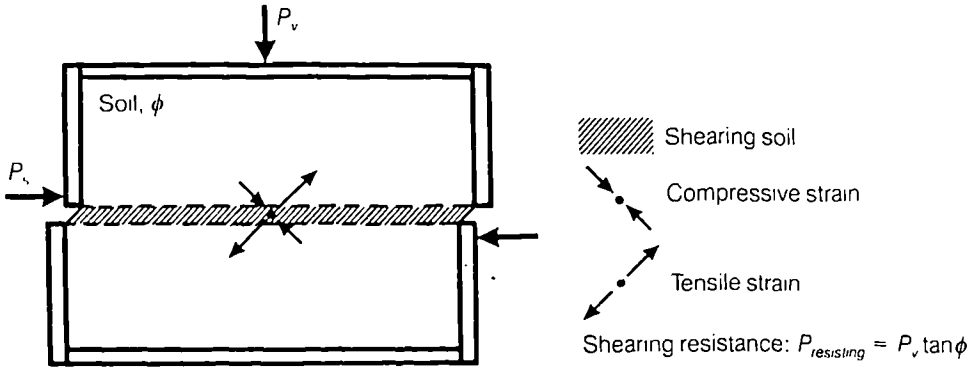

a) Compressive and Tensile Strains during Shear

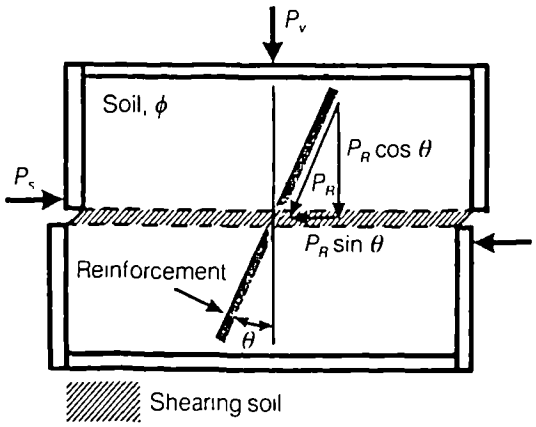

Shearing resistance:
From soil alone: $P_v \tan\phi$
Reduction in forces causing failure: $P_R \sin\theta$
Increase in forces resisting failure: $P_R \cos\theta \tan\phi$

Total shearing resistance:
$P_{resisting} = P_v \tan\phi + P_R(\sin\theta + \cos\theta \tan\phi)$

b) Reinforcement reducing the forces which cause failure and increasing the forces which resist failure

Fig. 2.2	Illustration of the action of Reinforcement in a Direct Shear Test (after Jewel and Wroth, 1987)

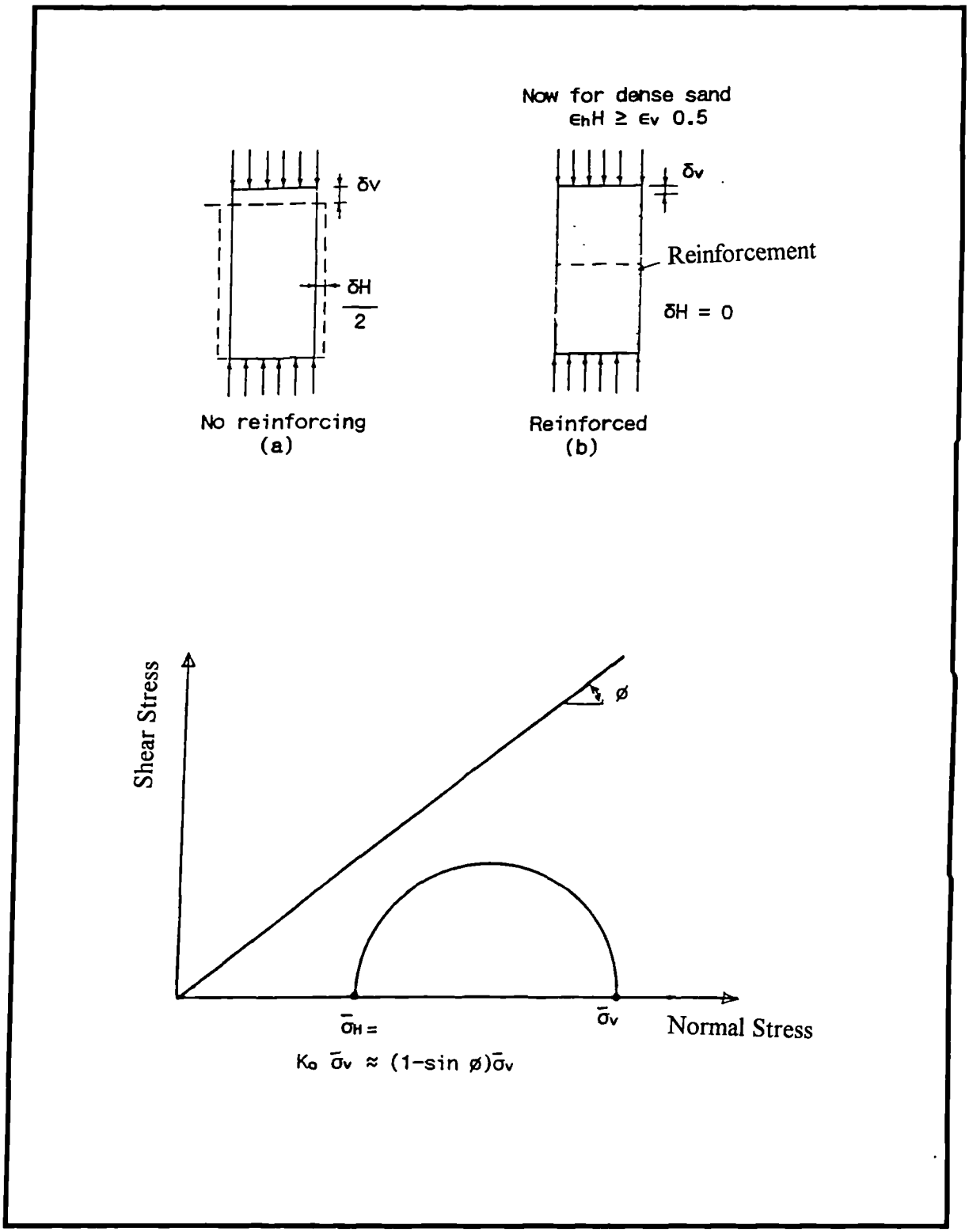

Fig. 2.3	Effects of Reinforcement on Soil (Vidal, 1969)

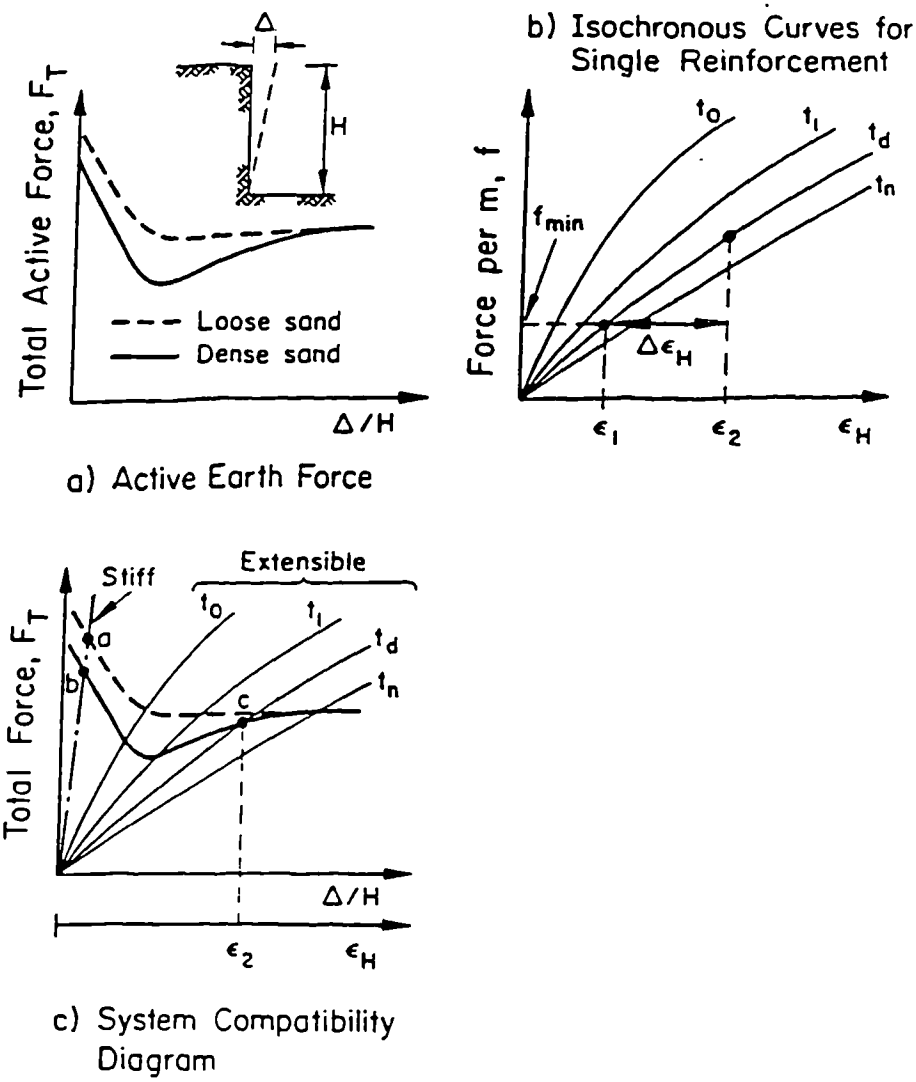

Fig. 2.4	System Compatibility of Strains and Forces for Reinforced Soil Structures (after O'Rouke and Jones, 1990)

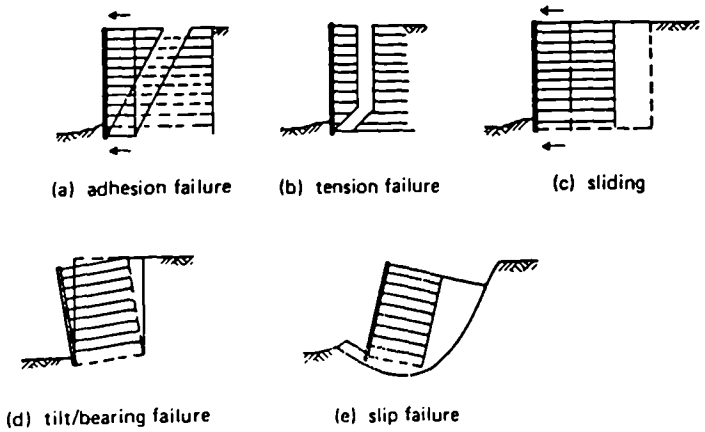

Fig. 2.5: Failure Mechanisms of Vertically Faced Reinforced Soil Structure

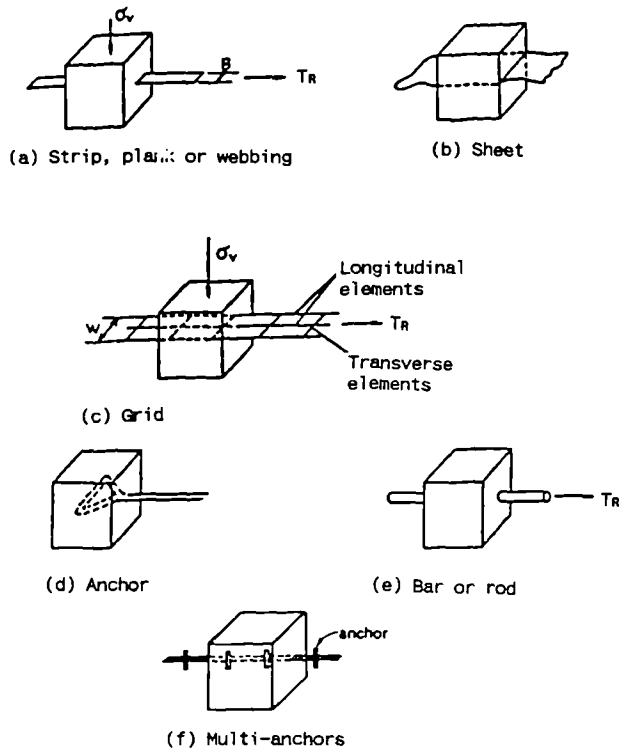

Fig. 2.6: Common Forms of Soil Reinforcement

Fig. 2.5	Failure Mechanisms of Vertically Faced Reinforced Soil Structure (after Jones, 1985)
Fig. 2.6	Common Forms of Soil Reinforcement (after Jones, 1990)

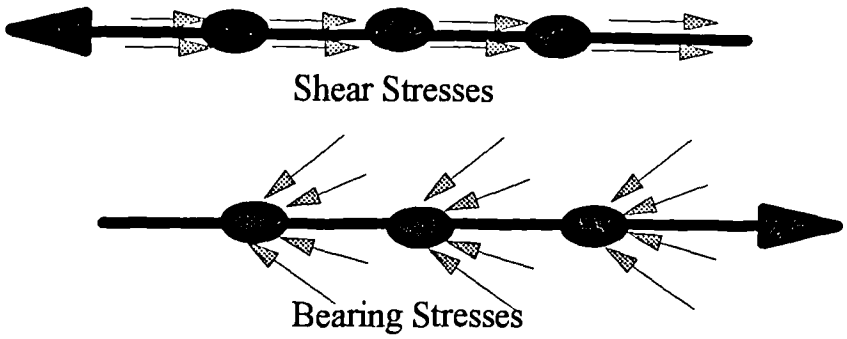

Fig. 2.7: Load transfer between soil and grid reinforcement

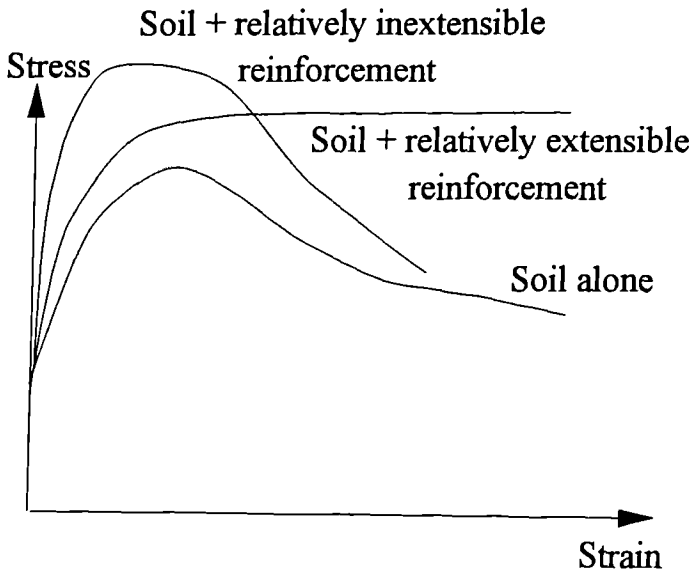

Fig. 2.8: Typical Composite behaviour (after McGown et. al.)

Fig. 2.7	Load Transfer between Soil and Grid Reinforcement
Fig. 2.8	Typical Composite behaviour

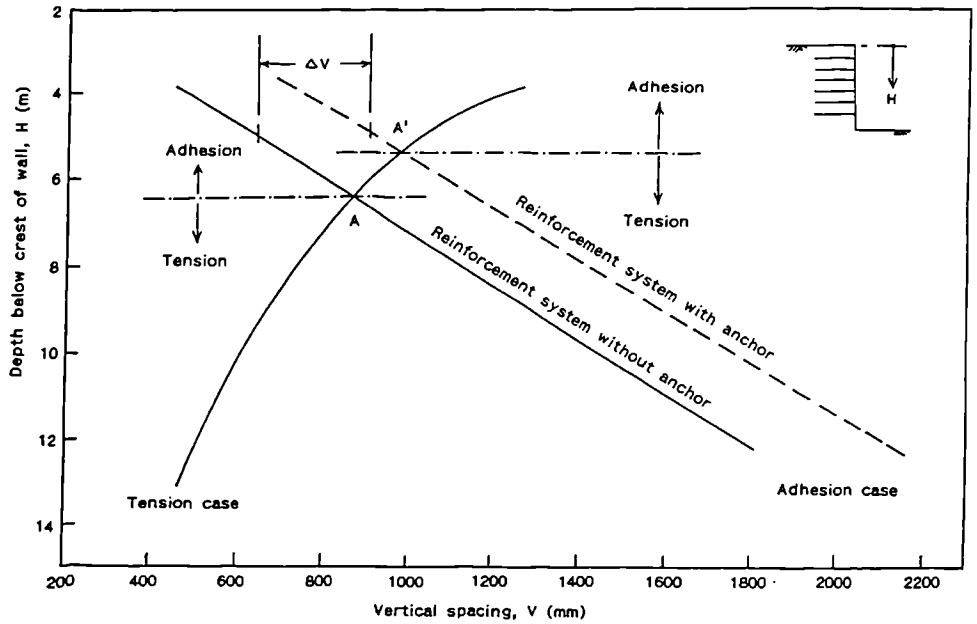

NB:
Graph is based on the following design assumptions:
1. Surcharge loading=37.5 units H.B.
2. Fill properties:
   γ =19 kN/m^3
   c'=0
   ø'=37°
3. Reinforcement system:
   Length of reinforcement, L=0.7H
   Length of anchor, L_S=667mm
   Diameter of anchor, D_S=20mm
   Average horizontal spacing of reinforcing strap, S=333mm
4. Factor of safety against rupture and pull-out=3

Fig. 2.9	Beneficial Effects of Transverse Bar Anchors (after Hassan, 1992)

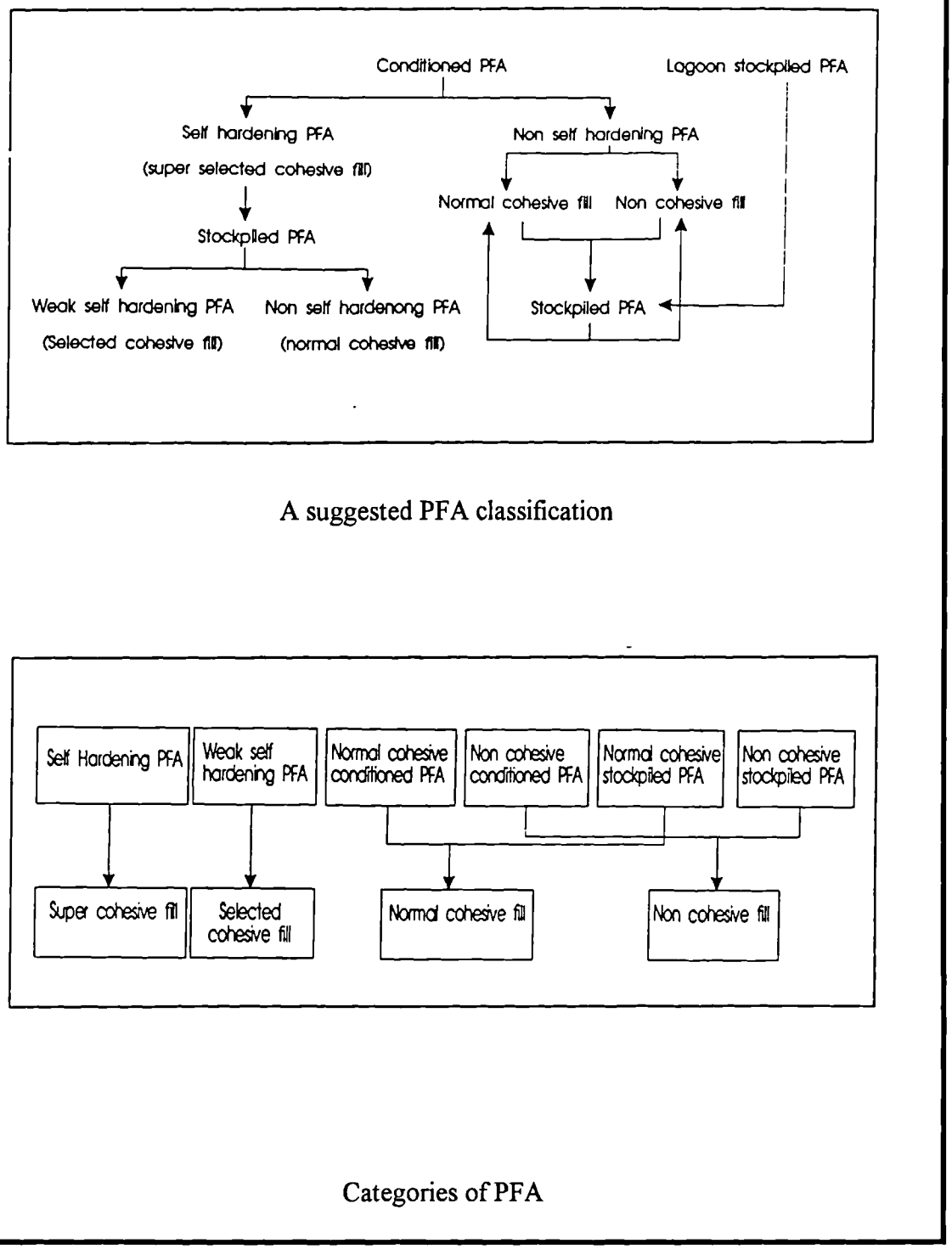

Fig. 2.10	Classification of PFA (after Yang, 1992)

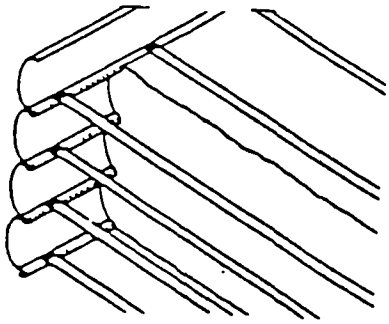

i) Concertina Method
(Vidal 1969)

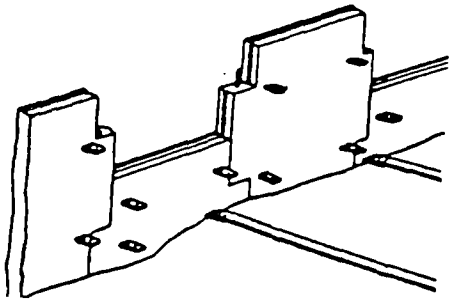

ii) Telescopic Method
(Vidal 1978)

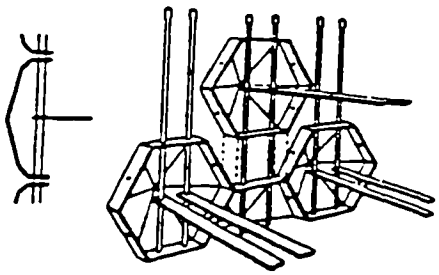

iii) York Method (Jones 1978)

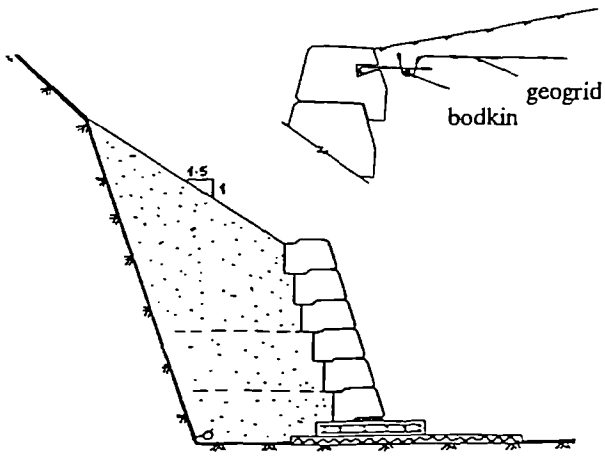

iv) Hybrid Method

Fig. 2.11	Construction Methods of Reinforced Soil

CHAPTER THREE

THE AIMS OF THE RESEARCH

3.1 INTRODUCTION

In this chapter the aims and objective of the research are identified and the geosynthetics used in the research are described. The tests undertaken as a part of the research are described.

In many parts of the world frictional fills are difficult to obtain at economic rates and consequently the use of reinforced soil in the these areas is curtailed. In many cases poor quality on-site soils are available. If these could be shown to be adequate for reinforced fill the requirement for expensive imported cohesionless soil could be eliminated and greater use could be made of reinforced soil.

The logical reinforcement for cohesive soils are geosynthetics. Some researchers have recommended against the use of cohesive fills in conjunction with geotextiles, Halibuton, (1987). The restriction was due largely to the fact, that the soil / geosynthetic friction resistance can be low, Christopher and Holtz, (1984).

Improvement to the friction characteristics could be made if the fine grained soil was well drained. This leads to the concept of composite geosynthetics that combine the function of drainage and reinforcement. Preliminary studies of the combined function of geosynthetics in providing reinforcement and drainage have shown that there is considerable potential in this application of geotextiles, Heshmati, et. al. (1990) and Jones and Heshmati (1993).

3.2 AIMS AND OBJECTIVES OF THE RESEARCH

The aim of the research was to study the fundamental behaviour of a cohesive soil such as clay (kaolin), and the action of geosynthetics in providing drainage and reinforcement. An objective of the research was to identify the separate effects on the strength properties of the

cohesive soil provided by the drainage function and separately that provided by the reinforcing function of the geosynthetics.

A range of geotextile materials have been studied to derive the characteristics, properties and mechanisms of improvement so that optimum combinations could then be postulated of material composites.

To study the degree of improvement of a cohesive soil (Kaolin), laboratory tests were designed based on conventional Rowe cells and Triaxial cells. A Scanning Electronic Microscope was used to investigate the interaction between the cohesive soil and the geosynthetics materials.

3.3 THE MATERIALS USED IN THE RESEARCH

3.3. 1 Cohesive soil

Clay minerals generally occur in the form of platy particles. The most important property of a clay soil is its plasticity. This is the ability of a clay to take up water and for the clay water mass at its optimum consistency to be shaped and to hold that shape after forming forces are removed.

The shear strength behaviour of a clay soil is determined by its consolidation and stress history rather than its density as in the case of cohesionless materials. Most clay soils derive their shear strength from cohesion and friction, however, saturated clays may appear to possess cohesion only and are therefore referred to as "cohesive soils"

Kaolin was used in this study, the index properties of the kaolin sample used in all tests are shown in Table 3.1. Details and characteristics of Kaolin are discussed in Chapter 4.

3.3.2 Geosynthetics used in the Research

A large number of woven and nonwoven geotextile and geogrid materials developed by a number of established manufacturers were considered for use in the study. A range of materials representing different materials, all of which appeared to have potential in respect of the study, were selected.

The geotextiles used in this study to provide reinforcement are the geogrids G2, G3, G4, and the geotextiles G5 and G7. The drainage function was provided by materials Gl and G6.

The geotextile material G5 was used with cohesive soil in the Colorado Walls Symposium, USA devoted to the prediction of the behaviour of full scale reinforced soil walls, Wu (1991). The objective of using the material, in this research, was to study its performance in respect of it drainage and reinforcement potential. The result of the research could be used to undertake . further prediction of the behaviour of the Colorado Walls. (see Chapter 9).

The action of geotextile G1 was limited to provide a drainage function only by cutting the intact material thereby destroying any inherent reinforcement properties, G1CT. Similarly the material G6 could be made to provide reinforcement properties only by removal of the outer filter membranes, G7. G1 and G6 were used to provide both reinforcement and drainage functions, and Gl and G2 were combined together to provide both reinforced and drainage functions, G1G2.

The index properties of the geotextiles used in the tests are shown in Table 3.2. The form of the geotextiles considered in the study are shown in Fig. 3.1a and 3.1b. The nature of the materials tested are shown in Table 3.3.

3.4 TESTS UNDERTAKEN AS PART OF THE RESEARCH

3.4.1 Triaxial Tests

A number of consolidated undrained tests (UD) and consolidated drained tests (CD) were carried out to determine the angle of internal friction (ϕ'), cohesion (c'), coefficient of compressibility (m_v), and coefficient of consolidation (c_v) of the Kaolin while containing a variety of geotextiles. The case where no geotextile drainage / reinforcement was present was also considered.

Both the consolidated undrained (CU) and the consolidated drained (CD) triaxial compression tests were undertaken using 100 mm diameter samples containing a single layer of different geotextiles placed at mid-height in the sample. A major part of the experimental work was the deliberate separation of the reinforcement and drainage function provided by the geosynthetic materials, detailed above.

Unreinforced samples of kaolin were tested to provide base data and samples were tested at effective cell pressures of 150, 300, 500 kPa. Samples were prepared in the laboratory in accordance with BS1377 (1990).

The Triaxial tests undertaken are identified in Table 3.4. Details of the tests and test procedures are explained in Chapter 6. The advantage of using the Triaxial test is that the data provided from the tests can be used directly for the analysis of reinforced soil structures, this is discussed in Chapter 9.

3.4.2 Rowe Cell Tests

Rowe cell consolidation tests were carried out to determine the C_v, and M_v of the cohesive soil (Kaolin), with a variety of geotextiles and also without the action of a geotextile. A combination of the value of C_v and M_v would be used to determine the appropriate permeability of Kaolin with and without geotextiles.

In the Rowe cell consolidation tests it was possible to measure the drainage potential and strain compatibilty of the geosynthetics, associated with the compressibility and permeability of the Kaolin. Details of the Rowe cell tests and procedures are explained in Chapter 7.

3.4.3 Scanning Electron Microscope Tests

In order to obtain a better understanding of the interaction between the cohesive soil and the geosynthetics, a number of Scanning Elotronic Microscope (SEM) tests were carried out to investigate the binding of the clay materials on the surface of the geosynthetics. The study was undertaken in the University's Materials Division, Electron Microscopy Unit.

3.5 SUMMARY

(i) There is lack of information and understating concerning the relative improvement of the physical properties of a cohesive soil when used in construction with an appropriate geosynthetic used to provide drainage. Similarly there is a lack of information of the mechanisms of action of geosynthetic materials used as reinforcement for cohesive soils.

(ii) The combined function of drainage and reinforcement which could be offered by some geosynthetic materials has not been studied, although this combined function is a logical extension of the potential improvements that could be provided by both reinforced/drainage geotextiles.

(iii) A study of the shear strength behaviour of a cohesive soil, when reinforced with a geosynthetic material providing drainage and / or reinforcement was proposed as a method to study the potential of fine grained soil as fill for reinforced soil structures.

(iv) Consolidation tests was proposed to study the influence of appropriate geosynthetics on the drainage and performance of cohesive soil.

Table 3.1: Index Properties of Kaolin

Index Property	
Plastic Limit, P.L %	35.05
Liquid Limit, L.L %	61.00
Plasticity Index, P.I %	25.05
Specific Gravity, G.S	2.63
Dry Density, ρ_d, Kg/m^3	1.32

Table 3.2: Index Properties of Geotextiles used in this research

Material and Description	**G1**	**G2**	**G3**	**G4**	**G5**	**G6**
Weight (g/m^2)	500	200	200	200	100	940
Material Thickness (mm) With a Load of 200 kPa	5 2.5	2 2	2 2	3 3	0.3 0.3	7 6
Tensile Strength Longitudinal (kN/m) Transverse (kN/m)	8 10	7.6 6.7	5 4.8	20.5 12.5	3 2	12.5 11.7
Apeture Size (mm)	0.15	0.99	25×25	28×38	0.3	0.1
Permeability (K) × 10^{-2} (m/s)	10	_	_	_	2	7.2
Roll Size (m)	3.9× 100	2 × 100	2× 100	4× 50	3× 20	3× 20
Geogrid Type	-	✓	✓	✓	-	-
Drainage Function	-	✓	-	-	-	-
Reinforcement Function	-	✓	✓	✓	✓	-
Drainage and Reinforcemnet	✓	-	-	-	-	✓

Table 3.3: Nature and Form of the Geotextile Materials Tested

Test No.	Figures	Description
K		Kaolin only, (China Clay), 0.01 mm Particle Size
K + G1	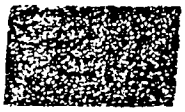	Kaolin + Netlon 514R, non woven needle punched polypropylene fibres. (providing both drainage and reinforcement)
K + G1CT	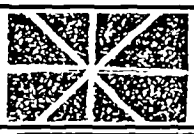	Kaolin + Netlon 514R, non woven needle punched polypropylene fibres cut to equal wedges. (providing drainage)
K + G2	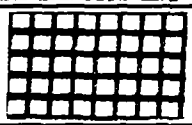	Kaolin + Conwed Strata Grid, geogrid, polyester 10x10 mm. (providing reinforcement)
K + G3		Kaolin + Conwed 5033 geogrid, polyester, 25x25 mm. (providing reinforcement)
K + G4	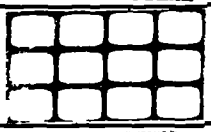	Kaolin + Tensar SS1 geogrid, PP, 28x38 mm. (providing reinforcement)
K + G5		Kaolin + non woven heat-bonded polypropylene geotextile.(providing reinforcement)
K + G6	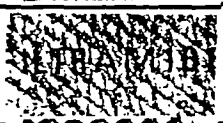	Kaolin + Filtram 1B1, Composite geotextile, mesh core spacer with filter on both side. (providing both drainage and reinforcement)
K + G7	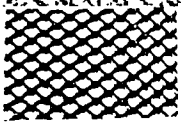	Kaolin + Filtram 1B1, mesh core, without filter on sides. (providing reinforcement)
K + G1G2	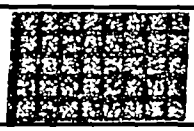	Kaolin + Combined both G1 and G2 together. (providing both drainage and reinforcement)

Table 3.4 : Consolidated Undrained Compression Triaxial Test (CU)
Consolidated Drained Compression Triaxial Test (CD)

Test No.	Test Condition CU - CD 100 mm	Effective Cell Pressure kPa 150 - 300 - 500			No. of Tests	Total Tests
K	✓	✓	✓	✓	3	3
K + G1	✓	✓	✓	✓	3	6
K + G1CT	✓	✓	✓	✓	3	9
K + G2	✓	✓	✓	✓	3	12
K + G3	✓	✓	✓	✓	3	15
K + G4	✓	✓	✓	✓	3	18
K + G5	✓	✓	✓	✓	3	21
K + G6	✓	✓	✓	✓	3	24
K + G7	✓	✓	✓	✓	3	27
K + G1G2	✓	✓	✓	✓	3	30
K	✓	✓	✓	✓	3	33
K + G1	✓	✓	✓	✓	3	36
K + G1CT	✓	✓	✓	✓	3	39
K + G2	✓	✓	✓	✓	3	42
K + G3	✓	✓	✓	✓	3	45
K + G4	✓	✓	✓	✓	3	48
K + G5	✓	✓	✓	✓	3	51
K + G6	✓	✓	✓	✓	3	54
K + G7	✓	✓	✓	✓	3	57
K + G1G2	✓	✓	✓	✓	3	60

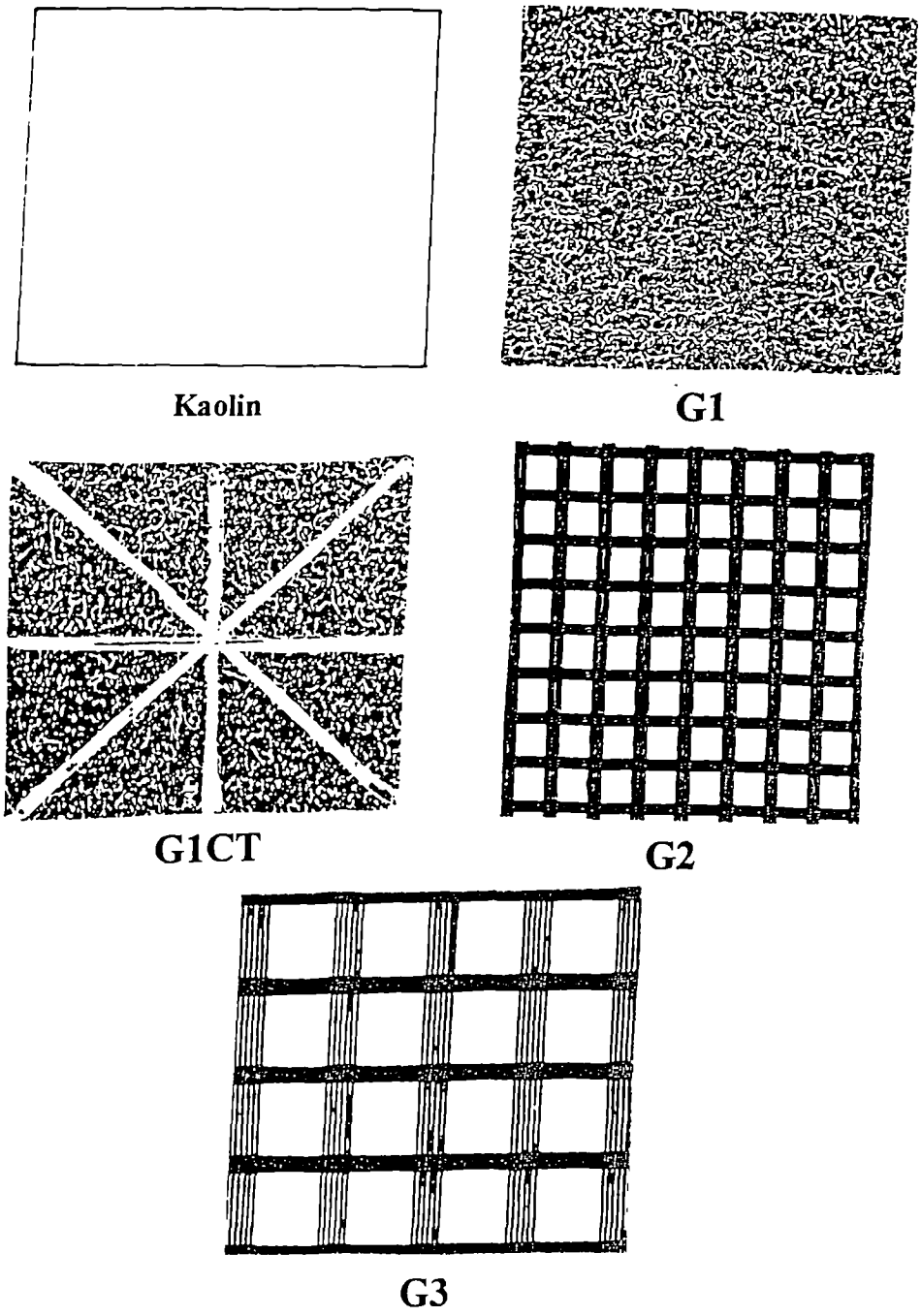

Fig. 3.1a	Types of Geotextiles used in the experimental work

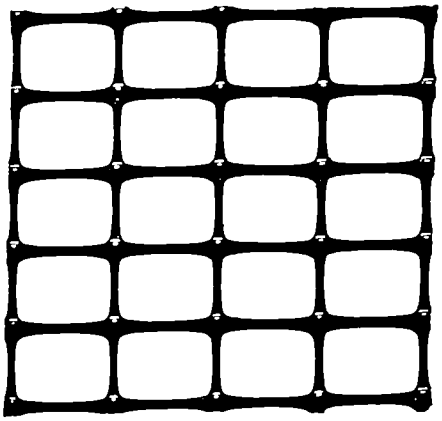

G4

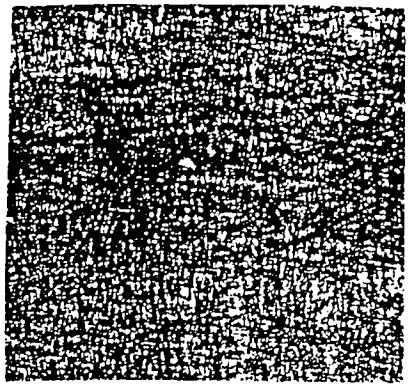

G5

G6

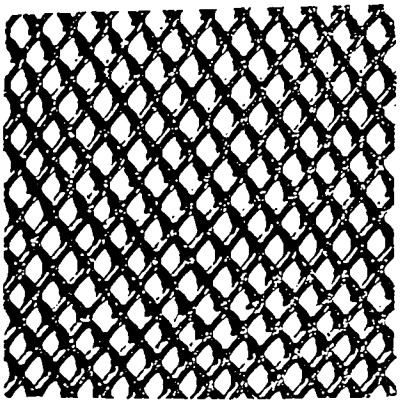

G7

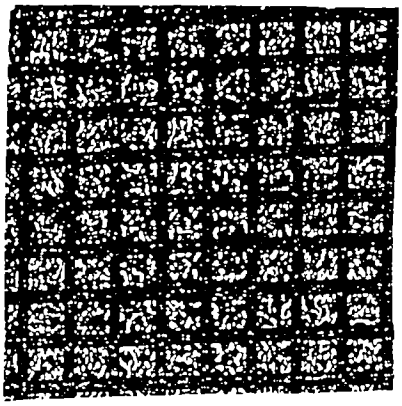

G1G2

Fig. 3.1b	Types of Geotextiles used in the experimental work

CHAPTER FOUR

COHESIVE FILL

4.1 INTRODUCTION

In this chapter the short term and long term stability of cohesive materials are considered in respect of reinforced soil. The mineralogy and properties of clay are discussed. The shear strength of clay and stress - strain characteristics of clay are explained. Finally, the properties of the Kaolin used in this study are identified.

Theoretically any soil could be used to form an earth reinforced structure. For practical purposes, only a limited range of soils are likely to be used, particularly in vertically faced reinforced soil structures, although marginal material may be used in embankments. The choice of which soil or fill material used will depend upon the technical requirements of the structure in question and also upon the basic economics associated with the scheme. In general, indigenous or waste material would be the most economic choice although these soils are likely to have inferior properties. The use of indigenous material may prove difficult for a variety of reasons especially with regard to long-term durability of the reinforcing elements and the ease with which the soil can be handled.

The main reasons and the problems why fine graded and cohesive soils are generally held to be unsuitable for reinforced soil construction are described in Chapter 2. Cohesive soil could introduce problems in respect of short / long term stability, durability and construction movement.

4.2 MINERALOGY AND PROPERTIES

4.2.1 Clay Minerals

Clay minerals generally occurring as platy particles in fine - grained aggregates which when mixed with water become yielding materials of varying plasticity. The clay particles may be crystalline or amorphous, and through normally very small, may vary from colloid size to those easily seen with an ordinary microscope.

The main groups of clay minerals and related sheet silicates may be listed as, Mineral Resources Consultative Committee (1982);
(i) Kaolinite group (from which we have kaolin), including kaolinite and halloysite;
(ii) Mica group, including micas, illite and glauconite;
(iii) Smectite group, including montmorillomite, hectorite, nontronite, saponite,
(iv) Hormite group, including attapulgite and sepiolite;
(v) Chlorites;
(vi) Vermiculite.

4.2.2 Clay Properties

The most important property of clay soils is their plasticity. Plasticity is the ability of a clay to take up water and for the clay-water mass at its optimum consistency to be shaped and to hold that shape after forming forces are removed. Plasticity can be affected by mineralogical composition, particle size, shape and distribution, action exchange capacity, pH and water content.

The shear strength behaviour of a clay is determined by its consolidation characteristics and stress history rather than by density as in the case of sands. Most clay soils derive their shear strength from both cohesion and friction, however saturated clays may appear to possess cohesion only and are therefore referred to as "cohesive soils"

When dealing with a clay soil, engineers generally aim to improve their permeability characteristics. Clays naturally contain a large amount of water in several forms including pore water or free water which is drawn into the clay by capillary action. The permeability of clay is very low compared to coarse-grained materials such as sands, and therefore it is very difficult for pore water to dissipate when load is applied to a clay foundation or fill. This leads to an increase in the pore water pressure and a decrease the effective shear strength. For this reason the use of geotextile drainage could improved the shear strength properties of clay soils.

4.2.3 Shear Strength of Clay Soils

The shear strength characteristics of clay soils are more complicated than cohesionless soils because of their more complex make-up. The behaviour of cohesive soil is influenced by surface forces rather than by mass forces because they exhibit particles which have large specific surfaces, Lambe (1951).

The shear strength of a cohesive soil is made up of two major components;
(i) internal friction, caused by particle interlocking and friction,
(ii) cohesion, caused by forces tending to hold particles together.

Coulomb (1773) suggested that the shear strength (τ_f), of a soil at a point on a particular plane can be expressed as a linear function of the normal stress (σ_n) on the plane at the same point;

$$\tau_f = c + \sigma_n \tan \phi \qquad (4.1)$$

Since it is possible to determine effective stress rather than the total stress, a more appropriate form of Columb's equation is ;

$$\tau'_f = c' + \sigma'_n \tan \phi' \qquad (4.2)$$

where;
c' = effective cohesion
ϕ' = effective angle of internal friction
τ'_f = effective shear strength of the soil
σ'_n = effective normal stress on the plane at a point
The shear strength of a soil can also be expressed in terms of effective major and minor principal stress σ'_1 and σ'_3 at failure at the point in question.

$$\tau'_f = 1/2(\sigma'_1 - \sigma'_3) \sin 2\theta \qquad (4.3)$$

$$\sigma'_f = 1/2(\sigma'_1 + \sigma'_3) + 1/2(\sigma'_1 + \sigma'_3) \cos 2\theta \qquad (4.4)$$

where $\theta = 45° + \phi'/2$ is the slope of the tangent to the Mohr circle when τ' is plotted against σ' (effective stress analysis).

This relationship is plotted for the triaxial test results during the compression stage. The relationship only shows the values for σ'_1 and σ'_3 at failure.

Plots like the Deviator stress (σ'_1-σ'_3) versus strain and the effective principal stress ratio versus strain that have been used for cohesive soils when predicting failure and are included

with the test results for comparison with the usual plots from routine Triaxial tests.

4.3 THE PROPERTIES OF KAOLIN

In assessing the apparent changes in soil properties employed by the addition of reinforcement it is first necessary to define the properties of the unreinforced soil. In this study all of the testing programme was conducted using commercially available kaolin clay in the form of English "China Clay". Over one tonne of material was used. Samples were taken regularly to monitor consistency.

4.3.1 Stress-Strain Characteristics

The stress-strain behaviour of clay soil depends on a number of different factors including density, water content, structure, drainage conditions, strain conditions, duration of loading, confining pressure, and shear stress. In many cases it may be possible to take account of these factors by selecting soil specimens and conditions which simulate the corresponding field condition. When this can be done accurately, it would be expected that the strain resulting from given stress changes in the laboratory would be representative of the strain which would occur in the field under the same stress change.

4.3.2 Suction

Soil is a multiphase material consisting of a particulate soil phase and pores which are filled with liquid and gas. There occurs specific interaction of these phases which, in turn, defines the overall mechanical integrity of the soil in terms of the interparticle forces. Numerous "effective stress" equations have been proposed by Bishop (1959) and Edil et. al. (1981) in order to relate the observed mechanical behaviour to the stress condition.

The stress variables normally include the total stress (σ), pore-water pressure (u_w), and pore-air pressure (u_a). Effective stress in soils is controlled, among other factors, by the difference between the pore-air and pore-water pressures, (u_a-u_w), which is called the matrix suction and is the negative gauge pressure at a point in the soil-water relative to the external gas pressure. It results from the capillary and adsorptive surface forces arising from the soil matrix. When expressed as energy per unit volume, suction reduces to a pressure unit. From thermodynamic or total energy considerations of the pore water, the total suction (ψ_t) can be subdivided into a matrix suction component (ψ_m) and an osmotic component (ψ_s) such that;

$$\psi_t = \psi_m + \psi_s = (u_a - u_w) + \psi_s \qquad (4.5)$$

Osmotic suction arises from the differences in the ion concentration of soil-water at different points in a soil. The main propose of this explanation is that soil suction can be considered to include implicitly the net effect of all the individual interparticle forces that influence the stress-strain and strength characteristics of the cohesive soil. In other words, soil suction may be considered an important stress viable which controls the "effective stress" and therefore the mechanical behaviour.

4.4 REINFORCED SOIL USING TRIAXIAL TESTS

4.5.1 Basic Mechanism of Reinforced soil

At present the fill material used in the construction of reinforced soil is restricted usually to non-cohesive materials in which the fully drained condition prevails both during construction and during the life of the structure. For simplicity the basic mechanism of reinforced soil may be described by reference to the behaviour of a mass of dry cohesionless soil such as sand.

Before considering the effects of any reinforcement it is useful to reconsider the behaviour of a sample of unreinforced soil. If the soil is tested in the form of a cylindrical sample with a height to diameter ratio of two (i.e. 200 - 100 mm) as used in the conventional triaxial compression test, the confining pressure σ'_c equals the minor principal stress σ'_3 similarly the vertical stress at failure σ'_f equals the major principal stress σ'_1.

These conditions are represented on the Mohr diagram given in Fig. 4.1 where a particular confining pressure, or minor principal stress, σ'_3 is associated with a particular failure stress, the major principal stress, σ'_1. Fig. 4.1 also shows that as the magnitude of σ'_3 increases so does the value of σ'_1 at failure. A line drawn tangential to the Mohr stress circles is found to pass through the origin and have a slope ϕ' equal to the internal angle of shearing resistance of the soil. This line defines the Mohr-Coulomb failure envelope for the soil. It follows from the geometry of the Mohr diagram that;

$$1/2\ (\sigma'_1 - \sigma'_3) = 1/2\ (\sigma'_1 + \sigma'_3) \sin \phi' \qquad (4.6)$$

Rearranging equation (4.6) leads to the familiar expression;

$$\sigma'_1 = \sigma'_3\ (1 + \sin \phi') / (1 - \sin \phi') \qquad (4.7)$$

$$\sigma'_1 = K_p \sigma'_3 \qquad (4.7a)$$

Thus for a constant value of ϕ' it follows that the major principal stress at failure is a linear function of the confining pressure which for an unreinforced sample equals the minor principal stress.

In an early study Vidal (1969), explained the concept of reinforced earth. It was pointed out that if a mass of dry cohesionless soil is unconfined then it has no compressive strength. This is confirmed by putting σ'_3 equal to zero in equation (4.7). However, a quite different result emerges if a layer of horizontal reinforcement is introduced into the soil mass as shown in Fig. 4.2. If a steadily increasing vertical stress $\sigma v'$, is then applied there would be lateral movement induced in the soil which would generate a frictional force between the soil and the embedded length, l, of the reinforcement. If the coefficient of friction between the soil and reinforcement is f, the change in tensile force, δT, generated in the reinforcement by the vertical stress is given by equation (4.8);

$$\delta T = \sigma' v \, b f \, \delta l \qquad (4.8)$$

for there to be no failure by slippage between the soil and the reinforcement;

$$\frac{dT}{2\sigma' v b dl} \leq f \qquad (4.9)$$

Reference to Fig. 4.2 reveals that δT is the difference between the tensile forces $T1$ and $T2$ generated at the ends of the reinforcement. As the action of loading the element of reinforced soil induces a tensile force in the reinforcement so there is a corresponding compressive lateral stress generated in the soil analogous to a confining pressure. This would impart some finite compressive strength to the soil mass. Two important conclusions of this study are that failure occurs either by slippage between the soil and the reinforcement or by tensile failure of the reinforcement.

A later and more extensive investigation was carried out by the Laboratories Central des Ponts et Chaussees (LCPC) using simple triaxial test techniques employing dry sand with the confining pressure applied by compressed air, Long et al (1972). Two possible comparison tests were carried out on both reinforced and unreinforced samples. The reinforcement used

was in the form of discs of aluminium foil cut to the same diameter as the sand sample. These were placed horizontally in the sample at a constant vertical spacing in any one sample. The effects of varying reinforcement spacing, Δh and reinforcement tensile strength T were investigated both experimentally and theoretically.

In the initial experimental work Long et al (1972) found that above a threshold confining pressure of approximately 50 kN/m^2 there was a constant increase in compressive strength, independent of applied confining pressure, for a sample with reinforcement of a given tensile strength at a constant spacing.

These results were interpreted on the assumption that the applied confining pressure equalled σ'_3 with the measured vertical stress equalling σ'_1. For the unreinforced samples the resulting Mohr's stress circles defined the familiar linear envelope passing through the origin. The failure envelope for the reinforced samples was also linear and parallel to that for the unreinforced sample, however, it intercepted the shear stress axis indicating an apparent cohesion. This is illustrated in Fig. 4.3 which shown stress circles for both reinforced sample and unreinforced samples tested at the same confining pressure. The difference in major principal stress at failure is $\Delta\sigma'_1 = [(\sigma'_1)_r - \sigma'_1]$. The results of the experimental work were later formulated by Schlosser and Long (1973) using the expression;

$$(\sigma')_r = K_p \sigma'_3 + \Delta\sigma'_1 \qquad (4.10)$$

This expression can be compared to the Rankine-Bell solution for a $c' - \phi'$ soil.

$$\sigma'_1 = K_p \sigma'_3 + 2\sqrt{K_p}\, c' \qquad (4.11)$$

From a comparison of equation 4.10 and 4.11, it was assumed that there was a direct correspondence between the second terms of both equations.

$$c' = \frac{\Delta\sigma' 1}{2\sqrt{KP}} \qquad (4.12)$$

Reference to experimental work showed the value of $\Delta\sigma'_1$ to be directly proportional to T and inversely proportional to Δh;

$$c' = \frac{T\sqrt{Kp}}{2\sqrt{\Delta h}} \qquad (4.13)$$

Subsequent work by Bacot (1974), Hausmann (1976), corroborated the early LCPC test data and reaffirmed the concept of the induction of an apparent anisotropic cohesion. A more unified theory was presented by Hausmann who modelled strength improvement as a pseudo cohesion above the threshold confining pressure where tensile failure prevails and as an enhanced friction angle at confining pressures below the threshold value when bond failure prevails.

Chapuis (1972) concluded that the assumption of vertical and horizontal stresses being principal stresses within a horizontally reinforced mass was erroneous. This followed from the fact that since the horizontal reinforcement induced horizontal shear stresses in the soil the horizontal plane could not be a principal plane, similarly vertical planes could not be principal. It was further argued that since the soil tested was truly cohesionless it should not be endowed with a pseudo cohesion. The argument was extended along similar lines to Vidal and led to the more logical conclusion that the reinforcement generated an enhanced confining pressure within the soil sample that must be associated with a stress circle conforming to the failure-envelope for a cohesionless soil. This concept was described by Yang (1972) who attributed the increased strength to an enhanced value of the minor principal stress within the sample, ($\sigma'c + \Delta\sigma'_3$) the magnitude of $\sigma'c$ being equal to the applied confining pressure at the periphery of the sample. This hypothesis is summarised as;

$$\sigma'_1 = K_p\,(\sigma'c + \Delta\sigma'_3) \qquad (4.14)$$

Yang offered experimental confirmation of this theory by testing both reinforced and unreinforced samples of sand compacted to the same relative density. Results from the unreinforced samples were used to define a value of the coefficient of active earth pressure, K_a, which was taken to be a constant of the sand compacted to a given relative density. This value of Ka was associated with the measured value of the vertical failure stress $\sigma'v$ of the reinforced sample. On the assumption that $\sigma'v = \sigma'_1$ a "true" value of σ'_3 was defined consistent with the sample failing according to the Mohr-Coulomb failure criterion. Knowing the corresponding value of the applied confining pressure, $\sigma'c$, the magnitude of $\Delta\sigma'_3$ can be determined;

$$\Delta\sigma'_3 = Ka\ \sigma'_1 - \sigma'c \qquad (4.15)$$

The significance of this can be seen from inspection of Fig. 4.4 which shows the stress circle for a reinforced sample interpreted using the $\Delta\sigma'_3$ concept, shown as a solid line, and the pseudo cohesion theory, shown in broken line.

In 1980 Ingold undertook a number of analytical and radiographic studies in clay, which quantified the magnitude and distribution of $\Delta\sigma'_3$ under drained triaxial loading, these were found to be a function of the coefficient of the soil-reinforcement friction, f, as well as the relative strain at the soil-reinforcement interface. The principal stress directions were found to suffer considerable rotation in diameter planes with the maximum rotation occurring at the free edge of the sample at the soil-reinforcement interface. It was concluded that the magnitude of $\Delta\sigma'_3$, at any radius r, could be determined by;

$$\Delta\sigma'_3 = \sigma'_c \{exp\ [f (R^2 - r^2) / h\ k_a R] - 1\} \qquad (4.16)$$

where R = the radius of the sample and h = the height of the soil element contained between consecutive reinforcing discs;

Studies by McGown et al (1978) have provided useful information on the effects of reinforcement stiffness, strength roughness and orientation. Tests were carried out on sand using a sophisticated plane-strain cell and the simple triaxial apparatus. The plane-strain cell where furnished with lubricated top and side platens with thick glass viewing panels incorporated in one pair of side platens to allow determination of internal sand deformations using stero-photogrammetric techniques. Reinforcement in the form of a single layer of either aluminium foil, aluminium mesh or non-woven fabric was tested in the cell at various inclinations to the internal principal strain direction for the sand alone. It was concluded that the modification of soil behaviour is strain controlled with the reinforcement, or inclusion, inhibiting lateral deformation.

The use of the triaxial test has been extended to determine the behaviour of geotextile reinforced clay subjected to undrained loading by Ingold (1982). Ingold found that even permeable geotextile reinforcement caused a consistent and substantial ***decrease*** in strength compared to that of an unreinforced sample, however, as the reinforcement spacing where decreased the strength of the soil improved and ultimately exceeded that of the unreinforced clay.

The failure stresses were investigated for reinforced and unreinforced (control) sample. Both reinforced and unreinforced sample have a linear envelop and reinforced samples showned a reduction of internal angle of friction at the higher normal stress levels. The effective stress paths for reinforced and unreinforced (control) samples are shown in Fig. 4.5.

This response reflects the fact that rapid loading is not necessarily associated with undrained loading if the reinforcement, which also acts as a drain, is installed at a sufficiently small spacing. Ingold's tests can be classified as sheared undrained tests either by virtue of the rapid rate of shear or by ensuring shear at constant volume. The phenomenon of strength ***reduction*** under rapid loading was observed in clay reinforced with porous plastic, however, this reduction in strength was only observed at large reinforcement spacing where a rapid rate of shearing is consistent with undrained loading.

On investigating the non-woven fabric and felt reinforced samples under truly undrained conditions it was found that they ***enhanced*** the compressive strength. This finding appeared anomalous since a gain in strength is associated with an increase in effective stress, however, the previous tests indicated that under undrained conditions there is likely to be a decrease in strength.

Broms (1977) carried out triaxial tests on uniform sand containing circular discs of woven geotextile. Tests were carried out by varying the relative density of the sand and the spacing of the fabric layers, Fig. 4.6. The experiments indicated an increase in the compressive strength of the sample, with decreased spacing of the fabric. Broms suggested that the restraint offered by the reinforcements, was equivalent to an additional confining pressure. The lateral earth pressure coefficient next to the fabric layer could be estimated from the relationship:

$$Kb = \frac{1}{(1+2\tan^2 \phi' a)} \qquad (4.17)$$

where ϕ'_a is the effective interface friction angle.
In between the two fabric layers, the active pressure coefficient K_a is given by;

$$Ka = \frac{1 - \sin \phi'}{1 + \sin \phi'} \qquad (4.18)$$

Broms then proposed an average value K_{av} to be used for the calculation of the equivalent confining pressure.

$$Kav = \frac{1}{2}(Ka + Kb) \qquad (4.19)$$

The vertical stress along the reinforcement can be then given by the equation;

$$\sigma' v = \sigma' v0 e \frac{2 \tan \phi' a}{DKav}(r0 - r) \qquad (4.20)$$

where σ'_{v0} is the vertical stress at the periphery of the sample ($r = r_0$) and D is the spacing between the fabric layers. The equation suggested that the vertical normal stress increases toward the centre of the sample. It was thus assumed that the tension at the periphery of the sample is equivalent to a uniformly distributed confining pressure.

Chandrasekaran (1988) carried out further tests to determine the strain distribution along the fabric layer. Tests were carried out with 100 mm and 200 mm cylindrical samples of angular medium coarse sand reinforced with horizontally placed non-woven and woven fabric disks. The fabric layers were strain gauged to measure the strain distribution. The spacing of the fabric layers were varied.

Typical stress-strain relationships for 100 mm diameter samples reinforced with different numbers of fabric layers showed increases of up to 300% in the ultimate strength as compared to unreinforced samples, Fig. 4.7. The strain distribution along the fabric layer identified a maximum axial strain with zero shear stress at the centre, Fig. 4.8. The latter property was caused by the relatively small displacement between the soil and fabric. Chandrasekaran (1988) proposed that the maximum mobilised friction resistance was at the centre of the layer, decreasing to zero at the periphery. The mobilised interface friction angle between the soil and reinforcement was found to be smaller than the interface friction angle (ϕ') of the soil determined by simple test (e.g. direct shear). A reduction of ϕ' was thus proposed.

$$\tau a = \sigma' v \frac{r}{r_0} \tan \alpha \phi' a \qquad (4.21)$$

The reduction factor α was found to be low as 0.5 for non-woven geotextiles.

Broms' (1977) vertical stress distribution equation was then modified to take account of the variation of the interface friction angle along the fabric layer.

$$\sigma'_v = \sigma'_{v0} e^{\frac{2 \tan \phi' a (r_0^2 - r^2)}{D K_{av} r_0}} \qquad (4.22)$$

A comparison of results from the equations proposed by Broms (1977) and Chandrasekaran (1988) is shown in Fig. 4.9a &b for 100 mm and 200 mm diameter samples respectively. The equations proposed by Chandrasekaran (1988) shown the importance of relative spacing between the soil and fabrics.

Al-Hassani (1978) carried out plane-strain tests on sand with and without reinforcements. Soil density, reinforcement stiffness, strength, roughness and orientation were varied in the tests. The results displayed a maximum tensile strain direction, while no change as compared to soil alone was seen when the reinforcement was placed in the direction of the maximum compressive strains. A weakening effect was obtained when reinforcement was placed along the compressive strain direction, Fig. 4.10. In these orientations the tensile resistance of the reinforcement was not mobilised. As the frictional resistance between the reinforcement and soil was lower than the internal friction angle of soil alone, weakening of the composite was obtained.

A preliminary triaxial study by Heshmati et al (1990) has provided data concerning the influence of composite drainage/reinforcement non-woven geotextile fabrics on improving the strength characteristics of cohesive soil (kaolin), are shown in Fig. 4.11. The study has been extended to determine the influence of woven and non-woven geotextiles fabrics on improving the strength characteristics of cohesive soil (kaolin), under condition of both undrained and drained loading, Jones and Heshmati (1993), see Fig. 6.6 in Chapter 6. The objective of these tests were to identify the separate roles of the geosynthetic in providing drainage and reinforcement.

From the above research works and the work of many others (Schlosser and Vidal 1969, Long et. al. 1972 and Hausmann 1976) the idea that reinforcements in a soil mass provide a beneficial effect has been characterised. However, the results of these unit cell tests cannot be applied directly to reinforced soil structures, as the behaviour of soil-reinforced structures are much more complicated. To obtain a full understanding of the behaviour of such structures, the use of laboratory and field tests to study different soil-reinforcement systems is necessary.

4.5 SUMMARY

(i) Fine grained cohesive soils are low cost materials which are available for potential use in many locations for use as reinforced fill.

(i) Cohesive soils are more complex than cohesionless fill and soil structures built with cohesive fills are susceptible to change in moisture content. Most cohesive soils are relatively impermeable if they are well compacted, hence water flow through these soils will be negligible.

(ii) The behaviour of cohesive soil is influenced by surface forces rather than by mass forces.

(iii) The shear strength of a cohesive soil is made up of two major components; internal friction and cohesion.

(iv) Drainage geotextiles can be used to improve the drainage of cohesive fills and the use of these materials frequently results in improved strength characteristics.

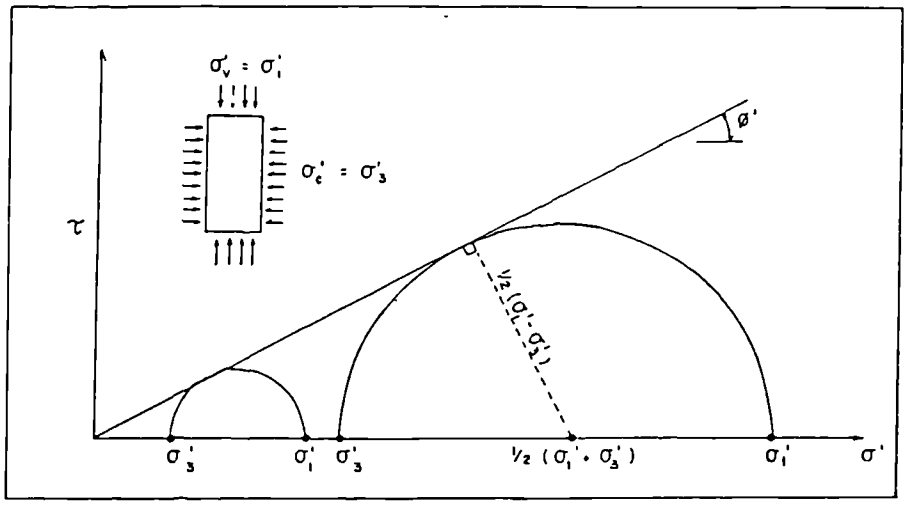

Fig. 4.1: Mohr Diagram- Unreinforced Sand

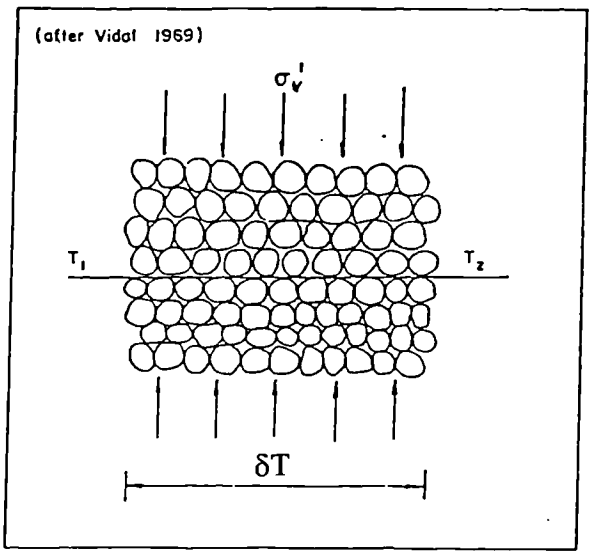

Fig. 4.2: The Effects of Reinforcement

Fig. 4.1	Mohr Diagram- Unreinforced Sand
Fig. 4.2	The Effects of Reinforcement

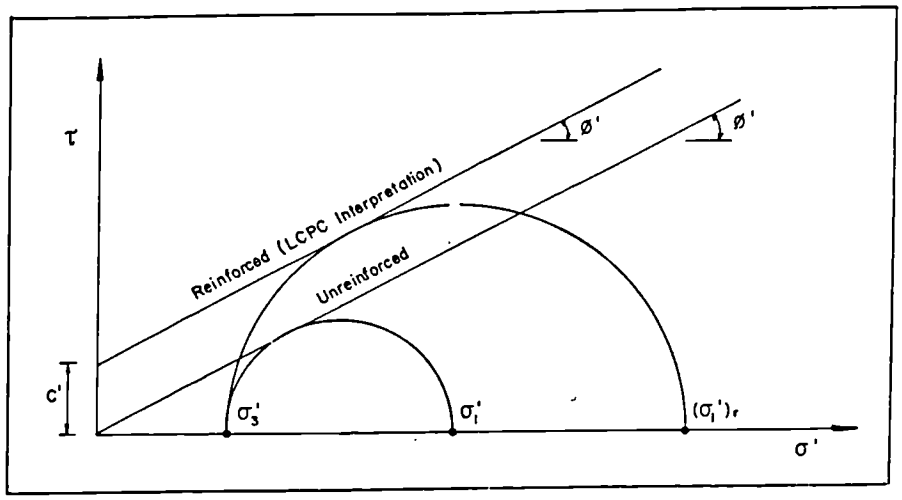

Fig. 4.3: The LCPC Interrelation (after Vidal, 1969)

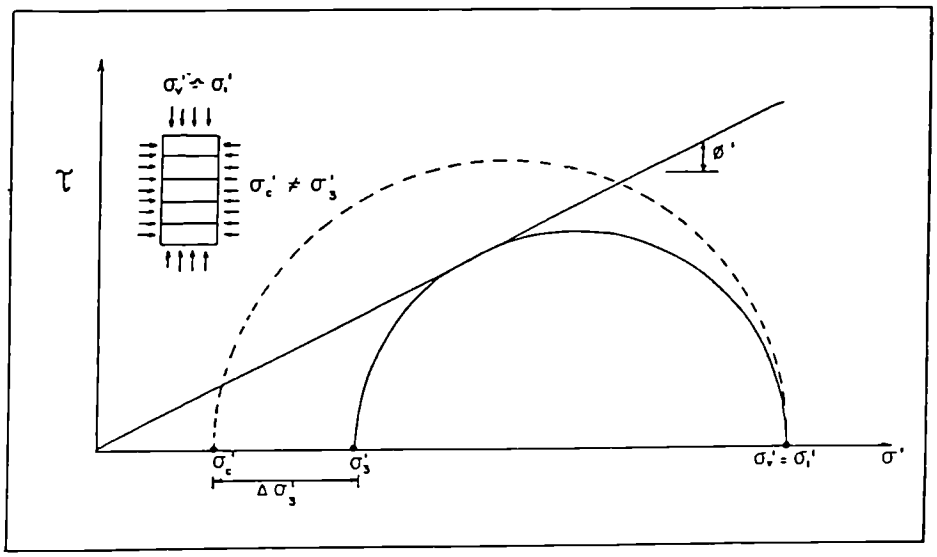

Fig. 4.4: The $\Delta\sigma'_3$ Interpretation

Fig. 4.3	The LCPC Interpretation (after Vidal, 1969)
Fig. 4.4	The $\Delta\sigma'_3$ Interpretation (after Vidal, 1969)

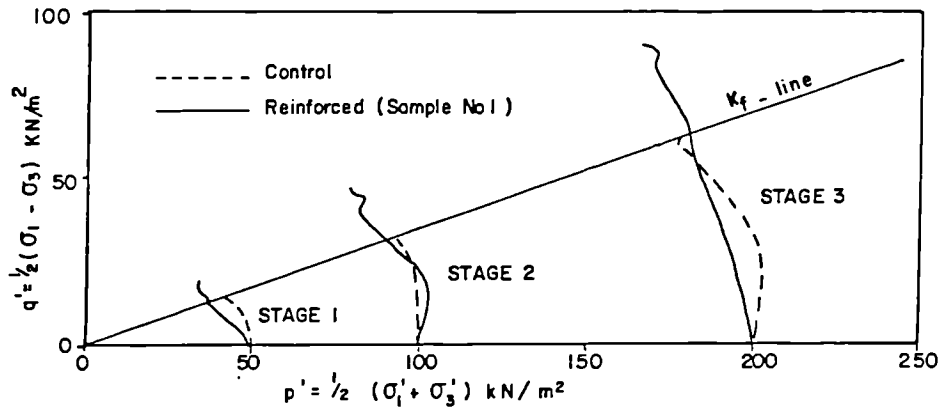

Fig. 4.5	Effective Stress Paths Reinforced and Unreinforced Sample (after Ingold 1980)

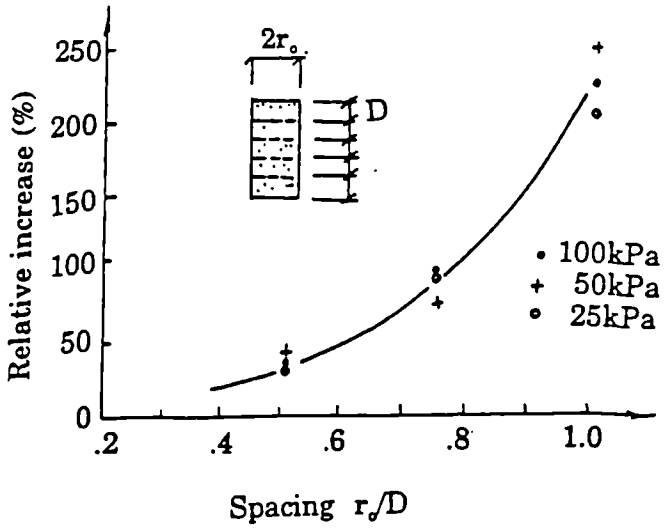

Fig. 4.6: Plot showing the relative increase of peak axial load with decreased fabric spacing and increased confining pressure (after Broms, 1977)

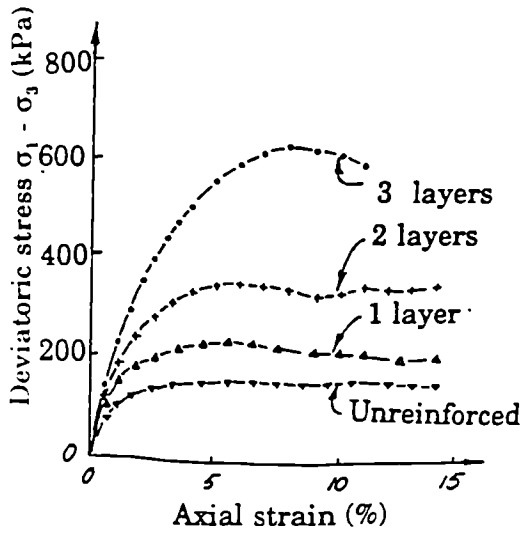

Fig. 4.7: Stress-Strain curve for unreinforced and polyester fabric reinforced soil samples (after Chandrasekaran, 1988)

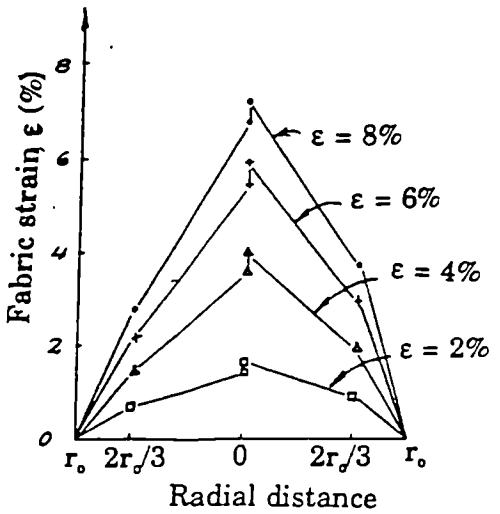

Fig. 4.8: Strain distribution along reinforcement (after Broms, 1977)

Fig. 4.6	Axial load (after Broms, 1977)
Fig. 4.7	Stress-Strain curve (after Chandrasekaran, 1988)
Fig. 4.8	Strain distribution (after Broms, 1977)

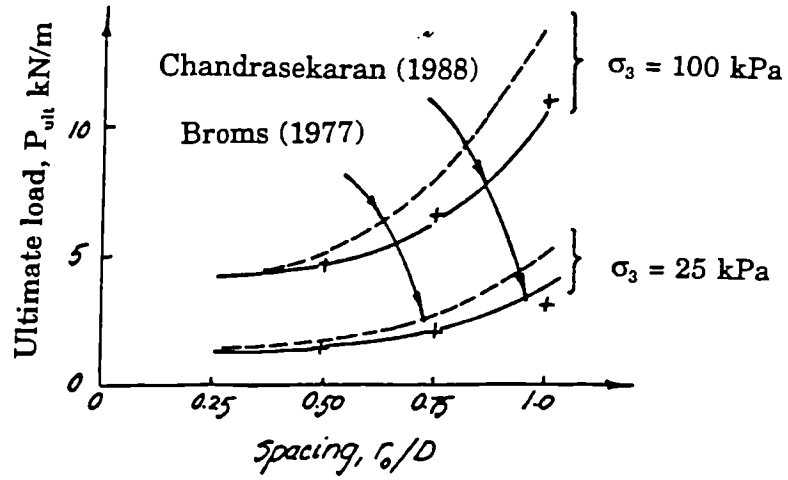

(a)

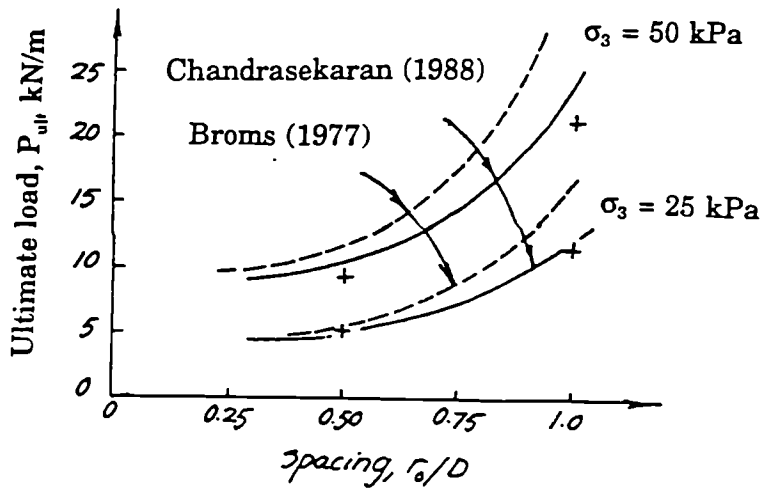

(b)

Fig. 4.9	Comparison of results from modes suggested by Broms (1977) and Chandrasekaran (1988), for (a) 100 mm samples and (b) 200 mm samples

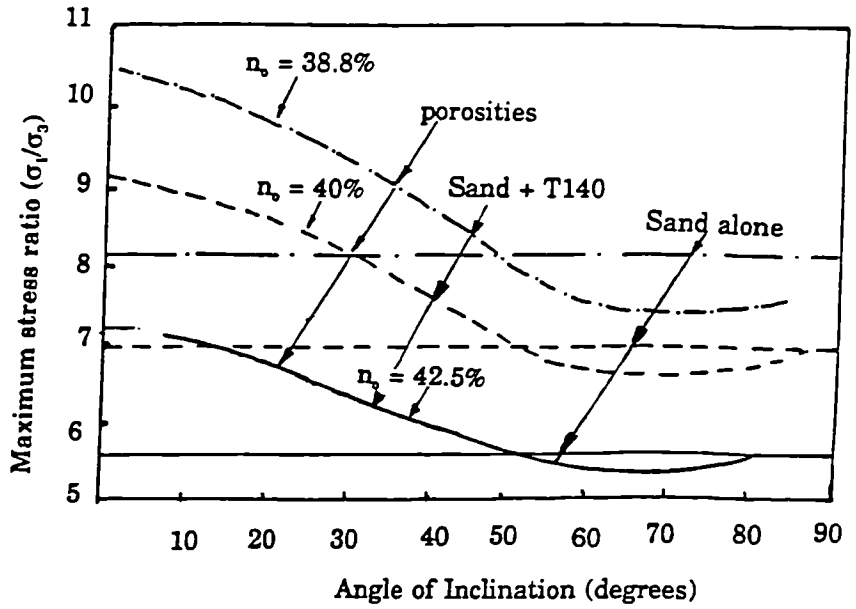

Fig. 4.10	Variation in peak stresses due to inclination of fabric for different porosities (after Al-Hassani, 1978)

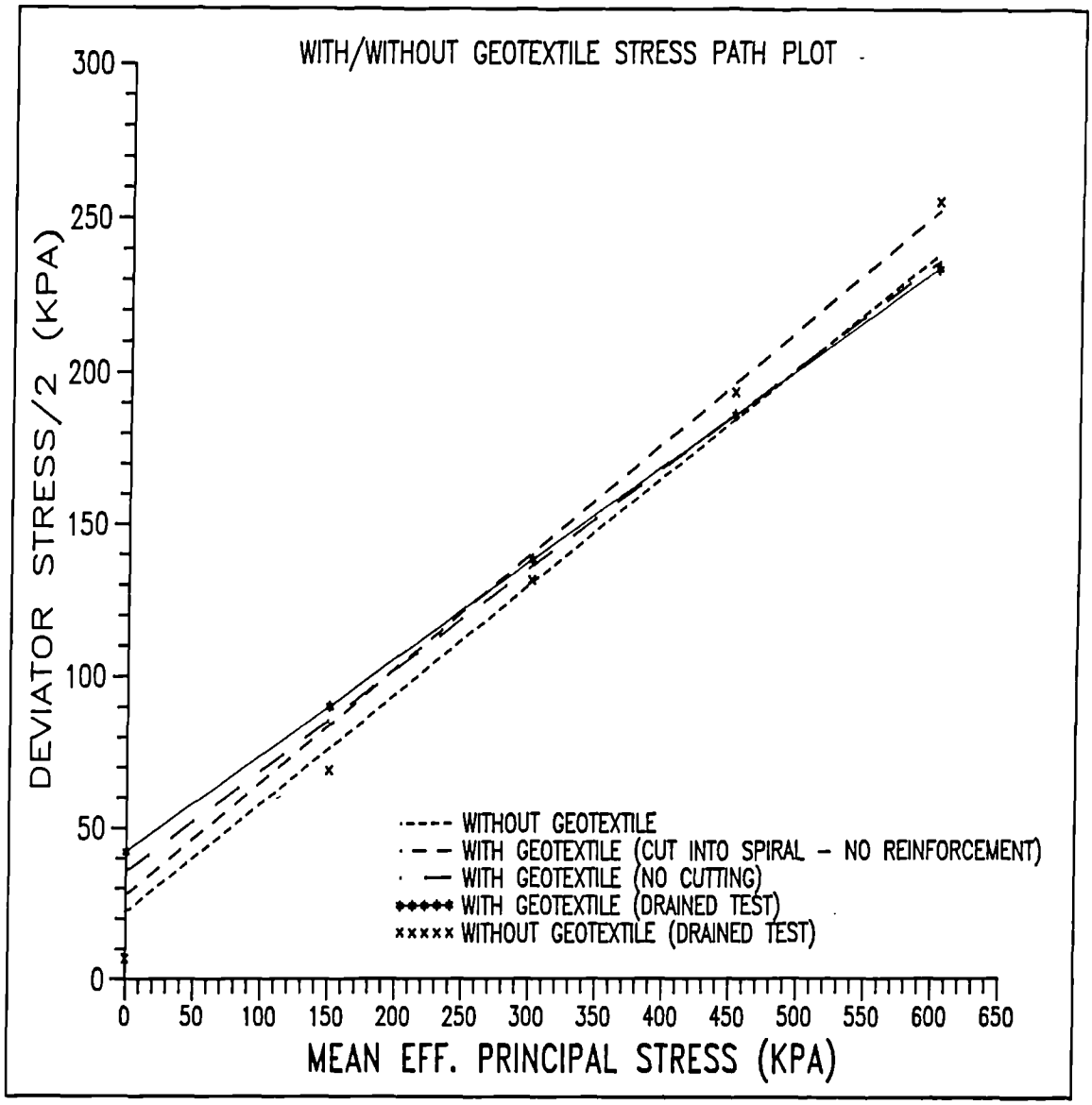

Fig. 4.11	Stress Path Plot for 100 mm samples with/without geotextile (after Heshmati et. al., 1990)

CHAPTER FIVE

IMPROVEMENTS TO CONSTRUCTION BY GEOSYTHETICS

5.1 INTRODUCTION

This chapter describes a brief history of geotextile and the related products. The functions and the characteristics of geotextiles are discussed. The geotextiles suitable for reinforcements and drainage with their factors are identified. The behaviour of a composite soil-geotextile under plane strain compression is also described.

5.2 GEOTEXTILES

Geotextiles and related products have become increasly important in geotechnical projects in recent years, Christopher and Holtz, (1984), Jones (1985), . Geotextiles have transformed geotechnical engineering to the point that their use is no longer considered exceptional.

Geotextiles, are made from polymers, such as polypropylene, polyester, polyethylene, polyamies (nylon) and glass fibres composites. These materials are highly resistant to biological and chemical degradation. Natural fibres such as cotton and jute can also be described as geotextiles, although with these materials their use is usually for temporary application

A convenient classification scheme for geotextiles and related materials is given in Fig. 5.1. Details on the composition, materials, and manufacturing processes for geotextiles and related materials, have been describe by Koerner and Welsh (1980), Rankilor (1981), and Koerner (1986). As Fig. 5.1 indicates, a number of processes can be used to manufacture geotextiles.

In manufacturing geotextiles, elements such as fibres or yarns are combined into planer structures called fabrics. The fibres can be continuous **filaments**, which are very long thin strands of a polymer or **staple fibres** in which the filaments are rather short, typically 20 to 50 mm long. The fibres may also be produced by **slitting** an extruded plastic sheet or film to

from thin flat tapes. In both filaments and slit films, an extrusion or drawing process elongates the polymers in the direction of the draw and increases the strength of the material.

The type of geotextile is determined by the method used to combine the filaments into the planar structure. The great majority of geotextiles are either **woven** or **non woven**. The weaving process and is typically used to make textiles for clothing. Nonwoven textile manufacture is a modern development, in which synthetic polymer filaments are extruded or spun onto a moving belt. The mass of filament or fibres are either **needle punched**, in which the filaments are entanged by a series of small needles, or **heat bonded**, in which the fibres are "welded" together by temperature and pressure at the point of contact in the nonwoven mass.

The manufacture of geotextile-related products is as varied as the products themselves, are shown in Fig. 5.2. Geonets, geomats, and geogrids, can be made from large and rather stiff filaments formed into a mesh and welded or glued at the crossover point, or they may be extruded from plastic sheets with holes punched in them.

A number of composite materials also exist, these may consist of two or more geotextiles combined in the manufacturing process or a combination of a geotextile and geotextile related product, Rankilor (1981). A typical example of a composite geosynthtiecs is 1B1 Filtram which is a form of prefabricated drain. Geocomposite drains are formed by either wrapping or covering a fluted or dimpled polymeric sheet, to act as a conduit for water, with a geotextile to perform as a filter.

5.3 BRIEF HISTORY

One of the first recorded uses of geotextiles occurs in the British Military Manual used in the 19th Century, where canvas sheets were used as reinforcement in revetments Pasley (1822).

In this Century woven cotton fabrics were used as an early from of geotextile/geomenbrane in a series of road construction field tests started in 1926 by the South Caroline Highways Department, Beckham and Mills (1935). The first application of polymer-based geotextiles were woven industrial fabrics used between concrete block revetment in the late 1950s, Bell, et. al. (1984).

Geotextiles were first used by Dutch engineers in 1956, Keown and Oswalt (1984). The early Dutch interest in geotextiles, stems largely from the need to find innovative construction solutions for use on the massive Delta Works Scheme. The use of woven geotextiles in Coastal protection works to became established during the early 1960s, and a related application was the use of geotextiles as a filter in rip-rap blankets for stream protection. This technique was used by the U.S Army Group of Engineering in the repair of rip-rap revetments in the Memphis District in 1962, Keown and Oswalt (1984).

The Dutch were the first to conceive the idea of using two layers of geotextile, pinned together at intervals, as a flexible form work for cast in-situ concrete revetments. A British Patent granted Holland for this concept had a priority date of Oct. 1964, Hillen (1968). This technique was first introduced into the United States in 1968, and the largest early installation was a 17m slope on the shores of the Allegheny Reservoir, Lamberton (1983). From 1986 onwards the American Federal Highway Administration (FHWA) monitored many pavement overly repair schemes where geotextiles were installed with the intention of controlling reflective cracking in the asphalt surfacing. Although this technique was fairly widely used in the United States the results appeared very sensitive to the condition of the road and variations in the installation method.

Geotextile nets started to become established around 1968 when the Japanese found that low strength polyethylene nets exported from Britain offered a means of alleviating the damage caused to embankments by seismic activity and heavy rainfall. Initially these were mainly used to strengthen the face of embankments, Iwasaki and Watanabe (1978).

The development of non-woven geotextiles in the 1960's by the Rhone Poulec Company in France widened the range of geotextiles and their applications. These were comparatively thick needle-punched polyester materials which were developed into the Bidin range of products, which were first used in dam construction at Valcros Dam in France during 1970, Giroud, et. al. (1977). At the same time ICI started to develop the Terram range of non-woven geotextiles which were quite different from the Bidim range, being thinner heat-bonded materials. One of the first applications of these geotextiles was as a separator between the underlying soil and the imported aggregate in the construction of roads, a noteable early application being the M1 motorway at Rotherham in 1967, Jones (1992). Early in the 1970's four other major geotextile applications were developed covering the fin drain, Healy and Long (1971), the use of woven geotextile based reinforcement beneath embankments, Holtz (1975), geotextile reinforced soil walls, Puig and Pasquet (1977), and

the use of geosynthtices reinforcement in the form of glass fiber strips, Jones (1973). Initially the fin drain concept was developed at Connecticut University in 1969 under contract to the Connecticut Department of Transportation. It was required to provide a system of installation that was immune from construction errors. The concept of using woven geotextile sheets as basel reinforcement in embankments was similar to the Japanese use of geotextile nets, except that the separation function was enhanced by using sheets.

5.4 FUNCTION OF GEOTEXTILES

The four primary functions of geotextiles and related materials are: Filtration, Drainage, Separation, and Reinforcement.

Geotextile applications are usually defined by the principal function of the geotextile for the particular application. For example, geotextiles are used as ***filters*** to prevent soils from migration into drainage, aggregates or pipes, while maintaining water flow through the system. They are similarly used below rip-rap and other materials in coastal and stream bank protection systems to prevent soil erosion.

Geotextiles can also be used as ***drainage*** or ***transmission*** media by allowing water to drain from or through soils of lower permeability. Applications include the dissipation of pore water pressures at the base of embankments. For situations with higher flow requirements, prefabricated drains and other geo-composites have been developed. These materials are used as pavement edge drainage, interceptor drains in slopes, and for drains behind abutments and retaining walls.

Geotextiles often find application as ***separators*** to prevent road base material from penetrating into the underlying soft subgrade, thus maintaining the design thickness and integrity of the roadway.

Geotextiles and related materials such as geo-grids and polymric strips can be used as ***reinforcement*** to add tensile strength to a soil matrix, and thereby produce a more competent structural material. Reinforcement enables stable embankments to be constructed over very soft foundations and permits the construction of steep slopes and retaining walls.

Geocomposites, in a soil reinforcement context, generally consist of high strength fibers set within a polymer matrix or encased within a polymer skin. The fibres provide the tensile properties for the material while the matrix or skin provides the geometical shape and

protects the fibers from damage. Geocomposites can also be defined as products which combine two or more of the primary function of geotextiles. This is the definition used in this study in which materials combining the ***reinforcement*** function and ***drainage*** function are considered. These two functions are considered in greater depth below.

5.5 GEOTEXTILES SUITABLE AS REINFORCING MATERIALS

Geotextiles are well suited to reinforce soils. They can be made from highly stable and durable polymers which can be engineered during manufacture to provide the required properties in terms of tensile strength and extension. In addition, they can be formed into specific geometric shapes which optimise the bond characteristics between the geotextile and the adjacent soil. In determining the most appropriate geotextile properties for reinforced soil applications there exists a complex interaction between many inter-related factors; such as, **tensile strength, extension, structure, time, temperature, environment,** and **economics**. This complexity restricts the choice of possible reinforcement types to several well-defined and proven forms and polymer types.

The geotextile properties of relevance to reinforced soil can be divided into two general categories, those properties which are non-time specific and those which are time specific. Non-time specific properties are concerned with the initial tensile strength/extension characteristics of the geotextile reinforcement and its resistance to the effects of site installation. Time specific properties are concerned with the creep characteristics of the geotextile reinforcement and its resistance to the environment in which it is placed.

It should be noted that some geotextile properties also depend on temperature; typically an increase in temperature reduces the ultimate tensile strength of the material and increases the rate of creep. Consideration of temperature should be taken into account in those applications where predicted ambient temperatures are significantly greater that adopted to establish the various engineering characteristics of the geotextile reinforcement

5.5.1 Reinforcement Function of a Geotextile

Geotextiles can be divided into two categories - conventional geotextiles and special geotextiles.

Conventional geotextiles are products of the textile industry and include woven, non woven, knitted and stitch-bonded geotextiles. **Special geotextiles** are of non-textile origin. They include geostrips, geobars, and geocomposite materials.

The tensile stiffness and strength are very important in reinforcement. Deformation characteristics of reinforced soil is determined by stiffness and strength.
The general characteristics of the various geotextile types, and the techniques used to determine their appropriate engineering properties for reinforced soil design. There are four main requirements for geotextile reinforcement materials:

(i) Strength,
(ii) Stiffness,
(iii) Bond,
(iv) Durability.

First, and most importantly, reinforcement must have **sufficient strength** to support the force required to achieve equilibrium in the soil The magnitude of the required reinforcement force varies greatly depending on the application.

Secondly, the geotextile reinforcement must have **sufficient stiffness** so that the required force can be mobilised at a tensile strain which is compatible with the allowable deformation in the soil. Again, the magnitude of allowable tensile strain will depended on the application.

Thirdly, the geotextile reinforcement has to remain in equilibrium with the surrounding soil, and must **bond sufficiently** well to transmit required forces. This is less important for wide width reinforcement materials (geogrids and conventional geotextiles) than for geostrips or geobars. This is because the former have a much larger surface area over which to bond with the soil, than is the case with strip or bar reinforcement.

The influence of time must also be considered together with environmental conditions experienced by the geotextile reinforcement in the soil. The distinction here between the relatively short term application of reinforcing an embankment over soft soil, and slope or wall, is important.

(i) Strength

The magnitude of the force that the reinforcement has to carry depends upon the application. In a steep slope strengthened by a geotextile reinforcement layers, each reinforcement layer might have to support 10 - 40 kN/m, alternatively a single geotextile reinforcement layer in an embankment on soft soil might require 100 - 400 kN/m to ensure stability. In the case of reinforcment spanning a void under an embankment, strengths of 1000kN/m may be required. In the case of retaining structures the height of the wall will determine the quantity of reinforcement resistance required.

Tensile strength / extension

The tensile strength and extension characteristics of geotextiles are a function of the tensile properties of the constituent load carrying elements and the geometrical arrangement of these elements within the geotextile.

The tensile characteristics of the various load carrying elements used in geotextiles are listed in Fig. 5.3a and b. The tensile strength of the very strong polyaramid fibres can be greater than that of prestressing steel tendons, although polyaramid fibres are seldom used for geotextiles because of high cost. Polyester strips and grids, polypropylene tapes, glass fiber reinforced plastic strips and HDPE grids are most used.

(ii) Stiffness

The requirement of the geotextile to be stiff is so that the required forced can be mobilised at a tensile strain which is compatible with the deformation of the soil. The concept of strain compatibility between the reinforced and the soil is implicit in any reinforced soil structure, Jewell (1990). The allowable tensile strain depends on the application and in the case of a reinforced slope on soft soil the allowable extension can vary from 5-10 percent. In the case of a reinforced soil wall the design allowable tensile extension of the reinforcement is unlikely to exceed 2-4 per cent, with a limitation of ≤ 1 per cent strain occurring after construction, Jones (1993). In an embankment on soft soil the design allowance extension might be 5-10 per cent.

Strength-stiffness of the polymer

The tensile strength and extension characteristics of geotextiles are a function of the tensile properties of the constituent materials and the geometrical arrangement of the elements within the geotextile. High density polyethylene grids can be manufactured as a grid which is immediately suitable for use as reinforcement, whilst polyester fibres can be produced as

specific constructions to enable their easy installation into soils. The influence of geometrical structure on the resultant geotextile stress-strain characteristics is shown in Fig. 5.3b, Lawson (1986). For maximum efficiency it is desirable that the geotextile reinforcement be able to reproduce as closely as possible the characteristics of the constituent load carrying elements. Grids formed as woven, stitch bonded, or extruded structures are preferred for reinforced soil applications.

Effect of long-term loads on strength-stiffness

For many polymeric based materials, ambient operating temperatures coincide with their visco-elastic phase, thus creep becomes a significant consideration in assessing their long term load carrying capacity. Creep is the increase in extension of a material under a constantly applied load. The stress-strain time characteristics (at constant temperature) of geotextile reinforcements can be visualised in terms of a three-dimensional body with stress, strain and time comprising the three axes, Fig. 5.4.

(iii) Bond

The mechanical requirement for bond between the reinforcement and the soil is important but often a function of the polymer reinforcement. Geogrids and conventional geotextiles in the form of sheets provide good bond with the soil either due to the large surface offered by the geotextile or by soil/reinforcement interlock in the case of geogrids. In the case of strip or bar reinforcement bond can become a critical consideration particularly in the top of a reinforced soil structure, Hassan (1992).

Bond mechanisms

The rate of change of axial force in reinforcement embedded in soil is limited by bond strength. For reinforcement in an embankment or retaining wall the changes in axial force close to the free end of the reinforcement are important for determining the necessary lengths to enable the required axial forces to be generated.

Bond strength is generated by friction, between the soil and reinforcement, but the relative movements of the soil and reinforcement are different from those occurring in direct sliding. With grid reinforcement, bond is induced by shear along the surfaces of the reinforcing element and by bearing of the transverse or anchor elements of the grid against the soil, no soil to soil friction is developed as there is no relative movement of soil on either side of the grid, Fig. 5.5.

The maximum bond stress for a grid or geotextile may be expressed in terms of a bond coefficient (f_b) multiplied by the soil angle of friction ($tan\ \phi$) and the normal effective stress(σ'n);

$$\tau_b = \sigma' n \times f_b \tan \phi \qquad (5.1)$$

for a geotextile sheet reinforcement of length (L_r) and width (W_r), unloaded at one end, the maximum bond force is given by the expression;

$$(P_r)_{max} = 2 \times L_r \times W_r \times \sigma' n \times f_b \times \tan \phi \qquad (5.2)$$

Parameters and equations to describe the geometry and bond coefficient for grid reinforcements have been suggested by Jewell (1980). The expression for the bond coefficient may be written as;

$$f_b = \alpha_s [\frac{\tan \delta}{\tan \phi}] \pm \frac{1}{2} [\frac{\sigma' b}{\sigma' n}] \times [\frac{B \alpha b}{S}] \times \frac{1}{\tan \phi} \qquad (5.3)$$

where:
δ is the direct shear friction angle between the soil and the reinforcement material surface, and $\sigma' b / \sigma' n$ is the ratio of bearing stress to normal effective stress in the soil.
For a geotextile, the coefficients $\alpha s = 1$ and $\alpha b = 0$, and equation (5.3) may be simplified to give;

$$f_b = \frac{\tan \delta}{\tan \phi} \qquad (5.4)$$

Two important features of the above analysis for wide-width reinforcement are;
(i) the normal effective stress (σ'_n) is calculated from the soil overburden and is not enhanced by dilation of the soil on shearing (in contrast to the case of strip or rod reinforcement, Schlosser and Elias, (1978).

(ii) the value of the bond coefficient is limited by the inequality; $f_b \leq 1.00$, which ensures that the reinforcement cannot be "rougher" than the soil.

The value of the bond coefficient for geotextiles in cohesionless soil was founded to lie between 0.7 to 1.0 by Jewel (1980). The main component of bond for grids is usually the bearing stresses on the transverse members. In any particular soil, the condition for the grid to behave as a fully rough sheet with f_b = 1.0 can easily be assessed. With extensible reinforcement, whether grid or geotextile, mobilisation of bond is progressive and may require considerable displacement to be fully achieved.

Where a frictional bond is to be utilised, it is recommended that the following relationship be used to establish the required bond development length for the geotextile reinforcement.

$$L_b \geq f_f \times P_R / 2 \times \sigma'_v \times W \times f_b \times \tan \phi' \qquad (5.5)$$

where:

L_b = Required bond development length for the geotextile.

The soil/geotextile frictional bond coefficient, f_b should be determined for each individual geotextile using the appropriate soil type. The appropriate value of f_b should be arrived at by the use of 'pull -out' friction tests as it is this mechanism which most closely approximates in situ conditions.

The partial factor of safety, f_f, is chosen based on the consequences of bond failure in the reinforced soil structure. If the structure is in a low risk category, and all the other variables in Equation 5.5 have been determined conservatively, then f_f can equal 1.0. However, if the structure is in a medium-to-high risk category, then f_f should have the value 1.5.

For planar geotextile reinforcement (i.e. conventional geotextiles and geogrids) the required bond length is normally very small (typically a maximum of 1 m). This is because the reinforcement provides a large surface area for bond development. For strip reinforcement, however, a considerable bond length is normally required because the width of the geotextile reinforcement is small compared to the total soil surface area available.

Sliding

Where sliding resistance is required, the length (along the geotextile reinforcement) over which this can potentially occur must ensure that the sliding resistance is greater than the outward thrust of the slope contained within the potential failure plane. That is:

$$L_S \geq f_S \times P_a / \sigma'_v \times W \times f_b \times \tan\phi' \qquad (5.6)$$

Where Ls = Required sliding resistance length for geotextile, W = the width of the geotextile reinforcement, f_b = the soil/geotextile interaction coefficient, and f_S = a partial factor of safety sliding resistance.

The soil/geotextile frictional interaction coefficient, f_b, should be determined for individual geotextile constructions using the appropriate soil type. The appropriate value of f_b should be arrived at by use of 'direct shear' friction tests as it is this mechanism which most closely approximates insitu conditions.

The partial factor of safety, f_S, is chosen based on the consequences of sliding failure in the reinforcement soil structure. Conventionally, a value of f_S = 1.5 has been adopted.
When conventional geotextiles are used as reinforcement the sliding resistance should be checked. For strip geocomposite geotextile, sliding resistance is never a limiting factor, and hence does not have to be checked during be design. For geogrids, sliding resistance should be checked, however, it is unlikely that this will be a limiting criterion for design.

(iv) Durability
Durability of the geosynthetics is influenced by time and has to be considered together with the environment conditions. With permanent structures durability is the dominant consideration of the designers.

5.6 GEOTEXTILES USED FOR DRAINAGE

In reinforced soil structures drainage is an important consideration. If the structure is allowed to become waterlogged the tensile forces in the reinforcing elements increase and the properties of the fill and retained fill may change. For example, the force on the facing may increase and any pore water pressures may reduce the overburden pressure on the reinforcements thus reducing pull-out capacity.

Geotextiles can serve two important hydraulic functions related to cross-plane flow (filtration) and in-plane flow (in-plane drainage). Some thick geotextiles which have sufficient interconnecting pore structures to allow fluid flow within the plane are becoming increasing popular in in-plane drainage applications. However, relatively less study has been done on the in-plane hydraulic conductivity of geotextiles when compared to that of the

cross-plane function, Koerner et al (1984). Koerner has identified a number of common application in which the in-plane flow capacity of a geotextile is an important design consideration including, permeability, compressibility, and flow through the material.

5.6.1 Permeability and Compressibility of Geotextiles

When considering the permeability of geotextiles a differentiation must be drawn between the permeability in the plane and in the perpendicular direction. Permeability in the plane of the geotextile is influenced by the degree of compressibility experienced by the material under normal stress.

Heerten, (1981) employed a compression-permeability-apparatus with a constant head and tested permeability of a packing of sheets. Since the flow is laminar and the thickness of the layer is exactly defined, the permeability-coefficient is dependent on the normal stress, and corresponds to the K-value of Darcy's law:

$$\partial Q / \partial t = K.A.\partial h/\partial l \qquad (5.7)$$

where, $\partial Q / \partial t$ = the rate of water movement through the soil (in volume terms), A = bulk cross-sectional area emitting flow, $\partial h/\partial l$ = the hydraulic gradient, K = the coefficient of permeability or hydraulic conductivity of the soil.

The coefficient of permeability is a measure of the ability of the soil (or more specifically the voids in the soil) to allow water to pass through its mass. It is a property intrinsic to the soil itself and is influenced by the soil characteristics such as soil gradation, soil structure and soil density.

In Equation 5.7 the hydraulic gradient is the driving force producing seepage flows. It is a measure of the difference in hydraulic head between two points divided by the distance the water has to travel between those two points.
In most cases it is common practice to present Darcy's law in a more simplified form:

$$q = K.A.i \qquad (5.8)$$

where q = the volume flow rate and i = the hydraulic gradient. The units of q are volume per unit time (e.g.m/sec), i = dimensionless. while K = distance per unit time (m/sec).

5.6.2 Flow normal to the plane

Flow normal to the plane may be determine using the method described in BS 6906: Part 3. The flow rate per unit area (F) normal to the plane of a geotextile under a standard head (h_g) of 0.1 m. If flow is assumed to be laminar, the permeability (K_g) of the geotextile may be obtained from the relation;

$$K_g = (F/h_g) \times t_g \qquad (5.9)$$

(where t_g is the thickness of the geotextile).

Flow. The flow through the geotextile and adjacent soil can be compared using the inequality, CFGG (1989);

$$(K_g / t_g) \times h_g > n' . K_s . i_s \qquad (5.11)$$

(where i_s is the hydraulic gradient in the adjacent soil). The factor n' is the product of several factors (type of structure, compression under load, hydraulic gradient in soil, head loss in geotextile).

5.6.3 Flow in the plane

Flow in the plane of the geotextile can be determined using BS Test 6906: Part 7. The relationship between the hydraulic gradient (h) and flow per unit width in the plane of the geotextile (q_{pg}). Can be obtained from Eq. 5.11, provided the flow is laminar.

$$K_{pg} = q_{pg} / i \qquad (5.12)$$

The BS Test recognises that flow is not laminar and that transmissivity should be quoted for a hydraulic gradient appropriate to the application. The test is a short-term one, under immediately applied load. Two factors must be taken into account in estimating the design flow in plane.

(i) First, the drain will be in contact with the soil and this may deform the geotextile stretched over the plastic core and reduce the cross-sectional area available for flow.
(ii) Second, the drain will be subject to compression creep under normal or shear loading due to transient compaction stresses during installation and to subsequent long-term overburden stresses. It is therefore necessary to determine the long term thickness under compressive creep, and then simulate this condition in the short-term transmissivity test, Murray and McGown (1992).

5.7 GEOTEXTILE DESIGN IN RESPECT OF DRAINAGE

The design of geotextiles for drainage is essentially the same as designing graded granular filters. A geotextile is similar to a soil in that it has voids (pores) and particles (filaments and fibres). However, with geotextiles, the geometrical relationships between filaments and voids is more complex than in soil because of the shapes and compressibility of the filaments. In geotextiles, it is general to try to measure the pore size directly or to estimate the pore size. Once the pore size has been measured, relatively simple relationships between the pore size and the particle sizes of the soil to be retained can be developed. Looking at particle retention, three drainge concepts are:-

(i) If the size of the largest pore size in the geotextile is smaller than the largest particles of soil the soil will form a filter bridge over the hole, which in turn, filters smaller particles of soil, in turn, retaining the soil and preventing piping.

(ii) If the smaller openings in the geotextile are sufficiently large such that the smaller particles of soil are able to pass through the filter, then the geotextile will not "clog" or "blind".

(iii) A large number of openings should be present in the geotextile that proper flow can be maintained even if some of the openings later become plugged.

These concepts and analogies with soil filter design criteria can be used to establish design criteria for geotextiles, Christopher and Holtz (1988). Specifically;
(i) the geotextile must retain the soil (retention criterion) while
(ii) allowing water to pass (permeability criterion) during
(iii) the life of the structure (clogging resistance criterion)
(iv) to perform effectively, the geotextile must also survive the installation process (survivability criterion).

5.7.1 Retention Criteria

Current design rules are have been reviewed by Giroud (1988), Fischer et al (1990), Heerten (1986). To meet the retention criterion, most specifications require a certain minimum ratio between a selected geotextile pore size and a selected base soil particle size. Often this ratio will be varied according to the structure of the geotextile filter and commonly there is differentiation between woven and nonwoven geotextiles.

$O90/D90 < 1.0$ for woven
$O90/D90 < 1.8$ for nonwoven

The relationship between a geotextile filter and the type of soil and their coefficient, reported by Holtz (1988) are shown as;
AOS or O_{95}(geotextile) $\leq B\,D_{85}$(soil)

Where ;
AOS = apparent opening size, mm,
O_{95} = opening size in the geotextile for which 95% which are smaller, mm,
B = a coefficient,
D_{85} = particle size for which 85% are smaller, mm.

The coefficient B ranges from 1 to 2 and is a function of the type of soil to be filtered, its density, the uniformity coefficient, Cu, if the soil is granular, the type of geotextile (woven or nonwoven) and the flow conditions.

For sands, silty sands, and clayey sands (less than 50% passing the No. 200 U.S. Sieve), B is a function of the uniformity coefficient, Cu, therefore;

$$Cu \leq 2 \text{ or } \geq 8: \quad B = 1$$
$$2 \leq Cu \leq 4: \quad B = 0.5\,Cu$$
$$4 \leq Cu \leq 8: \quad B = 8/Cu$$

Where; $Cu = D_{60} / D_{10}$

Sandy soils, which are not uniform tend to bridge across the openings and thus the larger pores may actually be up to twice as large (B=2) as the larger soil particles because, two particles cannot pass through the same hole at the same time. Therefore, using B= 1 would be a conservative design for retention.

For silts and clays (more than 50% passing the No. 200 U.S. Sieve), B is a function of the type of geotextile:-

For **woven**, $B = 1 \quad : O_{95} \leq D_{85}$
For **non woven**, $B = 1.8 \; : O_{95} \leq 1.8\, D_{85}$, and
For **both**, the AOS or $O_{95} \leq 0.3$ mm (No. 50 U.S. Sieve)

Due to their random pore characteristics and, in some materials, their felt-type nature, non-woven materials will generally retain finer particles than a woven geotextile of the same AOS. Therefore, the use of B= 1 is conservative for both woven and non woven materials.
If the geotextile is not properly weighted down, soil particles can move behind the geotextile and it is better to reduced B to 0.5, or $O_{95} \leq 0.5\, D_{85}$.

5.7.2 Permeability Criteria

For non-critical applications and less severe conditions repoted by Holtz (1988):
$K_g \geq K_s$
For critical application and severe conditions:
$K_g \geq 10\, K_s$

For actual flow capacity, the permeability criteria for non critical applications is conservative, since an equal quantity of flow through a relatively thin geotextile would take much less time than through a much thicker granular filter. Even so, some pores in the fabric may become blocked or plugged with time; therefore, for critical or severe applications, the more conservative relationship is recommended to provide an extra factor of safety.

$$K_{eff} = (t_g + t_s) / (t_g/K_g) + (t_s/K_s) \qquad (5.13)$$

Where;
$Keff$ = effective permeability
The variables t and K in this equation (5.13) refer to the thickness permeability respectively, of the geotextile (g) and soil (s).

5.7.3 Clogging Resistance

In situations where clogging is a possibility (e.g. gap graded or silty soils), the following optional qualifiers may be applied:

(a) For non woven geotextile material; porosity of the geotextile (n) ≥ 30%.
(b) For monofilament and slit film woven material; percent open area (POA) ≥ 4% .

For critical/severe conditions, filtration tests, which are performance tests, should be conducted. One type of filtration test is the gradient ratio test, which is applicable for sandy and silty soils with coefficients of permeability greater than 10^{-2} cm/sec.

For less critical/less severe conditions, a simple solution to avoid clogging would be to allow fine particles already in suspension to pass through the fabric and let the "bridge network" formed by the larger retained particles provided retention for the smaller particles. As the bridge network should develop rather quickly, the quantity of particles that would actually pass through the geotextile would be relatively small. The less critical/less severe clogging resistance criteria is thus required to have an AOS (O_{95})sufficiently larger than the finer soil particles (D_{15}) such that those particles will pass through the fabric. Unfortunately, the AOS value only indicates the size and not the number of O_{95} holes available. Thus, the finer soil particles can still be retained by the smaller holes in the fabric, and if they are sufficient in number, it could lead to a significant reduction in flow rate. Consequently, it may be desirable to use other qualifiers to control the number of holes in the fabric such as the porosity and open area requirements. There should always be a sufficient number of holes in the geotextile so that many of them will remain open even if some of them clog.

5.8 REINFORCEMENT GEOTEXTILE USED IN THIS STUDY

As already discussed *specific geotextiles can provided highly effective* reinforcement. The reinforcements geotextiles used in this study were selected to have sufficient strength bond capacity and stiffness so that the required force could be mobilised at an acceptable tensile strain. The materials used are discussed below. The nature and form of the reinforcement geotextiles used in the study are shown in Chapter 3, Fig. 3.1a and 3.1b. The index properties of the reinforcement geotextiles are shown in Table 5.1.

5.8.1 Material Properties

G2 and G3 are geogrid materials manufactured from high molecular weight/high tenacity polyester yarn. The yarns are knitted into a dimensionally stable, uniform network of apertures providing significant tensile reinforcement capacity in two principal directions. The polyester geogrid is engineered to be both mechanically and chemically durable, in both the harsh construction installation phase and long term aggressive soil environments. A black

PVC coating provides further chemical and mechanical, as well as ultraviolet protection. The material is usually acquired in rolls of two metre width and 100m length.

G4, is Tensar SS1 manufactured from co-polymer grade high density polyethylene. The manufacturing process of Tensar SS1 involves punching holes in a consistent manner and then heating and stretching the material in special machines. The direction in which the material is stretched is termed the 'machine direction'. The material is usually acquired in rolls of four metre width and 50m length.

G5, is a non-woven fabric produced by bonding the crossover points of a continuos polymer filament. Bonding is achived by application of controled heat and pressure called "melding".

G7, was formed from Filtram 1B1 manufactured from polymer. In the study the filter material on each side of the core was removed leaving a low strength grid.

5.9 DRAINAGE GEOTEXTILES USED IN THIS STUDY

There are many types of drainage geotextiles available, and it is possible to group these be various means. The most generally accepted method of classification, however, is by manufacturing process, which results in four different geotextile groups, non woven, woven, knitted, and stitch-bonded.

5.9.1 Material Properties

The properties of the selected materials include the following:

(i) mechanical, covering the strength characteristics of the drainage geotextile and its reaction to different loads,
(ii) endurance properties, covering the potential deterioration of the fabric and especially the fabric mechanical properties over time,
(iii) hydraulic properties, which covers the ability of the fabric to conduct a fluid and its ability to act as a filter.

The index properties of the selected materials can be identified from selected materials in BS 6906. The nature and form of the drainage geotextiles used in this study are identified as materials G1, G1CT, G6 and G1G2 shown in Chapter 3, Fig. 3.1a and 3.1b.. The index properties of drainage functions of geotextiles are shown in Table 5.2.

Material G1 is a non woven, needle-punched geotextile manufactured from polypropylene fibres. The fabric is resistant to the chemicals naturally found in soils and water. Material G6 is Filtram 1B1, formed from a mesh core acting as a spacer with filter on both sides. These materilas develop good interaction with the cohesive soil. (the fine particles are able to permeated in to the open surface of the drainage materials).

G1 and G6 provide better compaction of the cohesive soil and more efficient drainage from the interior of the fill. They provide effective tensile reinforcement while the drainage function maintains a high degree of suction forces within the cohesive fill.

During the tests G1 was cut into wedges so as to provide only drainage, this material is identified as G1CT. The combination of G1 and G2 produces a composite geotextile which could provide better compaction for the cohesive soil and more efficient drainage from the interior of the fill.

5.10 SUMMARY

(i) Little is known about the drainage function of geotextiles, but drainage can be complementary to the reinforcement function, by "improving" the propreties of soil fill.

(ii) Geotextiles can provide two important hydraulic functions related to cross-plane flow and in-plane drainage when embedded in soil.

(iii) Thick geotextiles, which have sufficient interconnecting pore structures to allow fluid flow within its plane, can be used to provide inplane drainage.

(iv) Geogrids alone can provide sufficient strength, bond capacity and stiffness so that the required force in a reinforced soil structures can be mobilised at an acceptable tensile strain.

(v) The geosynthetics materials chosen for the study are representative of available materials and conform to the requirements identified for both geotextiles offering drainage functions and materials acting as reinforcement.

Table 5.1: Index Properties of Reinforcement Function of Geotextiles

Material and Description	G2	G3	G4	G5	G7
Geogrid Type	✓	✓	✓	-	✓
Reinforcement Function	✓	✓	✓	✓	✓
Weight (g/m^2)	200	200	200	100	800
Material Thickness (mm) With a Load of 200 kPa	2 1.5	2 1.0	3 0.8	0.3 0.3	6 5
Tensile Strength Longitudinal (kN/m) Transverse (kN/m)	 7.6 6.7	 5 4.8	 20.5 12.5	 3 2	 12.5 11.7
Aperture Size (mm)	10×10	25×25	28×38	0.3	0.7×0.7

Table 5.2 : Index Properties of Drainage Function of Geotextiles

Material and Description	G1	G6
Drainage Function	✓	✓
Drainage and Reinforcement	✓	✓
Weight (g/m^2)	500	940
Material Thickness (mm) Without any Load With a Load of 200 kPa	 5.5 2.5	 7 4
Tensile Strength Longitudinal (kn/m) Transverse (kn/m)	 8 10	 –
Effective of Opening Size (mm)	0.15	0.1
Permeability (k) × 10^{-2} (m/s)	10×10^{-2}	7.2×10^{-2}
Non woven Needle Punched Polypropylene Fibres	✓	–
Non woven Heat - Bonded Polypropylene Fibres	–	✓

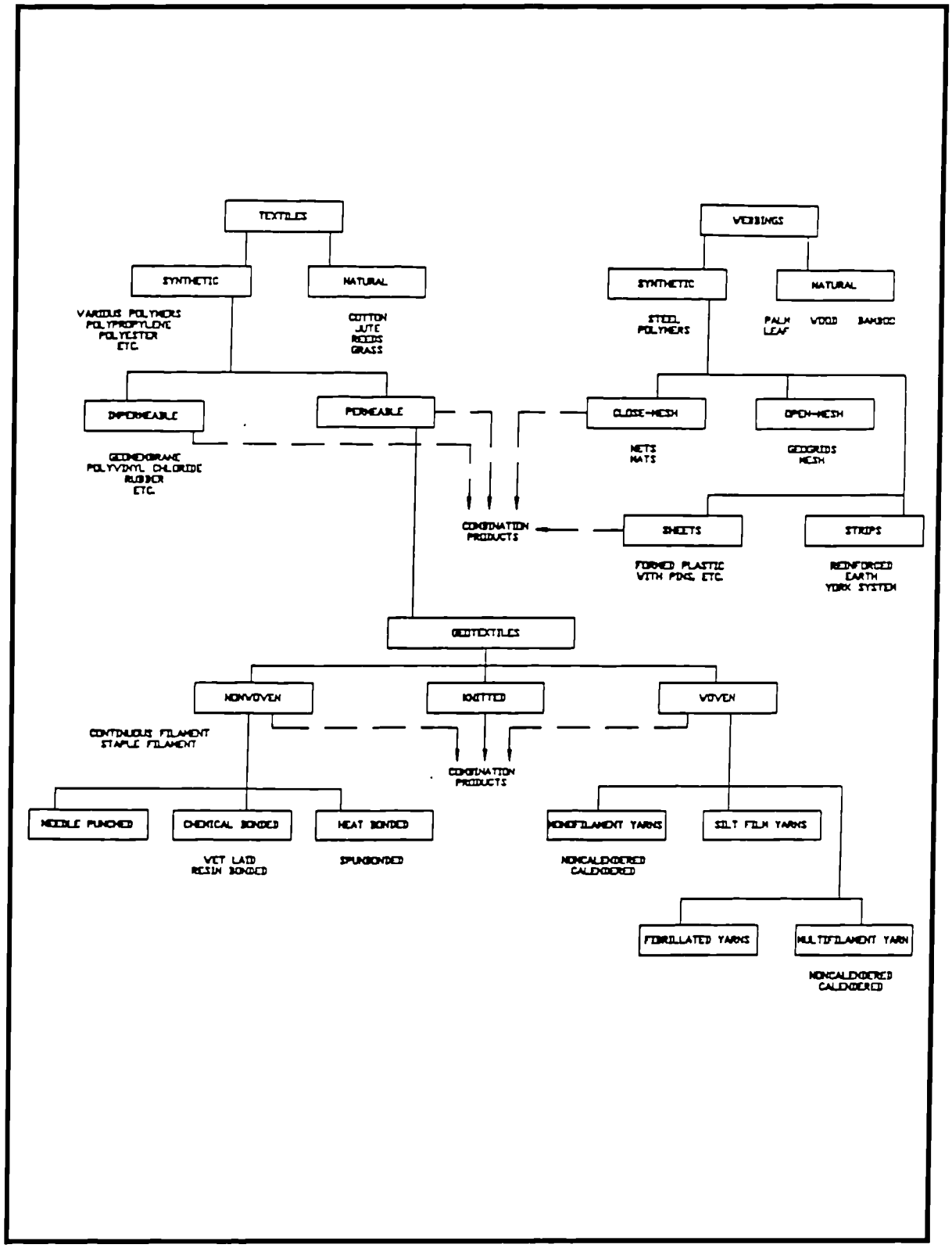

Fig. 5.1	Classification of Geotextiles (after Rankilor, 1981)

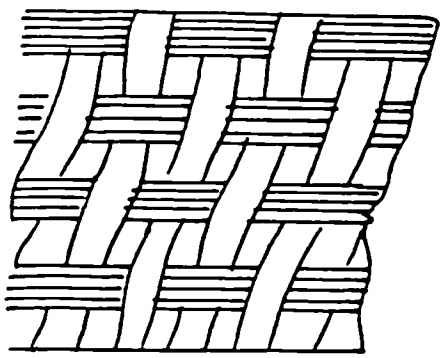

Woven

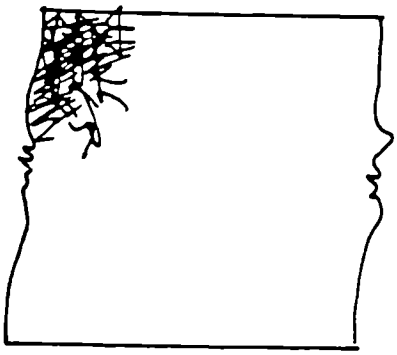

Non-Woven

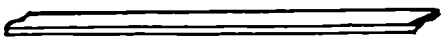

Straps

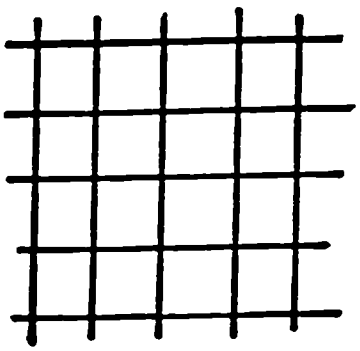

Nets

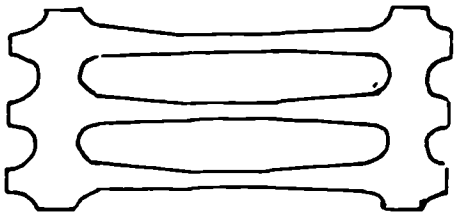

Grid

Fig. 5.2	Forms of Geotextiles and Related Products

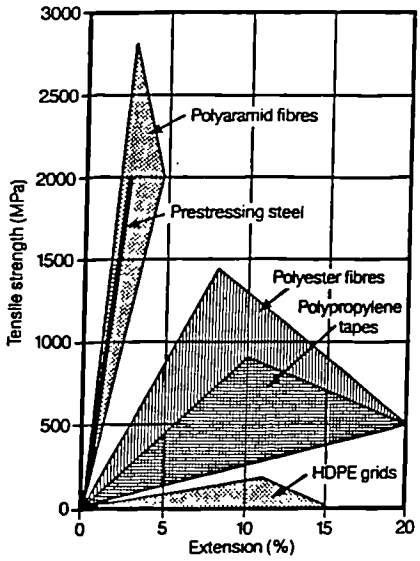

a) Tensile strength/extension characteristics of various geotextile load carrying elements and that of prestressing steel

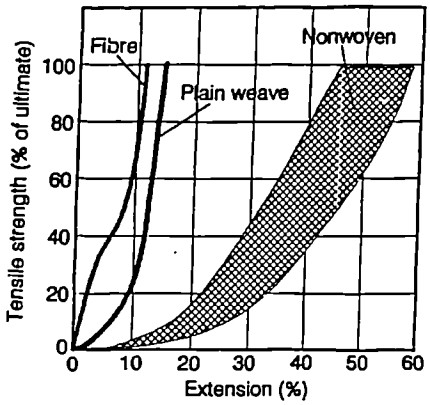

b) Effect of geotextile construction on resulting extension characteristics using polyester fibres

Fig 5.3	Load/Extension characteristics of Geotextiles and influence of Construction (after Lawson, 1986)

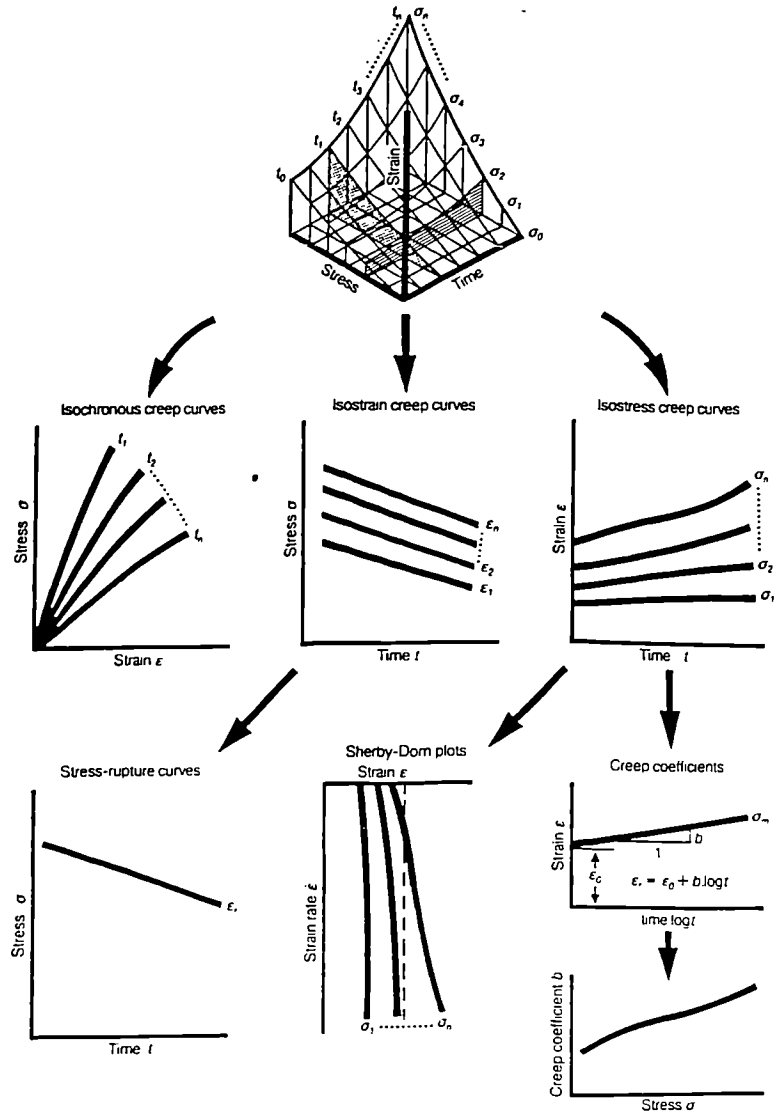

Fig. 5.4	Various ways of representing creep data (at constant temperature), (after Lawson, 1986)

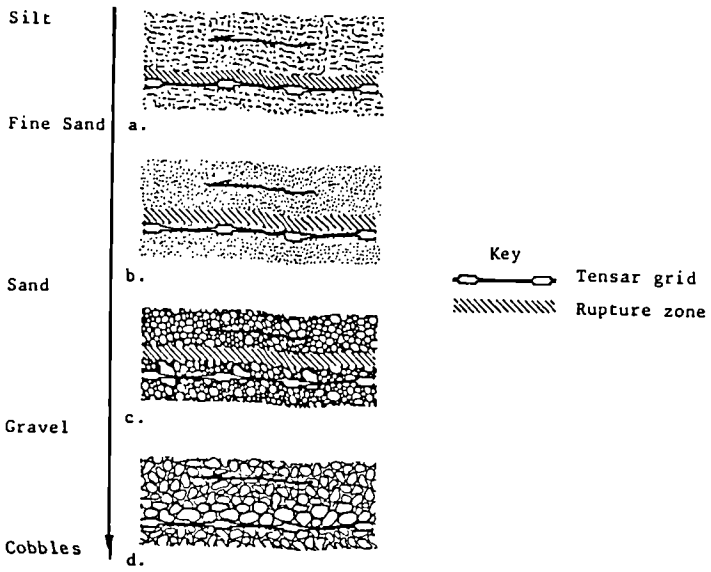

a) Qualitative effect of increasing soil particle size on direct sliding. View in cross-section across direction of sliding

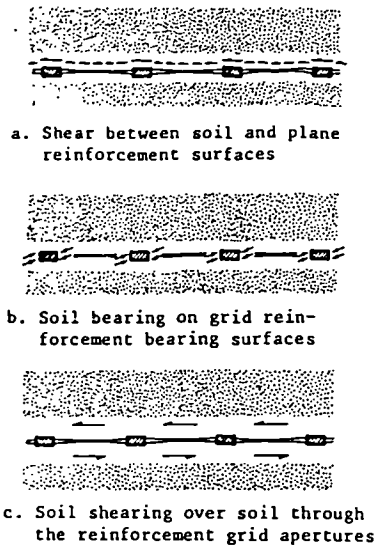

b) Three mechanisms resisting direct sliding

Fig. 5.5	Mechanisms Resisting Direct Sliding (after Jewel et. al. 1984)

CHAPTER SIX

TRIAXIAL TESTS, SAMPLE PREPARATION AND PROCEDURE

6. 1 INTRODUCTION

This chapter considers the details of the experimental aims and procedures used to undertake the consolidated drained and the consolidated undrained triaxial compression. Sample preparation, the experimental set-up and apparatus used are described and the calibration of the transducers are explained. The results of the tests are given.

6.2 REVIEW OF REINFORCED SOIL AND UNIT CELL STUDIES

Vidal (1969), Schlosser et. al. (1969), Yang (1972), Broms (1977), Long, et al. (1972), Ingold (1980, 1981), McGown, et. al. (1987), Al-Hassani (1978), Chandrasekaran (1988), Ling et. al. (1992), Heshmati el. at. (1990), and Jones and Heshmati (1993b), have used the unit Cell concept to examine the behaviour of reinforced soil. These have been reviewed in Chapter 4.

6.3 TRIAXIAL TESTS

The triaxial test apparatus was used for the measurement of shear strength of the reinforced kaolin for the following reasons:

(i) the principal stresses can be varied to simulate field conditions,
(ii) the failure plane is not predetermined as in the shear box,
(iii) the pore pressures can be measured, therefore an effective stress analysis can be undertaken.

Both the Consolidated Undrained Triaxial compression test (CU-test) and the Consolidated Drained Triaxial compression test (CD - test) have been used. An increasing axial load was

applied to the sample while maintaining a constant surrounding (cell) pressure. In the undrained test, the pore pressures were measured to enable the effective stress analysis to be carried out.

The benefits in using the undrained triaxial test are;
(i) pore pressures can be measured and an effective, as well as a total stress analysis can be carried out,
(ii) the experiment can be carried out faster than the drained test,
(iii) the experiment can be performed to simulate site conditions, where construction may be faster than the rate of pore pressure dissipation.

The drained triaxial test offers the following advantages;
(i) it provides accuracy when using a very slow rate of strain to failure,
(ii) no excess pore pressures are developed during the shearing stage, therefore a direct measurement of the effective stress parameters can be obtained,
(iii) it can be used to simulated field conditions following construction when drainage has taken place.

6.4 APPARATUS

The apparatus used for the project is detailed in Table 6.1. The layout of the apparatus used in the experiment is shown in Fig. 6.1. Explanatory notes on the use of this equipment for automatic control in the laboratory have been proposed by Head (1986).

6.5 CALIBRATING THE TRANSDUCERS

In order to achieve accuracy of the results, all transducers used in the project were calibrated. A correlation of 0.999 was considered satisfactory for the work.

6.6 SAMPLE PREPARATION

Samples were prepared in the laboratory by compacting 3.5 Kg of kaolin which had been mechanically mixed after adding approximately 29.5% of water by weight in accordance with BS1377 (1990). The optimum moisture content of the kaolin is shown in Fig. 6.2.
The dry density for each sample was calculated from the phase relationships:

$$\rho = M_t / Vt \qquad (6.1)$$

$$\rho_d = \rho / 1 + w \qquad (6.2)$$

where;
M_t = total wt. of soil
V_t = volume of soil (total)
ρ = bulk density
W = moisture content
ρ_d = dry density

The plain samples of kaolin were compacted in six layers using 27 blows per layer. For the samples including the geotextiles, the procedure was the same, with the geotextile material being introduced in the middle of the sample (after the first 3 layers). Drainage from the geotextile positioned in the centre of the sample was provided through a slot in the membrane. The slot was at approximately centre height except for the cases when geotextiles were included in these cases the slot considered with the exact position of the geotextile, is shown in plate 6.1. The triaxial sample assembly in the cell is illustrated in Fig 6.3.

6.7 TEST PROCEDURE

Both the Consolidated Undrained Triaxial tests and Consolidated Drained Triaxial tests were undertaken in five stages, Head (1986);

(i) Initial B-values,
(ii) Saturation,
(iii) B - Test,
(iv) Consolidation,
(v) Shearing (compression).

6.7.1 Initial B-values

The Initial B-Test was carried out by applying cell pressure in at least two increments to a desired pressure level. During the test, the increase of pore water pressure was monitored until it was constant and the next increment of cell pressure then applied. The test was considered finished when no increase of pore water pressure was needed following the last increment of cell pressure. A B-value can be calculated by dividing the change of pore pressure by the increment of cell pressure.

Using the Initial B-value, a quick check can be made to determine any leakage of the membrane. Leakages were identified by a rise in the B-value.

6.7.2 Saturation

Saturation is effected by raising the pore pressure to a level high enough for the water to be absorbed into solution. At the same time the confining pressure was raised in order to maintain a small positive effective stress in the sample.

Saturation was carried out by application of a back pressure to the system of 100 kN/m^2, this was 10 kN/m^2 less than the confining pressure to ensure that the effective stresses remained positive. The advantages of using the back pressure system are summarised below:

(i) When full saturation is reached, air in the void spaces within the sample is forced into solution. As a result there was no separate air phase in the voids which could have give erroneous pore pressure measurements.
(ii) Any trapped air remaining,
(iii) Any air bubbles remaining in the pore pressure and back pressure systems are eliminated,
(iv) Reliable measurements of permeability can be made on soils that are initially partly saturated if saturation is first achieved by applying a back pressure, Head (1986).

The sample was considered saturated when the pore pressure approached the back pressure value and if no further volume change occurred. The sample was considered to be saturated when B-values of more than 0.95 were obtained.

6.7.3 B-Test

The tests were carried out after the specimen had been saturated. A back pressure was applied on the sample (s) while monitoring any volume change and the pore pressure (s). Whenever the pore pressures approached the back pressure value, B-value 0.97, and the volume change showed no further flow of water (or negligible change) then test completed.

6.7.4 Consolidation

The samples were consolidated isotropically under a confining pressure by allowing water to drain out into the back pressure system, as a result the pore pressure dissipated gradually. The samples were considered to be completely consolidated, when the pore pressure equalled the back pressure.

All the samples tested had been consolidated in the CU-Tests and CD-Tests to nearly 100 %. Comparison of the samples with and without geotextiles where made using the time taken for each sample to reach 100 % consolidation. It was assumed that if a geotextile could improve the drainage properties of a sample, then the time taken for the sample containing the geotextiles to reach the consolidated state would reduce. All the tests were continued for a period of 80 to 100 hours, at which time consolidation was complete.

6.7.5 Shearing (Compression)

In the Drained test, the axial load was gradually increased under conditions of full drainage until failure occurred. The total confining pressure remained constant during application of the axial load.

The test took much longer (6 or 7 times) than the undrained test because the rate of applied loading was restricted to permit the drainage to be completed and without the development of excess pore pressure.

In the Undrained tests, no change in water content was allowed while the sample was being compressed. Compression was applied slowly to allow pore pressure changes to equalise throughout the sample and the pore pressure was monitored at the base.

6.7.6 Time to Failure

The term "failure" usually relates to the maximum ("peak") deviator stress which the sample can withstand. The strain, ε_f, at which this is likely to occur is usually estimated, but depends on the type and condition of the soil, Head (1986).

The time to failure in the drained tests was taken as $t_f = 14/t100$ minutes, and the time to failure for the undrained tests was $t_f = 1.8\backslash t100$ minutes, where $t100$, can be obtained from the plot of volume change versus root time at the end of the consolidation stage, and cannot be less than 120 minutes. The rate of strain therefore can be calculated using equation (6.3), Head (1986);

$$(\varepsilon_f\% \times L) / 100 \times t_f \quad mm/minute \qquad (6.3)$$

where:

ε_f % = the strain at failure which Head recommends as being 10%;
L = the length of sample, mm;
t_f = the time to failure,
The calculation procedures are tabulated in Appendix C.

6.7.7 Error Corrections

Some systematic and unavoidable errors can occur in the triaxial test and need to be corrected when processing the data. The following potential problems were identified;

i) water leakage, from the cell
ii) cell piston friction,
iii) deformation of the load cell
iv) volume change error

i) Water leakage, A very slow rate of leakage from valves and connections attached to the cell can occur during the consolidation and compression stages of the tests. The volume change was measured by the volume of water moving into or out of the specimen. To resolve any problem, trial tests were carried out to find a leakage time relationship for each testing machine. A linear relationship between the leakage and square root of time was found, Fig. 6.4a. In Fig. 6.4a the unconnected volume change - time curve shows that the curve has two parts, a non-linear and linear part. The linear part which is the result of leakage, was used for the correction, Fig. 6.4b.

Almost water leakage was found during the consolidation stages and no significant water leakage occurred during the compression stage of the tests.

ii) Cell piston friction, The friction between the load piston and cell bush needed to be corrected. This friction was not unique, therefore the error in the load caused by the friction could only be corrected for each test. A gap of approximately 1 mm between the piston and the load cap were observed in each test, the loads measured in closing this gap is a measure of the cell piston friction are shown in Fig. 6.5.

iii) Deformation of the load cell, It was possible for the load cell to deform during a triaxial test, this will cause some error when measuring the displacement of the specimen. The error

is linear with the load and has a unique relationship for any given load cell, and was easily corrected.

iv) Volume change error, During the test, the piston moving into the cell can cause water to move out of the cell. The volume change of any specimen can be measured from the volume of water moving into or out of the cell. A linear and unique relationship between the movement of the piston and volume of water moving out the cell was determined, by a compression test undertaken without a specimen inside the cell. The actual volume change of any specimen was then the measured value, minus the volume change caused by the piston movement.

6.8 TESTS RESULTS

The results of the both the Undrained test (CU - test) and the Drained test (CD - test) are tabulated in Appendix A. A summary of all the results obtained from the laboratory experiment are shown in Tables 6.2 to 6.7. The stress path plot of the both the Undrained test (CU - test) and the Drained test (CD - test) are shown in Fig. 6.6.

Plate 6.2 shows the triaxial samples with Geotextile after failure, and Plate 6.3 Geotextile located in the middle of sample after failure.

Sample calculations showing how the physical parameters C_v and M_v were calculated from the test data are given in Appendix C.

Table 6.1: The component of the Triaxial apparatus used in the laboratory

No.	Component	Size and Range	Description
1	Extruder	100 mm diameters	
2	Triaxial Cells	for 1000 kN/m^2 pressure	Triaxial cells, fitted with a base, including the specimen pedestal and loading ram.
3	Pressure System	for 1000 kN/m^2 pressure	For maintaining cell pressure at a constant level to within 10 kN/m^2.
4	Nylon tube	for 1000 kN/m^2 pressure	Tube for connecting the pressure system to the cell.
5	Load Device	up to 10 kN/m^2 capacity	Load measuring device - a load ring.
6	Dial Gauge	25 mm travel range	Dial gauge of 25 mm travel reading to 0.01 mm for strain measurement.
7	Rubber membrane	100 mm diameter	Rubber membranes for 100 mm diameter specimens.
8	Loading Frame	10 kN/m^2 to 10000 kN/m2	Loading frame, 10 kN/m^2 capacity or larger and motorised with a wide range of speeds.
9	Porous Discs	100 mm diameter	Porous discs or 100 mm diameter specimen.
10	Pressure Transducer	for 1000 kN/m^2 pressure	Pressure transducers capable of measuring up to a capacity 1000 kN/m^2.
11	Linear Transducer	for 30 mm travel range	Linear transducers of 30 mm movement
12	Volume Change	150 ml Capacity	Volume change Transducer, Imperial College type, connected to triaxial cell.
12	Filter Paper	-	Drainage proposes
13	ADU (Autonomous Data-acquisition Unit)	up to 200 channel	ADU (Autonomous Data - acquisition Unit) linked to a microcomputer that was capable of allowing full control of the whole procedure e.g. being able to over - ride the automatic functions when necessary. Test data could be obtained at any stage of the test.

Table 6.2: Initial and saturation Stage
Consolidated - Undrained Compression Triaxial Test (CU - Test)

Test No.	Effective Cell Pressure kPa	B - Values		Moisture Content%		Density Kg/m^3	
		Initial	After	Start	Finish	Bulk	Dry
K	150	0.59	0.94	28.6	27.4	1856	1429
	300	0.62	0.98	29.1	28.9	1885	1451
	500	0.55	0.93	29.7	28.3	1873	1442
K + G1	150	0.46	0.92	29.7	28.4	1927	1497
	300	0.38	0.91	28.3	29.2	1963	1433
	500	0.59	0.97	30.7	28.7	1888	1461
K + G1CT	150	0.55	0.93	29.1	28.2	1891	1465
	300	0.41	0.89	28.3	29.1	1978	1498
	500	0.46	0.98	-	28.7	1781	1402
K + G2	150	0.49	0.90	29.9	28.2	1887	1436
	300	0.55	0.99	29.0	29.1	1882	1461
	500	0.47	0.96	28.2	27.6	1855	1448
K + G3	150	0.53	0.98	30.0	29.1	1887	1473
	300	0.47	0.95	28.8	32.2	1851	1449
	500	0.58	0.94	31.1	32.3	1866	1455
K + G4	150	0.63	0.96	29.8	29.6	1848	1428
	300	0.59	0.95	-	28.3	1815	1430
	500	0.55	0.89	28.8	27.7	1884	1427
K + G5	150	0.38	0.95	29.7	28.1	1888	1429
	300	0.47	0.81	30.2	28.	1842	1447
	500	0.45	0.92	29.2	-	1858	1453
K + G6	150	0.45	0.89	30.1	29.7	1837	1462
	300	0.37	0.91	29.1	28.7	1845	1443
	500	0.52	0.93	29.2	-	1864	1452
K + G7	150	0.49	0.97	-	30.2	1894	1457
	300	0.49	0.98	29.6	28.9	1865	1452
	500	0.61	0.95	29.5	-	1833	1427
K + G1G2	150	0.57	0.98	30.3	29.5	1858	1435
	300	0.49	0.92	28.9	28.9	1841	1429
	500	0.52	0.89	29.8	27.6	1887	1452

Table 6.3: Consolidation Stage
Consolidated - Undrained Compression Triaxial Test (CU - Test)

Test No.	Effective cell Pressure kPa	Time for Consolidation Hours	√100 min	√90 min.	M_{vi} (m^2/mN)	C_v (m^2/yr)	K (m/s) $\times 10^{-9}$
K	150	102	19.5	17.2	0.44	4.03	0.55
	300	97	19.0	18.4	0.29	2.78	0.25
	500	89	18.4	18.1	0.24	2.55	0.19
K + G1	150	88	16.5	16.1	0.27	44.56	3.73
	300	83	16.0	15.8	0.33	35.09	3.59
	500	89	21.5	19.6	0.57	14.60	2.58
K + G1CT	150	77	14.8	13.6	0.24	45.16	3.36
	300	50	14.2	14.1	0.26	36.97	2.98
	500	81	18.7	17.9	0.71	11.72	2.58
K + G2	150	78	21.5	20.4	0.40	4.91	0.61
	300	94	10.0	9.3	0.38	2.97	0.35
	500	102	12.5	12.3	0.43	1.87	0.25
K + G3	150	79	15.0	14.7	0.31	2.60	0.25
	300	104	9.9	9.1	0.23	5.05	0.36
	500	96	19.5	18.6	0.27	5.73	0.48
K + G4	150	79	14.8	14.1	0.19	8.83	0.52
	300	96	16.1	16.1	0.25	4.38	0.34
	500	87	16.5	16.6	0.27	4.63	0.38
K + G5	150	104	19.0	18.7	0.16	23.99	1.19
	300	96	15.0	14.2	0.43	7.57	1.01
	500	93	14.1	14.0	0.36	6.09	0.68
K + G6	150	88	18.4	18.2	0.21	71.73	4.67
	300	93	23.6	21.2	0.25	50.70	3.93
	500	88	22.2	20.9	0.19	35.05	2.06
K + G7	150	86	16.1	15.91	0.16	10.28	0.51
	300	82	20.0	19.8	0.26	3.59	0.29
	500	86	19.1	19.0	0.42	1.92	0.25
K + G1G2	150	86	17.0	16.23	0.15	18.49	0.86
	300	87	12.5	12.1	0.19	20.21	1.19
	500	91	19.5	18.77	0.19	32.42	1.91

Table 6.4: Summary of Triaxial Tests Result
Consolidated - Undrained Compression Triaxial Test (CU - Test)

Test No.	Effective Cell Pressure kPa 150- 300- 500	Deviator Stress At Failure kPa	Strain At Failure	Shear Strength Parameter Cohesion - Int. Angle C'_{cu}	ϕ'_{cu}
K	150 300 500	118 220 308	10.4 10.5 10.0	9.1	23.6°
K + G1	150 300 500	220 287 335	10.7 9.5 11.3	26	20.1°
K + G1CT	150 300 500	170 343 422	9.9 11.3 11.8	16.5	20.6°
K + G2	150 300 500	140 184 376	7.7 8.9 9.1	25	20.4°
K + G3	150 300 500	162 273 368	9.7 9.2 9.8	17	21.7°
K + G4	150 300 500	151 264 418	9.1 11.4 12.2	16	20.5°
K + G5	150 300 500	175 243 406	9.0 9.2 10.8	18	19.3°
K + G6	150 300 500	198 346 403	9.1 9.7 9.9	39.5	18.6°
K + G7	150 300 500	239 286 393	9.1 10.4 11.2	36	21.2°
K + G1G2	150 300 500	160 283 407	8.8 9.2 9.9	16	20.5°

Table 6.5 : Initial and Saturation Stage
Consolidated - Drained Compression Triaxial Test (CD - Test)

Test No.	Effective Cell Pressure kPa	B - Values Initial - After		Moisture Content% Start - Finish		Density Kg/m^3 Bulk - Dry	
K	150	0.42	0.97	28.2	30.1	1856	1433
	300	0.61	0.95	28.7	29.3	1847	1451
	500	0.33	0.99	30.5	28.7	1839	1447
K + G1	150	0.55	0.89	27.6	26.9	1890	1465
	300	0.41	0.87	30.5	29.2	1886	1449
	500	0.58	0.92	29.8	28.8	1887	1452
K + G1CT	150	0.61	0.99	27.6	29.8	1863	1452
	300	0.52	0.93	29.1	30.2	1860	1447
	500	0.57	0.85	28.6	27.9	1861	1455
K + G2	150	0.39	0.91	30.4	29.7	1877	1471
	300	0.45	0.94	28.6	28.6	1890	1483
	500	0.47	0.96	31.1	27.9	1901	1496
K + G3	150	0.49	0.93	39.3	27.2	1907	1495
	300	0.51	0.96	29.7	29.1	1892	1484
	500	0.59	0.98	28.6	28.0	1879	1478
K + G4	150	0.51	0.98	31.4	29.1	1899	1476
	300	0.49	0.98	28.7	28.3	1904	1493
	500	0.47	0.97	26.4	29.9	1915	1495
K + G5	150	0.49	0.97	30.1	28.4	1836	1439
	300	0.53	0.96	28.6	29.6	1831	1427
	500	0.54	0.99	29.7	30.4	1837	1432
K + G6	150	0.49	0.96	38.2	29.3	1806	1421
	300	0.53	0.97	27.1	27.5	1821	1424
	500	0.52	0.96	26.2	28.6	1834	1430
K + G7	150	0.45	0.99	26.6	27.4	1881	1443
	300	0.44	0.93	28.1	28.8	1878	1455
	500	0.39	0.95	29.9	27.9	1880	1462
K + G1G2	150	0.37	0.87	30.2	29.5	1867	1427
	300	0.43	0.92	29.3	29.1	1872	1423
	500	0.54	0.98	28.7	29.6	1870	1441

Table 6.6: Consolidation Stage
Consolidated - Drained Triaxial Compression Test (CD - Test)

Test No.	Effective cell Pressure kPa	Time for Consolidation Hours	√100 min.	√90 min.	M_{vi} (m^2/mN)	C_v (m^2/yr)	K (m/s) $\times 10^{-9}$
K	150	93	19.2	18.6	0.40	4.51	0.56
	300	91	21.7	20.5	0.30	3.33	0.31
	500	79	21.5	21.1	0.25	2.83	0.22
K + G1	150	75	14.8	14.1	0.21	58.52	3.38
	300	77	15.3	14.8	0.27	41.33	3.46
	500	79	22.5	21.5	0.54	15.94	2.67
K + G1CT	150	87	10.1	9.4	0.20	52.47	3.25
	300	96	8.8	8.2	0.26	38.09	3.07
	500	99	17	16.8	0.70	11.56	2.51
K + G2	150	94	13.3	12.6	0.38	4.16	0.49
	300	103	15.1	15	0.41	2.44	0.31
	500	98	17	16.4	0.41	1.57	0.20
K + G3	150	69	18.9	17.1	0.22	7.33	0.50
	300	106	17.6	16.5	0.24	4.56	0.34
	500	67	15.9	15.6	0.27	2.63	0.22
K + G4	150	67	19.1	18.4	0.18	8.78	0.49
	300	112	15.6	14.8	0.26	4.84	0.39
	500	81	17.3	16.5	0.38	3.69	0.43
K + G5	150	68	16.5	16.1	0.34	12.92	1.36
	300	96	16.1	16	0.16	11.61	0.58
	500	69	14.2	13.5	0.18	19.17	1.06
K + G6	150	75	11.8	11.1	0.20	62.74	3.89
	300	75	21.5	19.6	0.29	38.71	3.48
	500	77	16.2	16.1	0.31	32.77	3.15
K + G7	150	86	12.2	11.9	0.36	1.70	0.19
	300	91	11.7	11.4	0.28	3.11	0.27
	500	68	16.8	16.5	0.17	9.29	0.49
K + G1G2	150	87	16.1	14.5	0.19	33.37	1.96
	300	86	15.6	14.9	0.18	24.19	1.35
	500	85	14.2	14	0.19	21.91	1.29

Table 6.7 : Summary of Triaxial Test Result
Consolidated - Drained Compression Triaxial Tests (CD - Test)

Test No.	Effective Cell Pressure kPa 150 - 300 - 500	Deviator Stress At Failure kPa	Strain At Failure	Shear Strength Parameter Cohesion -Angle of Internal Friction	
				C'_{cd}	ϕ'_{cd}
K	150	220	9.7	18.5	23°
	300	420	10.8		
	500	580	12.5		
K + G1	150	262	10.2	31.5	22.5°
	300	420	11.5		
	500	798	12.2		
K + G1CT	150	260	9.0	25	22.5°
	300	386	10.5		
	500	631	11.0		
K + G2	150	273	10.0	43	20.7°
	300	464	11.3		
	500	665	11.0		
K + G3	150	229	9.7	23	22.2°
	300	362	12.4		
	500	710	10.0		
K + G4	150	226	8.2	27	21.7°
	300	424	9.7		
	500	602	10.2		
K + G5	150	230	9.7	29.5	18.7°
	300	415	11.8		
	500	599	12.3		
K + G6	150	245	9.8	41.5	18.6°
	300	295	8.4		
	500	390	9.1		
K + G7	150	265	9.5	44	20.5°
	300	397	10.7		
	500	610	11.4		
K + G1G2	150	228	7.5	30.1	18.9°
	300	421	8.6		
	500	594	9.1		

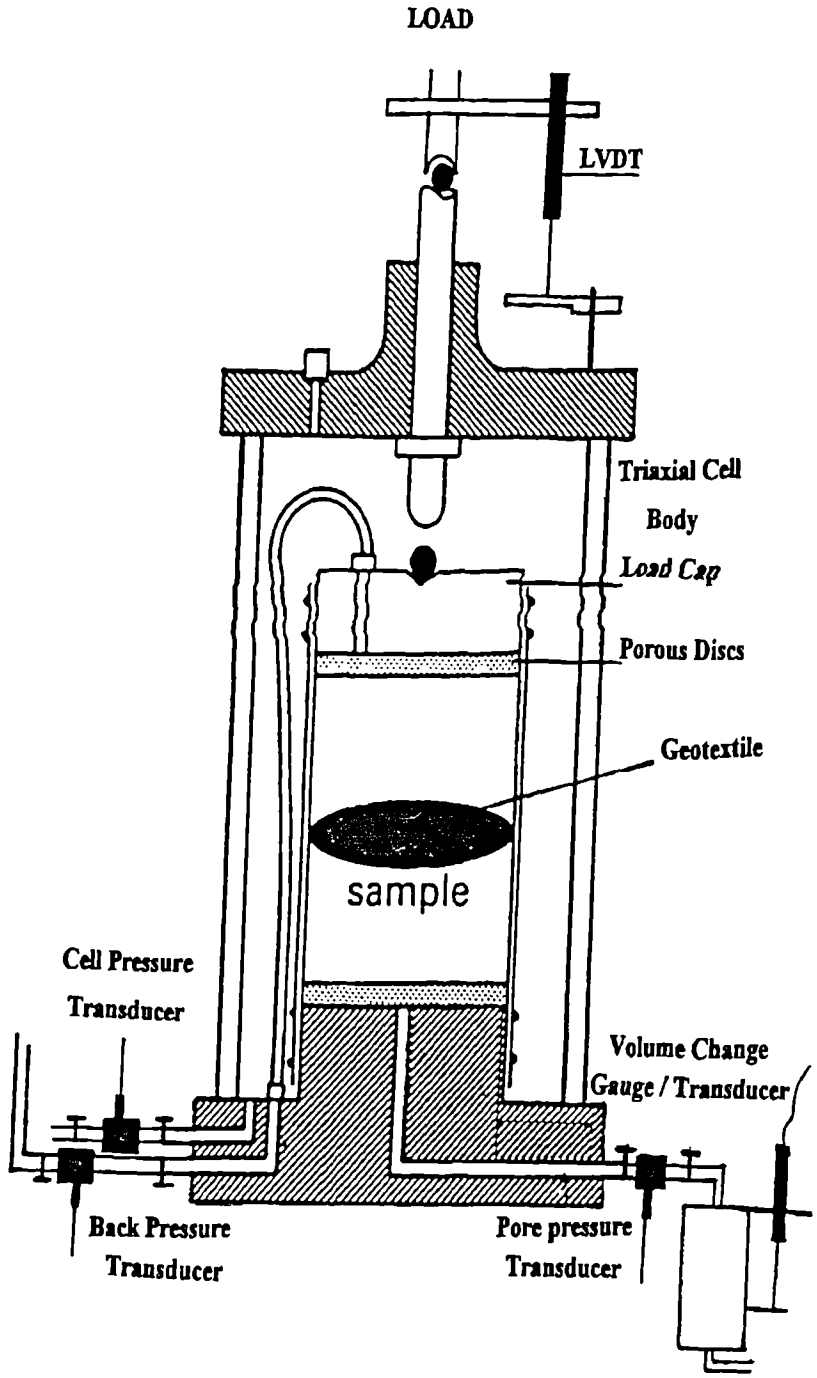

Fig. 6.1	Arrangement of the test apparatus and the specimen with the Geotextile

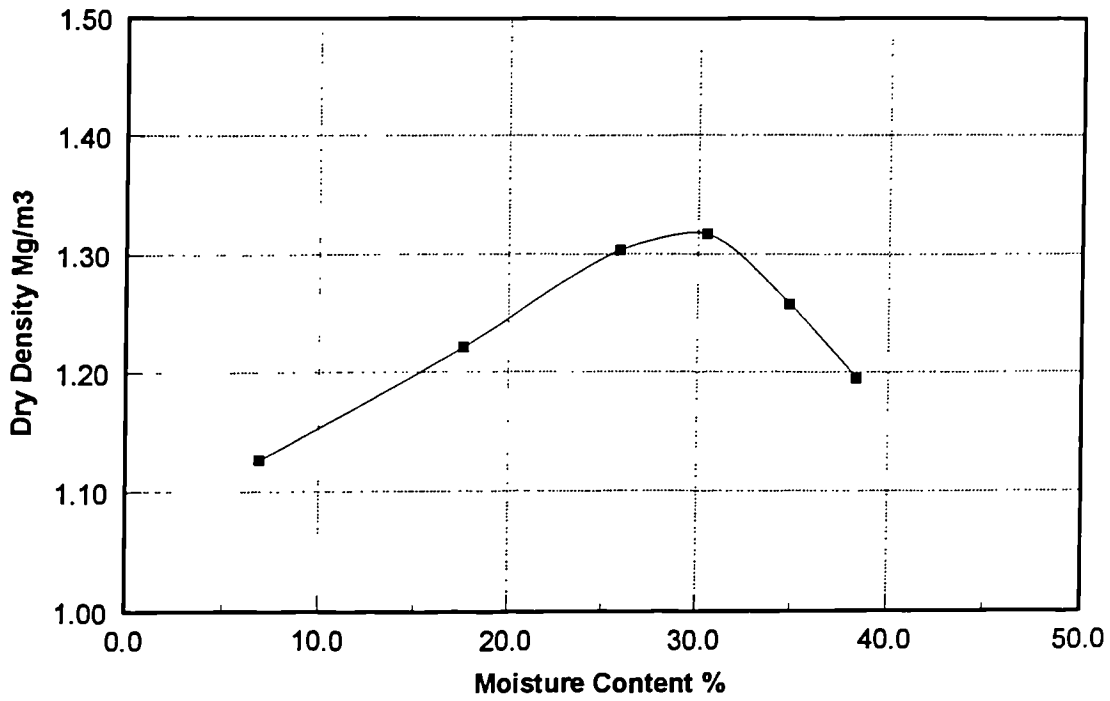

Type of Compaction : Proctor

No. of layers 3, No. of blows 27, weight of rammer 2.5 Kg

Specific gravity 2.63

MAXIMUM Dry Density 1.32 Mg/m3

OPTIMUM MOISTURE CONTENT 29.7 % Dry weight

Fig. 6.2	Compaction Test for Kaolin

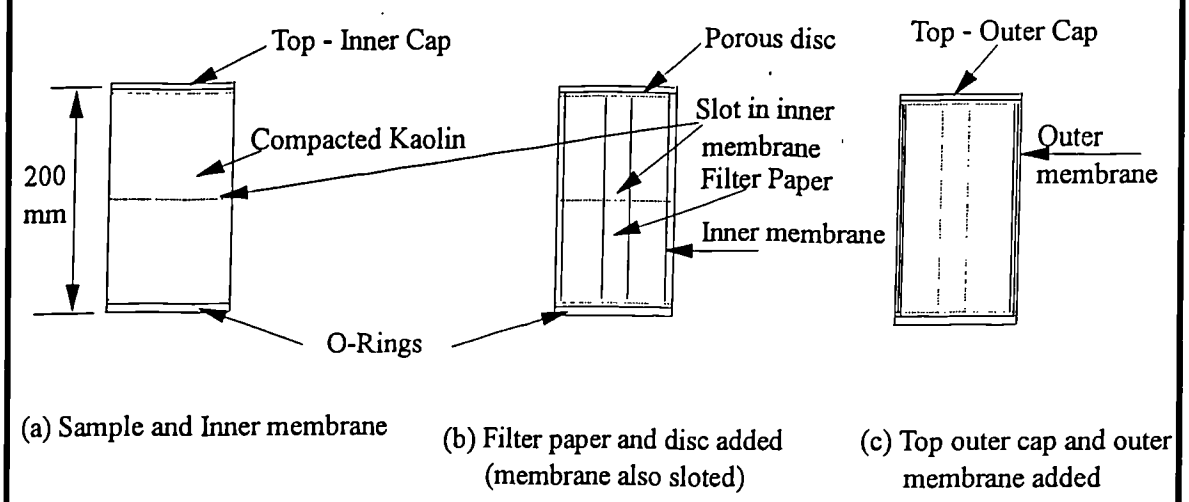

Fig. 6.3	Triaxial sample assembly in the cell

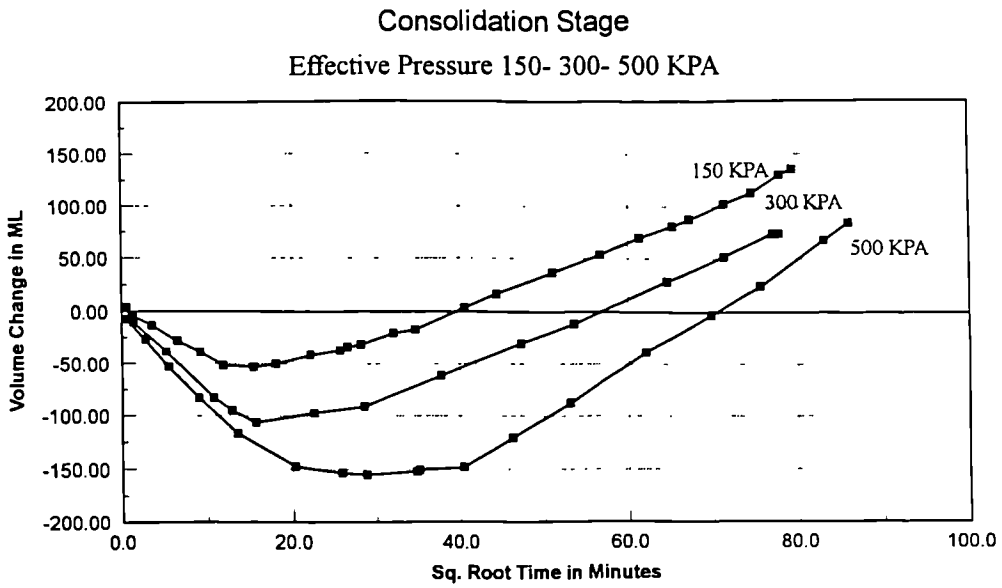

Fig. 6.4a: Uncorrected Consolidation Test

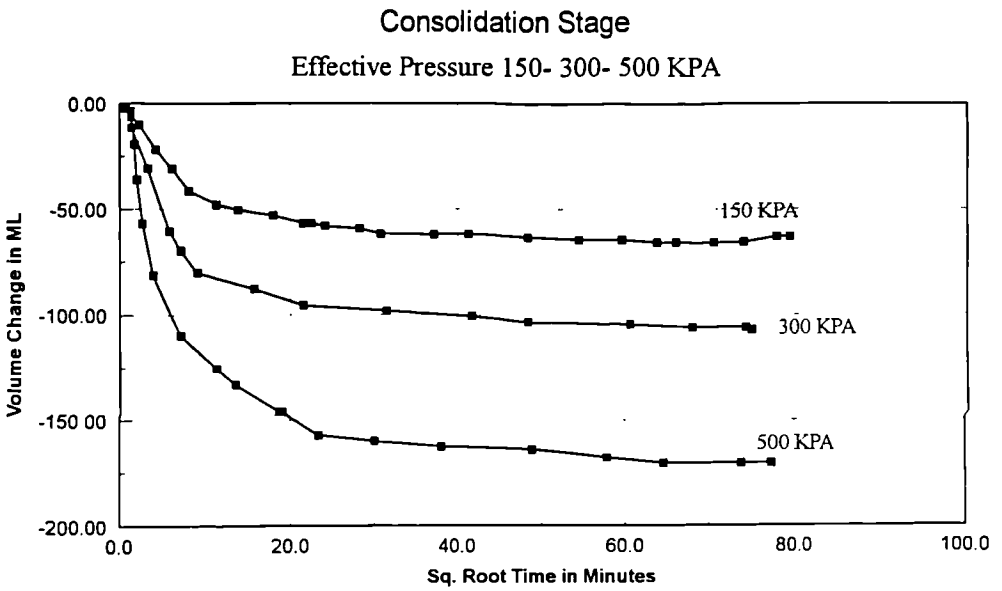

Fig. 6.4b: Corrected Consolidation Test

Fig. 6.4	Correction of Consolidation Test

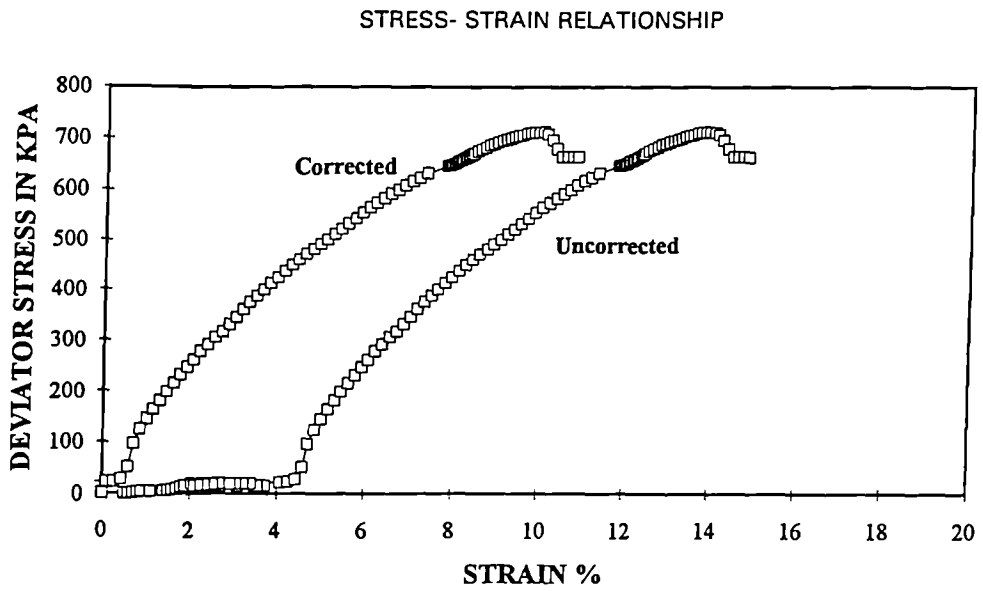

Fig. 6.5	Correction of Piston Friction

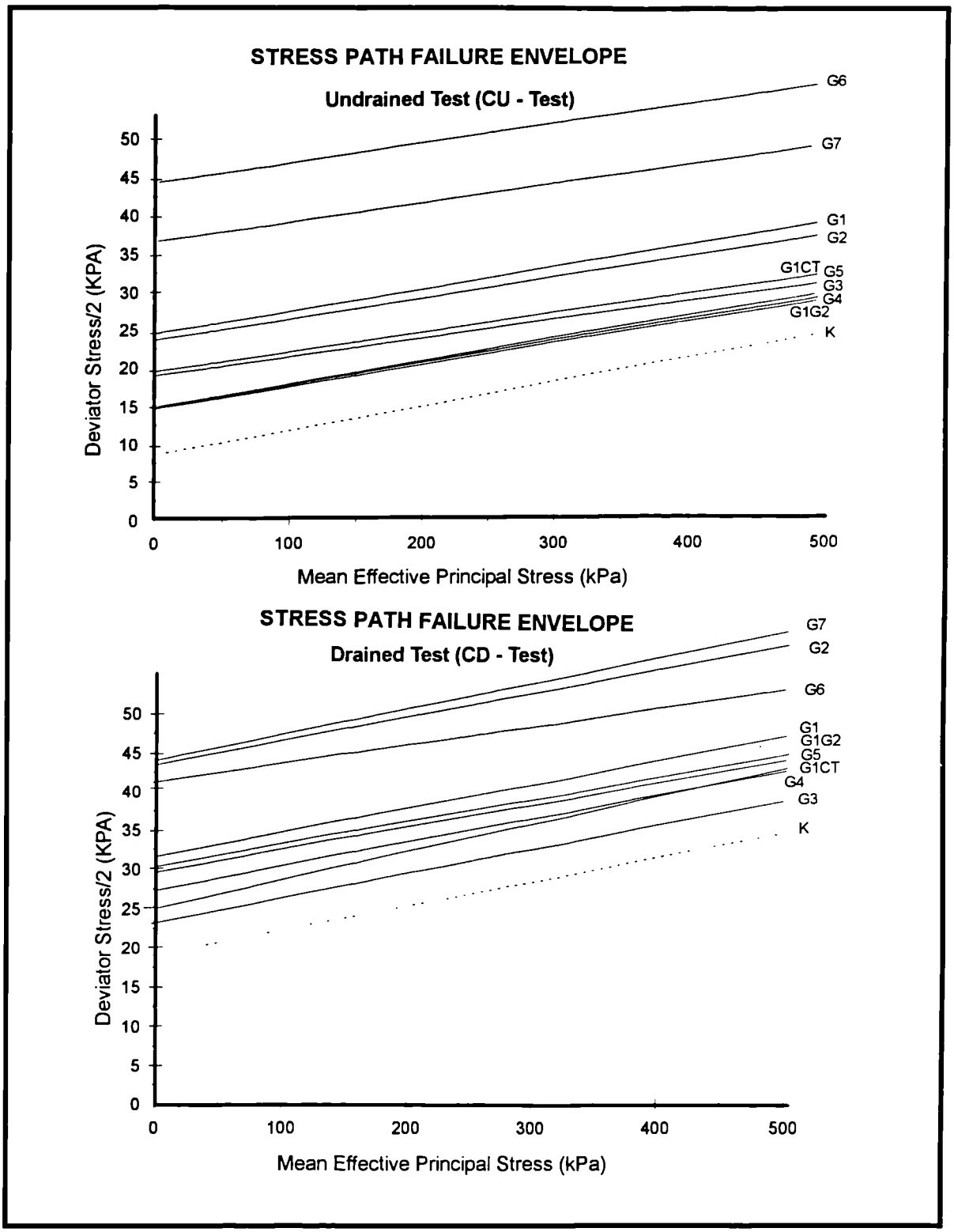

Fig. 6.6	Stress Path Failure Envelopes for Consolidated Undrained and Drained Compression Triaxial Tests

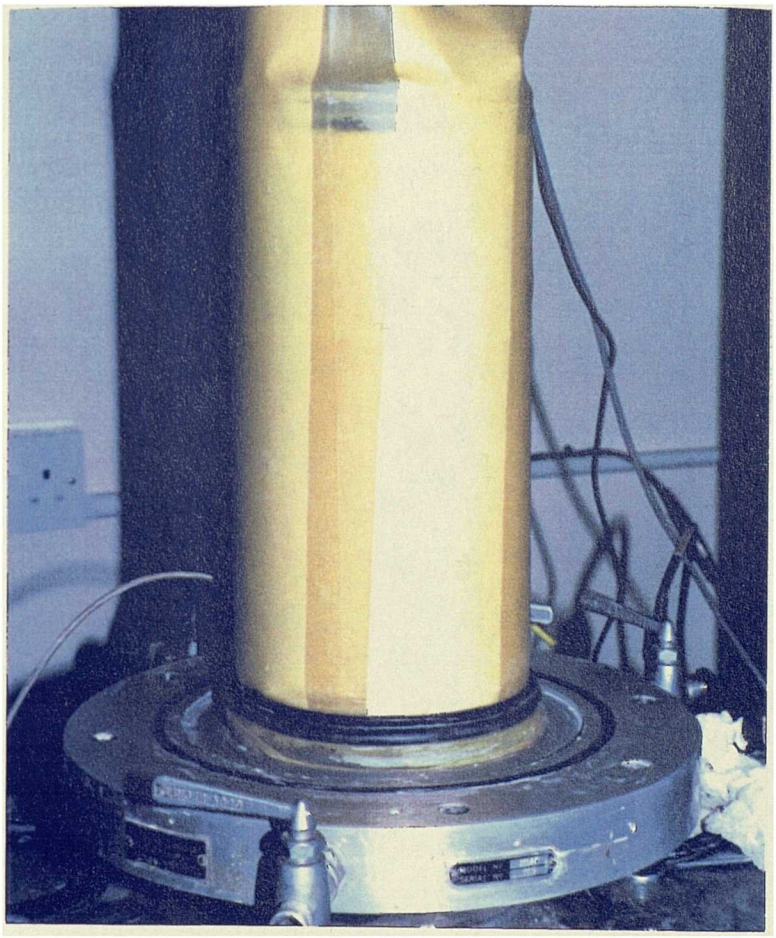

Plate 6.1	Triaxial sample assembly with two membranes

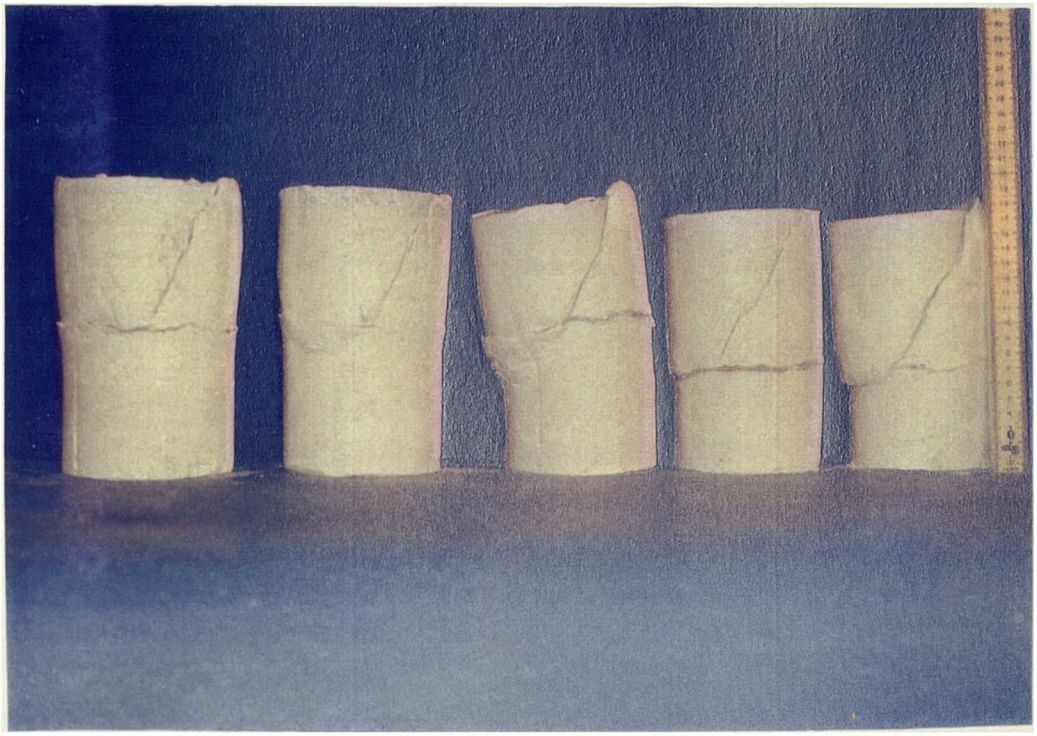

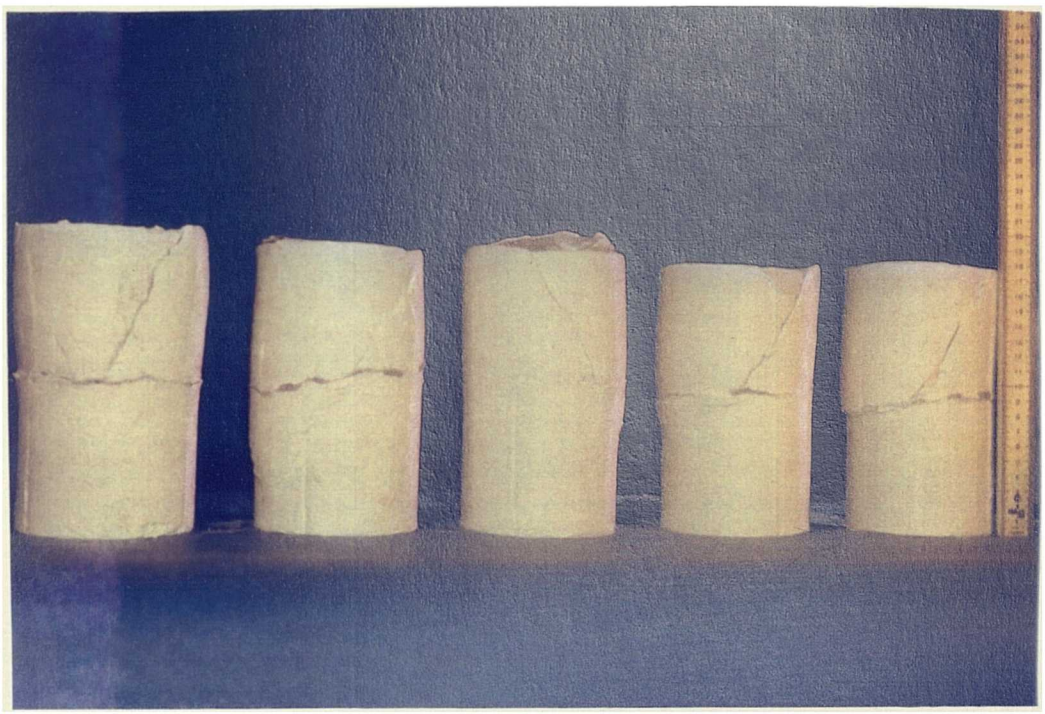

Plate **6.2**	Triaxial samples with Geotextile, after failure

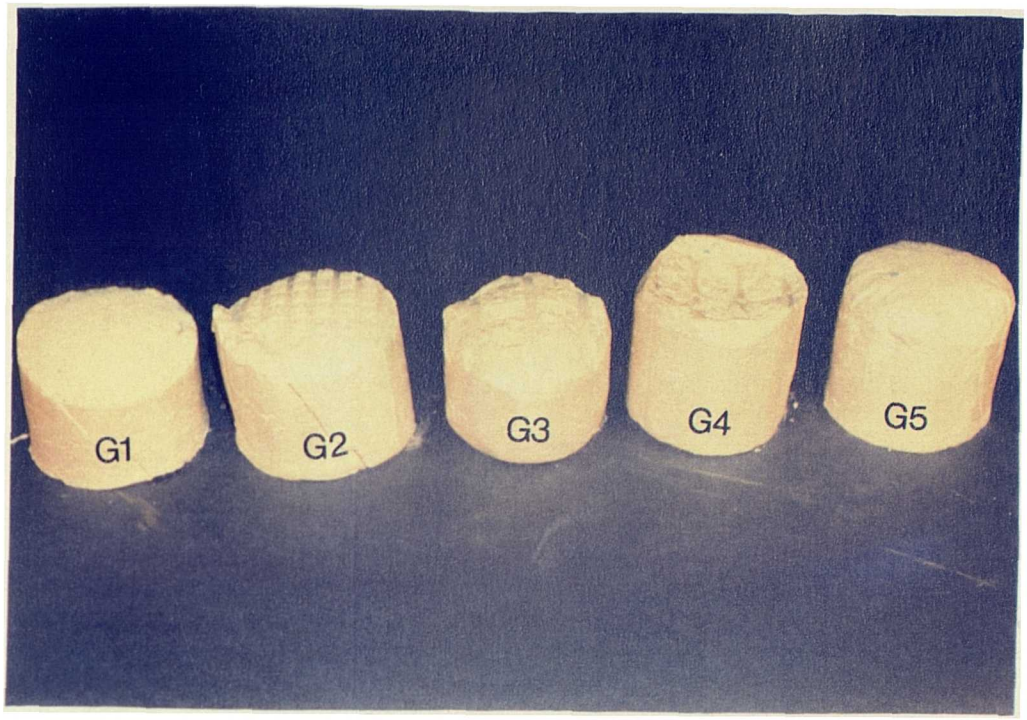

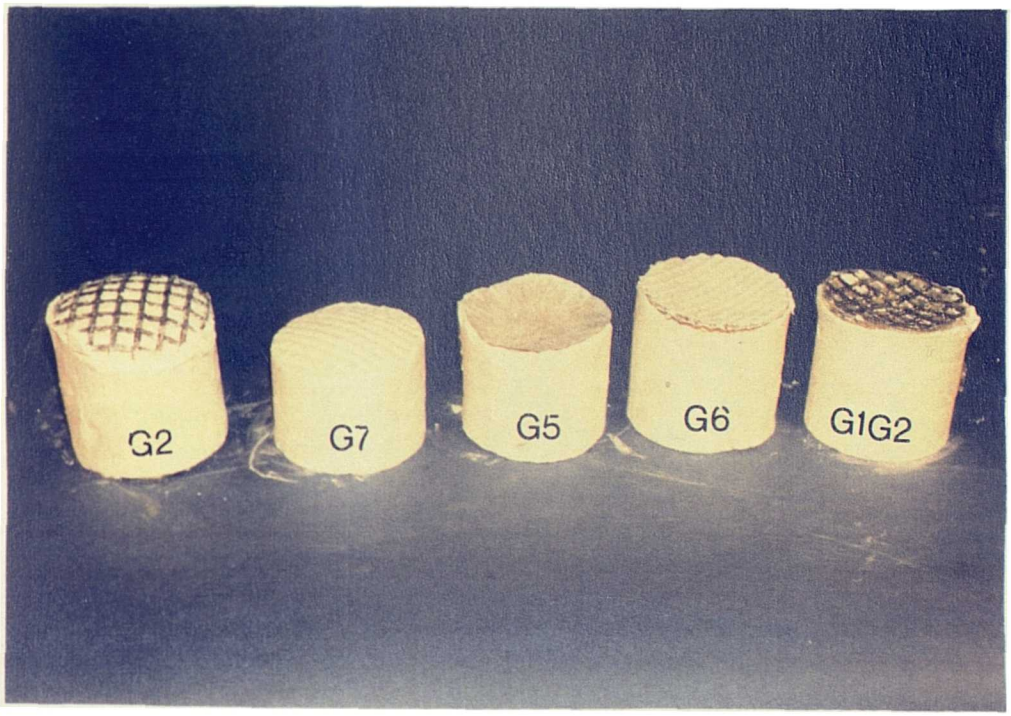

Plate **6.3**	Triaxial samples with Geotextile, after failure

CHAPTER SEVEN

ROWE CELL TESTS, SAMPLE PREPARATION AND PROCEDURE

7.1 INTRODUCTION

This chapter considers the experimental procedures used to undertaken the Rowe cell consolidation tests. Sample preparation, the experimental set-up and apparatus used are discussed. The results of the tests are given.

7.2 CONSOLIDATION

Consolidation is defined as the process where soil particles are packed more closely together over a period of time under the application of continued pressure. It is accompanied by drainage of water from the pore spaces between solid particles.

Soil consists of solid particles with spaces (voids) which may be filled with gas (usually air), a liquid (usually water), or a combination of both Head, (1986). The voids in fully saturated soil contain water only.

When a soil is subjected to a compression stress its volume tends to decrease, which for a saturated soil can take place by three means:
(i) compression of the solid grains
(ii) compression of the water within the voids
(iii) escape of water from the voids between grains

The theory of consolidation is based on (iii), the escape or 'squeezing out' of water from the voids between the 'skeleton' of the solid grains.

7.2.1 Consolidation of soils

The stress induced by the externally applied load is known as the "total stress" and is denoted by σ. The pressure of water in the voids between solid particles in a soil is known as the "pore water pressure" (pwp), or pore pressure, and is denoted by u. When an external load is applied to a saturated clay soil, the entire load is at first carried by the additional pore water pressure which is induced, referred to as the total applied stress.

If the clay is bonded by surfaces from which water can escape such as adjoining sand layers, the excess pressure will cause water to flow out of the clay into the adjoining layers. This will occur slowly, because of the low permeability of the clay, but as water drains out an increasing proportion of the load is transferred to the grains forming the soil 'skeleton' and the pore pressure correspondingly falls. The difference between the total applied stress and the pore water pressure at any instant, is known as the 'effective stress', and is approximately the same as the stress carried by the soil skeleton, Simons and Menzies, (1977). The equation is written as:

$$\sigma' = \sigma - u \qquad (7.1)$$

which is one of the most fundamental relationship in the field of soil mechanics, Terzaghi (1943).

7.2.2 Coefficient of volume compressibility, m_v

The coefficient of volume compressibility is defined as the volume change per unit volume per unit increase in effective stress. The units of m_v are the inverse of pressure (mN/m^2). The volume change may be expressed in terms of either void ratio or specimen thickness (i.e. one dimensional consolidation). If, for an increase in effective stress from σ'_0 to σ'_1 the void ratio decreases from e_0 to e_1, then:

$$m_v = \frac{\frac{1}{1+e_0} \times (e_0 - e_1)}{(\sigma'_1 - \sigma'_0)} = \frac{\frac{1}{H_0} \times (H_0 - H_1)}{(\sigma'_1 - \sigma'_0)} \qquad (7.2)$$

The value of m_v for a particular soil is not constant but depends on the stress range over which it is calculated, Craig (1987).

7.2.3 Coefficient of consolidation, c_v

The one dimensional case of consolidation for a clay layer subjected to uniform loading can be shown to be;

$$\partial U / \partial t = \left(\frac{k}{\rho_w g M_v}\right) \times \left(\frac{\partial^2 U}{\partial Z^2}\right) \qquad (7.3)$$

where;

U = excess pore water pressure at time t, of a given point

Z = vertical height of that point

K = coefficient of permeability of the clay

$_v$ = coefficient of volume compressibility of the clay

p_w = mass density of water

g = acceleration due to gravity

The expression above has a compound coefficient which is replaced by the coefficient c_v, called the coefficient of consolidation, where

$$c_v = \frac{K}{\rho_w g M_v} \qquad (7.4)$$

so that equation (7.3) becomes;

$$\partial U \quad \partial t = c_v \times \partial^2 U / \partial Z^2 \qquad (7.5)$$

and;

$$T_v = \frac{c_v t}{h^2} \qquad (7.6)$$

where h = length of the longest drainage path, and T_v = time factor.

7.3 ROWE CELL CONSOLIDATION TESTS

The Rowe consolidation test, was developed at Manchester University, Rowe and Barden (1966). The Rowe cell is used to overcome most of the disadvantages of the conventional

odometer apparatus when performing tests on low permeability soils, including non-uniform deposits described by Head, (1986).

The cell sizes range from 76 mm to the largest of 508 mm in diameter. The 254 mm diameter cells were used in the present study. This diameter was preferred over the conventional odometer apparatus for consolidation tests because;

(i) large samples can be tested using a large piece of geotextile in them.
(ii) pore pressures can be monitored using the pressure transducers connected to automatic data logging equipment (ADU).
(iii) it was possible to control the drainage of the sample and the drainage conditions could be modified.
(iv) the samples were less susceptible to a lever loading system in the odometer.
(v) pressures up to 1000 kN/m^2 could be easily applied on the large samples.

7.4 APPARATUS

The apparatus used in these tests were standard Rowe cells with the following modifications. Each cell had a plastic (impermeable) sheet with a central hole of diameter 10 mm just below a sintered porous disc (2 mm) which was glued along its periphery to one of the side holes where pore pressure of the sample would be monitored.

The apparatus was capable of measuring the pore pressure along the column of sand, the pore pressure of the sample at every stage of the experiment, the vertical displacement and the actual load (pressure) applied at the top of the sample. All readings were recorded with the help of an automatic data logging unit (ADU). The cells had the following facilities;

(i) pressure transducers for the measurement of the pore pressure and the total pressure,
(ii) linear transducers for the vertical displacement,
(iii) a motorise oil water system for the application of the total pressure at the top,
(iv) a sintered porous disc about 4 mm thick,
(v) a back pressure system which supplied a minimum pressure of 100 kPa,
(vi) a 25 mm dial gauge for measuring the vertical displacement,
(vii) an O-ring base seal.

7.5 SAMPLE PREPARATION

Each sample was made in the laboratory from 5 kg of Kaolin which was mechanically mixed after adding water with the aim of obtaining a moisture content of 29.5% using the procedure outlined in BS 1377, (1975).

The samples were compacted generally in 3 layers giving each layer 173 blows for the full height of the cell. The number of blows were determined by comparing the volumes of the Kaolin in the Proctor mould and that in the Rowe Cell. In some specified samples, the sample was compacted in two halves separately. One portion in the actual cell where the test was to be carried out and the other half extruded from a similar Rowe cell. In this second type of sample preparation, the unevenness of the small thicknesses of the porous discs were eliminated. The hammer was used to simulate a sheep's foot roller, typical of the plant used in the compaction of road embankments using cohesive fills.

A portion of the sample was placed in the oven for moisture content determination. The moisture content determination was carried out using an oven at 110'C.

The pore pressure transducer was used to monitor the pore- water pressure in the column of sand, which because of its free draining nature, was considered to be equivalent to the back pressure. A pressure transducer was used to record the pore pressure of the sample. It was located at the top rather than at the bottom of the cell as this was more realistic as the drainage and saturation was done from the top of the sample. This set up was used when no geotextile was present.

Extrusion of the samples was facilitated by using thin polythene sheets on the sides separated by a film of silicone grease.

For reproducibility of the results 7 grams of the sand was used each time in tubes and loosely packed so that allowance could be made for the consolidation of the Kaolin as far as it could without undue rigidity from the sand column.

The polythene used was flexible and only 0.125 mm thick to just allow the settlement of the centre core.

The sand column was introduced in order to be the only channel for conducting water upwards to the sintered porous disc above the plastic sheet with a central hole. The volume

of water being handled during the consolidation was limited so that the effects of the geotextile could be more noticeable.

The porous discs at the bottom side of the Rowe cell was to measure the pore pressure, the column of sand was monitored with the central bottom connection. This had the advantage of identifying whether the sand blocked or not. It was also a quick way of checking the end of a stage as the pore pressure would then approach a common value. The sample assembly in cell is illustrated in Fig. 7.1.

7.6 TEST PROCEDURES

The Rowe cell consolidation tests were carried out for cases with and without geotextiles, the tests consisted of the following stages, Head (1986);

(i) B-Test stage,

(ii) Saturation stage,

(iii) Consolidation stage.

7.6.1 B - Test

A few tests were carried out on the samples by applying an axial pressure in two stages of 100 to 150 kN/m^2. The first pressure was applied and usually took at least a day (24 hours), before the next increase of pressure. In each case, the applied axial load, pore pressure and back pressure were recovered on the automatic data logging unit. The stage was performed for the following reasons;

(i) to check that there is no leakage of total pressure water into the sample.

(ii) to pre-load the sample of soil to a known pressure.

(3) to eliminate the unevenness of the sample by bedding down the contact surfaces in the cell.

7.6.2 Saturation

The samples are saturated at a pressure of 110 kN/m^2 with a back pressure of 100 kN/m^2. Care was taken to ensure that there is a positive axial pressure on the sample. The back pressure was used to help remove the bubbles of air that tend to block the passage of water from flowing into the sample. The end of saturation was determined by plotting a graph of pore pressure versus time on the computer screen. When the pore pressure appeared level at approximately the back pressure value, it means that the stage is complete, otherwise the saturation would be allowed to continue even if the period took three days or more.

7.6.3 Consolidation

After the saturation stage, the sample was subjected to incremental axial loads. Each increment allowed the dissipation of pore pressure to equal the back pressure under which it was being consolidated. The back pressure under which it was usually maintained was 100 kN/m^2 partly because a number of experiments were running requiring the 100 kN/m^2 pressure and partly because the pressure during saturation as a back pressure was also 100 kN/m^2. To determine the end of consolidation, a graph of pore pressure versus time would be plotted when the pore pressure had stopped decreasing for all practical purposes, the next increment of load would be imposed. The loading pressures were 250, 400 and 700 kN/m^2 applied consecutively. The effective pressure of 600 kN/m^2 (700-100 kN/m^2) was used because the overburden pressure, (in high embankments) is within this limit, BS: 8006, (1991) and Tatsuoka, et. al. (1990).

7.7 TEST RESULTS

The results of the Rowe Cell Consolidation tests are tabulated in Appendix A. A summary of all the results obtained from the laboratory experiments are shown in Tables 7.1 to 7.3. Plate 7.1 shows the Rowe cell samples and geotextile located in the middle of sample.

Sample calculations showing how that physical parameters ε_v, m_v and K were calculated from the test data are given in Appendix C.

Table 7.1 : Rowe Cell Consolidation Test Result

Test No.	Consolidation Total Pressure kPa	$\sqrt{t_{100}}$ min.	$\sqrt{t_{90}}$ min.	Max. Pore Pressure kPa	Ratio of Pore Pressure
K	250	15.0	12.4	153	-
	400	17.5	8.2	195	-
	700	17.5	8.5	269	-
K + G1	250	7.8	7.2	121	1.26
	400	5.2	4.3	144	1.35
	700	13.5	10.5	201	1.33
K + G1CT	250	7.3	5.1	111	1.37
	400	7.2	5.4	131	1.49
	700	9.9	7.8	197	1.36
K + G2	250	15.7	10.0	147	1.04
	400	13.5	9.1	185	1.05
	700	15.7	10.4	267	1.01
K + G3	250	10.0	9.8	151	1.01
	400	17.1	13.5	189	1.03
	700	15.0	12.4	261	1.03
K + G4	250	11.4	7.5	148	1.03
	400	11.4	7.6	179	1.08
	700	12.8	7.7	271	1.01
K + G5	250	7.0	5.1	133	1.15
	400	11.7	11.6	154	1.26
	700	9.7	9.8	208	1.29
K + G6	250	9.14	8.8	103	1.48
	400	10.0	10.0	111	1.75
	700	12.1	10.1	183	1.75
K + G7	250	9.4	6.1	145	1.05
	400	9.3	9.5	189	1.03
	600	9.3	8.1	253	1.06
K + G1G2	250	12.8	8.8	139	1.10
	400	7.8	7.8	161	1.21
	700	6.4	5.1	209	1.28

Table 7.2 : Cv, Mv and corresponding K value Rowe cell consolidation tests result

Test No.	Consolidation Total Pressure kPa	Mv m^2/mN	Cv $m^2/yr.$	K $m/s \times 10^{-9}$
K	250	0.28	8.3	0.72
	400	0.16	7.1	0.35
	700	0.13	11.54	0.46
K + G1	250	0.27	66.74	5.59
	400	0.18	60.91	3.40
	700	0.13	54.38	2.19
K + G1CT	250	0.31	65.3	6.27
	400	0.22	45.6	3.11
	600	0.19	38.3	2.25
K + G2	250	0.23	6.34	0.46
	400	0.18	8.2	0.45
	700	0.14	11.2	0.48
K + G3	250	0.21	11.5	0.75
	400	0.19	10.1	0.59
	700	0.20	12.2	0.75
K + G4	250	0.27	8.9	0.74
	400	0.16	4.5	0.75
	700	0.11	4.1	0.47
K + G5	250	0.19	17.2	3.44
	400	0.17	10.78	1.93
	700	0.18	7.6	1.44
K + G6	250	0.19	97.8	5.76
	400	0.21	46.1	3.0
	700	0.18	39.7	2.21
K + G7	250	0.24	5.4	0.41
	400	0.19	4.2	0.24
	700	0.21	5.2	0.33
K + G1G2	250	0.18	36.1	2.01
	400	0.21	22.1	1.43
	700	0.24	14.2	1.05

Table 7.3 : Comparison of the permeabilities of the test results with and without geotextiles

Test No.	Consolidation Total Pressure kPa	Permeabilities $K \times 10^{-9}$ m/s	Factor of improvements between samples with and without geotextile
K	250	0.72	-
	400	0.35	-
	700	0.46	-
K + G1	250	5.59	7.7
	400	3.40	9.7
	700	2.19	4.5
K + G1CT	250	6.27	8.7
	400	3.11	8.8
	700	2.25	4.9
K + G2	250	0.46	0.63
	400	0.45	1.28
	700	0.48	1.03
K + G3	250	0.75	1.04
	400	0.59	1.6
	700	0.75	1.6
K + G4	250	0.74	1.02
	400	0.75	2.14
	700	0.47	1.02
K + G5	250	3.44	4.7
	400	1.93	5.51
	700	1.44	3.1
K + G6	250	5.76	8.0
	400	3.0	8.5
	700	2.21	4.8
K + G7	250	0.41	0.57
	400	0.24	0.68
	600	0.33	0.71
K + G1G2	250	2.01	2.8
	400	1.43	4.1
	700	1.05	2.28

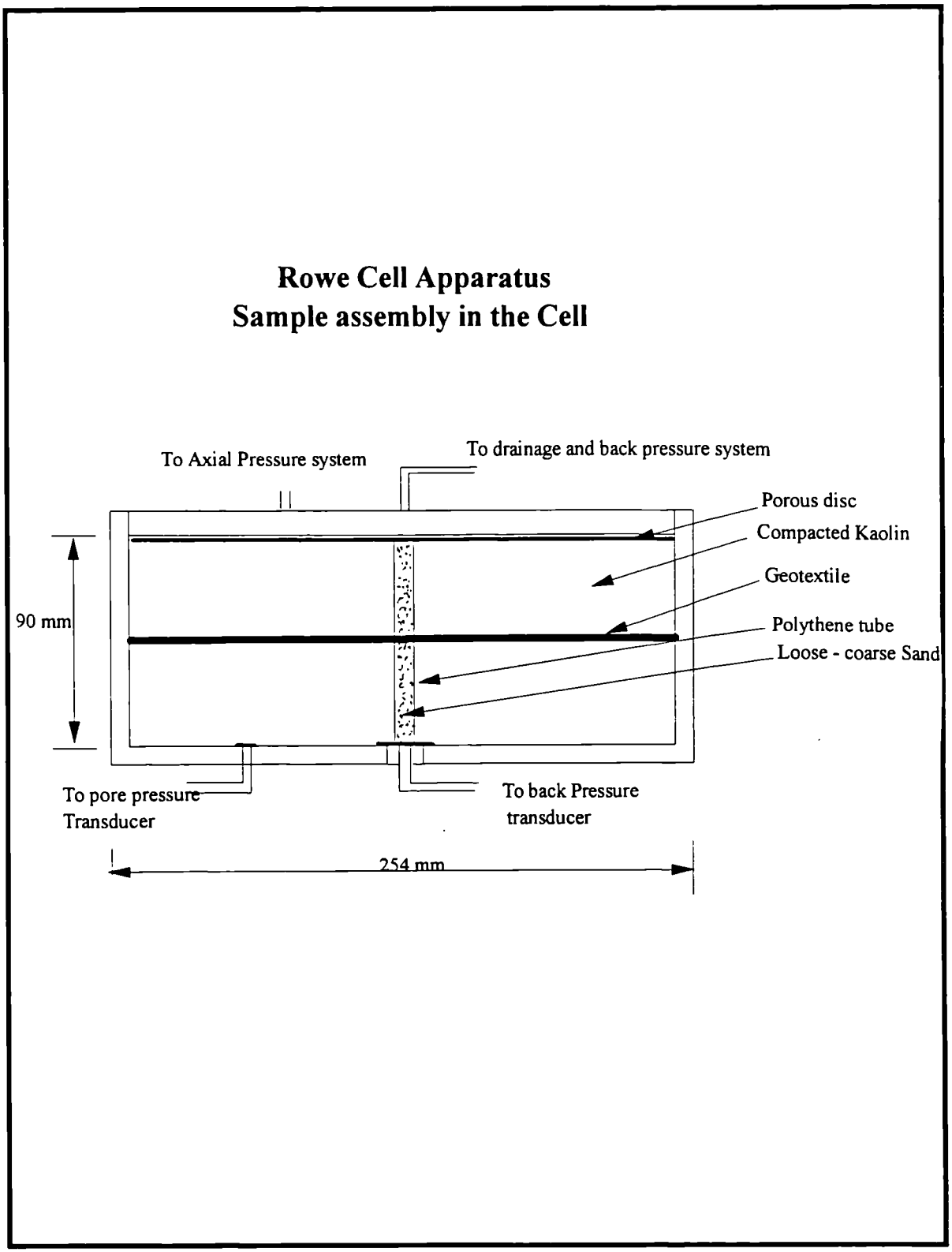

Fig. 7.1	Longitudinal section of sample in the Rowe Cell

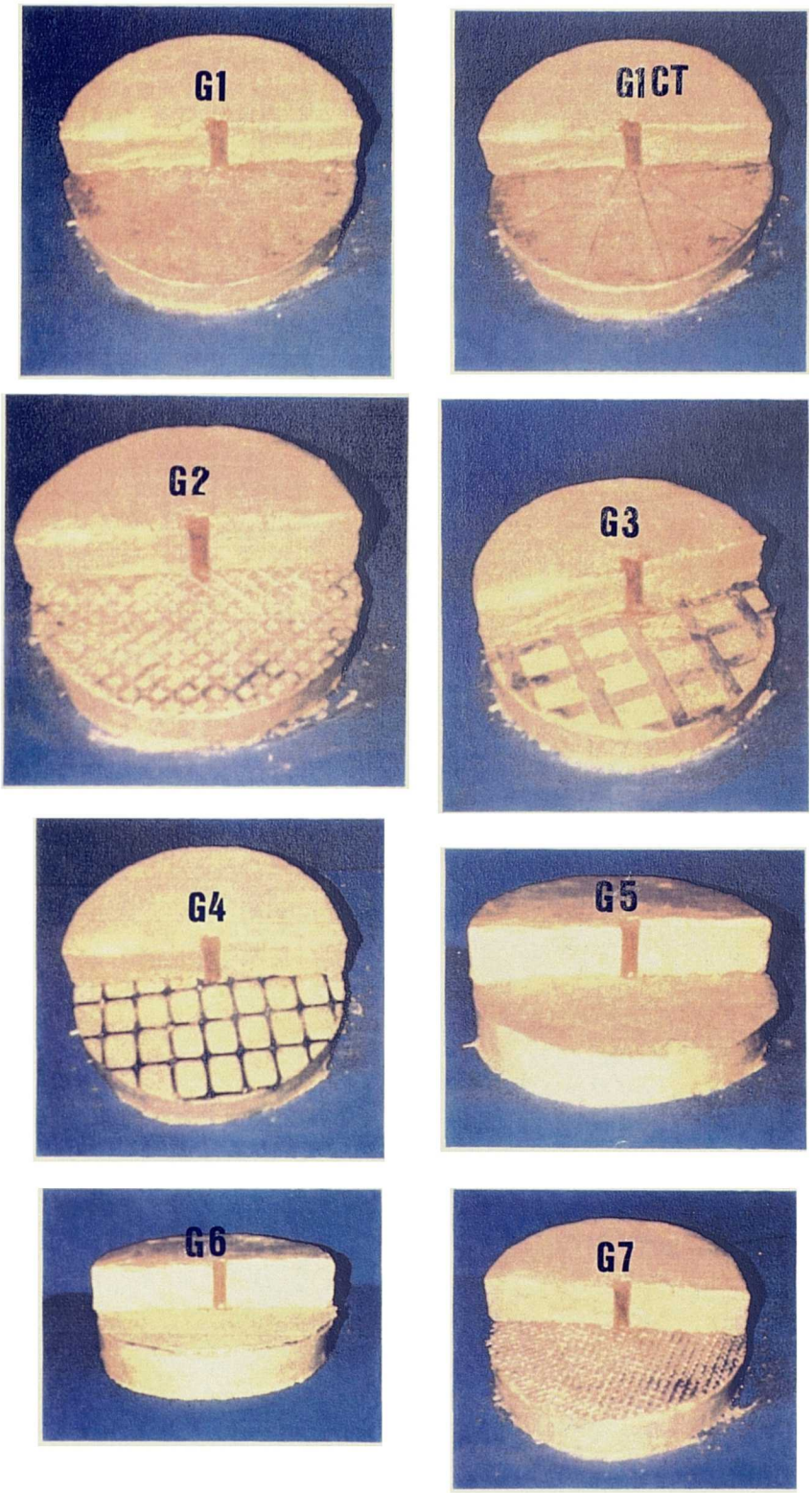

Plate 7.1	Geotextile located in the middle of the sample

CHAPTER EIGHT

INTERACTION BETWEEN GEOTEXTILE AND SOIL, RESULTS AND DISCUSSION

8.1 INTRODUCTION

In this chapter the mechanisms of interaction between geotextiles and soil are described. The binding, sliding and surface friction of the geotextiles and their behaviour on the geotextiles are considered. The interaction and scanning electron microscopy study of the geotextiles used in this research are identified. The results of the experimental works in this research are discussed.

8.2 INTERACTION BETWEEN GEOTEXTILE REINFORCEMENT AND SOIL

There are two main types of interaction between geotextile reinforcement and soil. The most significant is bond which determines the load transfer between the reinforcement and the adjacent soil. Fig. 8.1a. The assessment of bond is required when the critical (or potential) failure plane crosses the geotextile reinforcement. A second form of interaction is direct sliding resistance, which is particularly important for wide-width reinforcement materials. This allows the possibility of outward sliding across the surface of the geotextile reinforcement in the soil to be assessed, Fig. 8.1b. The assessment of direct sliding is required when a potential failure plane coincides with the surface of the geotextile reinforcement.

Tensile stresses in the geotextile reinforcement are transferred into the surrounding soil by means of the development of bond between the geotextile reinforcement and the adjacent soil. For reinforced soil, there are two possible bond mechanisms between the geotextile reinforcement and the surrounding soil, by friction, and end bearing.

Friction between the geotextile reinforcement and the surrounding soil occurs along a surface in a direction parallel to the reinforcement, whereas end bearing occurs along a surface normal to the plane of the reinforcement. These two reinforcement/soil bond

mechanisms are shown in Fig. 8.2. Conventional and flat strip geocomposite geotextiles develop bond by friction. Geocomposite anchors develop bond by end bearing, and while geogrids develop bond by a combination of friction and end bearing.

Fig. 8.2a depicts the development of a frictional bond between the geotextile reinforcement and the surrounding soil. To maintain equilibrium, this frictional bond must resist the maximum tensile load carried by the geotextile reinforcement.

The interaction coefficient f_b is a measure of the frictional bonding efficiency of the geotextile reinforcement with the adjacent soil-the greater the value of f_b, the greater the bonding efficiency. Because of their different constructions, different geotextiles exhibit varying frictional bonding efficiencies with the soil. Typical values are listed in Table 8.1.

8.2.1 Interaction between Geogrids and Soil

The major components which constitute a reinforced soil system, are the soil, the reinforcement, and the interaction between the soil and the reinforcement. In order to design safe and economical reinforced soil structures it is necessary to have a detailed appreciation of both the short-term and long-term characteristics of these components.

When the surface of the reinforcement includes some protrusions (i.e. ribs), the limit lateral friction is greatly increased as a result of the increase in the thickness of the sheared zone, while the coefficient of reaction is reduced. In the case of reinforcements with a complex geometry, such as grids, the frictional resistance is composed of many phenomena; surface friction, particle interlocking within the grid apertures, and passive thrust of the soil against the transversal elements, provided that the grid openings are sufficiently large with respect or the soil grain size.

The frictional characteristics have a primary importance in geotextiles used for soil reinforcement: in fact high frictional properties reduce the possibility of movements of reinforcing elements relative to the soil, and allow perfect transfer of the stresses from the soil to the reinforcing elements.

Soil dilatancy is an important factor which should be taken into account with respect bond developed between a geogrid and the soil. Dilatancy is caused by the shape of the geogrid material in which the soil is partially continuous (in that it is passes through the grid

apertures). When the reinforced soil deforms as the geogrid itself elongates, each geogrid transverse element makes the surrounding soil expand and the interaction behaviour is enhanced by direct friction between the geogrid longitudinal elements and the soil. This is illustrated in Fig. 8.3. Consequently, the vertical stress within the of soil mass increases and the total reinforcing effect is increased with the tensile capacity of the reinforcement.

8.3 INTERACTION AND SCANNING ELECTRON MICROSCOPE STUDY

In order to obtain a better understanding of the observation of the surface of the geotextiles used in this study, a SEM study was performed on representative samples retrieved from the geotextiles before and after the triaxial compression tests.

The observation of the surface of the geotextiles after shear failure, suggested some surface straining had occurred. It was further recognised that this strain was, to some degree, effected by the cohesion of the Kaolin and surface characteristics of the geotextiles i.e. non-woven needle punched polypropylene fibres, Plate 1 and 2. The contrary of this, is that the surface strain of some geotextiles such as HDPE geogrid is low, differential strain between the soil and the reinforcement can be identified by the striation visible on the smooth surface of the reinforcement material, Plate 3.

The resistance to shear failure of the geotextile is partly contributed by the interface *frictional resistance between the Kaolin and surface* of geotextile which may cause by cohesion of the Kaolin and roughness surface of geotextile, i.e. G1.

The drainage geotextiles have been shown good interaction with cohesive soil. The *interaction between soil/geotextile conform the shear failure* resistance of the surface of geotextile is partly contributed by the interface frictional resistance between Kaolin and surface of geotextile which may cause by cohesion of Kaolin and roughness surface of geotextile. This interaction may be associated with pore size, water permeability and thickness of the drainage geotextiles.

8.4 DISCUSSION OF THE TRIAXIAL TEST RESULTS

8.4.1 Angle of Internal Friction (ϕ') and Cohesion (c')

The results of the tests on the consolidated undrained tests (CU) samples, for both the reinforced and unreinforced uses are shown in Chapter 6, Table 6.4. The results of the consolidated drained tests (CD) are shown in Chapter 6, Table 6.7. Graphs of the stress

paths for the undrained tests (CU) and graphs of the stress path for the drained tests (CD) are shown in Chapter 6, Fig. 6.6.

In the consolidated undrained tests the non-woven geotextiles (G1, G1CT and G6) acted as drainage materials only. In the consolidated drained tests the non-woven geotextiles (G1, G1CT, G5 and G6) acted as drainage materials and also provided composite drainage and reinforcing functions.

It can be seen from the results that the inclusion of the drainage geotextiles in the fully consolidated undrained tests produced a ***reduction*** in the effective angle of internal friction (ϕ') [$K_{23.6°} \rightarrow G1_{20.1°}$], as did the cut geotextile [$K_{23.6°} \rightarrow G1CT_{20.6°}$], but a major increase in effective cohesion (c', kN/m^2) [$K_{9.1} \rightarrow G1_{26}$], as did the cut geotextile [$K_{9.1} \rightarrow G1CT_{16.5}$].

In the fully consolidated drained tests the geotextiles acting as a drainage layer only had no effect on the internal friction but produced an ***increase*** in effective cohesion (c') [$K_{18.5} \rightarrow G1_{31.5}$], as did the cut geotextile [$K_{18.5} \rightarrow G1CT_{25}$].

In the both the consolidated undrained and consolidated drained tests the geogrids (G2, and G7) acted as reinforcement which produced a ***reduction*** in the effective angle of internal friction (ϕ'); for the undrained tests [$K_{23.6°} \rightarrow G2_{20.4°} \rightarrow G7_{21.1°}$]; for the drained tests [$K_{23°} \rightarrow G2_{20.7°} \rightarrow G7_{20.5}$]. However, the presence of the reinforcement resulted in a major ***increase*** in effective cohesion (c') for the undrained tests [$K_{9.1} \rightarrow G2_{25} \rightarrow G7_{36}$], for the drained tests [$K_{18.5} \rightarrow G2_{43} \rightarrow G7_{44}$].

In both consolidated undrained and consolidated drained tests the increases of effective cohesion when using a reinforcement geotextile is generally in agreement with other researcher's works such as Yang, (1972) and Ingold (1980). Ingold's work showed a little increases in the effective angle of internal friction when geotextile introduced, (ϕ'= 20° - ϕ'= 25°). This may be caused due to, a) using rapid loading, and b) using multi-layers of reinforcement.

The results showed that the geogrids (G3 and G4) acting as reinforcement were not as effective as the materials (G2 and G7) probably due to the large aperture of the grids.

G1G2 was thought to have the properties required to provide the dual action of drainage

and reinforcement, but the results indicate a reduction in shear strength parameters. The possible explanation is that the composite material (reinforcement and drainage) provided a low friction plane at the geotextile/geogrid interface. This low friction plane could have been caused by the geotextile material attracting water which lubricated the interface, Fig. 8.4. Therefore, for perfect combination of drainage and reinforcement material it would be better to mixed the drainage and reinforcement material together rather than combined them. A proposed drainage and reinforcement material is shown in Fig. 8.5.

G5, was used in the Colorado Walls. It was represented at the Colorado Symposium that the post peak shear strength deflections of this material increased very rapidly indicating that this lightweight reinforcing geotextile had insufficient strength to provide stability. The finite element analysis of the Colorado Walls in this study provided an indication of the percentage mobilised shear strength of the reinforced soil during the construction stage and in the serviceability condition. It also provided an indication of the reserve of strength in the system and can be used to determine the potential failure plane (s) and also a measure of the factor of safety.

G5, in this study showed a reasonable improvement in shear strength parameters in both consolidated undrained and drained triaxial test and still better result in the consolidated drained triaxial test with compare of the conducted tests at Colorado Walls. This may be ignored the drainage potential of this material.

G1 and G6 are the best material associate with cohesive soil. The importance is that these materials could improve the shear strength parameters of a cohesive soil such as Kaolin and also provide improvement in the drainage characteristics.

G2 and G7 are also good materials to improve the cohesion and internal angle of friction of a cohesive soil, introduction of these materials into the cohesive soil improved the strength properties of the soil about five times.

8.4.2 Strain

In the both the consolidated undrained and consolidated drained tests, the strain to failure decreased with decreasing confining pressure for both the samples with and without geotextiles, Tables 6.4 and 6.7. This did conform to the normal pattern of behaviour at varying confining pressures suggested by Head, (1986).

The effective stress path plots for both the sample with and without geotextiles is given in Chapter 6, Fig. 6.6, and shows the state of stress for every stage until failure and slightly beyond. The stress paths are of a similar slope and pattern showing that the stress "history" of the samples was similar to what would have been expected.

There is no significant difference in the strain when using different geotextiles. However, in the case of reinforcement geotextiles (geogrids, G2, G3, G7 and G5), the strain to failure is slightly greater then for the drainage geotextiles, (G1, G1CT, and G6), Figs. 11-20 and 41-50, in Appendix A. The reinforcement geotextile have a high modulus than the drainage geotextile materials so less strain have been expected. The implication is that drainage materials have greater influence than the reinforcement materials.

8.4.3 Consolidation and Consolidation Parameters

The results in respect of the influence on consolidation of materials G1, G1CT, and G6, confirm that significant drainage occurred. The results of the consolidation tests, are shown in Tables 6.3 and 6.6, and Figs 21-30 and Figs 51-60 in Appendix A.

The results indicates that it was possible that the geotextiles maintained a water link in between the two membranes encasing the sample and in the plane of the sample, causing some reduction in the friction angle along the plane of failure. This may explain why the failure planes seemed to emanate from the geotextile surface downwards, shown in Plate 6.1 and 6.2.

8.5 DISCUSSION OF THE ROWE CELL TEST RESULTS

From the summary of the result in Table 7.1, 7.2 and 7.3 of c_v, m_v and K values, the following could be deduced;

(i) The drainage geotextiles (G1, G1CT, and G6) produced an improvement in the c_v value.

(ii) (a) the m_v values for those samples with drainage geotextiles were slightly lower when compared to those without a drainage material or provided with a reinforcement geotextile (G2, G3, G4, G5, and G7).
(b) lower Mv values were recorded as the level of pressure at which the

consolidation was carried out was increased.

(iii) the overall increase in permeability produced by the drainage geotextiles, (G1, G1CT, and G6) was up to 7 times. In the case of the reinforcement geotextiles, (G2, G3, G4, G5, and G7) no significance change in the permeability of the material was observed.

In both (ii) (a) and (b) the m_v values decreased with increase of the total axial pressure. Usually soils are more prone to high compressibility when they are silty and the values of m_v decrease with depth. It would therefore be expected and that the m_v values decrease with the increase level of pressure. In addition, the increase in pressure would trend to compress the geotextile drainage material thereby reducing the drainage properties.

Geotextiles Construction	Friction Coefficient f_b
Conventional geotextiles	
WOVENS	
Monofilament	0.6-0.8
Multifilament	0.75-0.9
Tape	0.5-0.7
NONWOVENS	
Melt-bonded	0.7-0.8
Needle-punched	0.7-0.8
Resin-bonded	0.6-0.7
KNITTEDS	
Weft	-
Warp	0.8-0.9
STITCH BONDED	0.75-0.9
Special geotextiles	
GEOGRID	
Cross-laid Strips	0.85-1.0
Punched sheets	0.85-1.0
GEOCOMPOSITES	
Strips	0.7-1.0
Bars	0.5-0.8
Lin structures	0.7-0.9

Table 8.1 Typical value of Friction for various geotextiles types (after ICI, 1990)

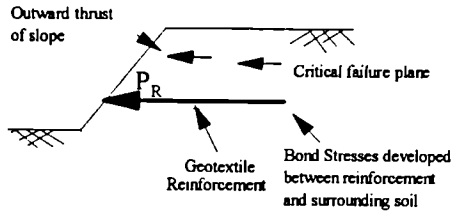

Fig. 8.1a: Application of bond between geotextile reinforcement/soil

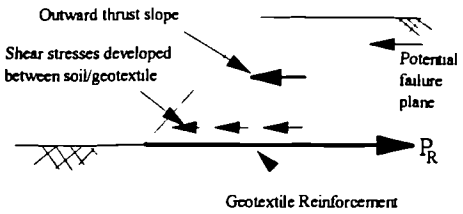

Fig. 8.1b: Application of direct sliding along surface of geotextile reinforcement

Fig. 8.1: Situation where the geotextile reinforcement interacts with the adjacent soils

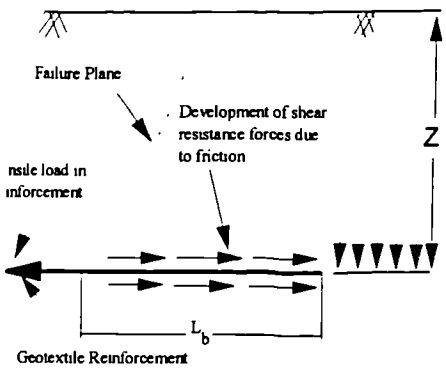

Fig. 8.2a: Soil / Reinforcement bond by friction

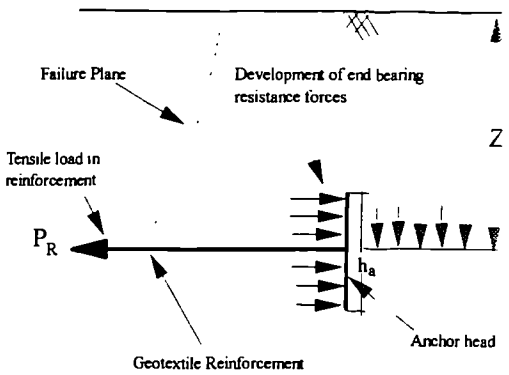

Fig. 8.2b: Soil / Reinforecment bond by end

Fig. 8.2: Soil / Reinforcement bond mechanisms

Fig. 8.1	Situation where the geotextile reinforcement interacts with the adjacent soil
Fig. 8.2	Soil/Reinforcement bound mechanisms

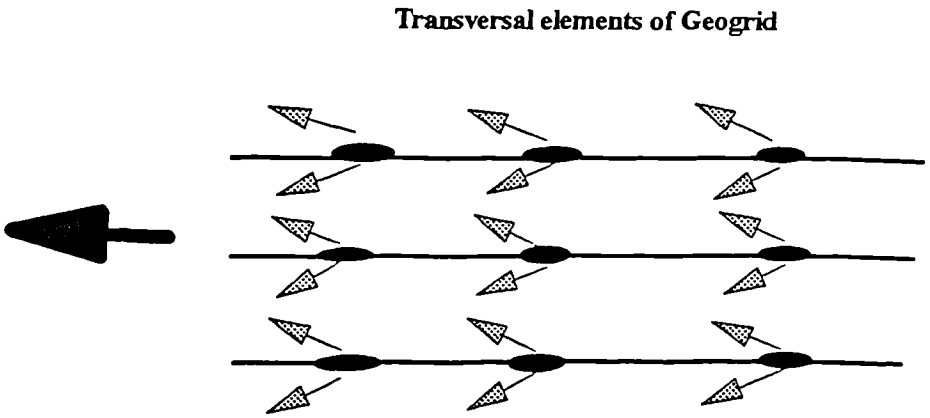

Fig. 8.3: Dilatancy behaviour of geogrid reinforced soil

Fig. 8.3	Dilatancy behaviour of geogrid reinforced soil

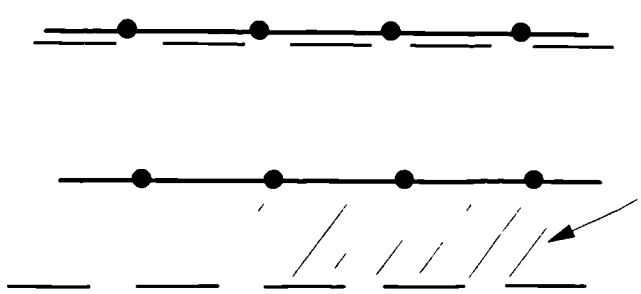

Combination of drainage geotextile (G1) and geogrid (G2) in the tests, (G1G2 sample)

Low friction due to the lubrication between surface of the geotextile

Drainage Geotextile *

Geogrid *

(* Graphical symbols IGS recommendation, 1991)

A proposed Geocomposite drainage and reinforcement material

Geogrid locked inside a thick non-woven geotextile (providing both drainage and reinforcement)

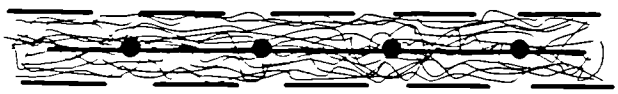

A thick non-woven geotextile (i.e. 4 - 8 mm thickness)

Fig. 8.4	Assumed the combination of drainage and reinforcement geotextile
Fig. 8.5	A proposed Geocomposite drainage and reinforcement material

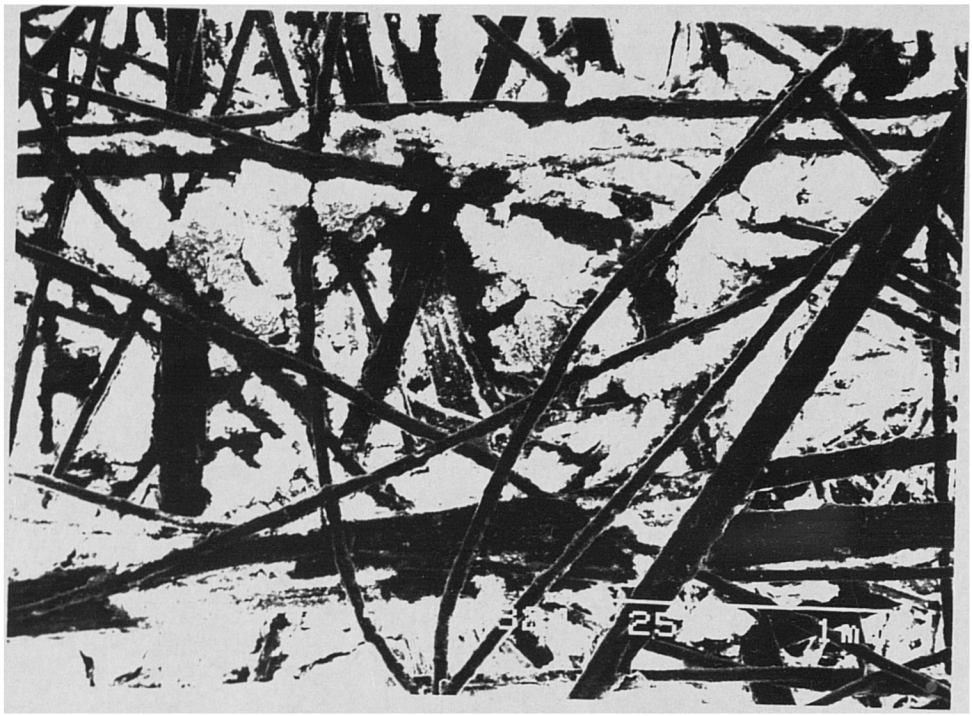

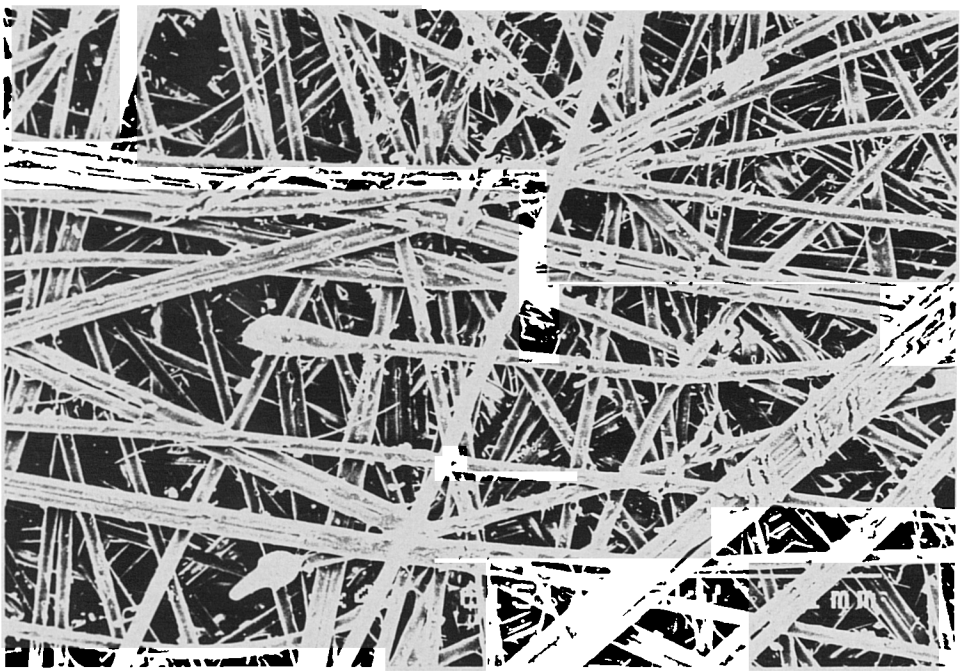

Plate 8.1	Surface Tensile Strain of Non-Woven geotextile, whit Kaolin and original closed appearance

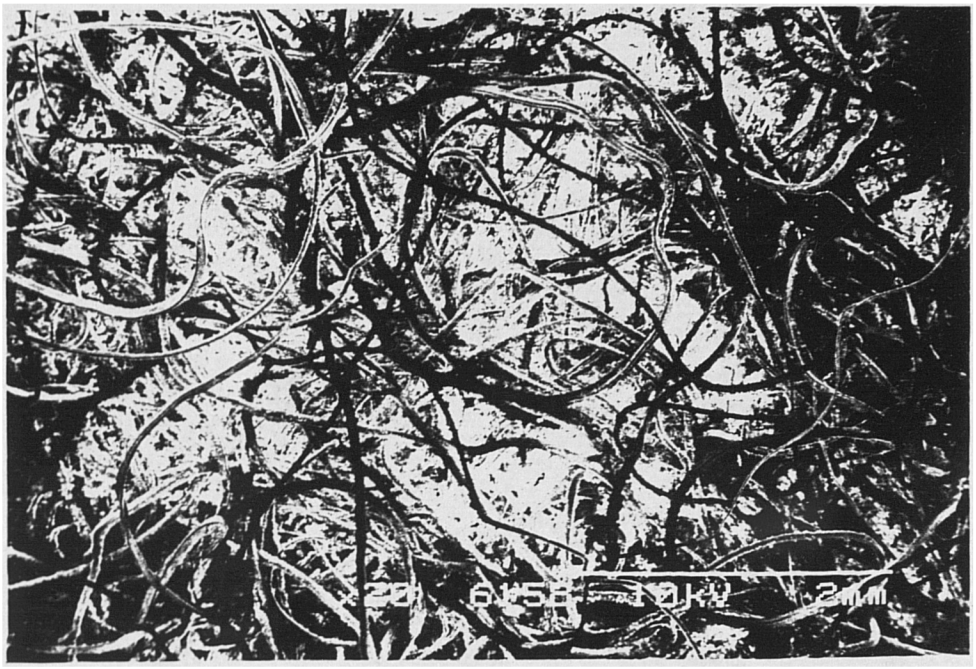

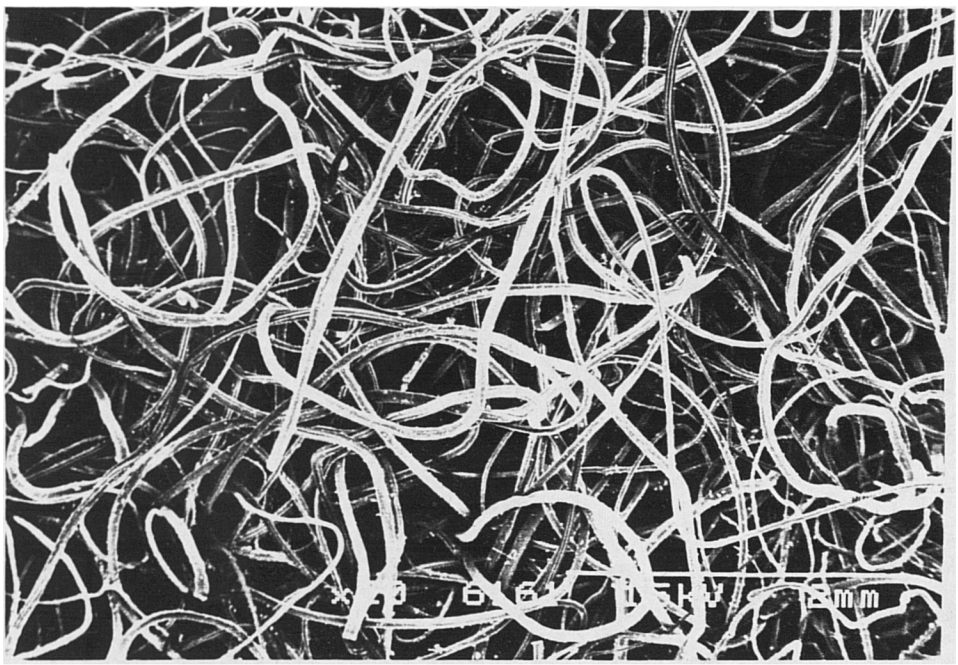

Plate 8.2	Surface Tensile Strain of Non-Woven geotextile, with Kaolin and original closed appearance

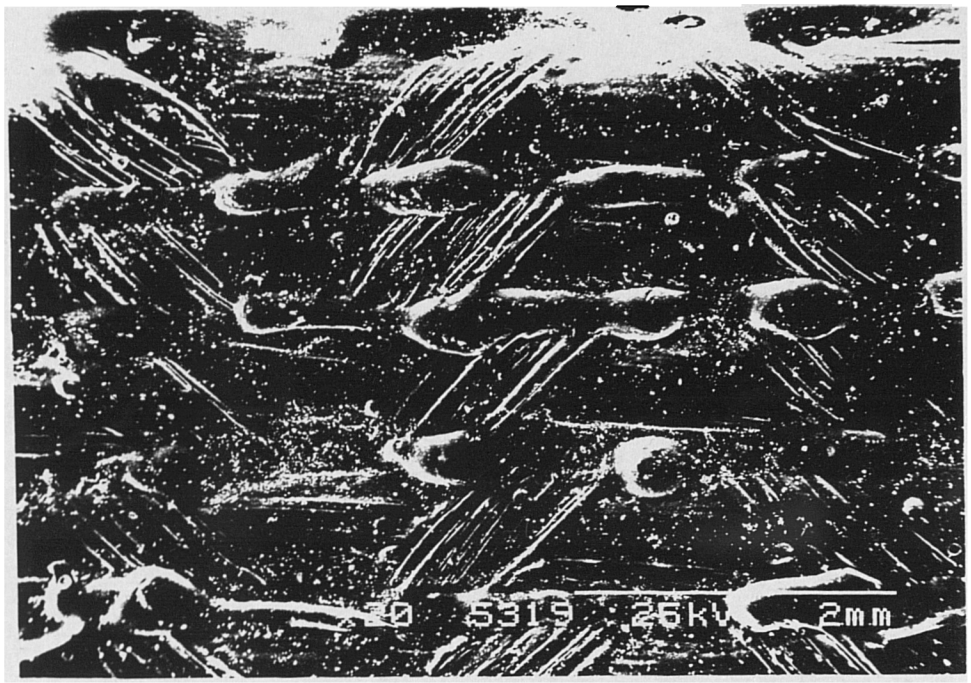

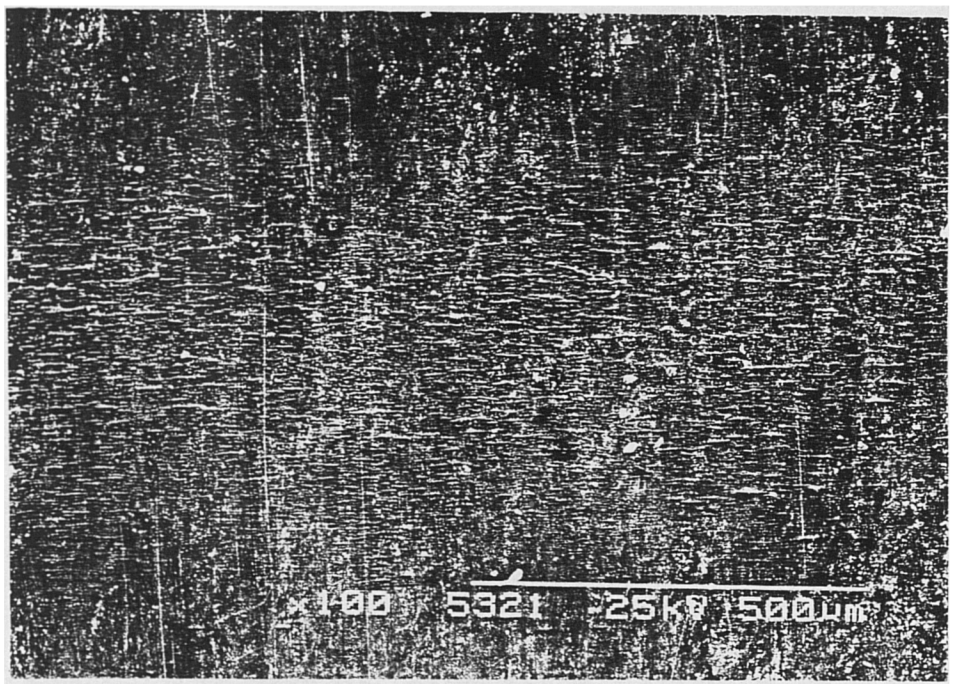

Plate 8.3	Smooth Surface of Geogrid, no sign of surface shear caused by Kaolin being sheared accrue the surface

CHAPTER NINE

ANALYSES OF REINFORCED SOIL AND DISCUSSION

9.1 INTRODUCTION

In this chapter the finite element modelling and analysis method is reviewed briefly. The advantages of using the finite element method for reinforced soil is discussed. The selection of appropriate parameters for reinforced soil analysis are discussed in the context of the experimental work undertaken in this study.

9.2 MODELLING AND ANALYSES

To describe the behaviour of engineering materials to loading, a number of conceptual models have been developed based on mathematical theory or on the results of experiments. The real behaviour of any material does not fully confirm to any model and there are always some differences. However, the accuracy of some conceptual models is adequate for the purpose of most engineering design.

Terzaghi's effective stress concept presented a theoretical model. Terzaghi stated that all measurable effects of change in stress in soils (such as compression, distortion , or change in shearing resistance) is due to changes in effective stress. The constitutive models provide a complete pattern of the stress - strain behaviour of soils starting from small strains to larger strains near failure and also range from relatively simple theories of isotropic linear elasticity to work hardening plasticity. If time effects are to be considered viscoelastic and viscoplastic theories could be used, such as with the Cam clay and modified Cam clay elasto-plastic models, Roscoe et. al. (1958 and 1963); Schofield and Wroth (1968).

Limit equilibrium analysis has been used in the design of earth structures for about 70 years. It has been extended to the design of geosynthetic-reinforced soil structures and this method of analysis is the normal, DOT, BE3/78 (1978) and BS 8006 (1991). The attractive feature of this analysis is its relatively simple input data. This leads to limited but useful output

design information. Practitioners can assess the reasonableness of the results of any analysis based on their experience and through simplified charts or hand calculations.

The most sophisticated modelling approach is finite element analysis. It can account for important factors associated with the design, construction, and detailing and, typically, it provides information in excess of what is needed for ordinary design. A hindrance in its routine use, however, is the extensive input data required to produce reliable results, and it does not provide a good estimation of the failure condition.

The alternative to analytical modelling of a problem is the testing of physical models. It is claimed that generalisations stemming out of such models should be made carefully. Small scale models do not necessarily duplicated the behaviour of full-scale prototypes. Alternatively, to conduct carefully-controlled full-scale tests, special constraints are imposed by the testing facility. Consequently, when extrapolating from full-scale tests to design, one must account for possibly different field conditions. However, one approach to achieve a reliable solution, is to analyses the data from a physical model using the finite element method thereby calibrating the model which can then be used to consider field conditions.

9.3 FINITE ELEMENT METHOD

9.3.1 Introduction

The commencement of a finite element analysis is the division of the component to be analysed into small elements. Some of the commonly available element types are shown in Fig. 9.1 . Each of these different sided elements can have different combination of degrees of freedom, depending on the use of the element. Element (g) in Fig. 9.1 for example is a simple bar element with two degrees of freedom at each node. However, if the element is given an additional bending stiffness, a further degree of freedom would be added to each node allowing the element (with the appropriate shape function) to be utilised as a bending element, (element h, Fig. 9.1). Similarly triangular and quadrilateral elements which have stress-strain functions could possess an additional pore-water-pressure function, allowing problems such as seepage in soil to be modelled.

In the simplest form, the minimum number of nodes in each element is equal to the number of corners in the element. Elements with one or more mid-side nodes are available for more accurate analysis, but it is doubtful if they offer much advantage on a "high order elements"

basis. The parabolic element with a single mid-side node is said to offer the best value per node, Naylor et. al. (1981).

In geotechnical work, triangular and quadrilateral elements in plane strain are generally employed. Truss elements with axial stiffness or beam elements with bending stiffnesses are employed to simulate the use of reinforcements, ties, beam or piles. Selection of the number, size and shape of element is dependant on experience and intuition. Smaller and greater numbers of elements are normally concentrated at potential areas of high stresses or strains, so as to obtain a better understanding of the behaviour in the area.

9.4 FINITE ELEMENT ANALYSIS OF REINFORCED SOIL

The finite element method provides a suitable analytical technique which is flexible enough to deal with a wide range of geotechnical problems. Following its formulation in the 1960s Zienkiwicz, et. al. (1970), the method has been used widely for embankment and dam studies (e.g. Hollingshead and Raymond 1971; Edwards and Jones 1978; Bassett and Leach 1980), more recently the method has been applied to reinforced soil. Several investigators including Andrawes et. al. 1982; Jones 1988; Heshmati, 1991; Tatsuoka 1992; and Wu 1992, have successfully used finite element techniques in the analysis of reinforced soil structures.

When applied to reinforced soil the method provides a powerful, alternative to limit equilibrium or plasticity techniques. In the most advanced formulation it has certain advantages over these other methods in that it gives specific details concerning displacements, stresses and strains at all points in the model at any time during construction or its working life. It can deal with complex loading conditions. In theory, any irregular geometry can be discretized using small elements of regular shape, usually triangles or quadrilaterals, and as a result it should be possible to use finite element analysis to solve all kinds of boundary problems that closed form analytical methods could not. A particular advantage of the finite element method lies in its ability to model non homogeneous and anisotropic materials, making it ideal theoretically for use in analysing reinforced soil.

The difficulties of producing accurate and consistent results in respect of reinforced soil analysis are illustrated by the wide spread of results presented at separate reinforced soil prediction symposiums including prediction Symposium held at King's College London in 1986; the NATO prediction Symposium held at the Royal Military College in Canada in

1987; and the Geosynthetics-Reinforced Retaining Walls Symposium, held at Denver, Colorado 1991.

One of the major sources of difficulty when applying the finite element method to geotechnical analysis arises from the constitutive models used to represent the behaviour of the soil. Jones (1985) notes that in practice there are two approaches to this problem. One is to model the soil by using a non-linear elastic model (Konder, 1963; Duncan and Chang, 1970). In this model a hyperbolic curve is used to represent the results of triaxial tests on the soil used as the fill. The hyperbolic mode is defined by two parameters only, related to the initial modulus ($1/a = E_I$) and the ultimate asymptotic strength (1/b), see Appendix B, Fig. B1. These hyperbolic models do not allow for dilatancy but do allow for a change in Poisson's ratio and have been the subject of criticism regarding the rate of volume change. However, when used over an appropriate stress and strain range they have found to produce accurate results, Jones (1988), Jones and Heshmati (1993).

The other type of model used to represent soil behaviour are the elasto-plastic stress-strain models based on the concepts of critical state soil mechanics. These model work in terms of effective stress parameters and attempt to predict the shear and volumetric behaviour of the soil. Finite element research into reinforced soil is now being done using these complex soil mode in various finite element programs. The relationship between stress and strain of soil is non-linear up to the design strength, as a result a non-linear analytical model of stress and strain for normal soil may be required for use with fine grained cohesive materials such as Kaolin.

The number of finite element programs have been developed for use with soils. Arguably the most successful in respect of reinforced soil is the FELSTA program initially developed by the former West Yorkshire Metropolitan County Council for the Department of Transport. FELSTA can be used as a plane strain or plane stress program and account can be taken of initial stresses, the construction sequence, and the presence of reinforcement or prestressing reinforcement. The program has been successfully used to predict accurately a range of reinforced soil structures. The hyperbolic stress-strain model used in the FELSTA program is described in Appendix B.

In the case of the FELSTA program the analysis also provides an indication of the percentage mobilised shear strength of the reinforced soil during the construction stages and in the serviceability condition.

$$MS = \frac{(\sigma'_1 - \sigma'_3)}{(\sigma'_1 - \sigma'_3)_d} \times 100\% \qquad (9.1)$$

Where:

MS = percentage of mobilised shear strength

σ'_1 = major principal effective stresses

σ'_3 = minor principal effective stresses

In the FELSTA program the elements, where the mobilised shear strength is equal to 100%, are eliminated from the solution and the stresses distributed. A plot of the percentage mobilised shear strength of the reinforced soil can be used to illustrate the remaining strength of the structure and can also be used to identify the predicted failure plane which in turn can be analysed using limit equilibrium methods, Jones (1988), Jones and Heshmati (1993).

An alternative to the relatively simple model represented by FELSTA is the Critical State Program (CRISP) written and developed at the Cambridge University since 1975, Britto and Gunn, (1987). This program has been used successfully by a number of researchers, Guest, (1989); Yogarajah and Yeo (1993), but it has not been conclusively documented that it can be model accurately the reinforced soil condition, Bolton (1992) and Sellahennadi, (1993). Sellahennadi has used the Critical State Program (CRISP) to model the triaxial tests described in this thesis but it was found that the commercial version of CRISP was not able to model either the triaxial test containing reinforcement or triaxial tests containing drainage. The triaxial tests containing no geosynthetic materials were modelled accurately. Consequently it can be concluded that CRISP is inferior to FELSTA in being able to represent a reinforced soil structure formed from fine grained soil and containing discreet drainage / reinforcement geotextiles.

9.4.1 Idealisation

Typically reinforcement is modelled using bar elements, which are capable of only tensile loads which are not subject to the usual restrictions on aspect ratio which state that normally formulated quadrilateral elements should be as near to square as possible. Between the reinforcement and the soil elements some researchers incorporate interface elements (Kwok, 1987). These interface elements allow for slippage to occur between the reinforcement and the soil after a threshold shear stress is acting on the interface. The model analysis provides

details covering the development of shear stress within the soil, the strains (and stresses) in the reinforcement and overall deflection of the facing and the base.

Interface or slip elements were initially created for rock joints and seams in which the influence of the joints rather than the rock types were thought to be dominant. Since then, the idea of providing an element to model the frictional properties between two materials has received wide attention, Goodman et. al, (1968); Clough and Duncan (1972); Romstad et al (1976); Naylor (1978); Hermann and Al-Yassin (1978); Andrawes et. al (1982); Desai et. al. (1984); Zienkiewicz (1988).

(i) Equivalent material approach

Romstad et. al. (1976) canvassed the idea of describing reinforced soil as a composite material, using the equivalent material approach Fig. 9.2a. In their study, they assumed a unit-cell concept in which reinforcement and adjacent soil together act to from an uniform material. The weighted average of the area and elastic modules of the two component elements (reinforcement and soil) are considered to determine the stress and strain in the system. The idealisation assumes that large amounts of reinforcement are used and that no slippage occurs between the reinforcement and the soil.

Naylor (1978), carried the equivalent material approach one step further by allowing for the provision of slip at the soil/reinforcement interface. Naylor's model allows for the transfer of shear stress by bond between the strips and soil and the transfer of shear through the soil. In the analysis, the shear stress is checked against the Mohr-Coulomb failure criterion. If the shear stress exceeds the limiting stress, slippage occurs and the shear modulus is adjusted accordingly to a specified value.

(ii) Spring Analogy

Hermann and Al-Yassin (1978) proposed a method of presenting the interface between the reinforcement and the soil elements by springs of specified stiffness. With the value of the shear displacement and the stiffness of the springs known, the shear stress along the interface can be obtained. A Mohr-Coulomb failure criteria was applied to limit the shear stresses developed.

Andrawes et. al. (1982) also used the spring analogy to model reinforced soil Fig. 9.2b. They assumed that the nodes between the two materials were attached to each other with springs of zero length, one parallel and the other perpendicular to the direction of sliding was large to avoid overlapping of the nodes at the line element, while the spring parallel to the

direction of sliding was based on a hyperbolic function. This modelling therefore allowed relative movement parallel to the direction of the reinforcement.

(iii) Thin element method

Zienkiewicz (1977) developed an element to model rock joints of finite thickness. The element was given a finite thickness, from the point of view of the stiffness formulation, although its nodes were assumed to coincide with its mid-section, Fig. 9.2c. The interface element was designed as an elastic material with shear stresses checked against Mohr-Coulomb yield criterion and corrected accordingly. To avoid numerical ill-condition, the thickness of the element was not to be too small and also the ratio of stiffness between the soil and interface be kept less than 1000.

Desai et. al. (1984) in a separate study developed a thin layer element for interfaces and joints with the same assumption made by Zienkiewicz (1977, 1988) regarding the non-zero thickness of the element. The element was formulated for either a linear-elastic, non-linear elasto-plastic material. Depending on the model used, slip was initiated when the shear stresses exceeded a predetermined value. The interface element was found to work best when the thickness to length (t/b) ratio was between 0.01 and 0.1.

(iv) Joint element method

Goodman et. al. (1968) developed eight-noded, zero thickness joint element, Fig. 9.2d. Based on an energy equation and allowing for absolute displacements, the element is built on the assumption that nodes have identical co-ordinates. The material property type is that of c', ϕ' material with a Mohr-Coulomb failure criterion. The stiffness parameters (k_s and k_n) are defined as shear and normal stiffness parameters. In the joint element method proposed, five different behavioural modes are discussed by Goodman et. al. (1968).

9.4.2 Interface Element

The interface element uses a strength of material concept. Modelling of interface requires careful treatment because of the sensitivity of the boundary conditions. Inappropriate boundary condition assignment may cause the elements to "break" and cause numerical ill-conditioning. Interface elements with different properties can be employed to model a range of adjoining surfaces, namely soil/soil, soil/wall and soil/reinforcement.

The soil/reinforcement interface element at the rear of the reinforced soil block can pose equilibrium problems in the analysis. Various modelling techniques have been developed to

accommodates this case. A typical connection arrangement used at the rear of the reinforcements is shown in Fig. 9.3. Elements 1 and 2 are assigned properties of frictional characteristics similar to reinforcement/soil frictional properties, while elements 3 and 4 represent a soil/soil interface with the soil parameters.

The properties used for the interface are dependant on the frictional characteristics developed along the two adjoining surfaces and are based on a ratio of the surface frictional properties between the soil and the adjoining surface. The soil/wall interface properties can be assumed to be two thirds of the soil/soil interface properties. For the cohesive soil the soil/wall interface properties can be assumed to be 2/3 of c and ϕ respectively.

9.5 SELECTION OF APPROPRIATE PARAMETERS FOR REINFORCED SOIL USING COHESIVE FILL

The design method currently employed for reinforced soil are essentially based upon Limit Equilibrium methods, Schlosser and Vidal (1969), Banerjee (1975), Department of Transport (1978) and BS 8006 (1991). The methods allow analysis of an assumed failure condition, but do not analyse working conditions. Analysis of the working condition requires a formulation of the soil-reinforcement system behaviour involving a valid kinematics behaviour model.

9.5.1 Limit Equilibrium Analysis

Selection of the analysis parameters for use with the Limit Equilibrium method are detailed in the design Codes and material specifications. These are based upon the shear strength properties of the fill material. The results of the triaxial tests undertaken as part of this work can be used directly with the limit equilibrium method. Arguably an increased value of the c′ or ϕ' parameter could be used to taken into account the improvement of properties provided by the different geotextile materials. Two design conditions can be identified for the results of the tests (i) the undrained (short term) condition which could hold during construction and (ii) the long term fully drained condition.

9.5.2 Finite Element Analysis

The use of the equivalent material approach is arguably the logical idealisation for the finite element analysis of reinforced soil structure formed from fine grained (cohesive) soils containing reinforcement / drainage geotextiles. The use of the critical state models represented by CRISP cannot be justified, but the simple hyperbolic model as used in

FELSTA could be used. The input data for the hyperbolic model is derived from triaxial tests of the soil and accordingly the results of the experimental work provide the complete input data. Assuming that the number of reinforcement layers would be large and that the spacing between each layer is small this approach could be justified. Any initial stresses could be provided, based upon compaction theory. The weakness of the approach would be the lack of information concerning the stresses in the reinforcement but at small strains these could be nominal.

9.6 SUMMARY

(i) The finite element method is a powerful and versatile method of carrying out parametric analyses of the behaviour of the reinforced soil structures.

(ii) The finite element program FELSTA, based upon a simple non-linear elastic hyperbolic model has been shown to provide accurate predictions of the behaviour of reinforced soil structures in use.

(iii) The input data for the hyperbolic model is data derived from triaxial tests conducted in the laboratory on the proposed fill material.

(iv) It can be concluded that the hyperbolic model can be used to describe the behaviour of fine grained cohesive soil containing different combinations of geosynthetic materials to provide drainage or reinforcement. The practical application of the model could be in the finite element program FELSTA in which idealisation of a reinforced soil structures would best be achieved using the unit cell concept.

(v) The commercial version of the Critical State Program (CRISP) could not be made to model the triaxial tests containing different geotextiles and therefore cannot realistically be used to model reinforced soil structures formed from the same materials.

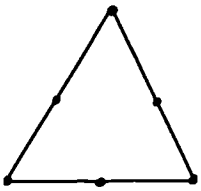

(a) linear strain triangular element
(6 nodes, 12 d.o.f)

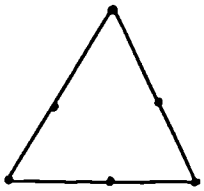

b) Linear strain triangular element
(6 nodes, 15 d.o.f.)

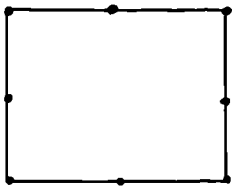

c) Linear strain quadrilateral element
(8 nodes, 16 d.o.f.)

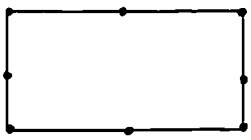

d) Linear strain quadrilateral element
(8 nodes, 20 d.o.f.)

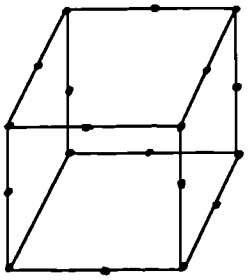

e) Linear strain brick element
(20 nodes, 60 d.o.f.)

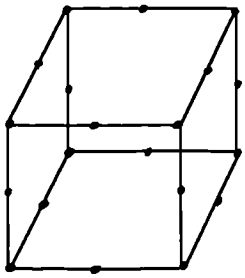

f) Linear strain brick element
(20 nodes, 68 d.o.f.)

g) Bar element
(3 nodes, 6 d.o.f.)

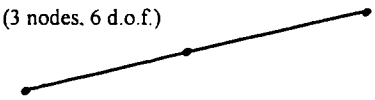

h) Beam element
(3 nodes, 9 d.o.f.)

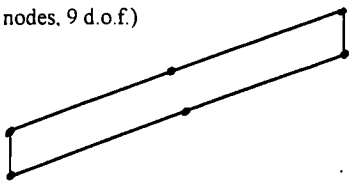

i) Interface element
(6 nodes, 12 d.o.f.)

Fig. 9.1	Typical Types of Elements

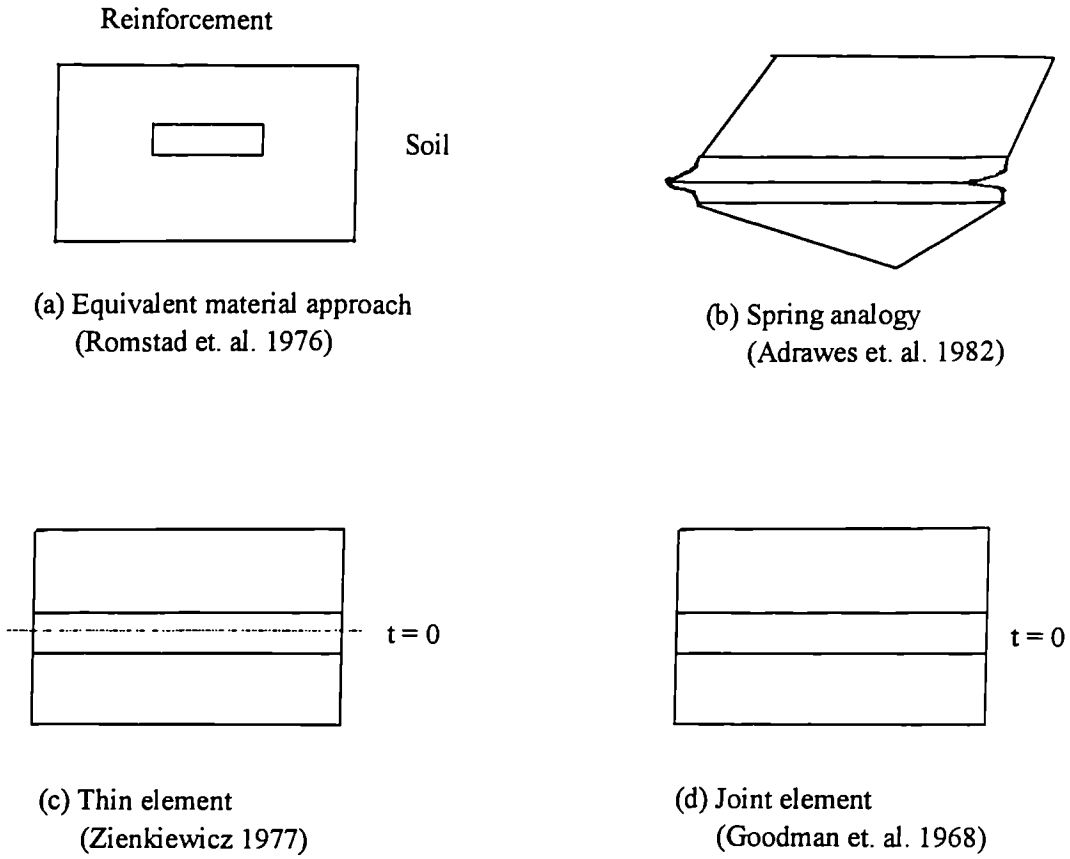

(a) Equivalent material approach (Romstad et. al. 1976)

(b) Spring analogy (Adrawes et. al. 1982)

(c) Thin element (Zienkiewicz 1977)

(d) Joint element (Goodman et. al. 1968)

Fig. 9.2	Type of Interface Elements

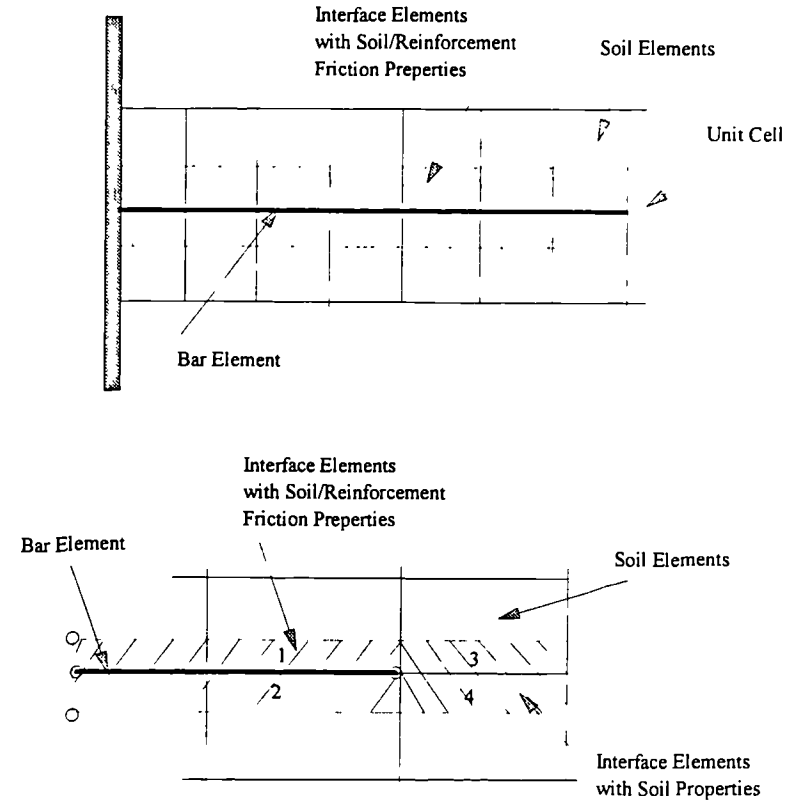

Fig. 9.4	Typical Connection Arrangement of Soil/Reinforcement Interface Element

CHAPTER TEN

CONCLUSIONS AND SUGGESTIONS FOR FURTHER RESEARCH

10.1 INTRODUCTION

Good quality frictional fills could be difficult to obtain at economic rates consequently the use of reinforced soil in some parts of the world is limited. Fine grained cohesive soils are low cost materials which are available for potential use in many locations for use as reinforced fill. However, cohesive soils are more complex and soil structures built with these materials are susceptible to change in moisture content. There is little experimental evidence to support the use of cohesive fill in reinforced soil structures and their use is excluded in many material design Codes. Most research on reinforced soil has constructed in the use of cohesionless fills. Recent studies in Japan indicate the cohesive soils with water contents up to 130 per cent can be adequate as reinforced soil fill provided the correct type of reinforcement is selected.

The presence of an inclusion can favourably effect the behaviour of the soil fill used in a reinforced soil structure. Various design approaches based on theoretical and experimental have been suggested by a number of researchers to describe the effect of inclusions mostly associated with good quality cohesionless fill and reinforcement. Little is known about the potential benefits of the drainage on soil containing an inclusion although this can be a complementary function, by "improving" the properties of soil fill.

From the Triaxial tests, it was concluded that the cohesion (c') of kaolin and the overall shear strength of the sample increased with the introduction of a range of geotextiles. This was due to the improved consolidation or reinforcement of the samples that was developed by the presence of the geotextiles. The magnitude of the cohesion improved by up to five times the original value, with the apparent cohesion of the kaolin rising from 9 to 45 kPa.

The value of the angle of internal friction (ϕ') was generally decreased by introduction of a geotextile material. There was no significant difference in the internal friction presented by the reinforced samples which used a reinforcement geotextile such as geogrid. There is a small difference of internal friction for the sample when a drainage geotextile was introduced. This lends support to the conclusion that the drainage geotextiles used were effective.

The use of a composite geosynthetic material made up of a drainage geotextile and a reinforcement geogrid did not result in an increase in shear strength properties. This was unexpected. It is possible that the drainage geotextile maintained a water layer in between the plane of the reinforcement inclusion and the drainage material causing some reduction in the friction angle at the this position. Failure probably occurred along this plane. A different geosynthetics in which the reinforcement is embedded within the drainage geotextile could produce a much different and more positive result.

10.2 CONCLUSIONS

(i) The results of both the consolidated undrained and consolidated drained triaxial compression tests obtained in this study suggested that:

a. The cohesion of the kaolin and overall shear strength of the sample increased with the introduction of a range of geotextiles. The improvement was the result of improved consolidation hastened by the presence of the geotextile.

b. The comparison of the laboratory results of both the consolidated undrained and consolidated drained triaxial compression tests with the requirements for fills for field use, indicates that properly selected geotextiles are capable of providing both drainage and reinforcement functions when used with a cohesive soil.

c. The consolidated drained test is more reliable than the undrained test when studying geotextiles with good hydraulic conductivity.

d. The reinforcements which offer the potential of being suitable for use with fine grained soils are geogrids and geotextiles.

e. Geogrids alone can provide an effective reinforcing function in cohesive soil, the main

criteria for success being selection of the correct grid aperture.

f. The mechanism of reinforcing is different according to the stiffness of reinforcements with stiff reinforcements such as geogrids, the soil is strengthen by frictional resistance between soil and reinforcements.

g. Polymer-based materials (woven and non-woven) are the best materials for the reinforcement of cohesive fill materials. Non-woven geotextile can provide the combined function of drainage and tensile-reinforcement.

h. Non-woven geotextiles can provide two important hydraulic functions related to cross-plane flow (filtration) and in-plane (drainage) when embedded in soil.

i. Thick geotextiles which have sufficient interconnecting pore structures to allow fluid flow within its plane, can be used to provide inplane drainage.

(ii) The results obtained from the laboratory Rowe Cell tests indicate:

j. Drainage geotextiles can be used to improve the drainage of cohesive fills and the use of these materials frequently results in improved strength characteristics of these soils.

k. The use of geotextile composite materials could help provide better compaction of cohesive fills and more efficient drainage from the interior of the fill whilst some geosynthetic materials can also provide effective tensile reinforcement. Some non-woven geotextiles function well as a drainage for cohesive soil, maintaining a high degree of suction (i.e. negative pore water pressure).

l. Thick non-woven geotextiles could be used as potential drainage materials not only in embankments but at any location where the rapid dissipation of pore pressures from a cohesive soil is required.

m. The use of drainage geotextiles in cohesive soils could be a means of construction embankments from fine grained soil to higher heights than are currently used.

n. The triaxial test results using geotextile materials as drainage/reinforcement indicate that the Japanese practice of using cohesive (fine grained) soil as fill for reinforced soil

structures is justified.

o. The use of fine grained soils in reinforced soil structures could result in major savings.

p. It is possible for cohesive soils to be used in embankments with a higher moisture content and much higher heights than previously constructed by the incorporation of geotextiles. In addition fill materials with high initial moisture contents could be used.

(iii) The conclusion from the SEM investigation and numerical studies suggested that:

q. The interaction between soil/geotextile is partly influenced by the interface frictional resistance between the Kaolin and the surface of the geotextile which may be caused by the cohesion of the Kaolin and roughness and the surface texture of the geotextile. The binding between particles of Kaolin and the surface of the geotextile, is a function of the moisture content of the fill.

r. The frictional properties of hard geogrids depends upon the interface friction angle along a contact surface between the soil and the materials.

s. Dilatancy is an important factor in determining the restraining effect of geogrid reinforced soil. This may not be a significant factor for geotextiles, which are in direct contact with the soil surface.

t. The finite element method is a particularly powerful and versatile method of carrying out a parametric analysis of the behaviour of the reinforced soil models. Some finite element models offer an advantage associated with the ultimate limit state as they can be used to identify potential failure planes, these can then be checked using limit equilibrium methods.

u. If the correct idealisation is made and the selection of material parameters is accurate, very close agreement can be achieved between the performance of the model and the real structure.

v. The hyperbolic model can be used to describe the behaviour of fine grained cohesive

soil combined as the geotextiles. The results of the experimental triaxial tests can be used directly as the input data for an established finite element program which itself has been used successfully in predicting the behaviour of reinforced soil.

10.3 SUGGESTIONS FOR FURTHER STUDY

The following recommendation are made for further study:

(i) Further investigation should be carried out as in these tests with higher moisture contents, i.e. > 100 per cent which could simulate a heavy rain fall in the construction.

(ii) In further investigations of the introduction of geotextiles in plane strain condition it would be better to study samples of a larger size (i.e. 300mm diameter). In addition the effect of using muli-layers of geotextile in the soil sample instead of just one layer in the middle should be studied.

(iii) The effect of compaction on the interaction between cohesive soil and geotextile should be studied. The friction between cohesive soil and geotextile should be investigated further.

(iv) Different geotextiles could be investigated to identify the potential for short / long term clogging of the geotextile.

(v) Measurement of the in-plane hydraulic conductivity of different geotextiles which could be used with cohesive soil are required.

(vi) It may be worthwhile to study the effect of geotextiles when using waste materials especially PFA instead of using kaolin even though the PFA itself already has a high value of shear strength.

(vii) The use a combined drainage / reinforcement geotextile produced an unexpected answer in that the expected improvement did not materialise. This should the subject of additional study. Using "***mixed***" materials rather than "***combined***" materials.

(viii) Improvements in the critical state soil model are needed in order that this advanced

model can be used to model cohesive soils containing inclusion offering drainage and reinforcement.

(iv) The improvement in the drainage of cohesive soil using electrically conduction geosynthetics materials based upon the principal of electo osmosis is a logical extension of the current research.

REFERENCES

Al-Hassani, M.M., (1978)
"Investigation of Stress-Strain Behaviour of Sand Tested in Plane Strain With and Without Sheet Inclusions", PhD Thesis, University of Strathclyde, Glasgow.

Al-Hassani, M.M., and Johnson, L.D (1978)
"Numerical Analysis of a Reinforced Earth Wall", ASCE Symp. on Earth Reinforcement, Pittsburgh, Pennsylvania, pp. 127-156.

Andrawes, K.Z., McGown, A. (1977)
"Alerations of Soil Behaviour by Inclusion of Materials with Different Properties", Proc. Sym. on Reinforced Earth and Other Composite Soil Techniques, TRRL/Heriot Watt Univ., Edinburgh. pp. 88-108.

Andrawes, K.Z., McGown, A., Wilson-Fahmy, R.F. and Mashour, M.M. (1982)
"The finite element method of analysis applied to soil-geotextile systems", Proc. 2nd Int. Geotextiles Conf., Las Vegas, pp. 695-700.

Bacot (1974)
"Etude Theorique et Experimentale de soutenement realise en terre armee", Claude Bernard University - Lyon.

Bagir, T. (1944)
"Iraq. Journal", pp. 5-6, British Museum.

Bassett. R.H., and Last, N.C. (1978)
"Reinforcing earth below footings and embankments", Proc. ASCE, Spring Convention, Pittesburgh, pp. 47-53.

Bassett. R.H., and Leach, G. (1980)
"A Comparison of Two Soil Models In a Finite Element Analysis of An Embankment". Proc. Sym. On Computing In Highway Eng. University of Cambridge, pp. 157-199.

Banerjee, P.K. (1975)
"Principles of Analysis and Design of Reinforced Earth Retaining Walls", Highway Eng. London, Vol. 22, No. 1, pp.13-18.

Beckham, W. K. & Mills, W. H. (1935)
"Cotton fabric reinforced roads", Engineering News Record 115, 14, 3, 453-455,

Bell, J. R. , Szymoniak, T. and Thommen, G. R. (1984)
"Construction of a steep sided geogrid retaining wall for an Oregon coastal highway", Proc. Polymer Grid Reinforcement Conf., London, Thomas Telford, 198-202.

Bishop, A.W. (1959)
"Teknisk Ukeblad", No. 39, 1959, pp. 859-863.

Bishop, A.W. and Henkel, D.J (1982)
"The Measurement of Soil Properties", Edward Arnold, London.

Blight, G.E., and Dane, M.S.W. (1989)
"Deterioration of a Wall complex Constructed of reinforced Earth, Geotechnique., Vol. 29, No. 1, pp. 47-53.

Bolton, M.D. (1986)
"The Strength and Dilatancy of Sands", Geotechnique, Vol. 36, No.1, pp. 65-78.

Bolton, M.D. (1992)
"Private Communication", Cambridge, 23 September 1992.

Britto, A. M. and Gunn, M.J. (1987)
"CRISP users and programmers manual", Cambridge University.

Britto, A. M. and Gunn, M.J. (1987)
"Critical State Soil Mechanics Via Finite Elements", Ellis Horwood, Chichester.

Broms, B.B. (1977)
"Polyester fabric as Reinforcement in Soil", Int. Conf. on the Use of Fabric in Geotech., Paris, Vol. 1, pp 129-135.

BS 6906 (1987)
"Determination of Tensile Properties, Using a Wide Width Strip", British Standard on the Methods of Testing Geotextiles", British Standard Institute, London.

BS 8006 (1991)
"Code of Practice for Strengthened reinforced Soil and Other Fills", British Standard Institute, London. draft for Public Comment.

BS 6906: Part 3 (1987)
"Determination of Water Flow Normal to the Plane of the Geotextile Under a Constant Head", British Standard Institute, London.

BS 6906: Part 7 (1987)
"Determination of In-Plane Water flow", British Standard Institute, London.

BS 1377 (1975)
"Methods of Test for Soils for Civil Engineering Purposes", British Standard Institute, London.

BS Institution (1988)
"Strengthened/reinforced Soil and other Fills", 1988 pp.16.

CFGG (1989)
"Recommendations pour l'emploi des g'eotextiles dans les syste'mes de drainage et de filtration", Committee Francais des Geotextiles et Geomembranes., Paris, 23pp.

Chapuis (1972)
"Report Research LCPC", Inst. Mech. Canadian Geotech. Jrnl. Vol. 14 No.3, PP. 389-398.

Chandrasekaran, B. (1988)
"An Experimental Evaluation of Fabric Strength Properties and Behaviour of reinforced Soil", M.Eng. Thesis, National University of Singapore.

Chang, J.C., (1977)
"Design and Field Behaviour of reinforced Earth Wall", J. Geotech. Eng. Div., ASCE, Vol. 103 No. GT7, pp 677-692.

Chang, J.C., Hannon, J.B. and Forsyth, R.A. (1977)
"Pull-out Resistance and Interaction of Earthwork Reinforcement and Soil", Transportation Research Record 640, Washington, D.C., pp. 1-7.

Christopher, B. R. and Holtz, R. D. (1984)
"Geotextile Engineering Manual", U.S. Department of Transportation, Federal Highway Administration, pp.1-6, 2-59, 2-63.

Christopher, B. R. and Holtz, R. D. (1985)
"Geotextile Engineering Manual", STS Consultants, Ltd., Northbrook, Illinois: Report to Federal Highway Administration, No. FHWA-TS-86/203. 10-44 pp.

Christopher, B. R. and Holtz, R. D. (1988)
"Geotextile Design & Construction Guidelines", U.S. Department of Transportation, Federal Highway Administration, NHI Course No. 13213, 297pp.

Clarke, B.G., TRI Utomo, S.H. and Jones, C.J.F.P (1990)
"Geotechnical properties of Tilbury Power Station Ash", Research Report, University of Newcastle upon Tyne.

Clough, G.W., and Duncan, J. M. (1972)
"Finite Element Analysis of Retaining Wall Behaviour. J. of Soil Mech. and Found. Div., ASCE, Vol. 93 SM4, pp 529-549.

Coulomb, C. A. (1973)
"Essai sur une Application des Regles des Maximis et Minimus a Quelques Problems de Statiques Relatifs a 1' architecture", Man. Acad. de Pres, Vol. 7, pp. 343-382, Paris.

Coyne, M.A. (1929)
"French Patent Specification No. 656.692.

Craig, R. F. (1987)
"Soil Mechanics", 4th Ed. pp 10 - 99 and 353.

Department of Transport (1978)
"Reinforced Earth Retaining Walls and bridges Abutments for Embankments", Technical Memorandum (Bridges) BE3/78 (Revised 1987), H.M.S.O., London.

Desai, C.S. and Siriwardane H.J. (1984)
"Constitutive Laws for Engineering Materials", Prentice-Hall Inc., NJ.

Duncan, J.M., Chang, C.Y. (1970)
"Nonliner Analysis of stress and strain in soils", Journal of the Soil Mechanics and Foundation Division, Proceedings of the American Society of Civil Eng.. pp. 1629-1653.

Edil, T.B., Motan, S.E., and Toha, F.X. (1981)
"Mechanical behaviour and testing methods of soils Laboratory shear strength of soil", Symp. of Soil and Rock for Eng. Purposes, American Society for Testing and Materials, University of Florida, 1981, pp. 114-129.

Edwards, L.W. and Jones, C.J.F.P. (1978)
"Non-linear finite element analysis of the trent embankments", J. Int. Numerical Methods in Geomechanics.

Work Yorkshire Metropolitan County Council (1977)
"Manual of the plane stress/strain finite element structural analysis including linear and non-linear stress-strain material properties", FELSTA. pp. 136.

Elias, V., and Swanson, P. (1978)
"Gautions of Reinforced Earth with Residual Soil", Transportation Research Record 919, pp. 21-24.

Fischer, G.R., Christopher, B.R. and Holtz, R.D (1990)
"Filter Criteria based on Pore Size Distribution", Proc. 4th Int. Conf. on Geotextiles, Geomembranes and Related products, The Hague, Vol. 1, 289-293.

Foreword, J., Legrad, J., Schlosser, F. (1976)
"Reinforecd Earth", Note D, information Technique, Laboratoires Central des Pont et Chaussees, 23 pp.

Giroud, J. P. (1982)
"Filter Criteria for Geotextiles", Proceedings Second International Conference on Geotextiles, Las Vegas, Vol. 1 pp 103-108.

Giroud, J. P. (1988)
"Review of Geotextiles Filter Criteria", Proc. First Indian Geotextiles Conf., Indian Institue of Technology, Bombay, Vol. 1, pp 1-6.

Giroud, J. P., *Gourc, J. P., Bally, P. and Delmas, P. (1977)*
"Behaviour of a nonwoven geotextile in an earth dam", Proc. Int. Conf. on the Use of Fabrics in Geotechnics, Vol. 2, 213-218. (In French.)

Goodman, R.E., Taylor, R.L. and Brekker, T.L. (1968)
"A Model for the Analysis of Jointed Rocks", J. Soil. Mech. Fdns. Div., ASCE, Vol. 94, SM3, pp. 637- 659.

Guest, D. R. (1989)
"An experimental and analytical study of Reinforced Earth Embankments". A PhD Thesis King's College, London

Guilloux, A., and Jailloux, J.M. (1979)
"Full Scale Failure Test on Reinforced Earth wall by Accelerated Corrosion", Proc. of Int. Conf. Soil Reinforcements, Paris (LCPC), pp. 503-508.

Guler, E. (1990)
"Lime Stabilized Cohesive Soil as a Fill for Geotextile Reinforced Retaining Structures", Proc. 4th Int. Conf. on Geotextiles, Geomembranes and Related Products, The Hague. Vol. 1, pp.39-44.

Haliburton, T. A., C. C. Anglin and Lawmaster, J. D. (1978)
"Selection of Geotechnical Fabrics for Embankment Reinforcement", Report to U.S. Army Engineer District, Mobile, Oklahoma State University, Stillwater, 138pp.

Hassan, C.A.B. (1992)
"The Use of Flexible Transverse Anchors in Reinforced Soil", PhD. Thesis, University of Newcastle upon Tyne.

Hausmann, M.R. (1976)
"Strength of Reinforced Earth", Proc. of 8th Australian Road Board Conf., perth.

Heerten, R. G. (1981)
"Geotextiles in Coastal Engineering", RILEM Materials and Structures, Research and Testing, No. 82, pp. 273-282.

Heerten, R. G. (1986)
"Functional design of Filters using Geotextiles", Proc. 3th Int. Conf. on Geotextiles, Vienna, Vol. 4, pp 1191-1196.

Hermann, L.R. and Al-Yassinn, Z. (1978)
"Numerical Analysis of Reinforced Soil System. Symp. on Earth Reinforcement, ASCE, Pittsburgh, pp. 428-457.

Head, K. H. (1982)
"Permeability, shear strength and compressibility", Manual of Soil Laboratory Testing Volume 1 and 2, London.

Head, K. H. (1986)
"Effective Stress Tests", Manual of Soil Laboratory Testing Volume 3. London. pp 787-788; 872-877.

Healy, K. A. and Long, R. P. (1971)
"Prefabricated subsurface drains", Highway Research Record 360 57.

Heshmati, S., Jones, C.J.F.P, and Zakaria, N.Z, (1990)
"Effect of Composites Non-Woven Geotextile on the Consolidation and Shear properties of Kaolin", Proc. First Int. Seminar on Soil Mech. and Found. Eng. of Iran, Tehran, Vol. 3. pp 864-870.

Heshmati, S. (1991)
"Prediction of the Behaviour of Two Test Walls by non-linear elastic analysis", Class A Prediction Symposium, Denver, Colorado, USA, August, 1991.

Hillen, H. J. F. (1968)
"A protective facing particularly for shore protection", Brit. Pat. No. 1111453.

Hollingshead, G.W., and Raymond, G.P. (1971)
"Prediction of Undrained Movements Caused By Embankments On Muskeg", Can. Geot. Jour., Vol. 8, No. 1. pp.23-35.

Holtz, R. D. (1975)
"Recent developments in reinforced earth", Proc. Seventh Scand. Geotechnical Meeting, Polyteknisk Forlag, Denmark 281-291.

ICI Geotextiles, (1988)
"Designing for subsurface drainage", The manual for designing with geotextiles, Chemical and Polymers Ltd. pp. 54.

International Geotextile Society, (1993)
"Recommended Mathematical and Graphical Symbols", A recommendation manual. 19 pp.

Ingold, T.S. (1979)
"The Effects of Compaction on Retaining Structures", Geotechnique, Vol. 29, No. 3, pp. 265-283.

Ingold, T. S. (1980)
"Reinforced clay", PhD thesis, University of Surrey. pp. 252.

Ingold, T.S. (1981)
"A Laboratory Simulation of Reinforced Clay Walls", Geotechnique, Vol. 31, pp 399-412.

Ingold, T.S. and Miller, K.S. (1982)
"The behaviour of geotextile reinforced clay subjected to undrained loading", Proceeding of Second International Conference on Geotextiles, Las Vagas. pp. 593-597.

Ingold, T.S. (1983)
"Laboratory Pull-Out Testing of Grid Reinforcements in Sand", Geotechnical Testing, J., Vol. 6, No. 3, pp. 101-111.

Iwasaki, K. and Watanabe, S. (1978)
"Reinforcement of railway embankments in Japan", Proc. ASCE Symp. on Earth Reinforcement, Pittsburgh, 473-500

Janbu, N. (1963)
"Soil Compressibility as Determined by Odometer and Triaxial tests", European Conference on Soil Mechanic & Foundation Engineering, Wiesbaden. Vol. 1, pp. 259-283.

Jewell, R.A (1980)
"Some Effects of Reinforcement on the Mechanical Behaviour of Soils", Ph.D. Thesis, University of Cambridge.

Jewell, R.A (1985)
"Limit Equilibrium Analysis of Reinforced soil Walls", Proc. Eleventh Int. Conf. on Soil Mechanics and Foundation Eng., Vol. 2, San Francisco, pp. 1705-1780.

Jewell, R. A. (1987)
"The Mechanics of Reinforced Embankments on Soft Soils", University of Oxford, Report No. OUEL 1694/87; and published in Geotextiles and Geomembranes, Elsevier, Vol. Vol.7, No. 3, 1988.

Jewell, R.A (1987)
"Direct shear tests on sand", Univ. of Oxford, Report No. OUEL 1719/88; Dept. of Eng. Science.

Jewell, R.A (1988)
"Compatibility, Serviceability and Design Factors for Reinforced Soil Walls", Theory and Practice of Earth Reinforcement, Proc. Int. Sym on the Theory and Practice of Earth Reinforcement, Japan, pp. 611-616.

Jewell, R.A (1990)
"Strength and deformation in reinforced soil design", Keynote Paper. Proc. Geotextiles, Geomembranes and Related Products, Hague. pp. 1-79, Balkema.

Jewell, R.A., and Jones, C.J.F.P. (1981)
"Reinforcement of clay soils and waste using grids", Proc. Tenth Int. Conf. on Soil Mechanics and Foundation Eng., Vol. 3, Stockholm, pp 701-706.

Jewell, R.A., and Wroth, C.P. (1987)
"Direct Shear Tests on Reinforced Sand", Geotech. 37, No.1. pp.53-68.

Jewell, R. A. and Greenwood, J. H. (1988)
"Long Term Strength and Safety in Steep Soil Slopes Reinforced by polymer Materials", Geotextiles and Geomembranes, Elsevier, Vol. 7, Nos. 1 and 2, pp 81-118.

Jewell, R. A., and Milligan, G.W.E. (1989)
"Deformation Calculation for Reinforced Soil Walls", Proc. 12th ICSMFE, Vol. 2, Rio de Janeiro, pp. 1257-1262.

Jewell, R. A., Milligan, G.W.E., Sarsby, R.W. and DuBois, D. D (1984)
"The interaction between soil and geogrids", Proc. Symp. on Polymer Grid Reinforcement in Civil Engineering, London. 22-23 March 1984.

Jones, C. J. F. P. (1973)
"Field Measurements of Earth Pressures Against Motorway Retaining Walls and Bridge Abutments", Symp. on Field Instrumentation, British Geot. Society, Part I, pp. 107-219.

Jones, C.J.F.P. (1978)
"The York Method of Reinforced Earth Construction", ASCE Sym. on Earth Reinforcement, Pittsburgh, Pennsylvania, pp. 501-527.

Jones, C. J. F. P. (1985)
"Earth Reinforcement and Soil structures", Butterworths, P. 192, (Revised reprint 1988), London.

Jones, C. J. F. P. (1988)
"Predicting The Behaviour of Reinforced Soil Structures", Theory and Practice of Earth Reinforcement, Proc. Intr. Gete. Sym. on the Theory and Practice of Earth Reinforcement, Japan, pp. 535-540.

Jones, C.J.F.P. (1990)
"Construction influences on the performance of reinforced soil structures", State of the Art Review, Int. Reinforced Soil Cons. pp. 67-92 Glasgow, Scotland.

Jones, C.J.F.P. (1991)
"Code of Practice for Strengthened/Reinforced Soils and Other Fills", British Standard 8006. Draft for Public Comment. October. pp.1-232.

Jones, C.J.F.P. (1992)
"The Economic Construction of Reinforced Soil Structures", Int. Symp. on Recent Case Histories of Permanent Geosynthetic-Reinforced Soil Retaining Walls-Seiken Symp., Tokyo Japan.

Jones, C. J. F. P. (1992)
"Polymer Reinforcements in Permanent Soil Structures", Geotropika' 92, University Teknologi Malaysia, pp 1-32.

Jones, C.J.F.P and Hassan, C.A. (1992)
"Compression movements within reinforced soil structures", Geotropika' 92, Johor Bharu, Malaysia, p. 8.

Jones, C.J.F.P and Hassan, C.A. (1992)
"Reinforced soil formed using synthetic polymeric anchors". Pro. Int. Symp. On Earth Reinforcement Practice, Kyushu.

Jones, C. J. F. P., and Heshmati, S. (1993)
"The use of the Finite Element Method to Predicted the Performance of Reinforced Soil Walls", Int. Congress on Computational Methods in Eng., Shiraz University, Shiraz, Iran, pp. 357-364.

Jones, C. J. F. P., Heshmati, S. (1993)
"The Action of Geotextile to Provide Combined Drainage and Reinforcement to the Cohesive Soil", Second Int. Seminar on Soil Mech. and Found. Eng. of Iran, Tehran.

Jones, C.J.F.P., and Sims, F.A. (1975)
"Earth Pressure Against Abutments and Wing Walls of Standard Motorway Bridges", Geotechnique Vol. 25, No. 4, pp. 731-732.

Kempton, G.T., Enwistle, R. W. *and Barclay, M.J. (1985)*
"An Anchored Fill Harbour Wall Using Synthetic Fabrics", Proc. Instn. Civ. Eng. Part 1. pp. 42-65.

Keown, M. P. and Oswalt, N. R. (1984)
"US Army Corps of Engineers experience with filter fabric for stream bank protection applications", Proc. Int Conf. Flexible Armoured Revetments Incorporating Geotextiles, London, pp. 227-238.

Koerner, R. M. (1986)
"Designing with Geosynthetics", Prentice-Hall, N. J.

Koerner, R. M. and Welsh, J. P. (1980)
"Construction and Geotechnical Engineering Using Synthetic Fabrics", John Wiley & Sons, New York.

Koerner, R. M., Bove, J. A., and Martin, J.P. (1984)
"Water and air transmissivity of Geotextiles", Geotextiles & Geomembrane, Vol. 1, 1984, pp. 57-73.

Kondner, R. L., (1963)
"Hyperbolic Stress-Strain Response of Cohesive Soils", Proceedings of the American Society of Civil Engineers. Vol. 1, pp. 289-33.

Kwok, C.M. (1978)
"Finite Element Studies of Reinforced Embankments on Soft Ground", PhD. Thesis, Sheffield University.

Ladd, C. C. , Foott, R. , Ishihara, K. , Schlosser, F. and Poulos, H. G. (1977)
"Stress-Deformation and Strength Characteristics", State-of-the-Art Report, Proc. Ninth Int. Conf. on Soil Mechanics and Foundation Eng., Tokyo

Lambe, T.W., (1951)
"Soil Testing for Engineers", John Wiley and Sons , USA.

Lambe, T.W., (1967)
"Stress Path Method", Journal of the Soil Mechanics and Foundation Division, Proc. of the American Society of Civil Engineers. Vol. 3, pp. 117-141.

Lamberton, B. (1983)
"Fabric-Formed Revetment Technology", Geotechnical Fabrics Report 1,Vol. 1.pp. 4-10

Lawson, C. R. (1982)
"Geotextile Requirements for Erosion Control Structures", Proc. Sym. on Recent Developments in Ground Improvement Techniques, Asian Institute of Techailand, pp 177-192.

Lawson, C. R. (1986)
"Geosynthetics for Soil Reinforcement", Proc. Sym. on Geotextiles in Civil Engineering, Institution of Engineers, Australia, Newcastle, July, pp 1-35.

Lawson, C. R. (1986)
"Geotextile Filter Criteria for Tropical Residual Soils", Proc. Third Int. Conference on Geotextiles, Vienna, Vol. 2, pp 557-562.

Ling, H. I. and Tatsuoka, F. (1992)
"Nonlinear analysis of Reinforced Soil Structures by Modified CANDE Programme", Proc. of Int. Sym. on Geosynthetic Reinforced Soil Retaining Walls, Denver, Colorado, Balkema, Rotterdam.

Ling, H. I. and Tatsuoka, F. (1992)
"Effects of anisotropic consolidation on the performance of soil-geosynthetic composite at plane strain compression", Geotechnical Engineering Laboratory Report, Institute of Industrial Science, University of Tokyo, Japan. pp. 165-168.

Long, N.T. (1977)
"Some Aspects about Fill Material in Reinforced Earth", Proc. TRRL/ Heriot-Watt Univ. Sym. Reinforced Earth and other Techniques, pp. 246-249.

Long, N.T., Guegany, Y., and Legeay, G. (1972)
"Triaxial Apparatus", Research Report LCPC, No. 17. pp 16-33.

McGown, A. and Ozelton, M. W. (1973)
"Fabric membranes in flexible pavement construction over soils of low bearing strength", Civil Engineering and Public Works Review Vol. 68, No. 798, pp. 25-29.

McGown, A., Andrawes, K.Z., and Al-Hasani, M.M. (1978)
"Effect of Inclusion Properties on the Behaviour of Sand", Geotechnique. Vol. 28, No. 3, 327-346.

McGown, A., Andrawes, K.Z., and Kabir, M.H. (1982)
"Load Extension Testing of Geotextiles confined in Soil", Proc. 2th Int. Conf. on Geotextiles, Las Vegas, Vol.3 pp. 793-798.

McGown, A., Paine, N., and DuBois, D.D. (1984)
"The use of geogrid properties in design", Proc. Symp. Polymer Grid Reinforcement in Civil Eng., London. pp. 18-30.

McGown, A., Murray, R.T., and Andrawes, K.Z. (1987)
"The influence of Lateral Boundary Yielding on the Stresses Exerted by Backfills", Conf. of Soil Structure Interaction, Paris, pp. 585-592.

McGown, A., Jewel, R.A. and Murray, R.T. (1988)
"State of the Art Report on Reinforced Soil", Proc. Int. Conf. on Geotextiles, Rio De Janeiro, Brazil.

McGown, A., Yogarajah, I., and Yeo, K.C. (1992)
"The choice of Soil Properties in Limit State Analysis of Reinforced Soil Retaining Structures", Proc. Int. Conf. on Retaining Structures, Cambridge, UK.

McKittrick, D.P. (1978)
"Reinforced Earth- Application of Theory and Research to Practice", Proc. Sym. Soil Reinforcing and Stabilising Techniques, Sydney, Australia.

Milligan, G.W.E., (1982)
"Some scale model tests to investigate the use of reinforcement to improve the performance of fill on soft soi", Q. J. Eng. Geological Society, London, Vol. 15, pp. 209-215.

Milligan, G.W.E., and Love, J.P. (1985)
"Model testing of geogrids under an aggregate layer on soft ground", Polymer Grid Reinforcement. Thomas Tefford Limited, London, 1985.

Mitchell, J. K. and Villet, W. C. B. (1987)
"Reinforcement of Earth Slopes and Embankments", National Cooperative Highway Research Program Report 290, Transportation Research Board, National Research Council, June.

Mineral Resources Consultative Committee, (1982)
"Common Clay and Shale", Mineral Dossier, No.22.

Ministry des Transports (French Ministry of Transport/LCPC (1979)
"Reinforced Earth Structures Recommendations", Rules of the Art.

Munster, A. (1925)
"United States Patent Specification", No. 1762343.

Murata, O, Tateyama, M., Tatsuka, F., Nakamura, K., and Tamura, Y. (1991)
"A reinforcing method for earth retaining wall using short reinforcing members and a continuos rigid facing", ASCE Geotechnical Eng. Congress, Denver.

Murray, R. T. (1977)
"Research at TRRL to develop design criteria for Reinforced Earth", Symp. Reinforced earth and other composite soil techniques. Heriot-Watt University, TRRL Sup. 457

Murray, R.T. (1983)
"Studies of Behaviour of Reinforced and Anchored Earth Walls", PhD. Thesis, Heriot- Watt University, Edinburgh.

Murray, R.T. and Irwin, M.J. (1981)
"A Preliminary study of TRRL Anchored Earth", TRRL Supplementary Report 674, Transport and Road Research Laboratory, Growthorne, Uk.

Murray, R.T., and McGown, A. (1992)
"Ground Engineering Applications of Fin Drains for Highways", Dep. of Transport, Application Guide 20, TRRL, Crowthorne.

Naylor, D.J. (1978)
"A Study of Reinforced Earth Walls Allowing Strip Slip", ASCE Sym. on Earth Reinforcement, Pittsburgh, Pennsylvania, pp. 618-643.

Naylor, D.J., Pande G.N., Simpson, B. and Tabb, R. (1981)
"Finite Elements in Geotechnical Engineering", Pineridge Press., Swansea.

O'Rouke, T.D. and Jones, C.F.J.P. (1990)
"Overview of Earth Retention Systems, 1970-1990", ASCE Geotechnical Spec. Publication. No. 25, pp 22-51.

Osman, M.A. (1977)
"An Analytical and Experimental Study of Reinforced Earth Retaining Walls", PhD. Thesis, University of Glasgow.

Osman, M.A., Finlay, T.W., and Suntherland, H.B. (1979)
"The Internal Stability of Reinforced Earth Wall", Proc. Int. Conf. on Soil Reinforcement, Paris (LCPC), Vol. 1, pp. 107-112.

Ogink, H. J. M. (1975)
"Investigations on the Hydraulic Characteristics of Synthetic Fabrics", Delft Hydraulics Laboratory, Publication No. 146.

Palmeira, E. M. and Milligan, G. W. E. (1987)
"Scale and Other Factors Affecting the Results of Pull-Out Tests of Grids Buried in Soil", University of Oxford, Report No. OUEL 1678/87.

Pasley, C.W. (1822)
"Experiments on revetments", Vol. 2, Murray, London.

Puig, J., Bilvet, J. C. and Pasquet, P. (1977)
"Earth fill reinforced with synthetic fabric", Proc. Int. Conf. on the Use of Fabric in Geotechnics, Vol. 85-90.

Rankilor, P. R. (1981)
"Membranes in Ground Engineering", John Wiley & Sons, Inc.,
London, England, pp. 377.

Romstad, K.M., Hermann, L.R. and Shen, C.K. (1976)
"Integrated Study of Reinforced Earth-I: Theoretical Formulation", Geotech. Eng. Div., ASCE, Vol. 102, No. GT5, pp. 457-471.

Roscoe, K.H., and Burland, J.B. (1958)
"On the generalised Stress-Strain behaviour of Wet Clay, Engineering Plasticity", 2nd European Conf. in Soil Mech., pp. 535-607.

Roscoe, K.H., and Poorooshasb, H.B. (1963)
"A Theoretical and Experimental study of Strain in Triaxial Compression Tests on Normally Consolidation Clays", Geotechnique, Vol. 13, pp. 12-38.

Sellahennadi, D. (1993)
"Use of CRISP in Cohesive Triaxial Tests", MSc. Thesis, University of Newcastle upon Tyne.

Schlosser, F. and Vidal, H. (1969)
"Reinforced Earth", Bull. de Liaison des, Laboratories, Routiers Ponts et Chaussees, Paris No. 41, pp101-144.

Schlosser, F. and Vidal, H. (1969)
"Le Terre Arme'e", Bulletin de liaison LCPC, No. 41, pp. 101-144.

Schlosser, F. (1972)
"La terre armee - recherches et realisations", Bull. de liaison LCPC, No. 62, pp. 79-92.

Schlosser, F. and Elias, V. (1978)
"Friction in Reinforced Earth", ASCE Symp. on Earth Reinforcement, Pittsburgh, Pennyslyvaia, pp. 735-763.

Schlosser, F. and Long, N.T (1973)
"Recent results in French Research on Reinforced Earth" J. Construction Div., Am. Soc. Civ. Eng., Vol. 100, No. CO3, pp. 2223-237.

Schober, M. and Teind, H. (1979)
"Filter-Criteria for Geotextiles", Proc. Seventh European Conference on Soil Mechanics and Foundation Engineering, Brighton, Vol. 2, pp 121-129.

Schofield, A. N., and Worth, C.P. (1986)
" Critical State Soil Mechanics", McGraw Hill, London.

Sims, F. A., and Jones (1974)
"The Use of Soil Reinforcement in Highway Schemes", Proc. Int. Conf. Soil Reinforcement, Paris, Vol. 2, pp 361-366.

Simons, A. and Menzies, C. (1977)
"A Short Course In Foundation Engineering", ELBS, London.

Smith, A.K.C. (1977)
"Experimental and Computational Investigation of Model Reinforced Earth Structures",

PhD. Thesis, Cambridge University.

Terzaghi, K. (1943)
"Theoretical Soil Mechanics", Wiley.

Tatsuoka, F., Sate, T., Iwasaki, K., Yamada, S. and Naito, S. (1983)
"Performances of a Test Embankment of Kanto-Loam Reinforced with Nonwoven Fabric", JSSMFE, Vol. 3.

Tatsuoka, F., Ando, H., Iwaski, K., and Nakamura, K. (1985)
"Reinforcing of Cohesive-soil-Embankment with Nonwoven Fabric", JSSMFE, Vol.3.

Tatsuoka, F. and Yamauchi, H. (1986)
"A reinforcing method for steep clay slopes with a non-woven geotextile" , Geotextiles and Geomembrane, Vol.4, pp. 241-268.

Tatsuoka, F., Ando, H., Iwasaki, K., and Nakamura, K. (1986)
"Performances of Clay Test Embankments Reinforced with a Non-Woven Geotextile", Third International Conference on Geotextiles, Vienna, Austria. Vol. 2. pp. 355-360.

Tatsuoka, F, Musata, O, Tateyyama, N. K., Tamuta, Y, Ling, H.I., Iwasaki, K. and Yamauchi, H. (1990)
"Reinforcing steep clay slopes with a non-woven geotextile", B.G.S. Int. Reinforced Soil Conference, Glasgow, Scotland. pp 24-35.

Tatsuoka, F. (1992)
"Permanent Geosynthetic-Reinforced Soil Retaining Walls for Railway Embankment In Japan", Int. Symp. on Recent Case Histories of Permanent Geosynthetic-Reinforced Soil Retaining Walls, Tokyo, Japan.

Walkinshaw, J. L. (1975)
"Reinforced Earth Construction", Dept. of Transportation FHWA Region 15 Demonstration project No. 18

Westergaard, H. M. (1938)
"A problem of elasticity suggested by a problem in soil mechanics, Soft material reinforced by numerous strong horizontal sheets", Harvard University

Wu, J.T.H. (1991)
Proc. of Int. Symposium on Geosynthetic Reinforced Soil Retaining Walls, Denver, Colorado, Balkema.

Wu, J.T.H., Barrett, R. and Chou, N.N.S. (1992)
"Developing cost-effective geosynthetic-Reinforced Soil Walls, Recent Efforts in Colorado U.S.A.", Inte. Symp. on Recent Case History of Permanent Geosynthetic-Reinforced Soil Retaining Walls, Tokyo, Japan.

Vidal, H. (1969)
"The principal of Reinforced Earth", Highway Research Record, No. 2 pp. 1-16.

Vidal, H (1978)
"The Development and Furtuer of Reinforced Earth", ASCE Sym. on Earth Reinforcement, Pittsburgh, Pennsylvania, pp. 1-61.

Wamaya, B.M (1989)
"Effects of a Geotextile on the Drainage, Consolidation and Shear Properties of Kaolin as a Construction Material in Embankments", MSc. Thesis, University of Newcastle upon Tyne.

Yang, Z (1972)
"Strength and deformation characteristics of reinforced sand", Ph.D. Thesis, University of California at Los Angeles, 233 pp.

Yang, Y. (1992)
"Study of the mechanical properties of pulverised fuel ash for use in geotechnical application", PhD Thesis, University of Newcastle upon Tyne.

Yang, Y., Clarke, B.G., and Jones, C.J.F.P. (1993)
"A classification of pulverised fuel ash as an engineered fill", Proceeding of Int. Conference Engineered fills, University of Newcastle upon Tyne. pp 367-397.

Yogarajah, I. (1993)
"Effects of construction procedures on the behaviour of geogrid reinforced soil walls", PhD thesis, University of Strathclyde, Glasgow, UK.

Yogarajah, I., and Yeo, K.C. (1993)
"Finite Element Modelling of Pull-Out Tests with Load and Strain Measurements", (In press, Geotextiles and Geomembrane).

Zakaria, N.A. (1990)
"Effects of a Geotextile on the Drainage and Shear Properties of Kaolin as a Construction Material in Embankments", MSc. Thesis, University of Newcastle upon Tyne.

Zienkiewicz, O. C., Best, B., Dulage, C. and Stagg, K.G. (1970)
"Analysis of Non-Linear Problems in Rock Mechanics with Particular Reference to RockMechanics", Jou. of Strain Analysis, pp. 172-182.

Zienkiewicz, O. C. (1977)
"Finite Element Method", 3rd. Ed. McGraw-Hill.

Zienkiewicz, O. C. (1988)
"Finite Element Method", Vol. 1. Ed. McGraw-Hill.

APPENDIX A

Triaxial Test Results and Rowe Cell Test Results

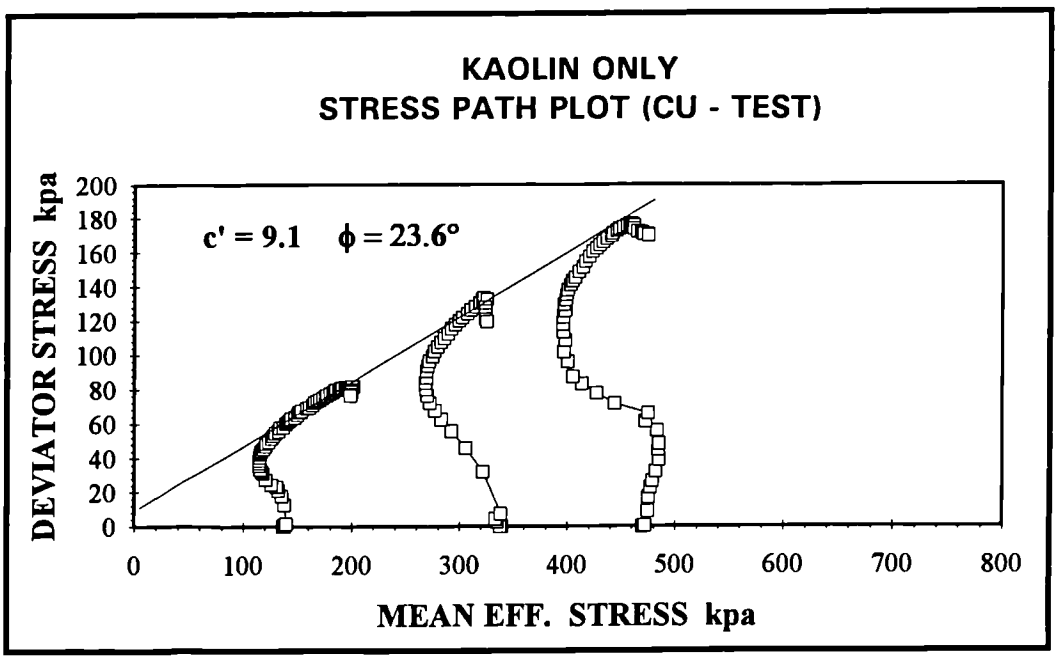

Fig. 1 Stress path plot, consolidated undrained compression triaxial test

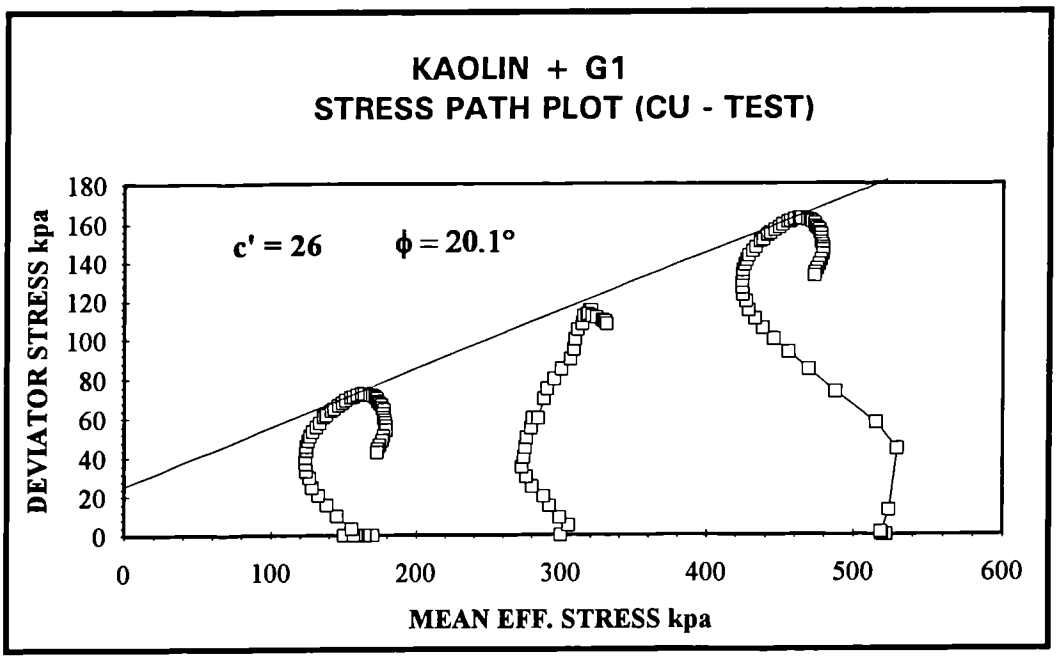

Fig. 2 Stress path plot, consolidated undrained compression triaxial test

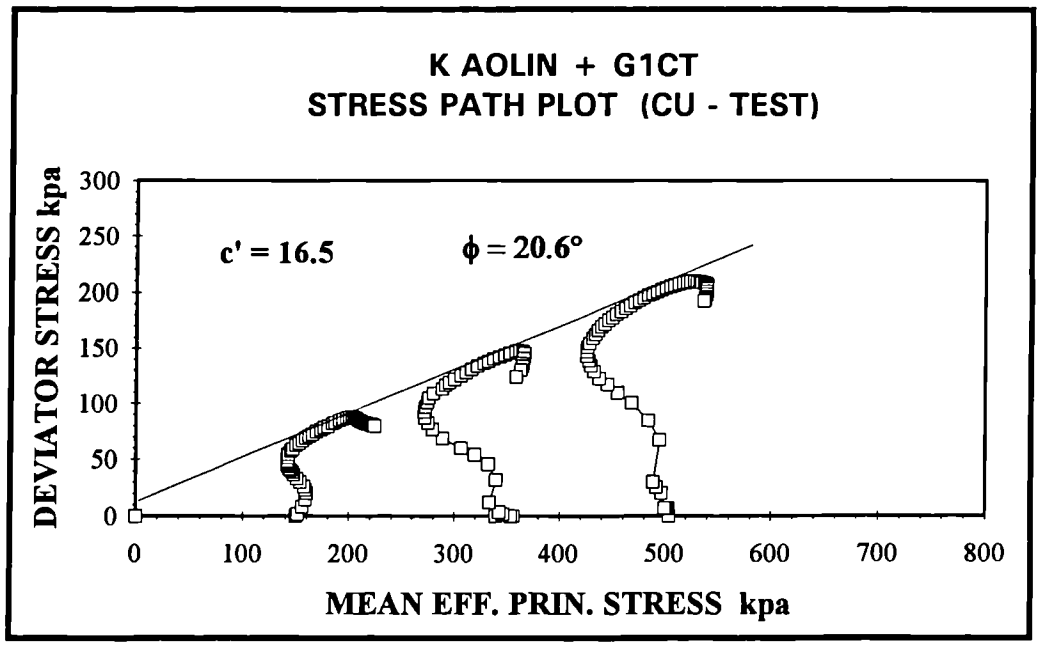

Fig. 3 Stress path plot, consolidated undrained compression triaxial test

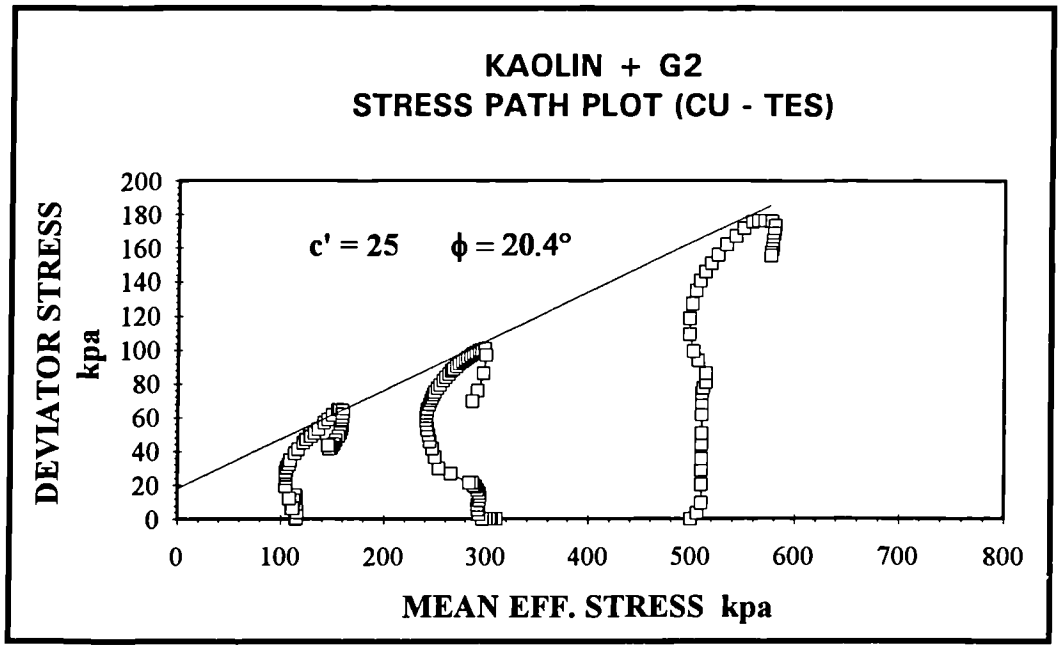

Fig. 4 Stress path plot, consolidated undrained compression triaxial test

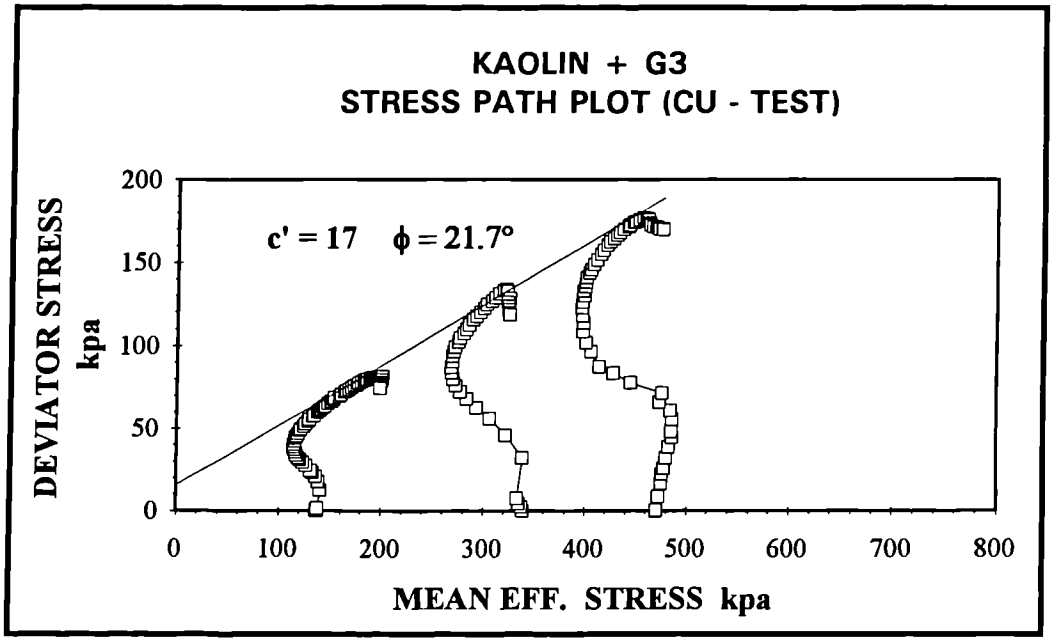

Fig. 5 Stress path plot, consolidated undrained compression triaxial test

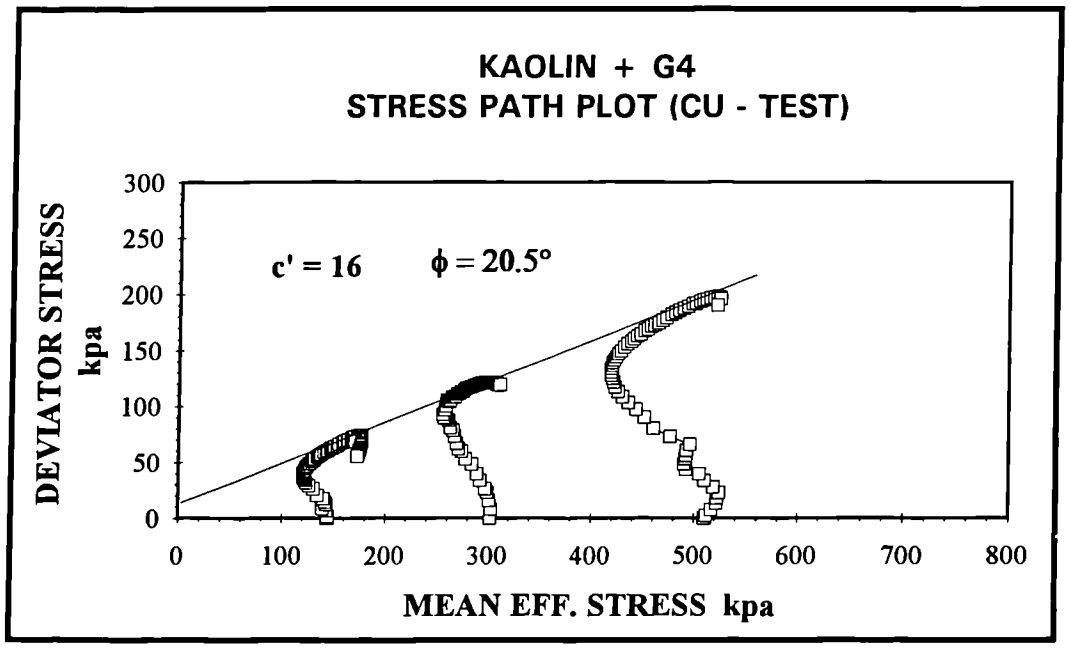

Fig. 6 Stress path plot, consolidated undrained compression triaxial test

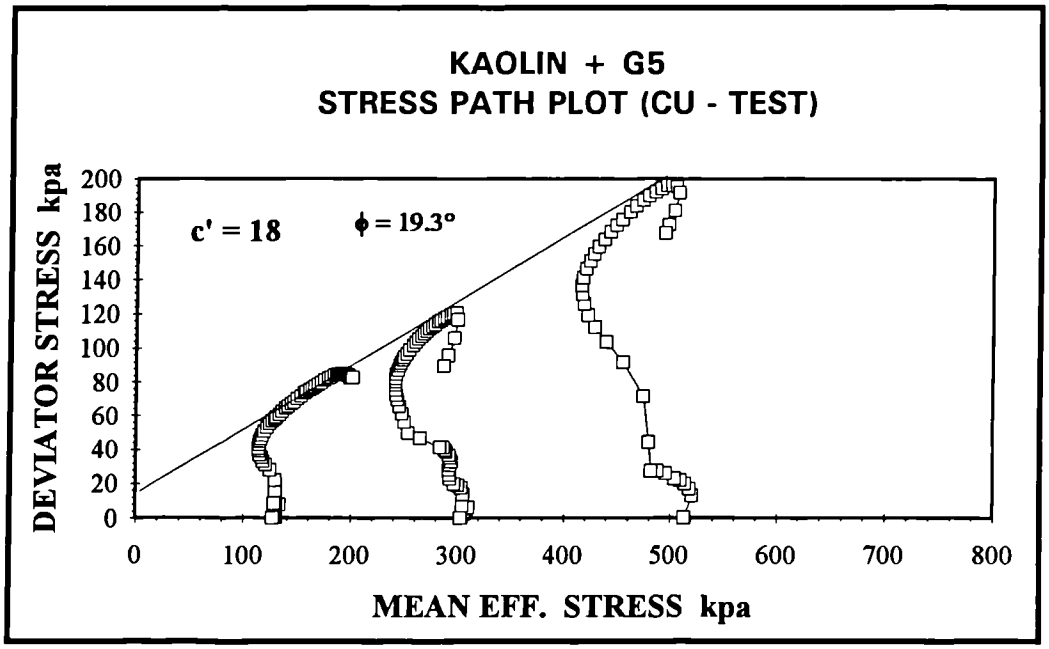

Fig. 7 Stress path plot, consolidated undrained compression triaxial test

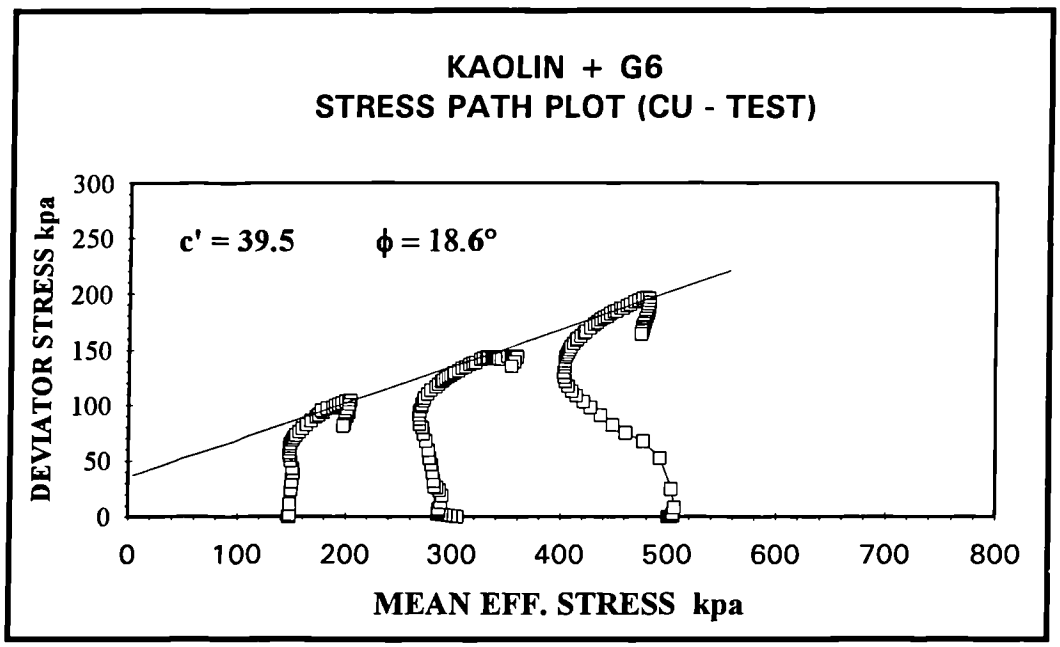

Fig. 8 Stress path plot, consolidated undrained compression triaxial test

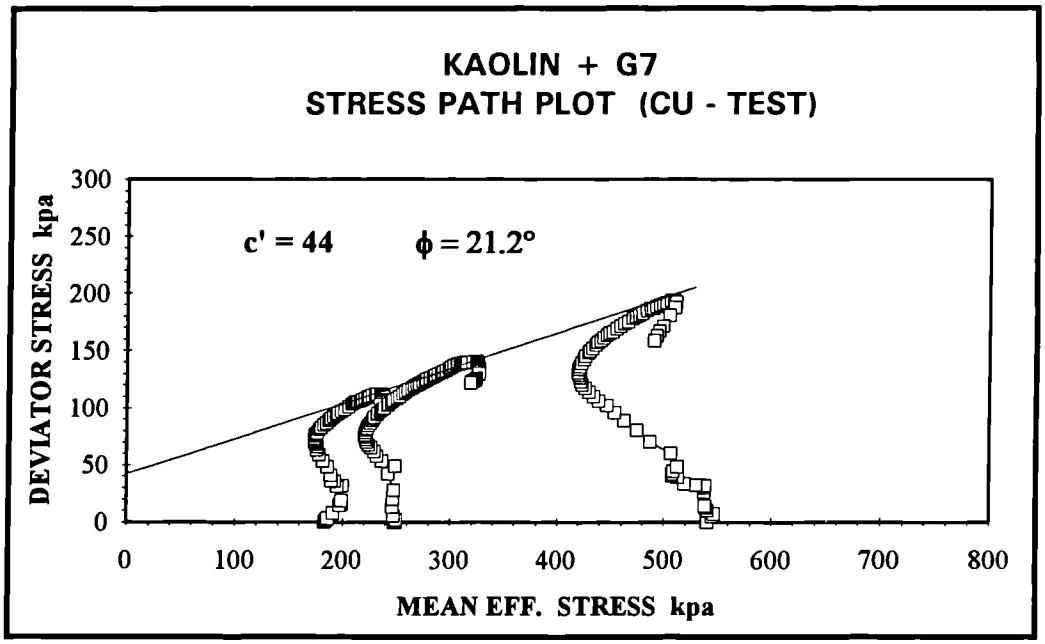

Fig. 9 Stress path plot, consolidated undrained compression triaxial test

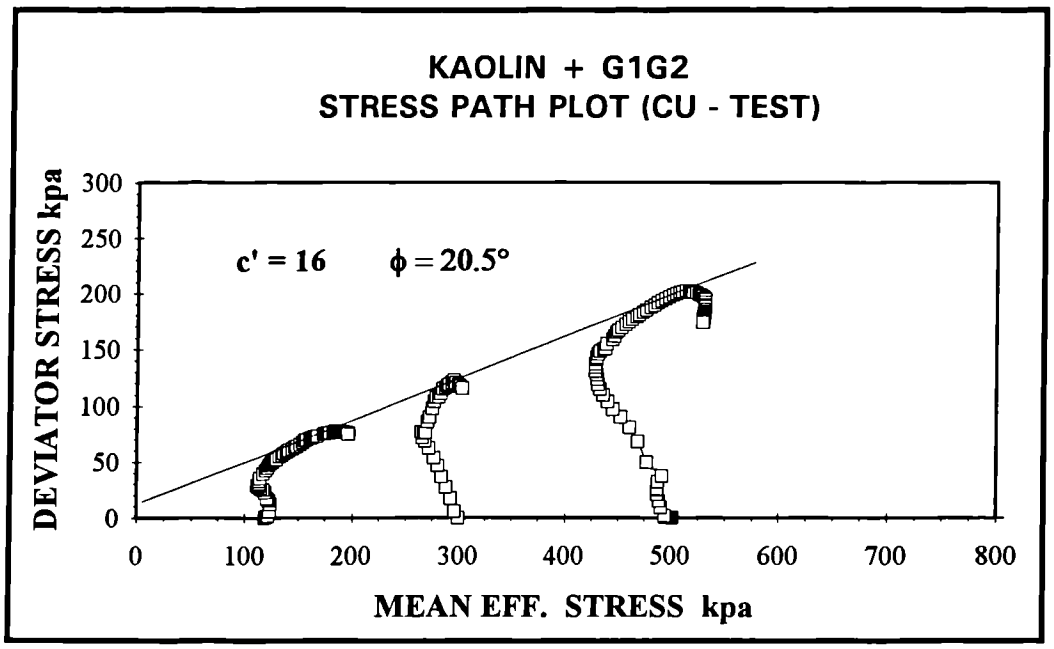

Fig. 10 Stress path plot, consolidated drained compression triaxial test

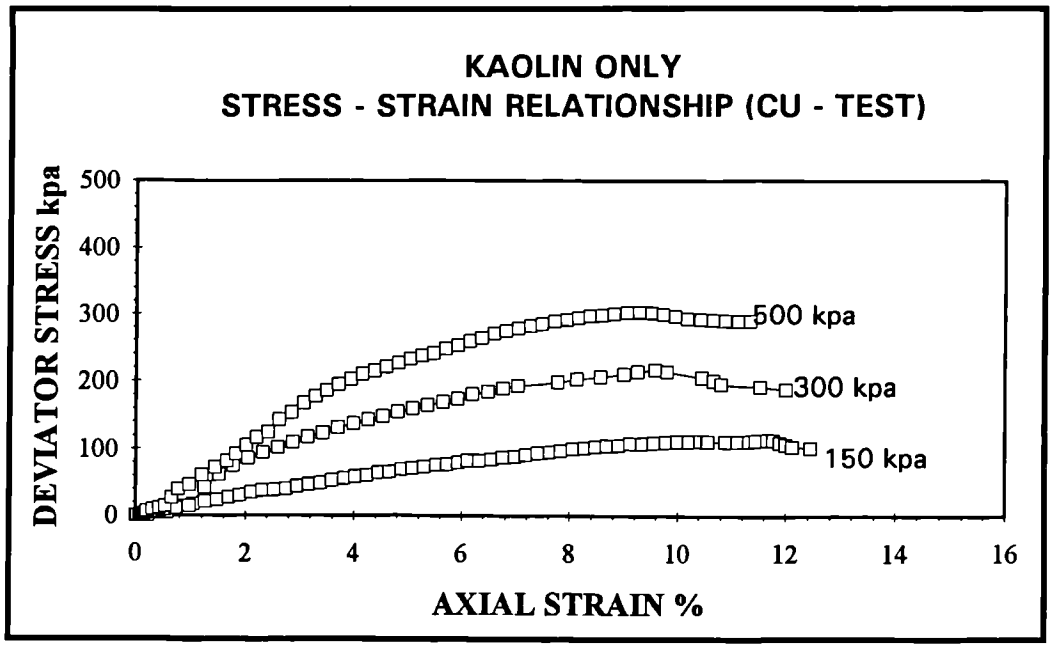

Fig. 11 Deviator stress vs. strain, consolidation undrained compression triaxial test

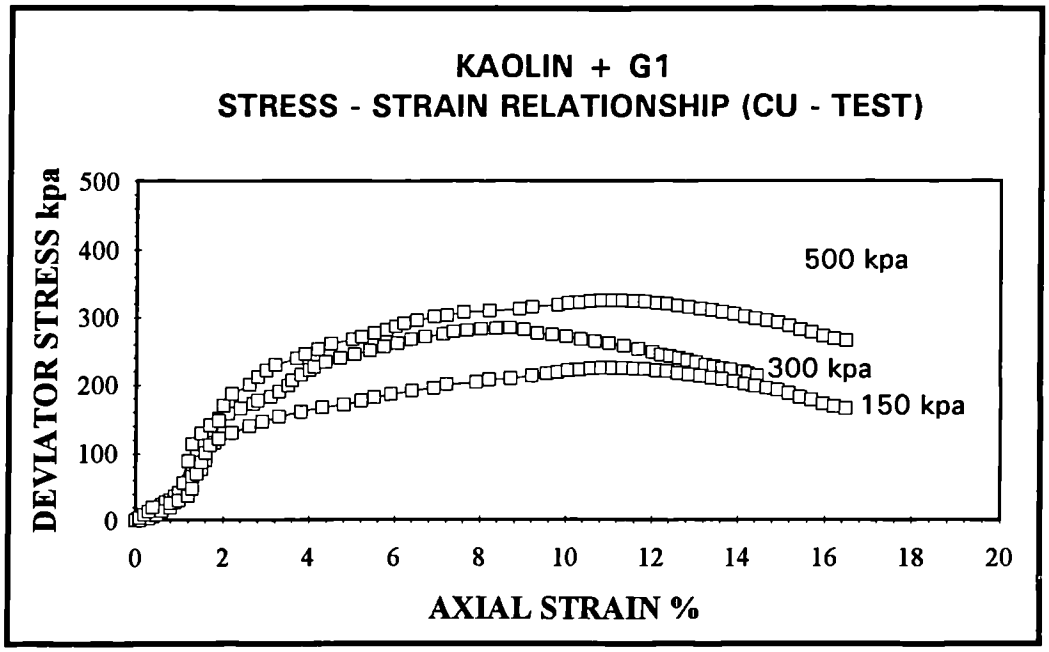

Fig. 12 Deviator stress vs. strain, consolidation undrained compression triaxial test

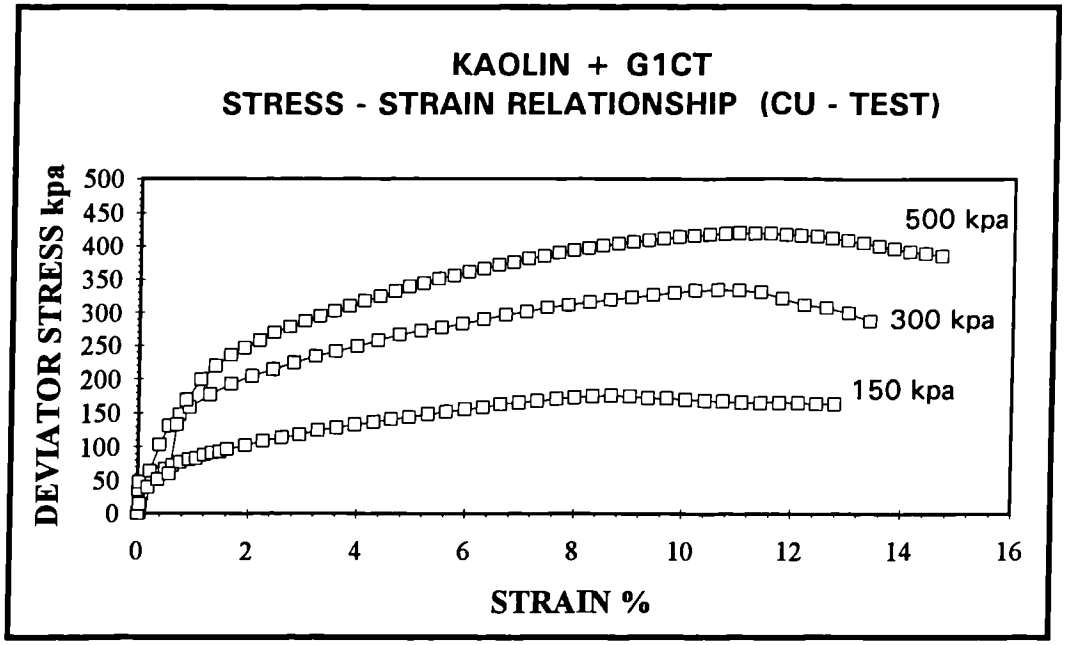

Fig. 13 Deviator stress vs. strain, consolidation undrained compression triaxial test

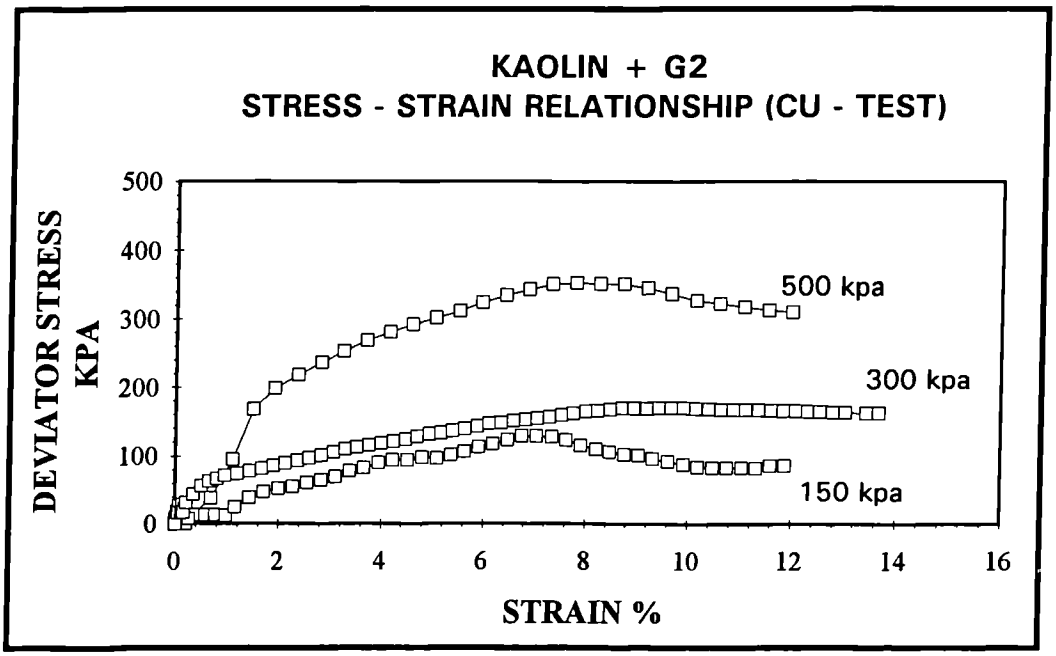

Fig. 14 Deviator stress vs. strain, consolidation undrained compression triaxial test

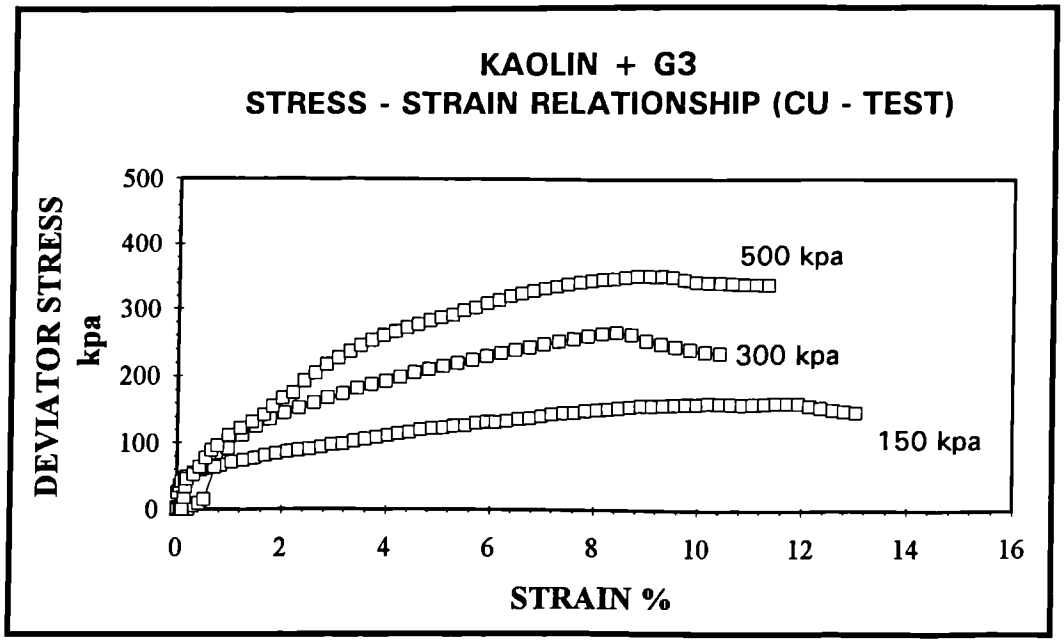

Fig. 15 Deviator stress vs. strain, consolidation undrained compression triaxial test

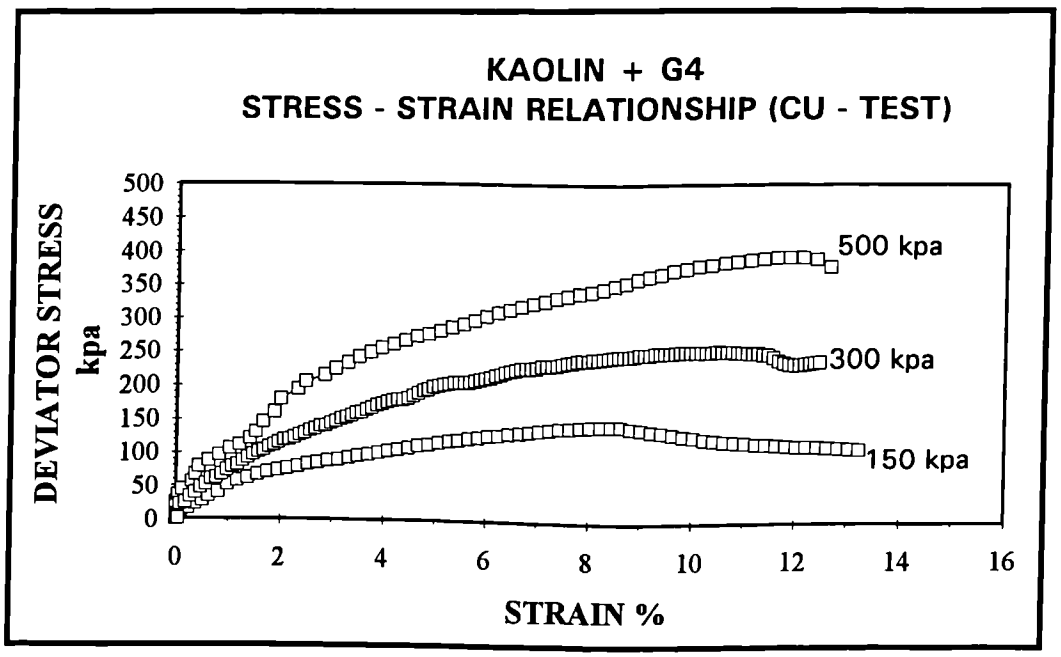

Fig. 16 Deviator stress vs. strain, consolidation undrained compression triaxial test

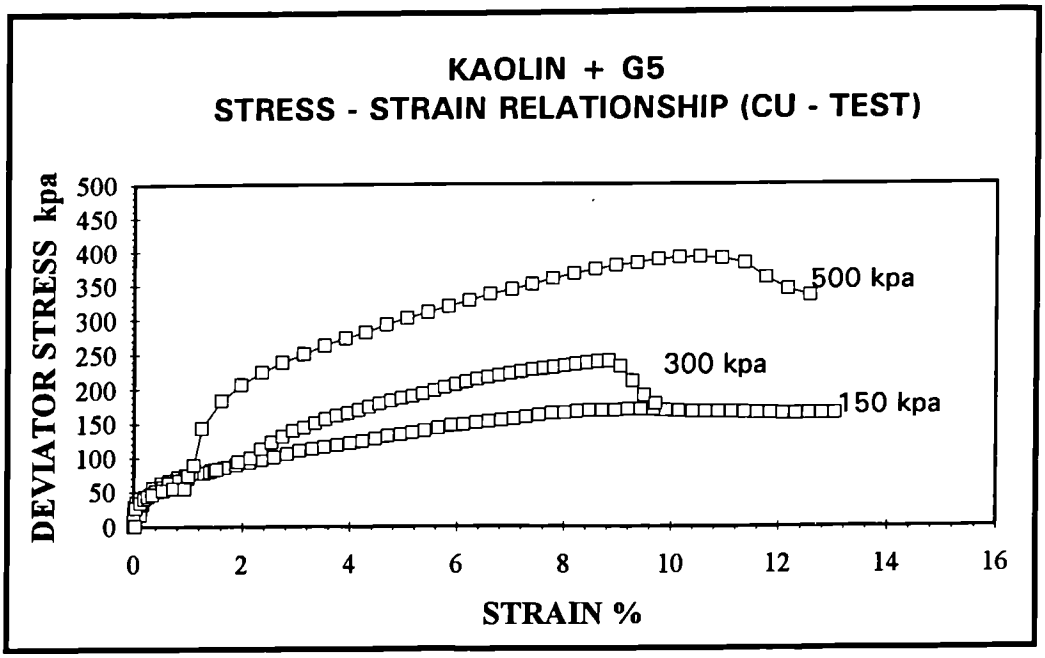

Fig. 17 Deviator stress vs. strain, consolidation undrained compression triaxial test

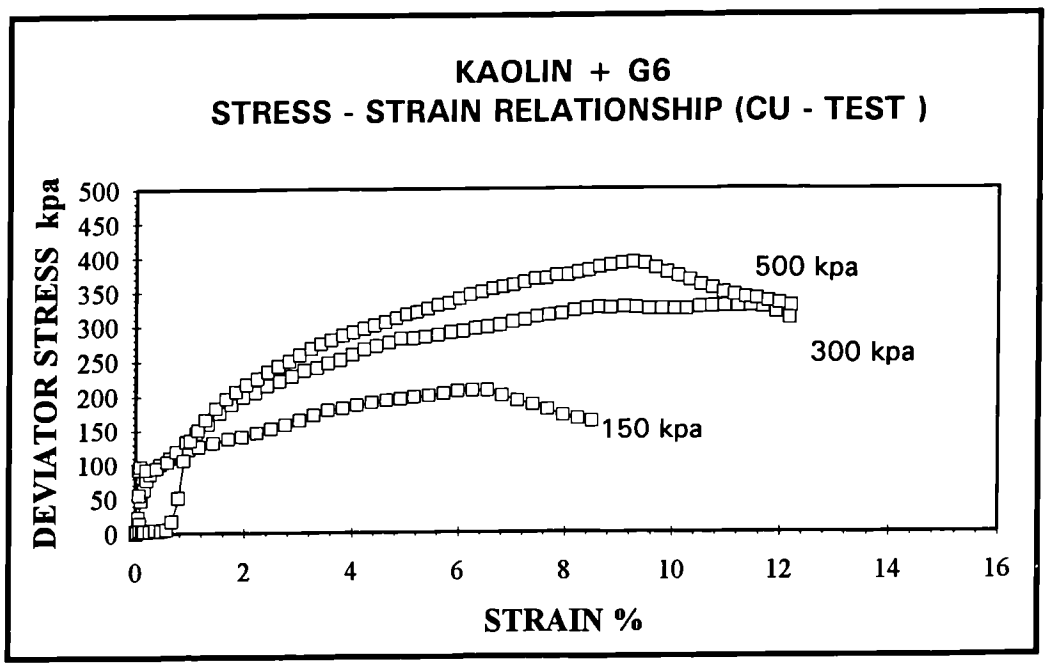

Fig. 18 Deviator stress vs. strain, consolidation undrained compression triaxial test

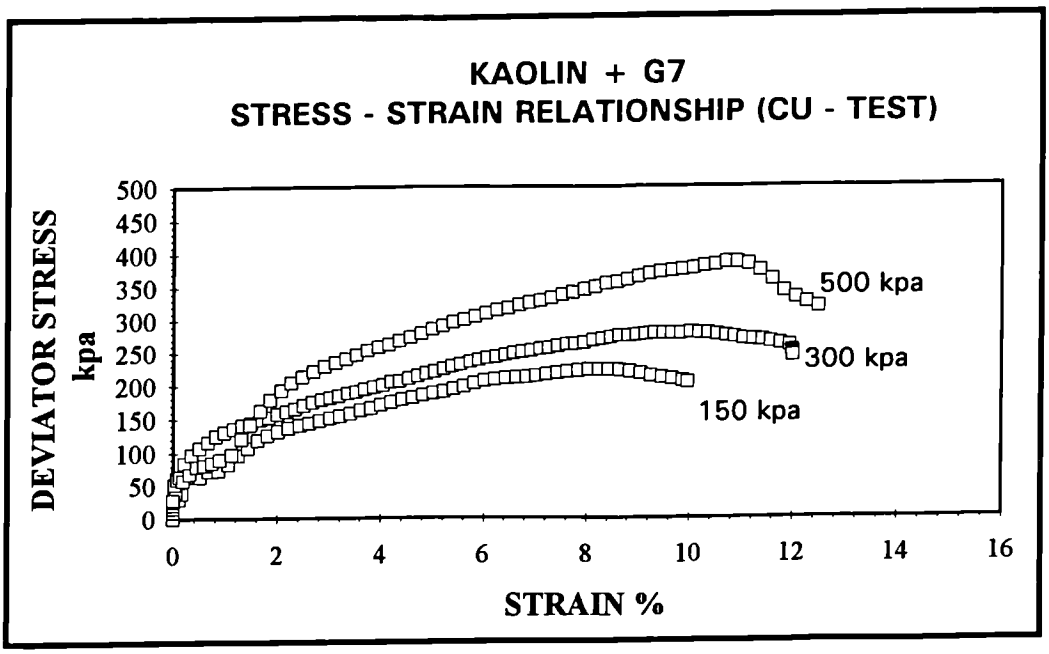

Fig. 19 Deviator stress vs. strain, consolidation undrained compression triaxial test

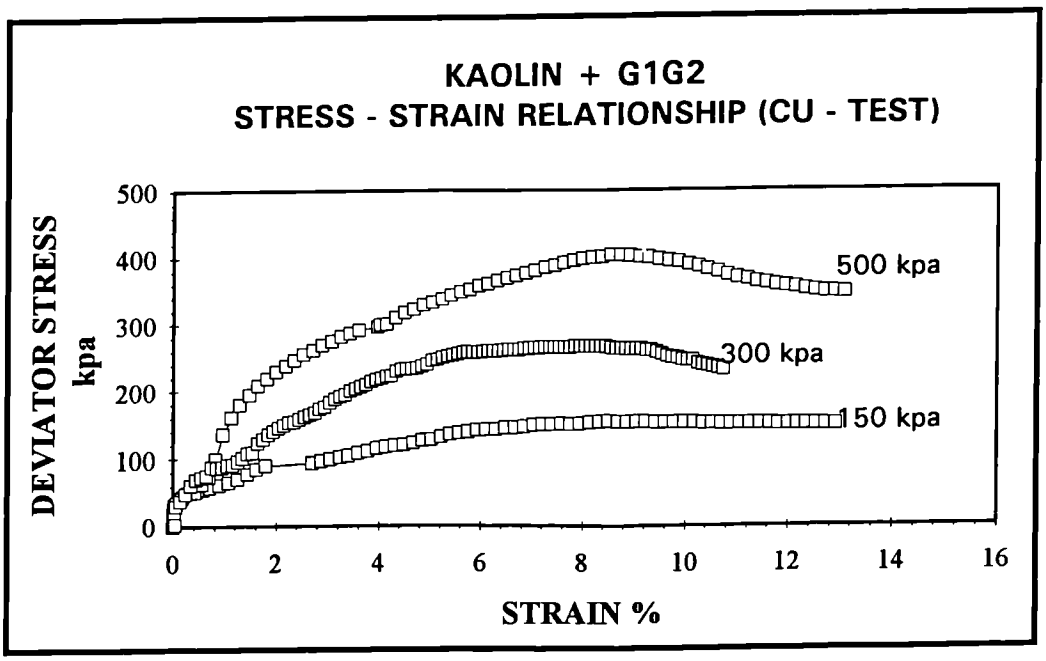

Fig. 20 Deviator stress vs. strain, consolidation undrained compression triaxial test

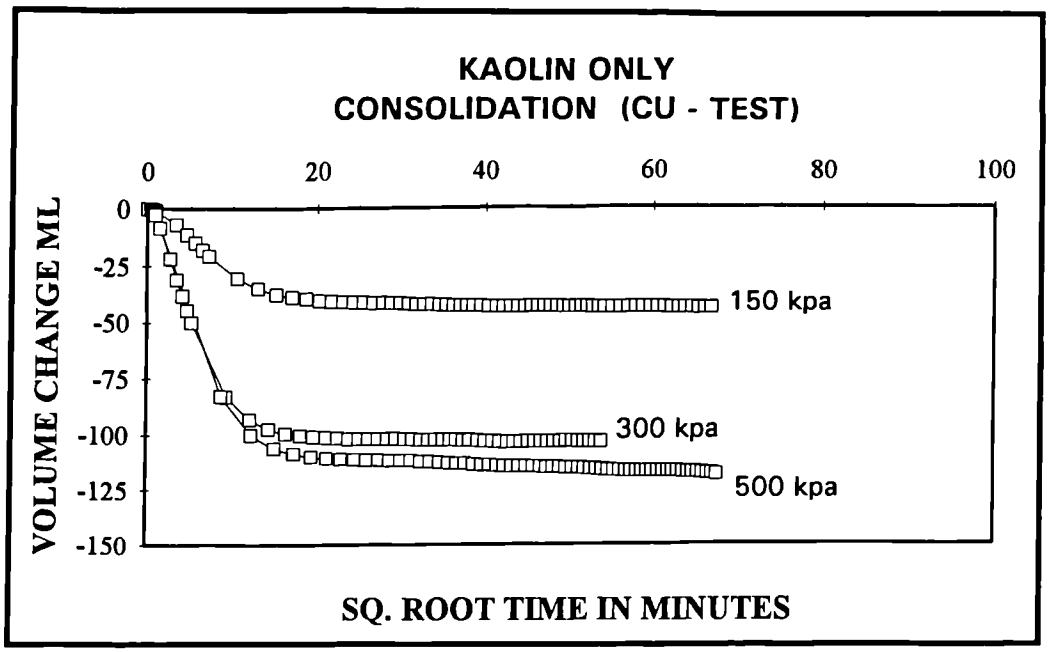

Fig. 21 Volume change vs. sq. time, consolidation undrained compression triaxial test

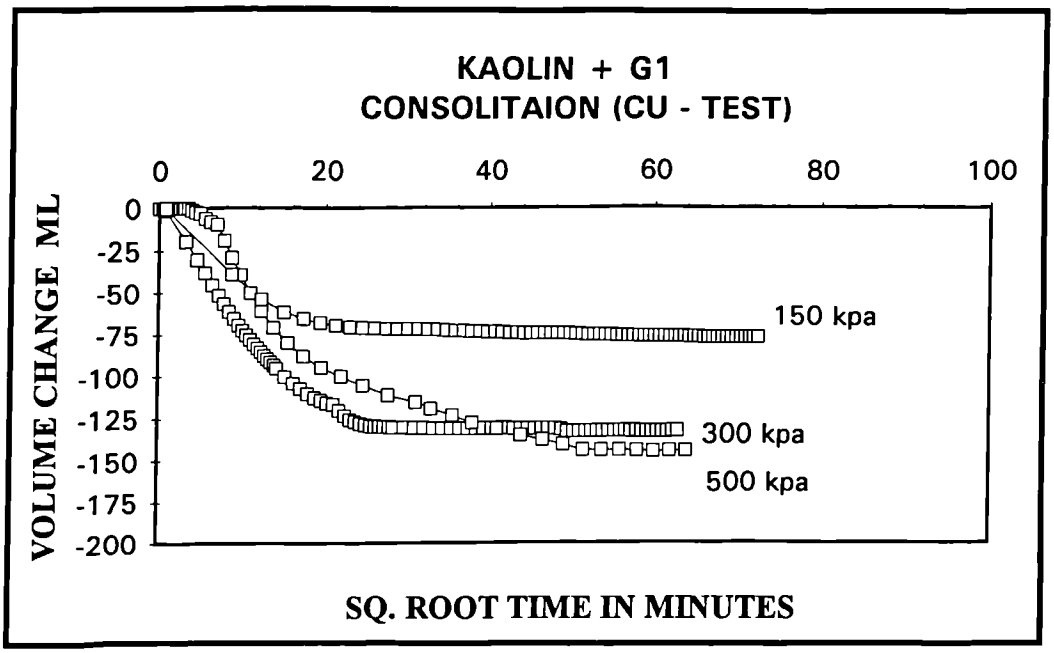

Fig. 22 Volume change vs. sq. time, consolidation undrained compression triaxial test

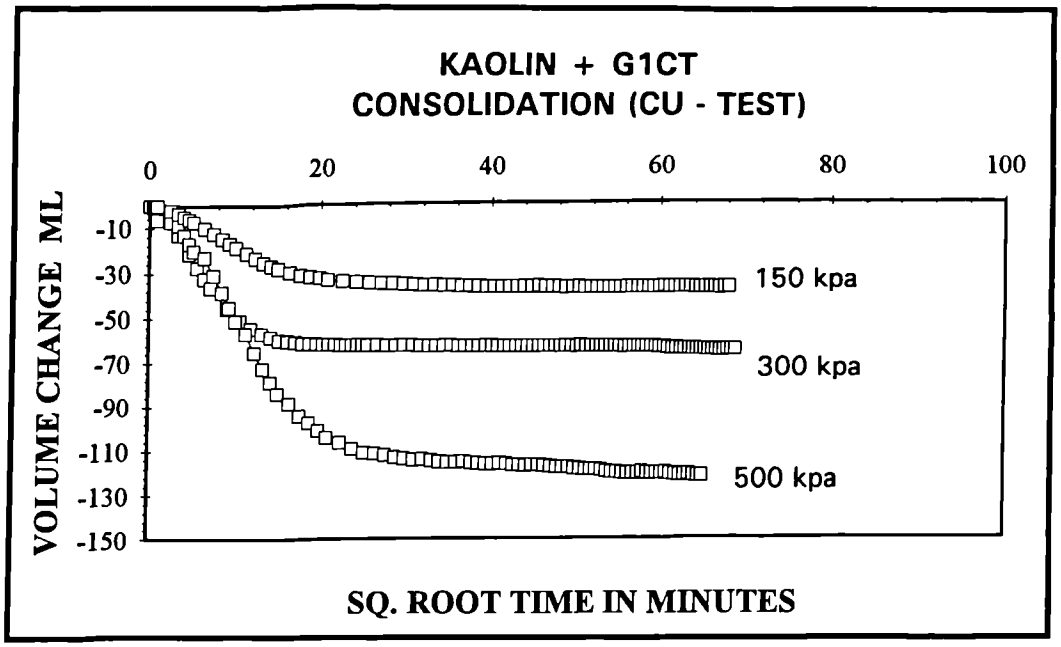

Fig. 23 Volume change vs. sq. time, consolidation undrained compression triaxial test

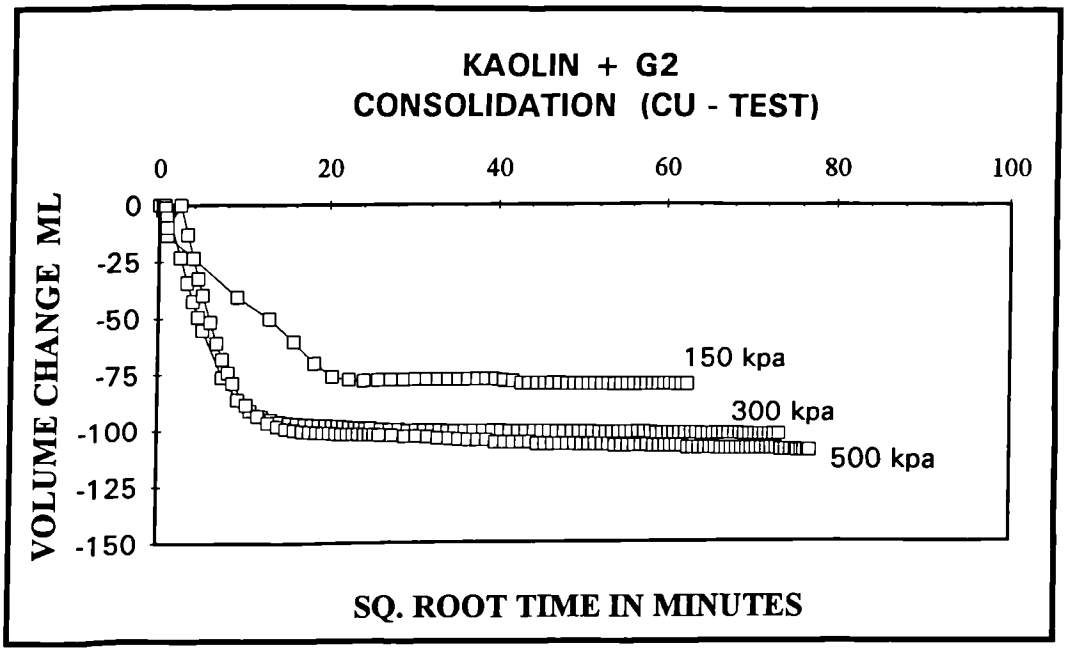

Fig. 24 Volume change vs. sq. time, consolidation undrained compression triaxial test

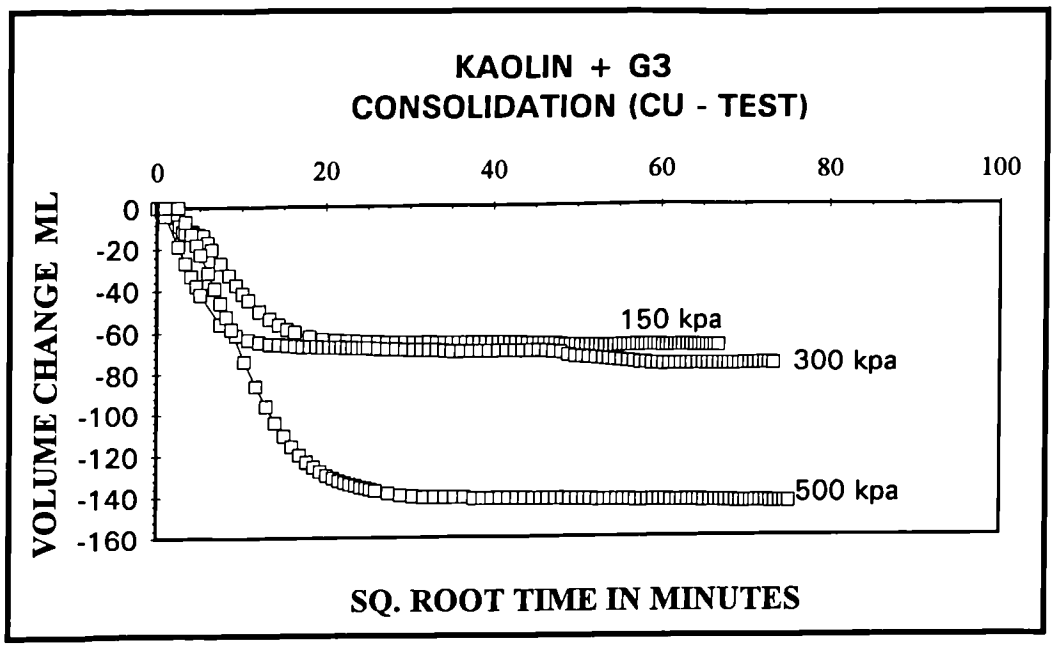

Fig. 25 Volume change vs. sq. time, consolidation undrained compression triaxial test

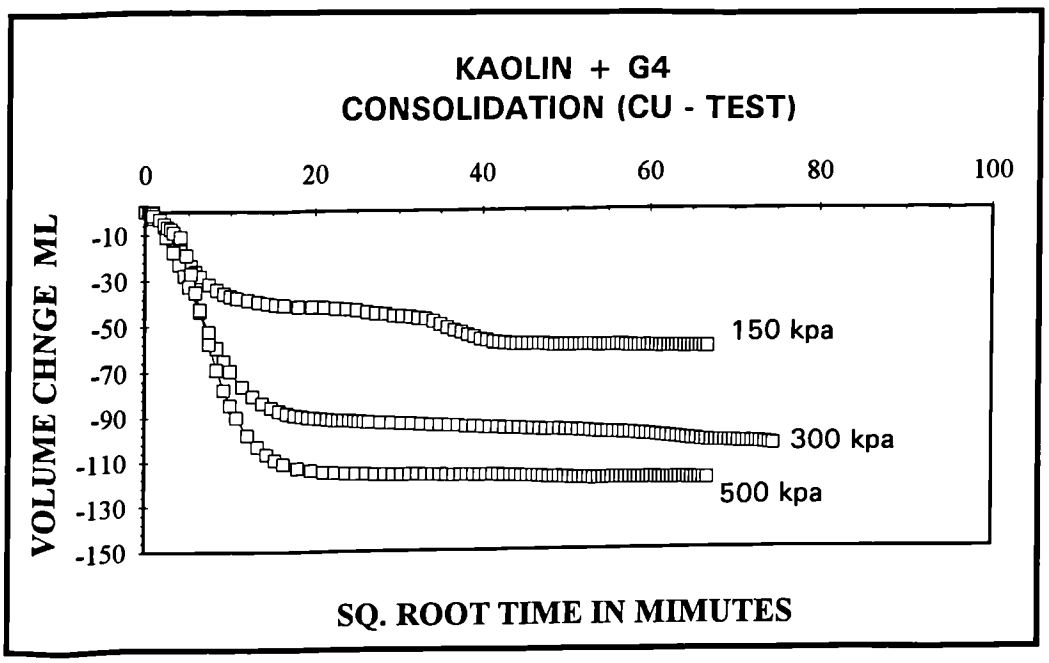

Fig. 26 Volume change vs. sq. time, consolidation undrained compression triaxial test

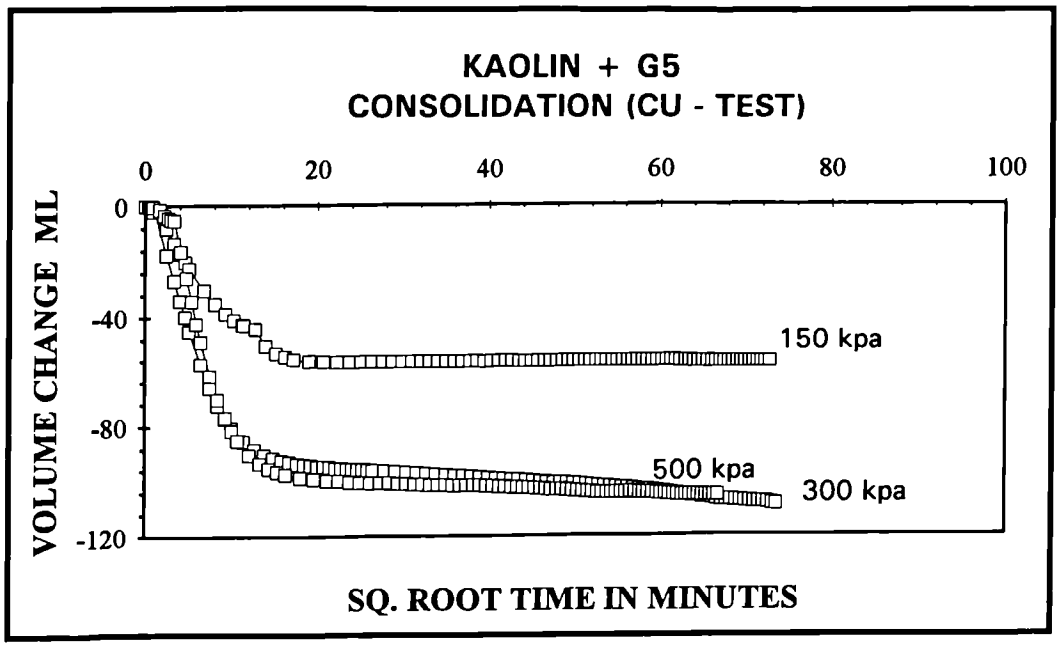

Fig. 27 Volume change vs. sq. time, consolidation undrained compression triaxial test

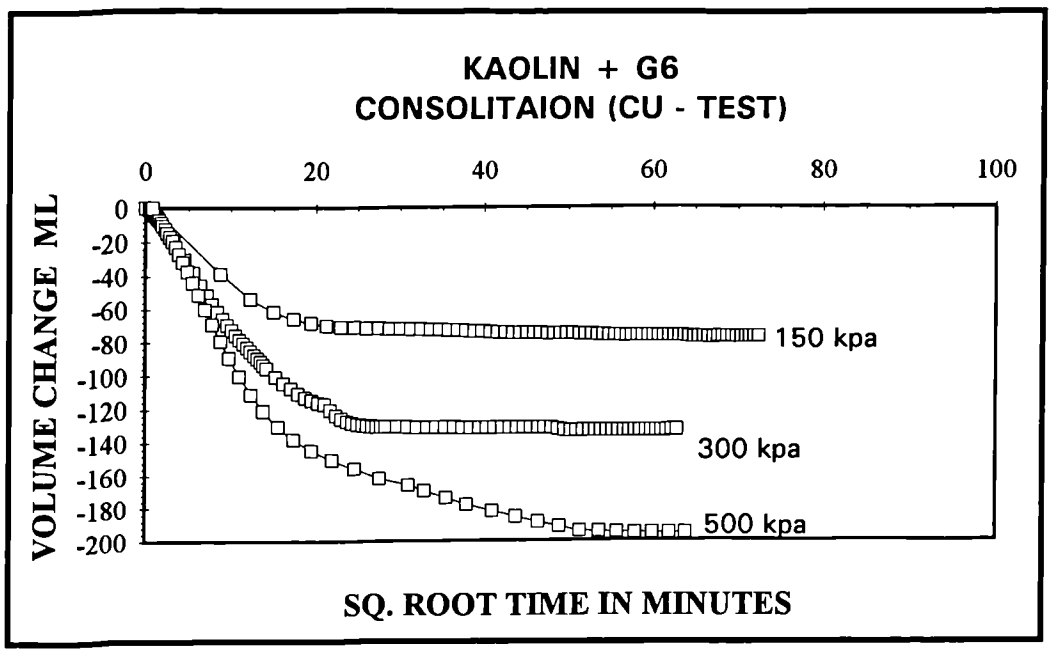

Fig. 28 Volume change vs. sq. time, consolidation undrained compression triaxial test

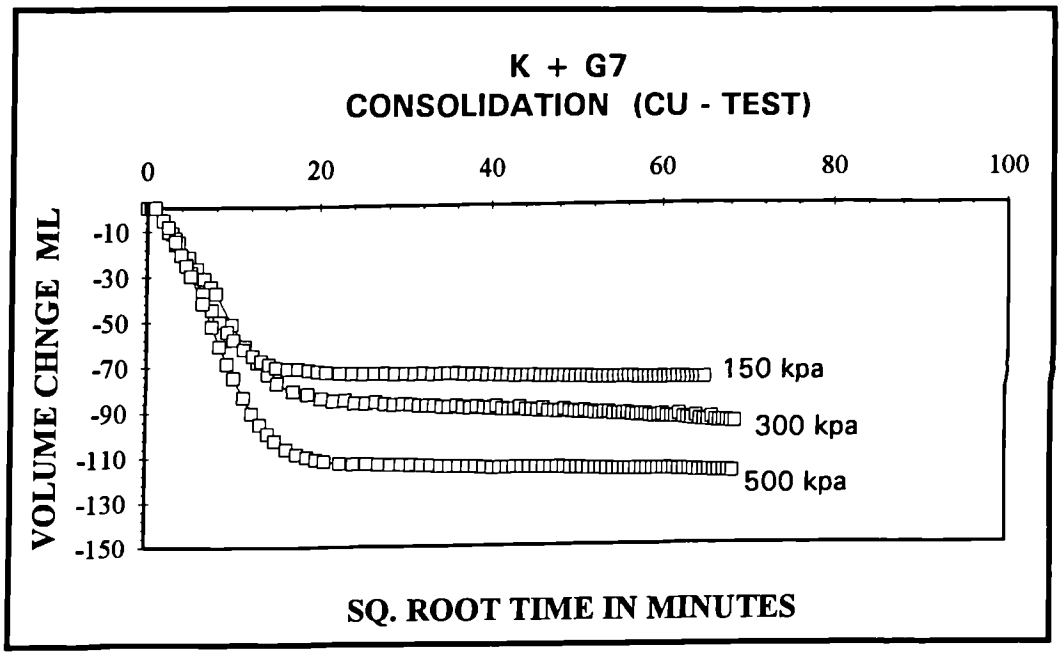

Fig. 29 Volume change vs. sq. time, consolidation undrained compression triaxial test

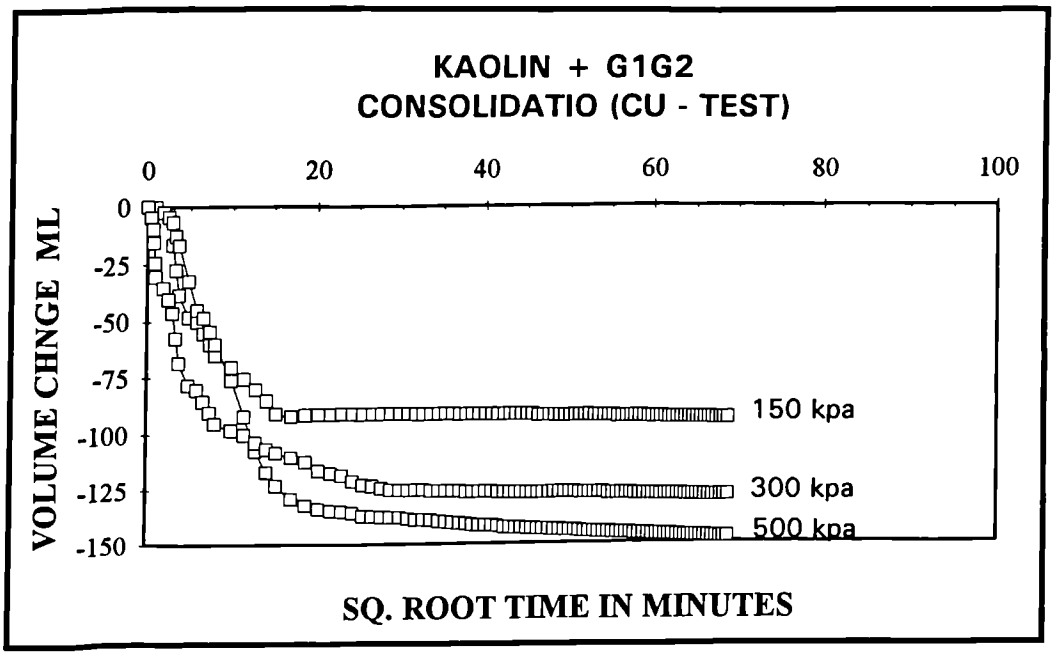

Fig. 30 Volume change vs. sq. time, consolidation undrained compression triaxial test

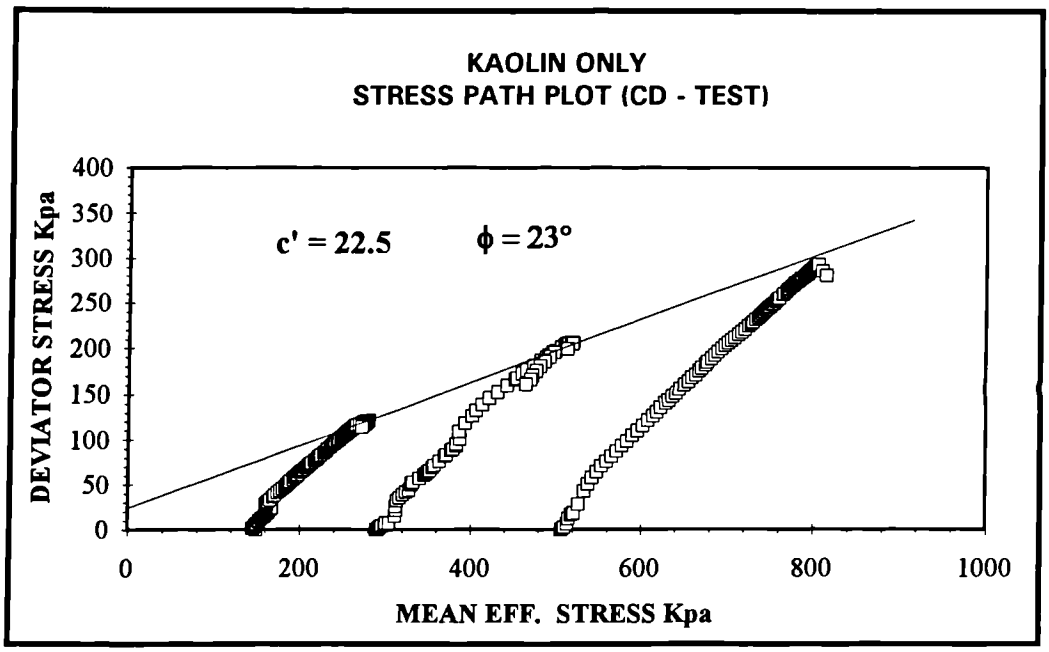

Fig. 31 Stress path plot, consolidated drained compression triaxial test

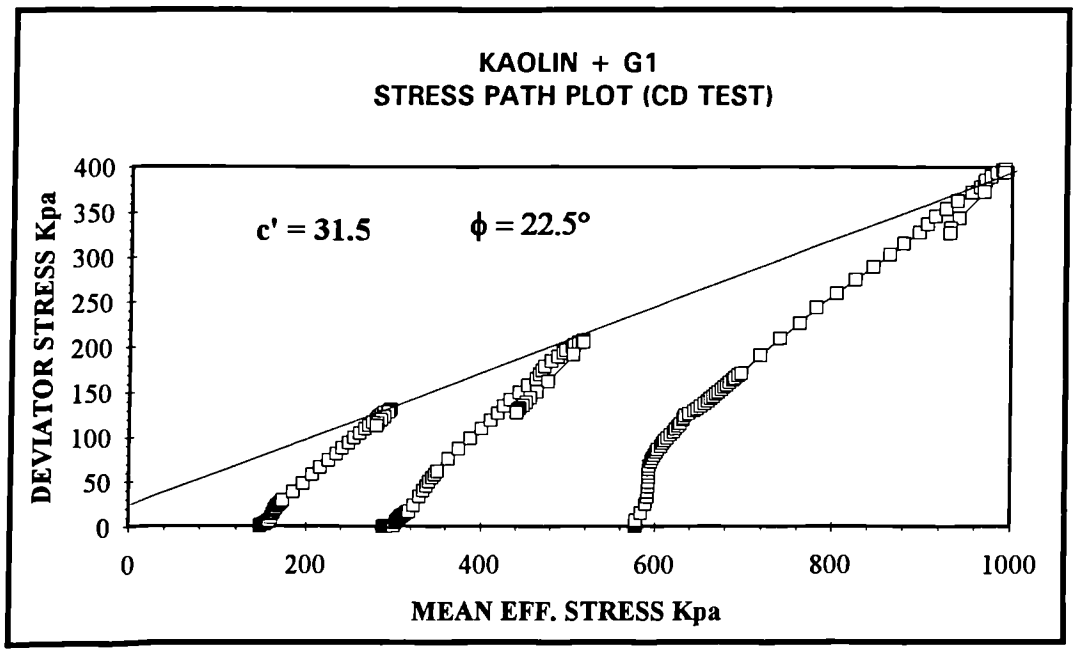

Fig. 32 Stress path plot, consolidated drained compression triaxial test

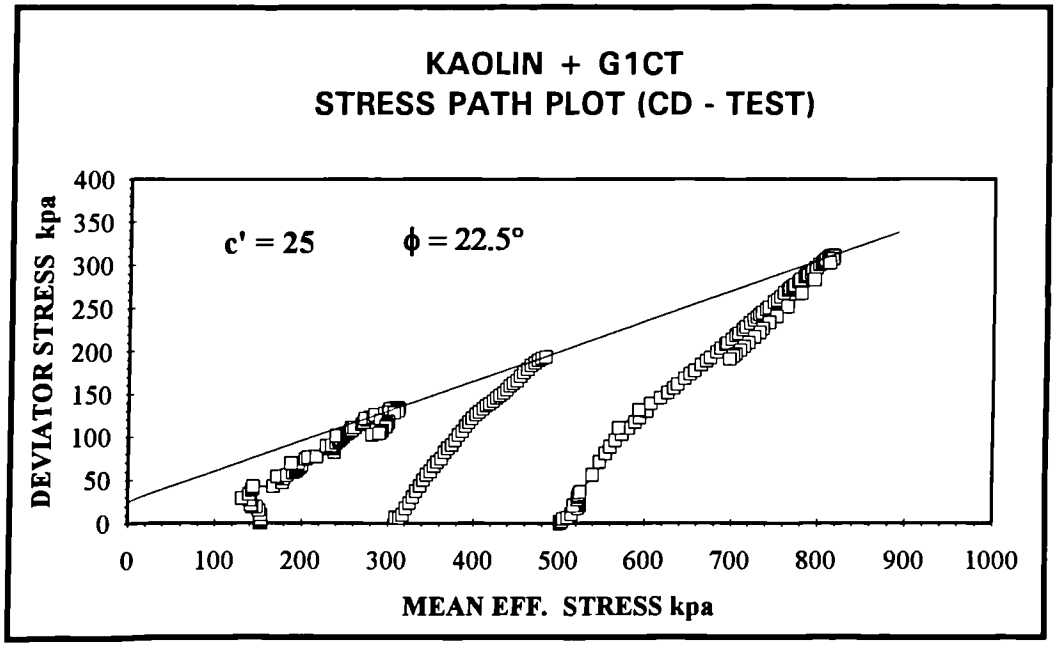

Fig. 33 Stress path plot, consolidated drained compression triaxial test

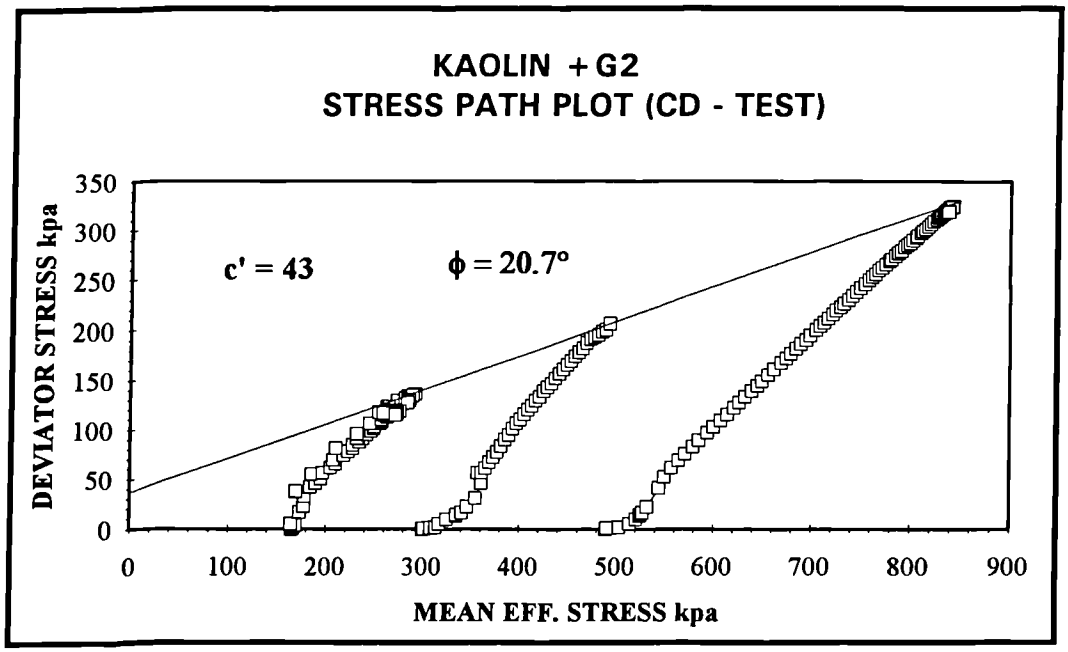

Fig. 34 Stress path plot, consolidated drained compression triaxial test

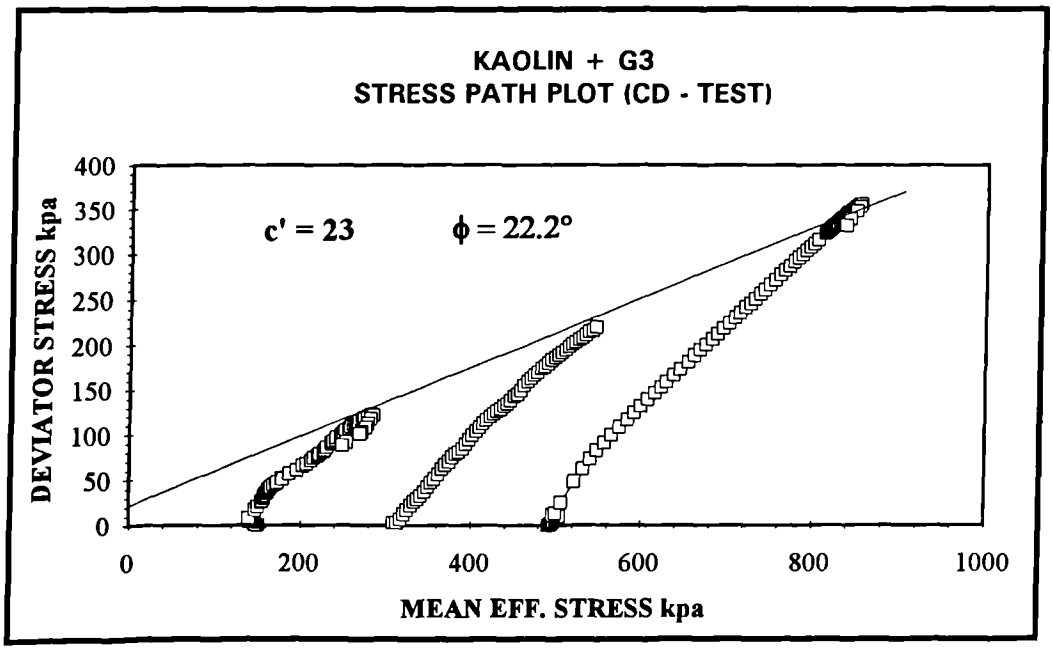

Fig. 35 Stress path plot, consolidated drained compression triaxial test

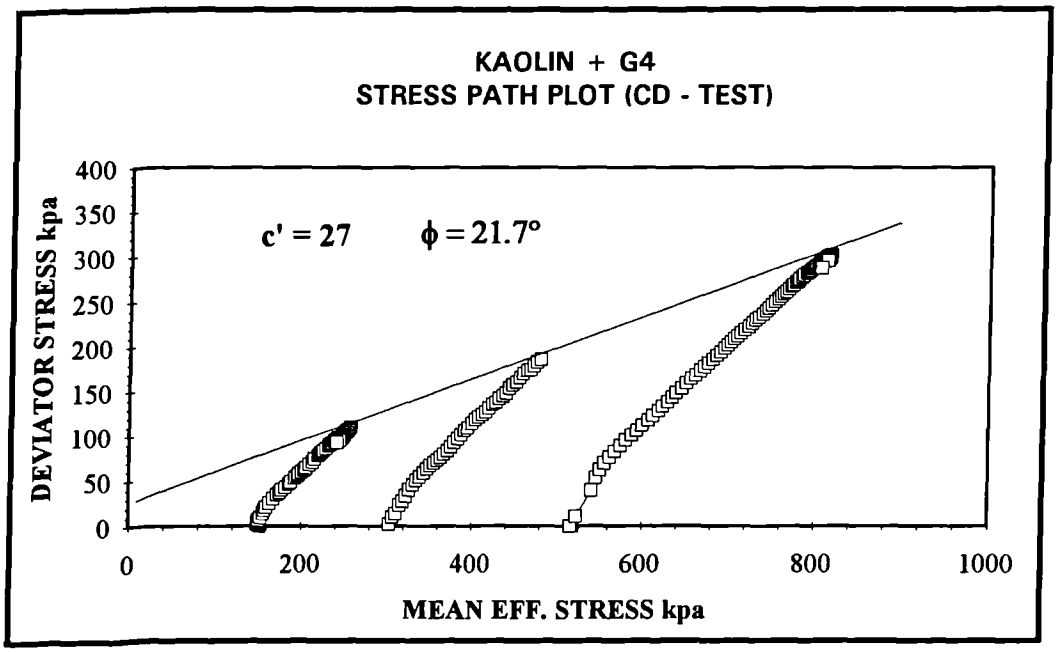

Fig. 36 Stress path plot, consolidated drained compression triaxial test

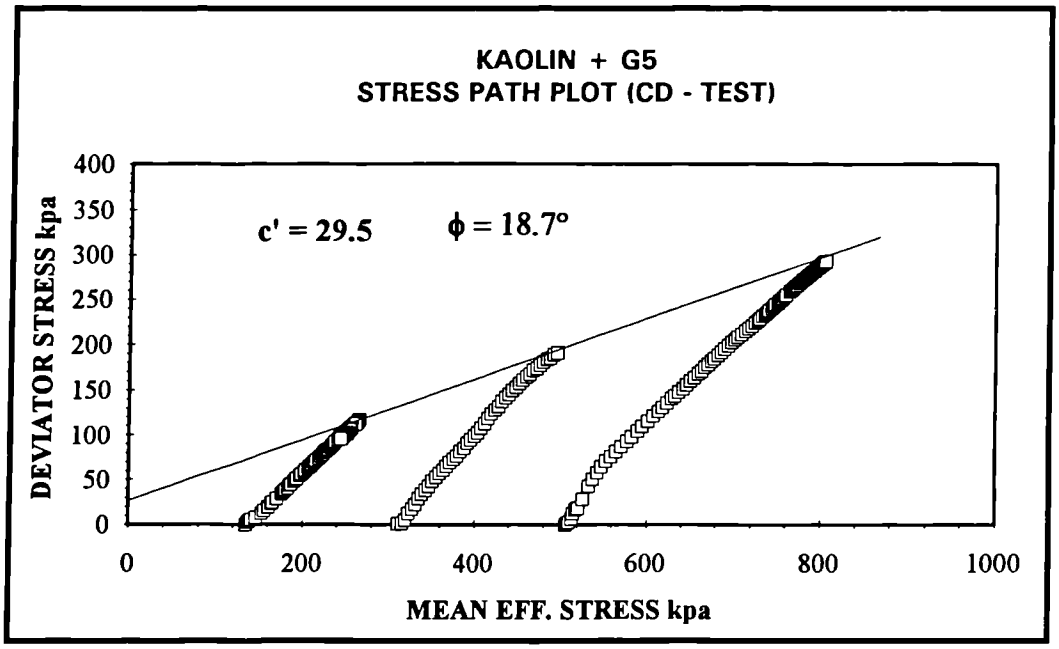

Fig. 37 Stress path plot, consolidated drained compression triaxial test

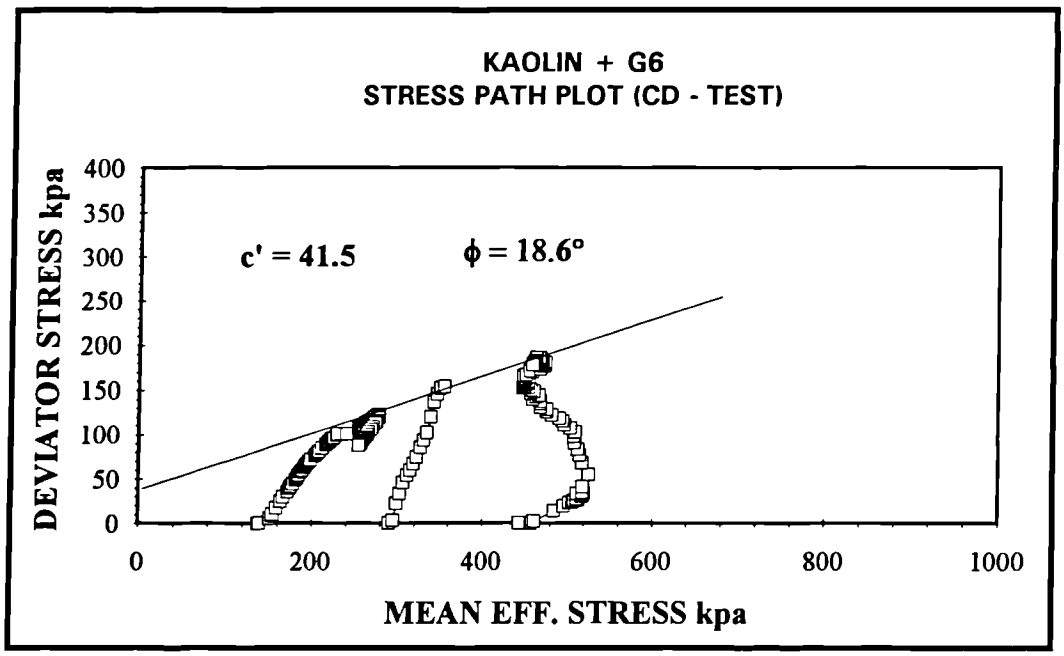

Fig. 38 Stress path plot, consolidated drained compression triaxial test

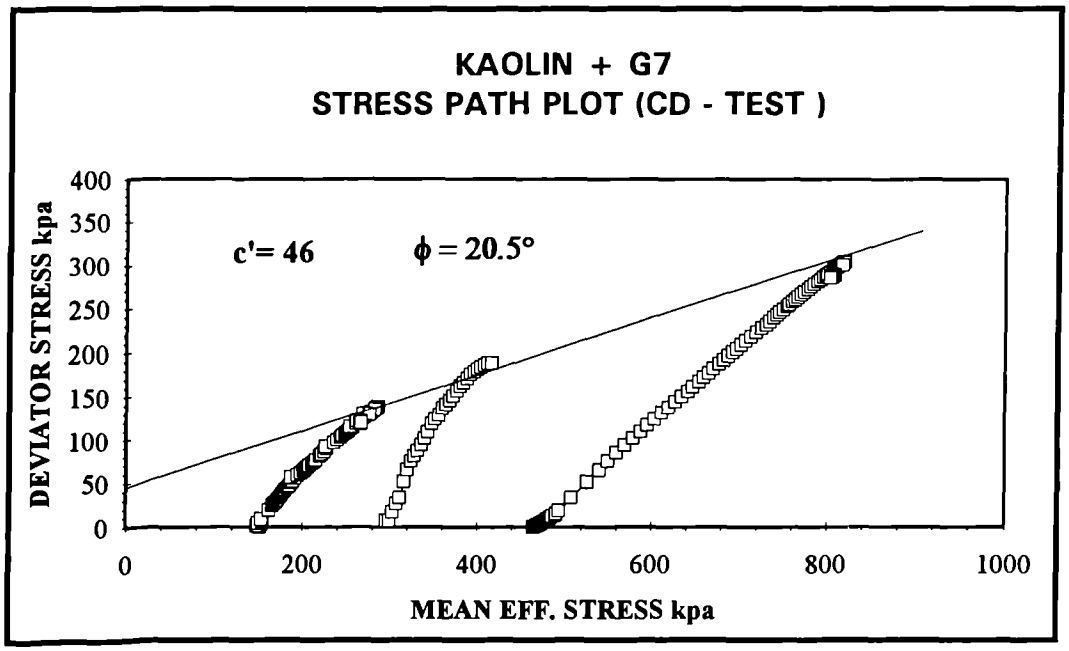

Fig. 39 Stress path plot, consolidated drained compression triaxial test

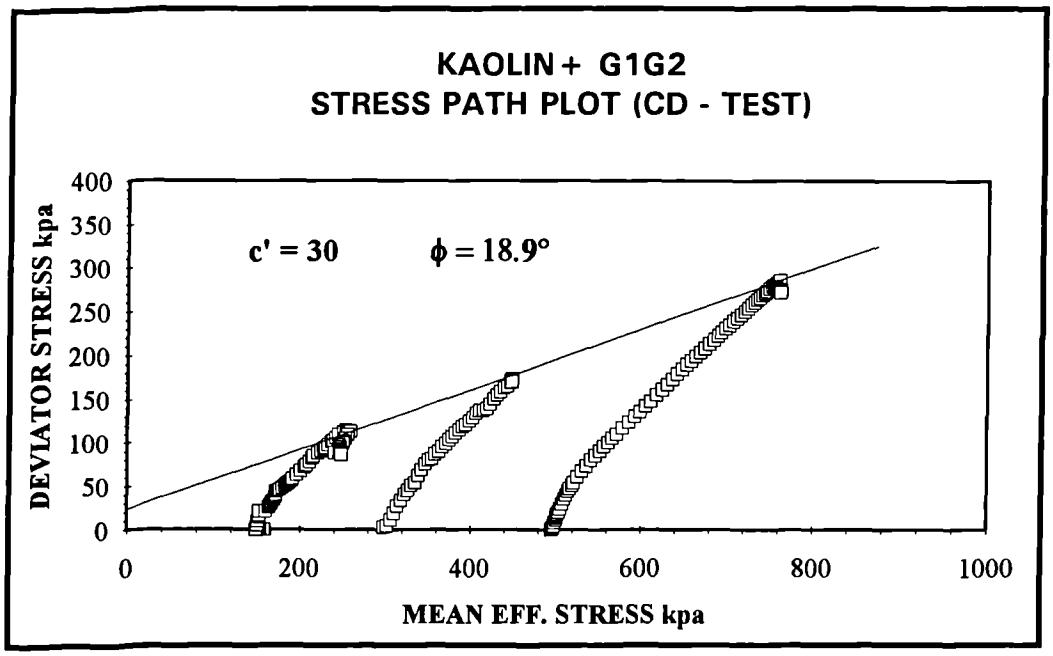

Fig. 40 Stress path plot, consolidated drained compression triaxial test

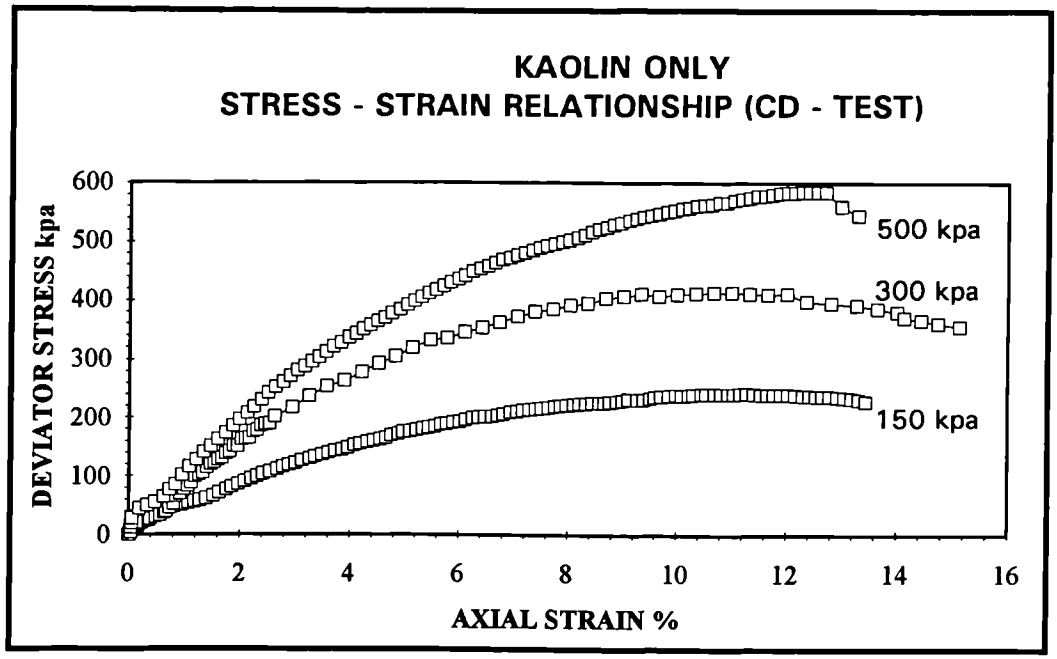

Fig. 41 Deviator stress vs. strain, consolidation drained compression triaxial test

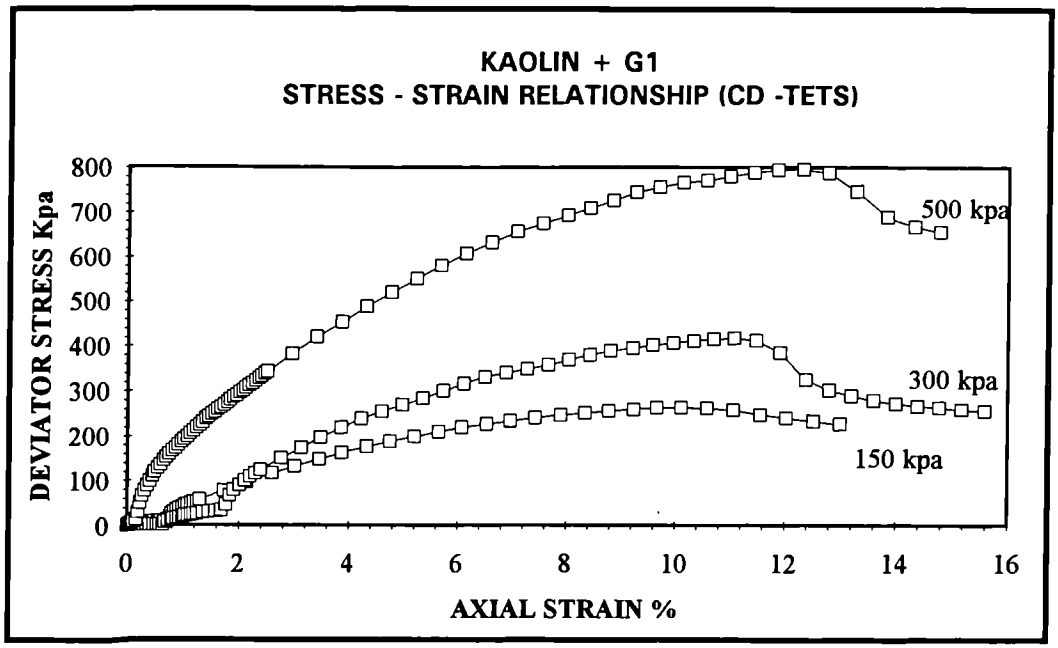

Fig. 42 Deviator stress vs. strain, consolidation drained compression triaxial test

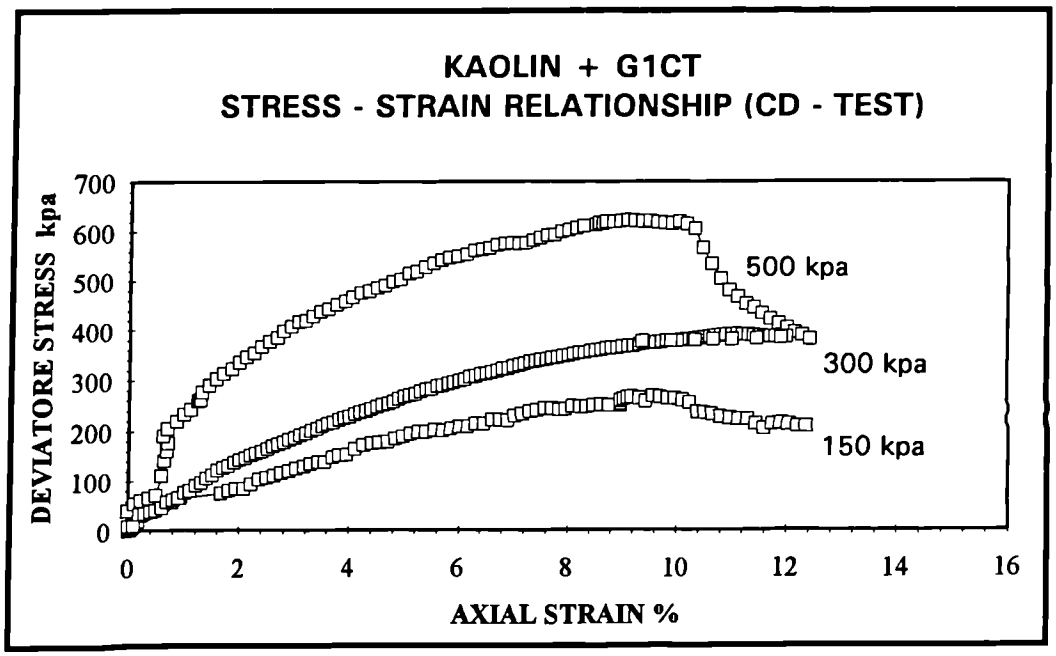

Fig. 43 Deviator stress Vs. strain, consolidation drained compression triaxial test

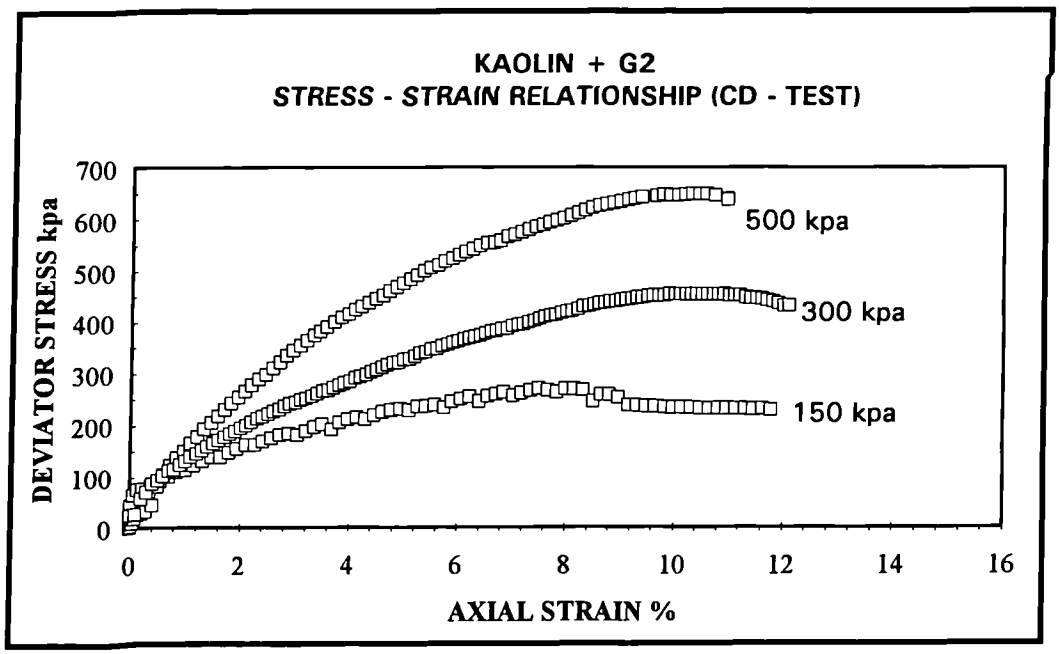

Fig. 44 Deviator stress Vs. strain, consolidation drained compression triaxial test

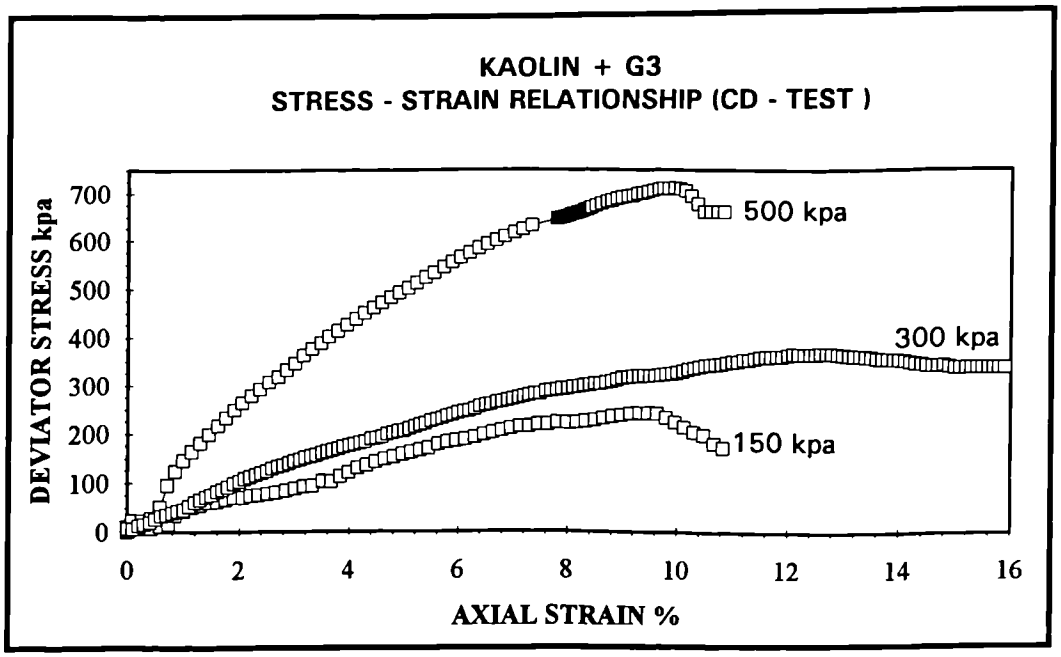

Fig. 45 Deviator stress vs. strain, consolidation drained compression triaxial test

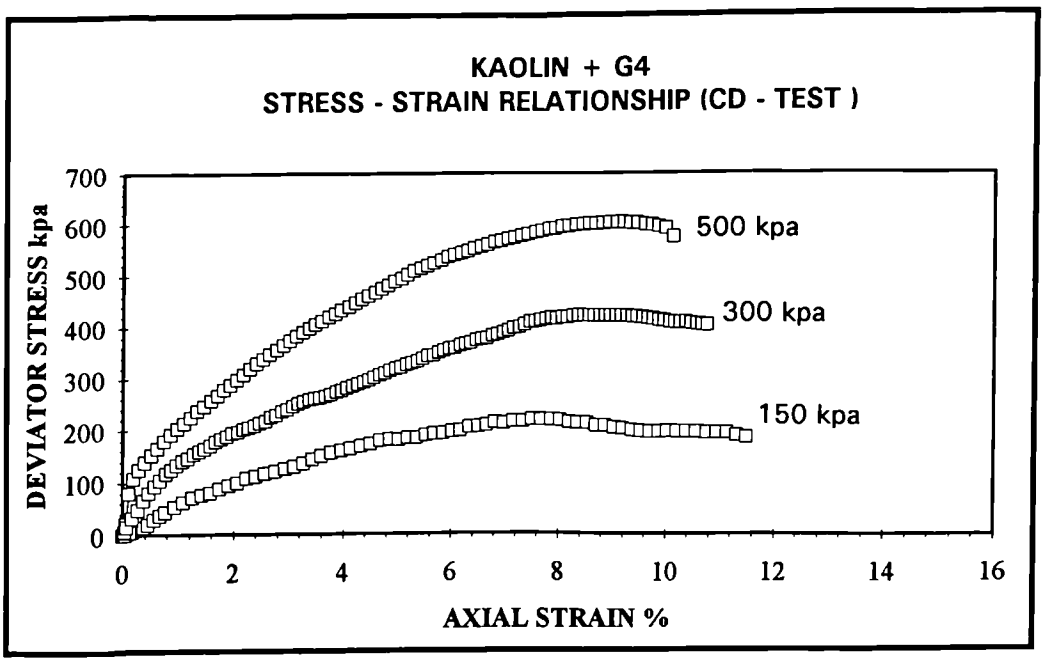

Fig. 46 Deviator stress vs. strain, consolidation drained compression triaxial test

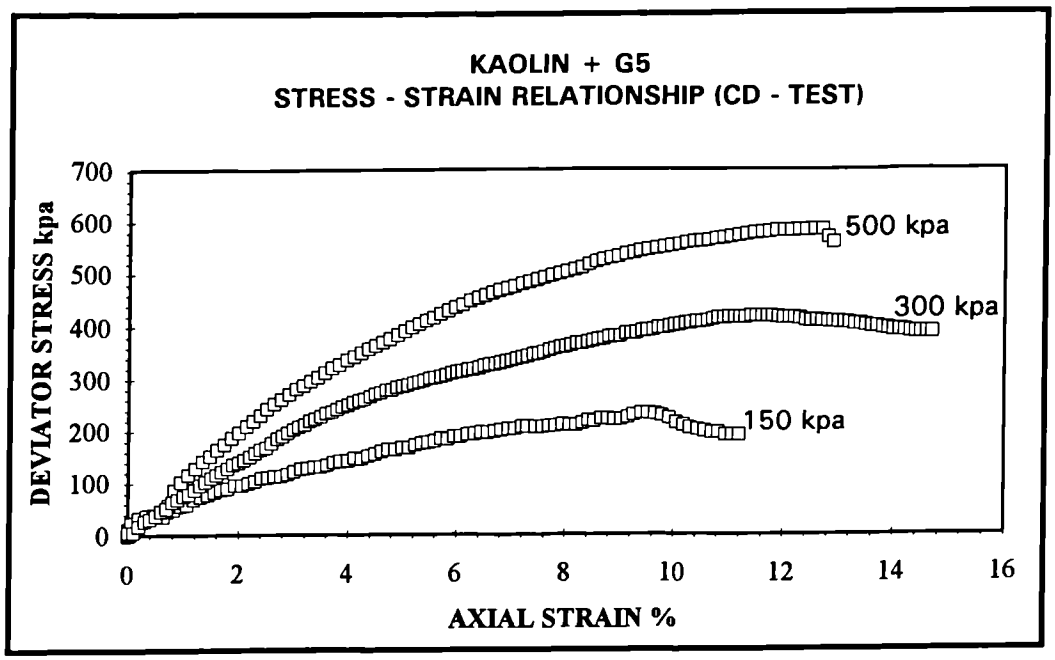

Fig. 47 Deviator stress vs. strain, consolidation drained compression triaxial test

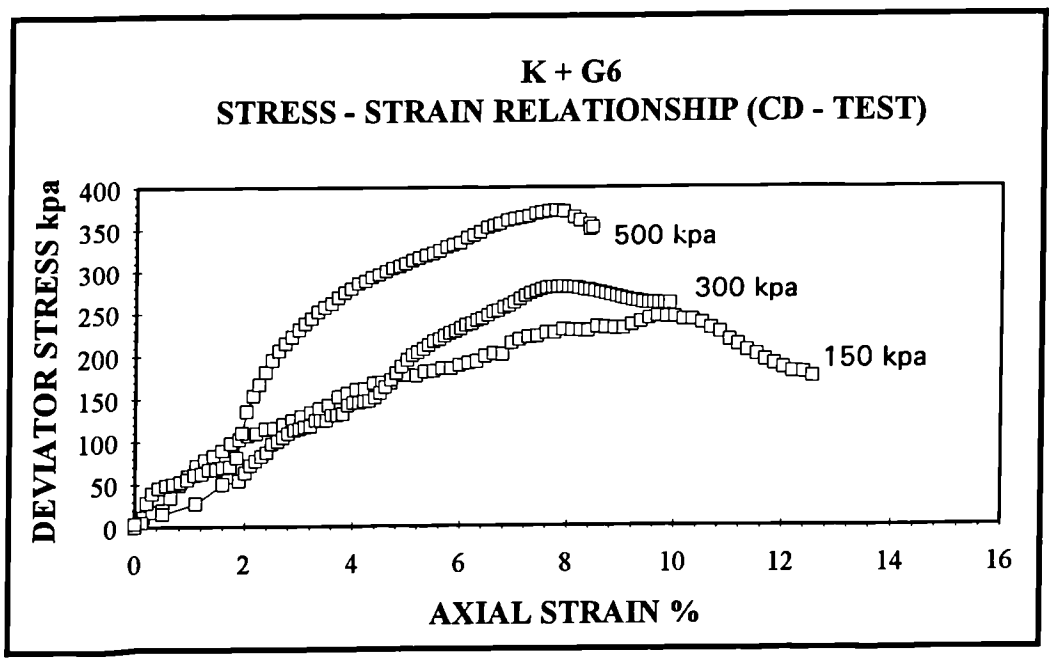

Fig. 48 Deviator stress vs. strain, consolidation drained compression triaxial test

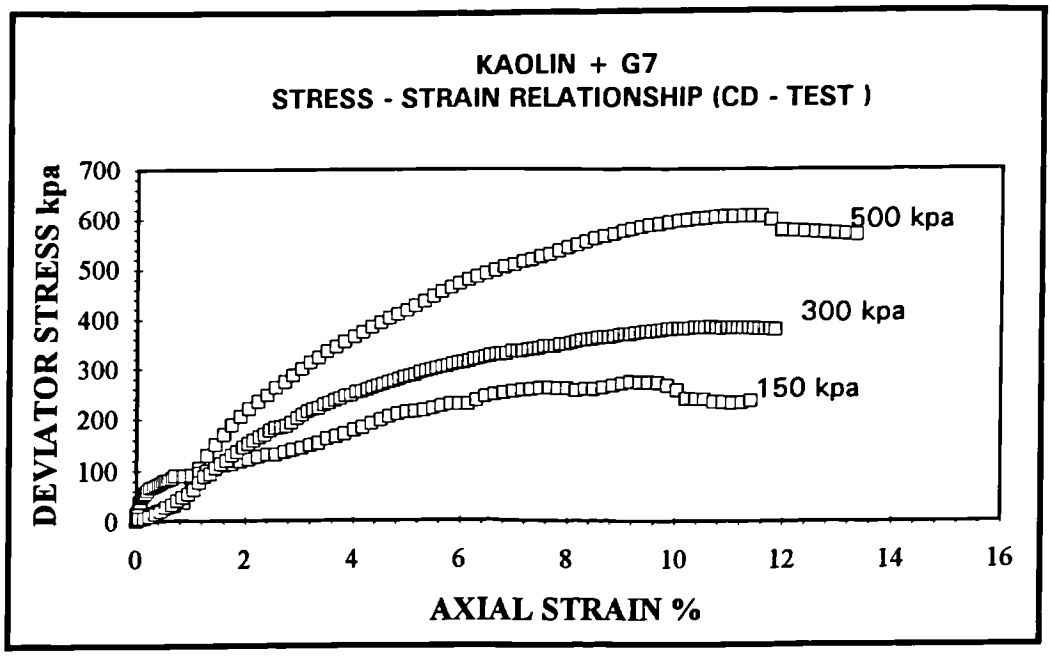

Fig. 49 Deviator stress Vs. strain, consolidation drained compression test

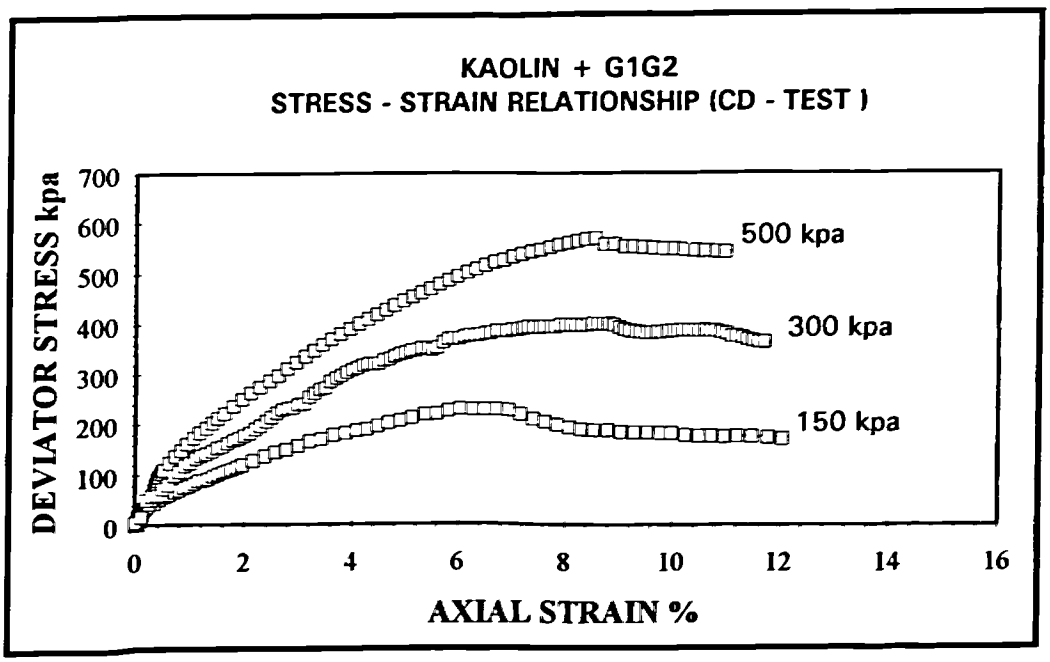

Fig. 50 Deviator stress vs. strain, consolidation drained compression triaxial test

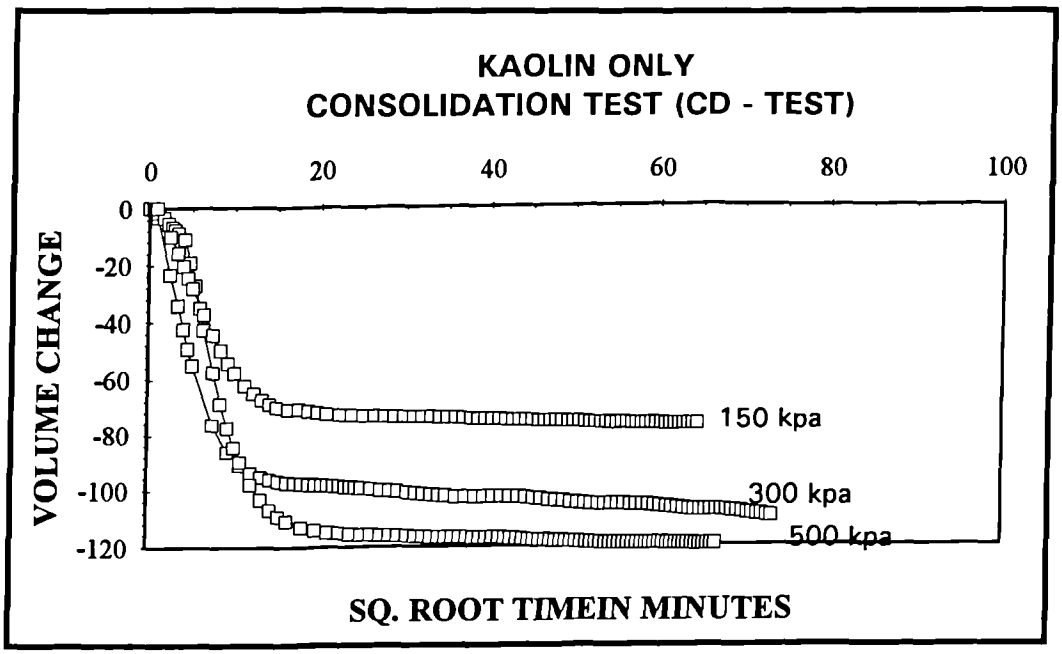

Fig. 51 Volume change vs. sq. time, consolidation drained compression triaxial test

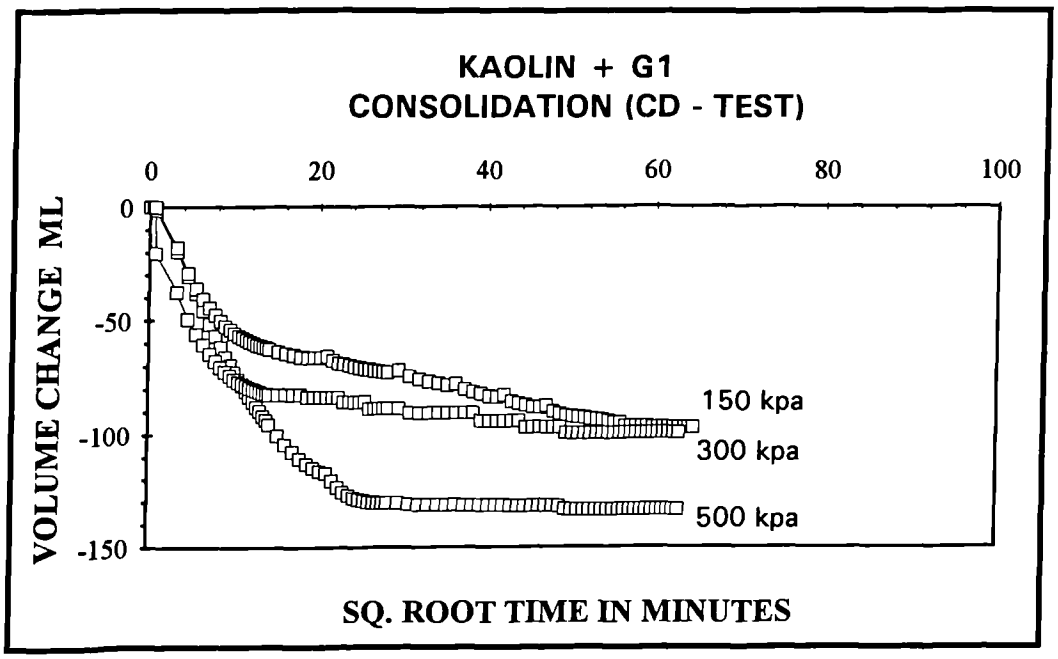

Fig. 52 Volume change vs. sq. time, consolidation drained compression triaxial test

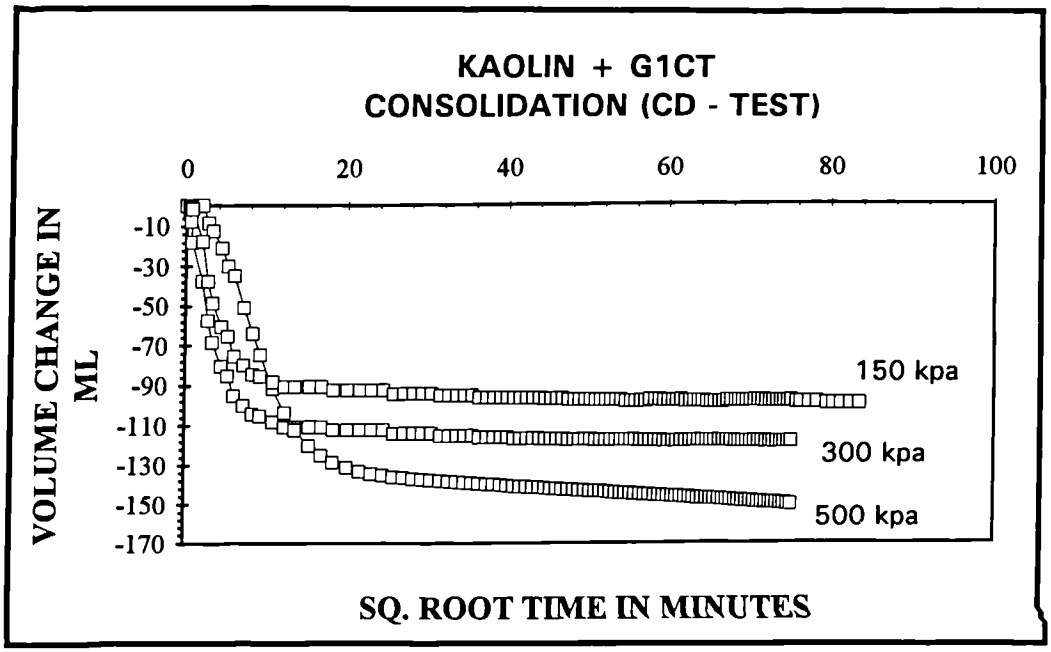

Fig. 53 Volume change vs. sq. time, consolidation drained compression triaxial test

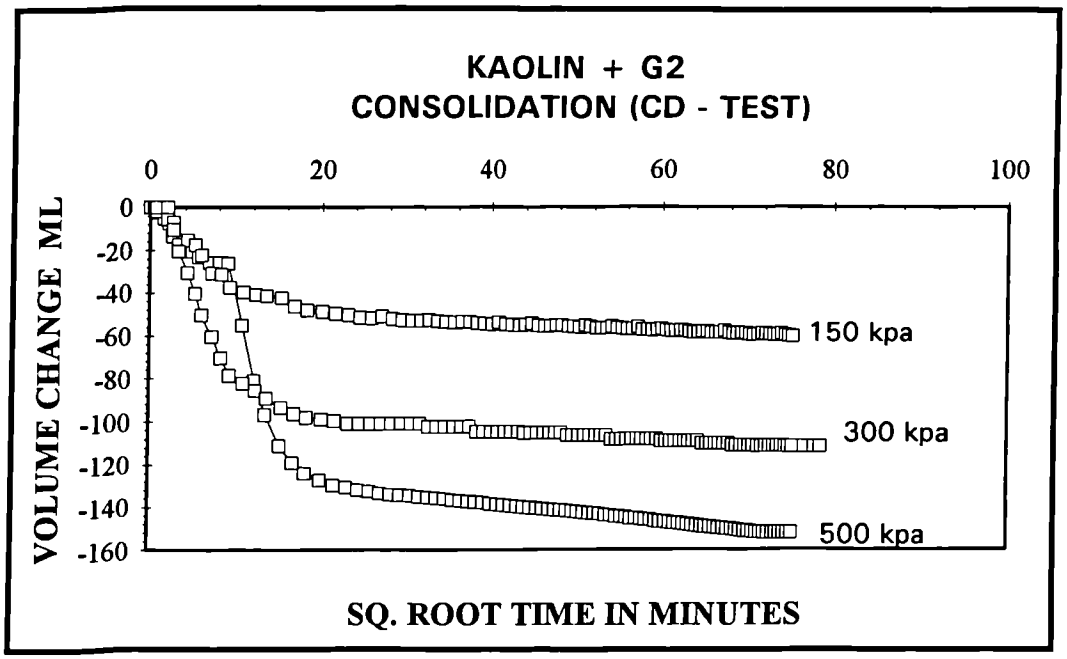

Fig. 54 Volume change vs. sq. time, consolidation drained compression triaxial test

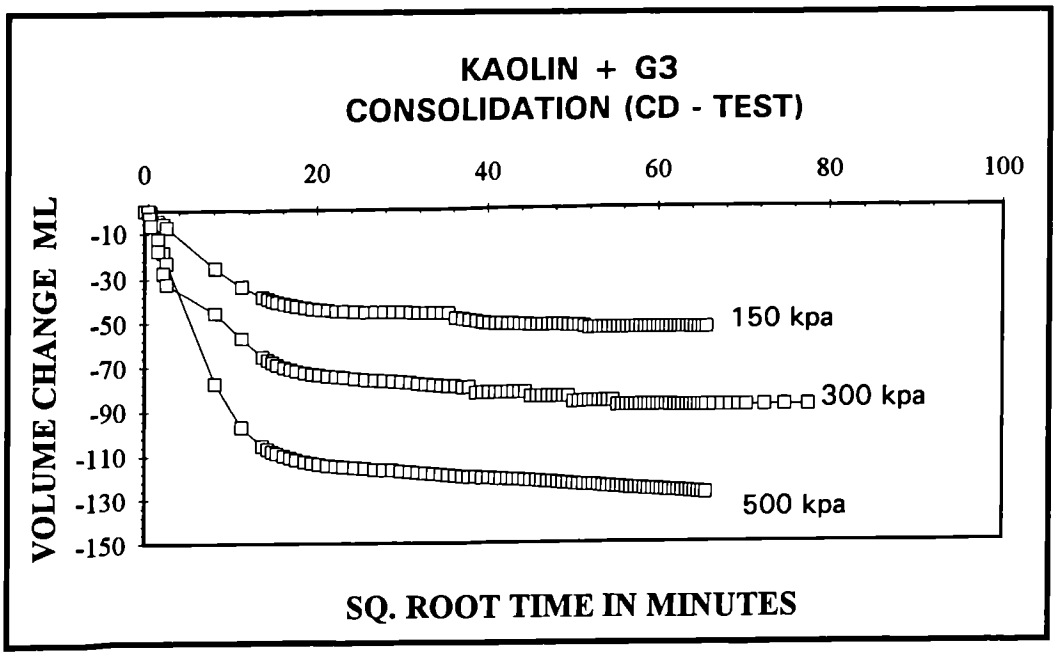

Fig. 55 Volume change vs. sq. time, consolidation drained compression triaxial test

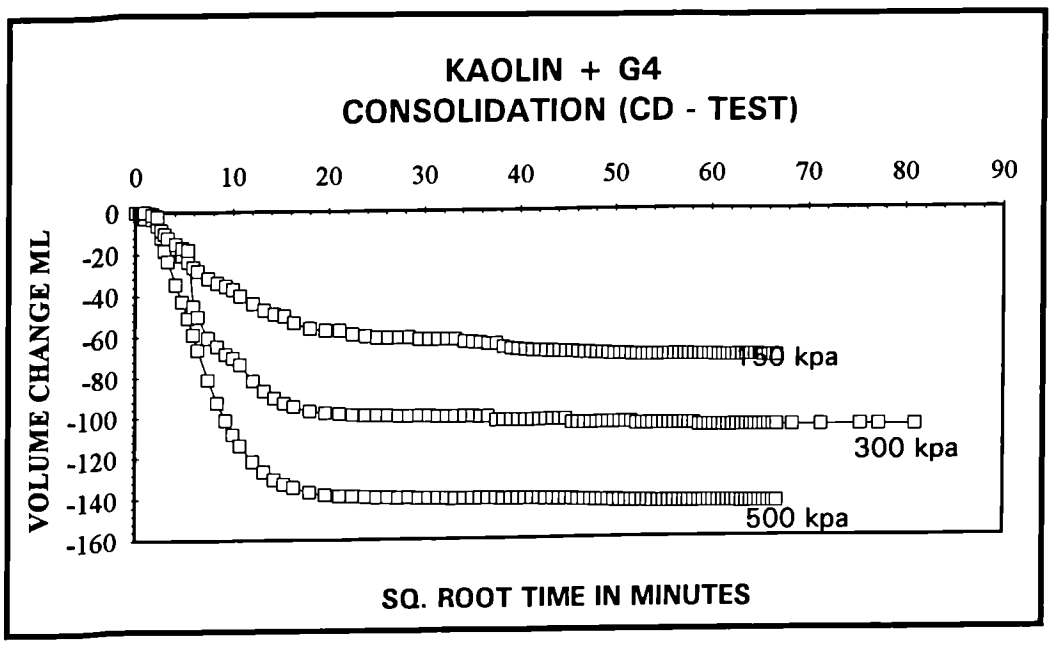

Fig. 56 Volume change vs. sq. time, consolidation drained compression triaxial test

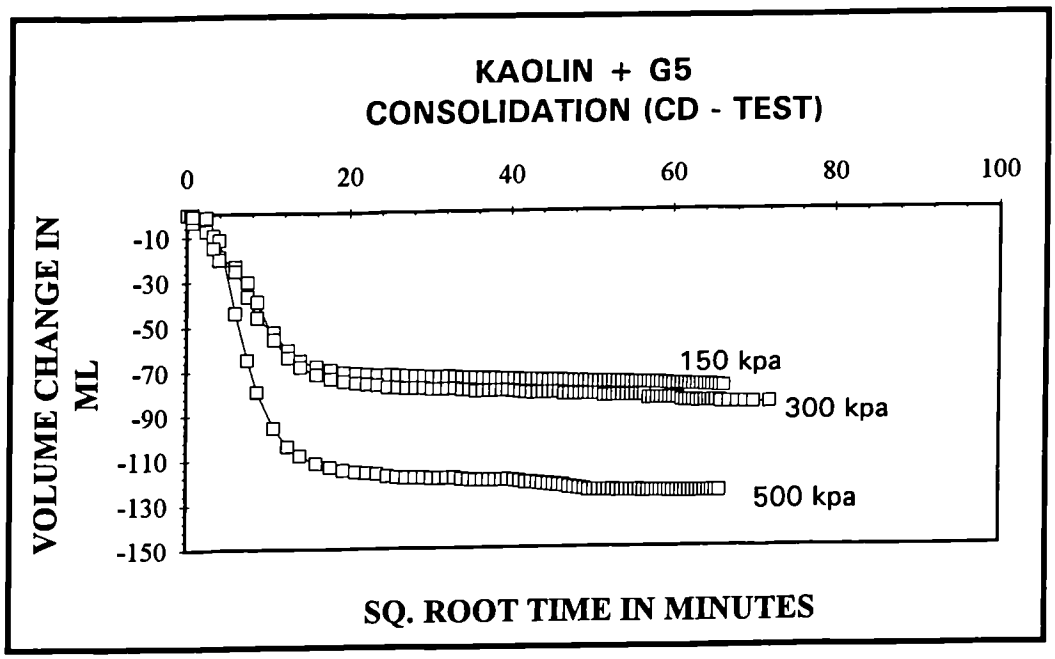

Fig. 57 Volume change vs. sq. time, consolidation drained compression triaxial test

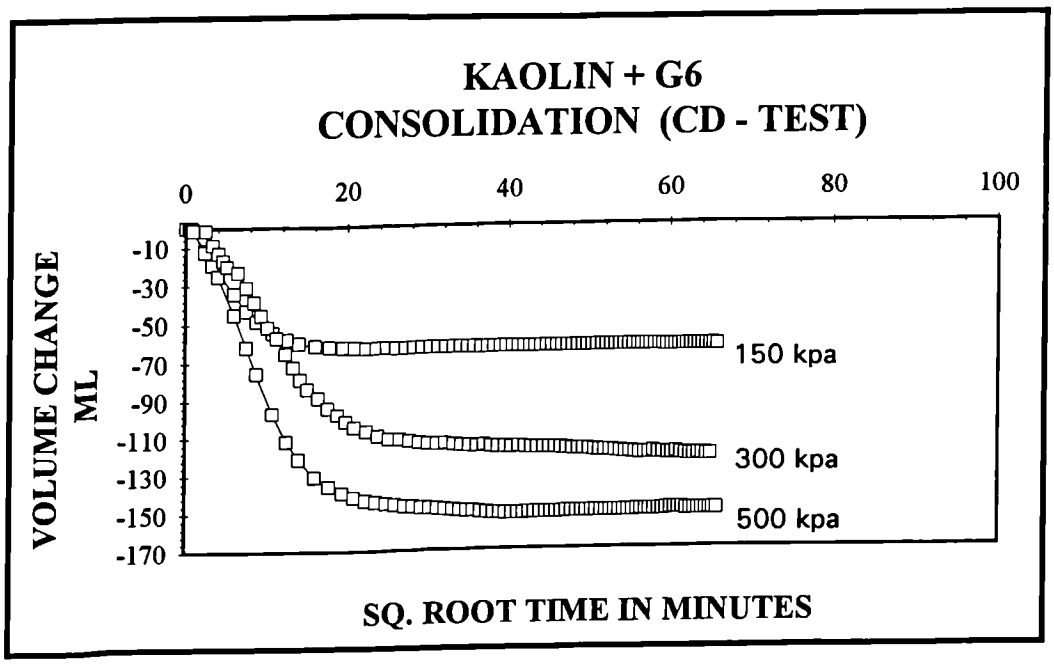

Fig. 58 Volume change vs. sq. time, consolidation drained compression triaxial test

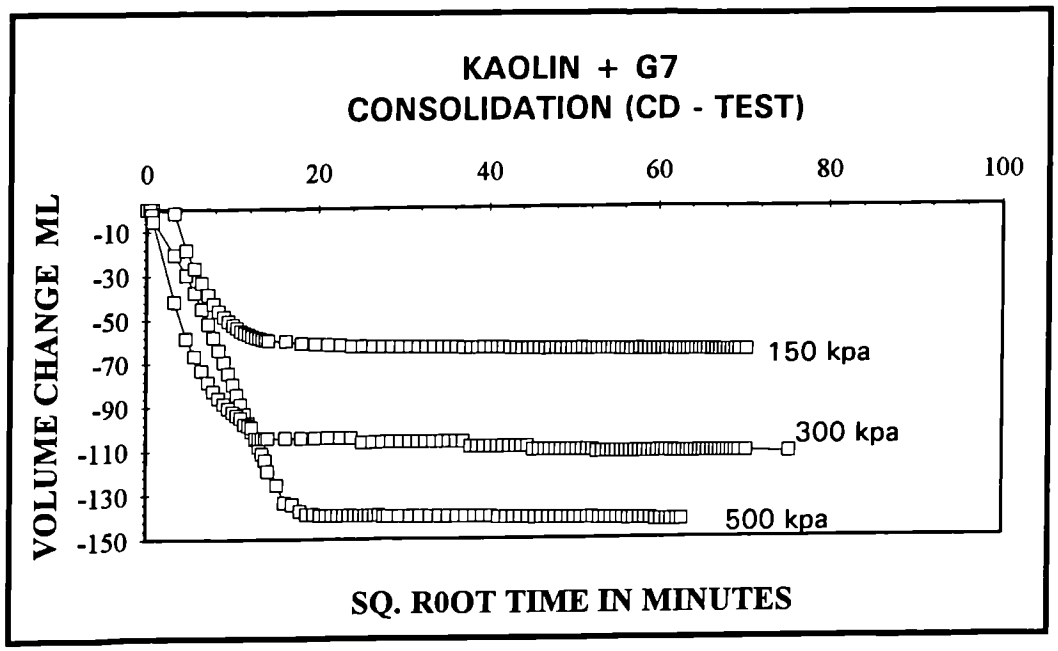

Fig. 59 Volume change vs. sq. time, consolidation drained compression triaxial test

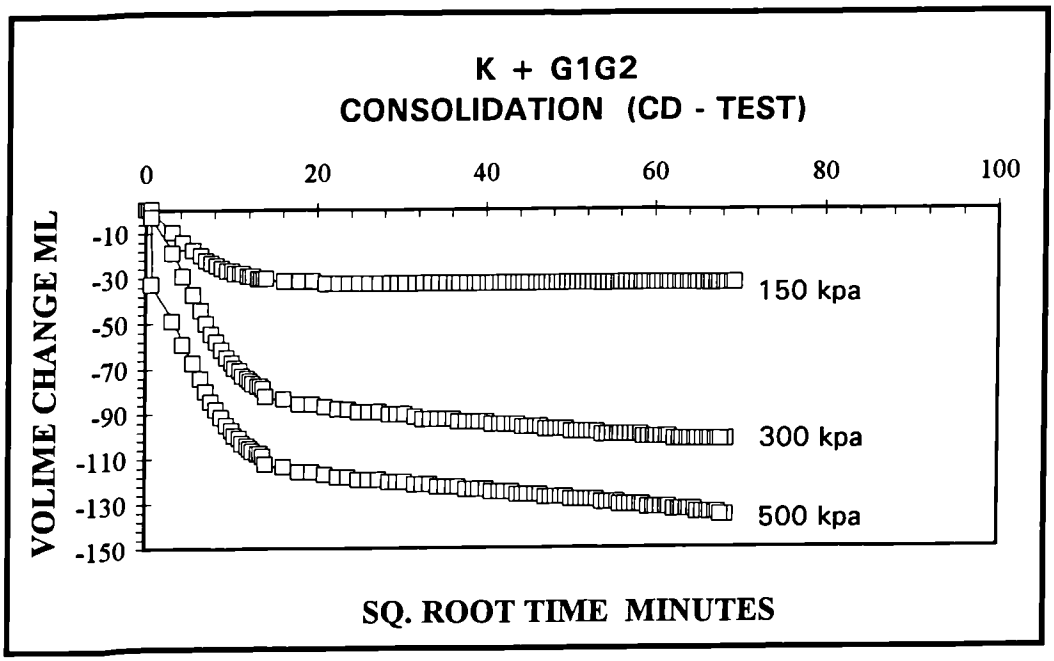

Fig. 60 Volume change vs. sq. time, consolidation drained compression triaxial test

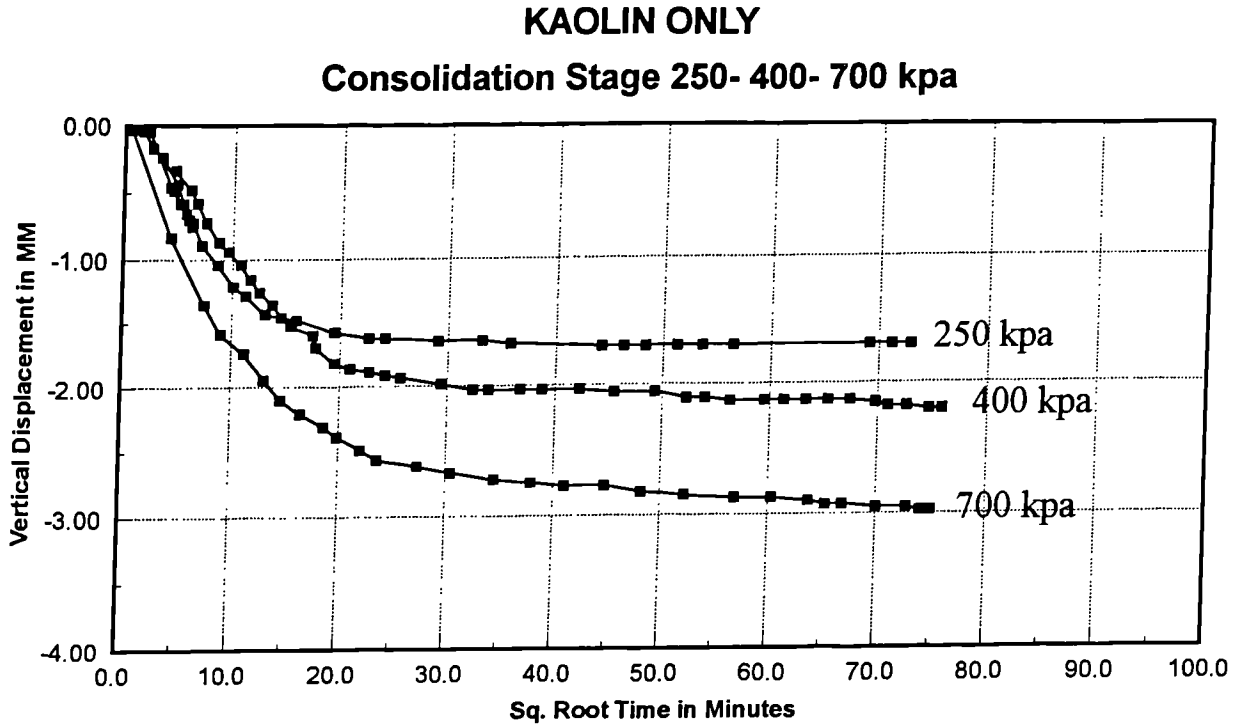

Fig. 61: Vertical displacement vs. sq. root time, Rowe Cell Consolidation test

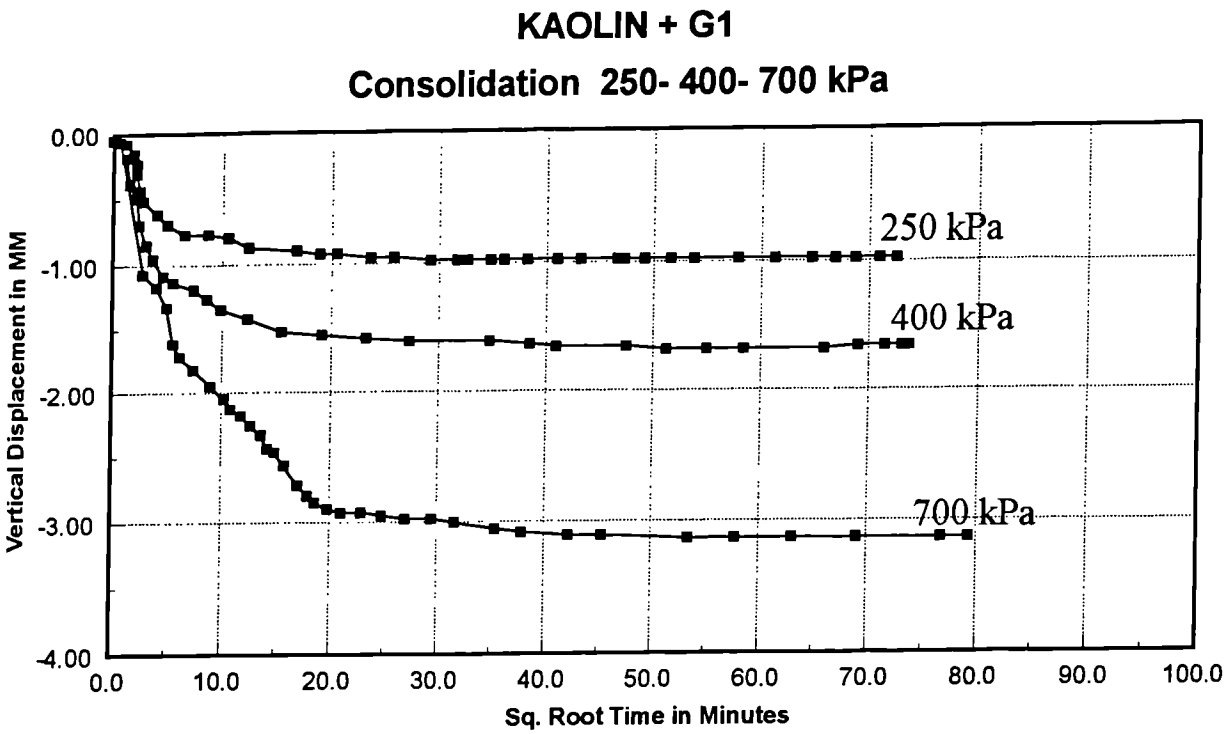

Fig. 62: Vertical displacement vs. sq. root time, Rowe Cell Consolidation test

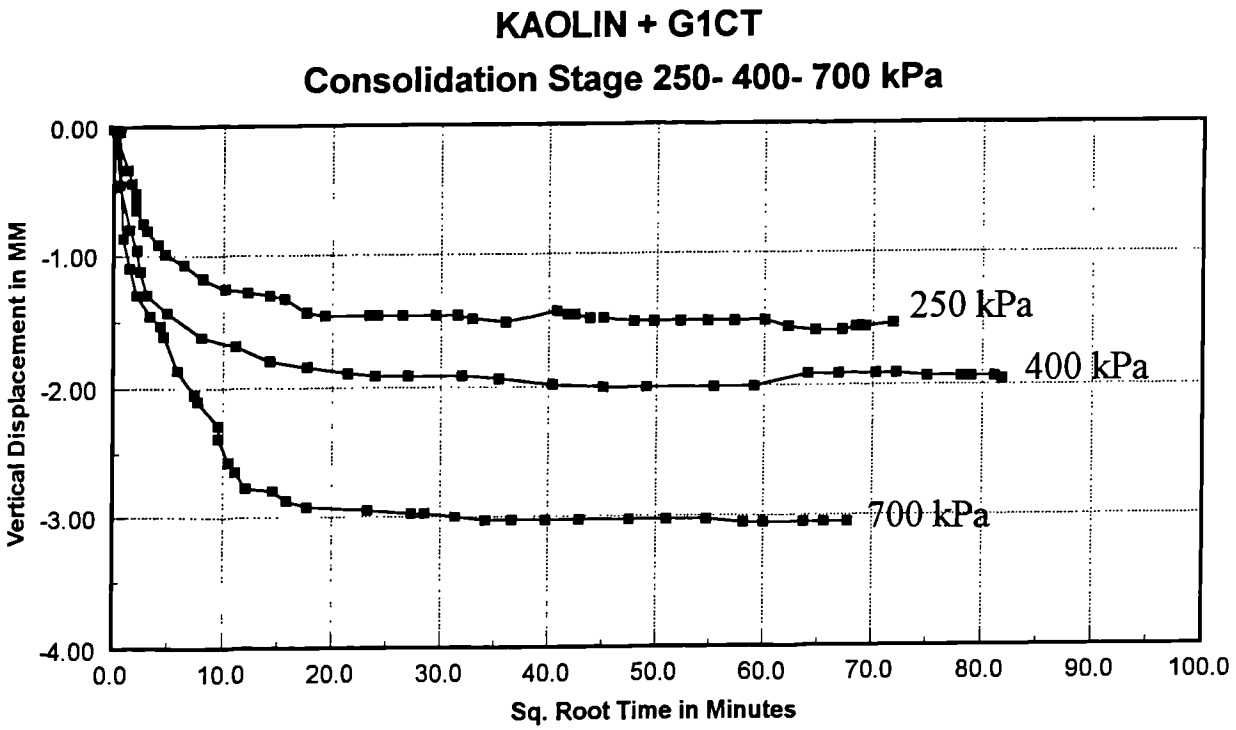

Fig. 63 Vertical displacement vs. root time, Rowe cell consolidation test

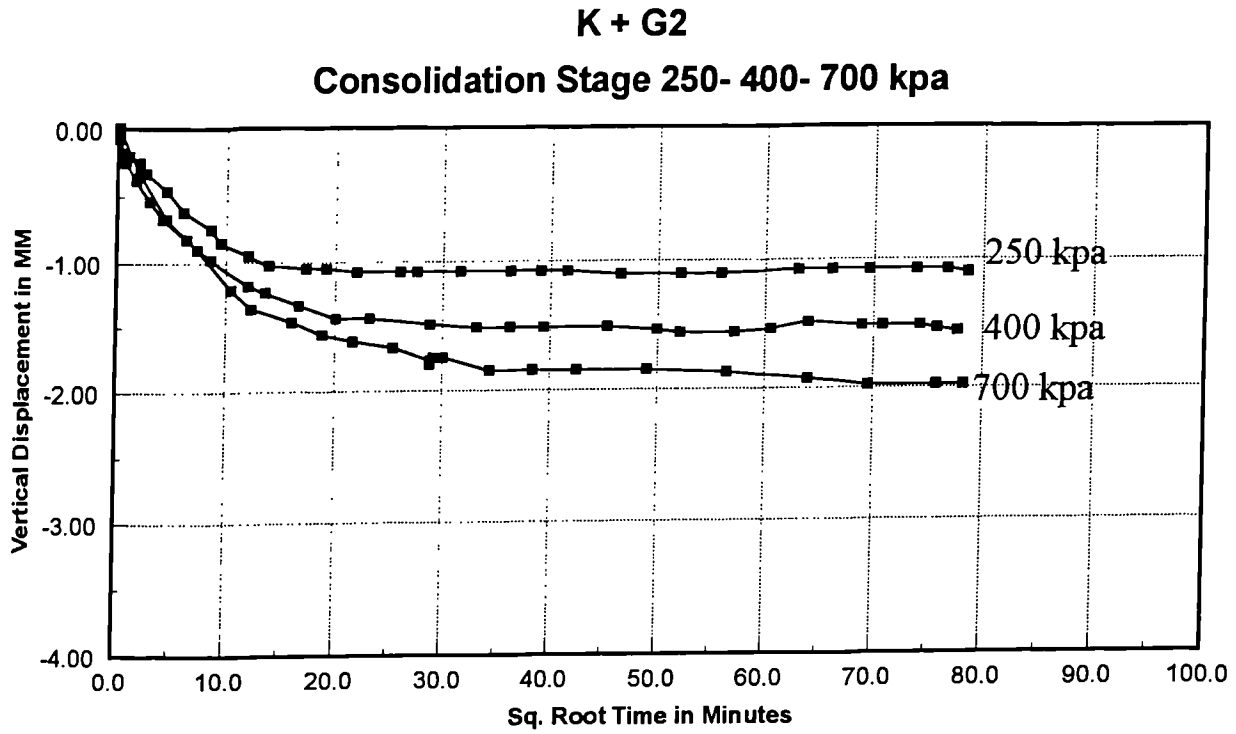

Fig. 64 Vertical displacement vs. sq. root time, Rowe cell consolidation test

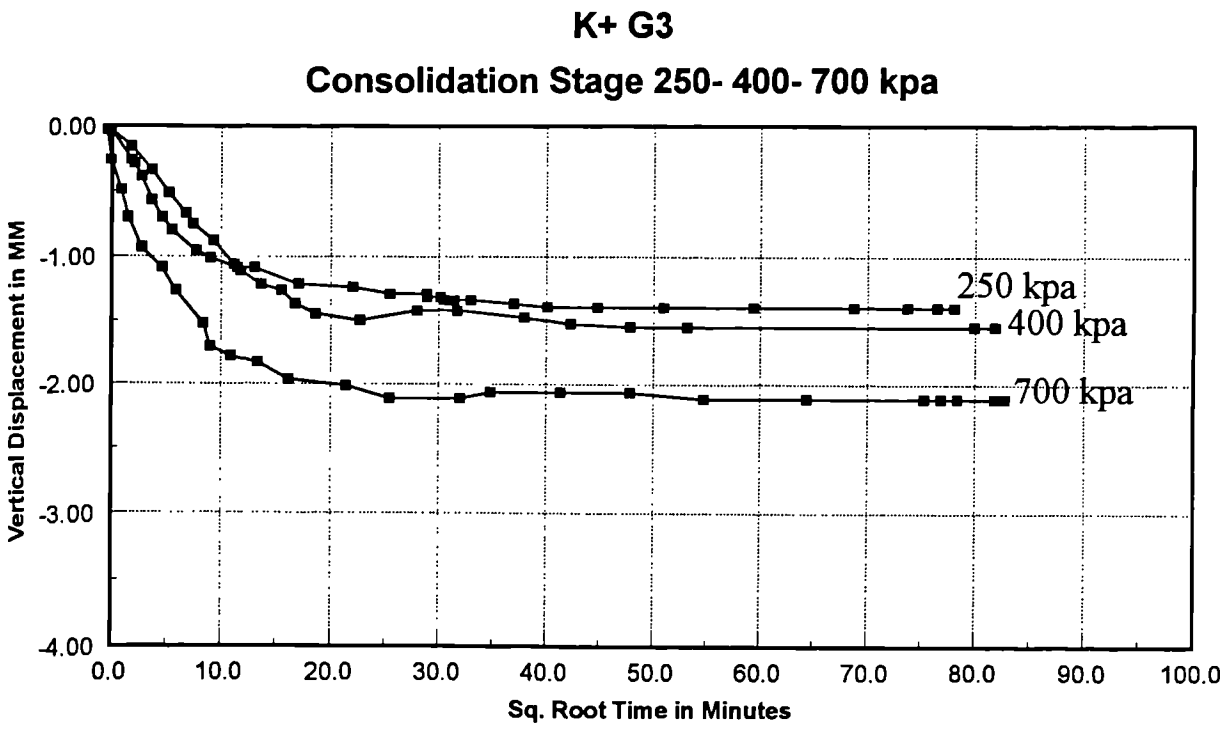

Fig. 65 Vertical displacement vs. sq. root time, Rowe cell consolidation test

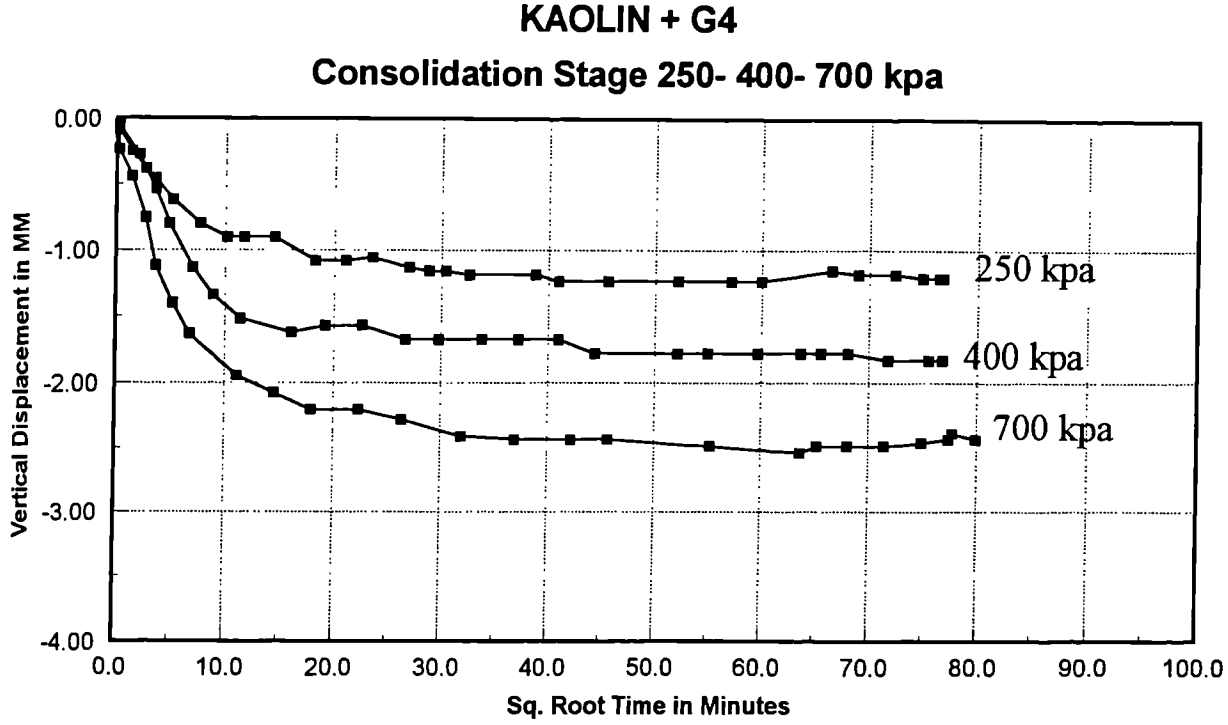

Fig. 66 Vertical displacement vs. sq. root time, Rowe cell condolidation test

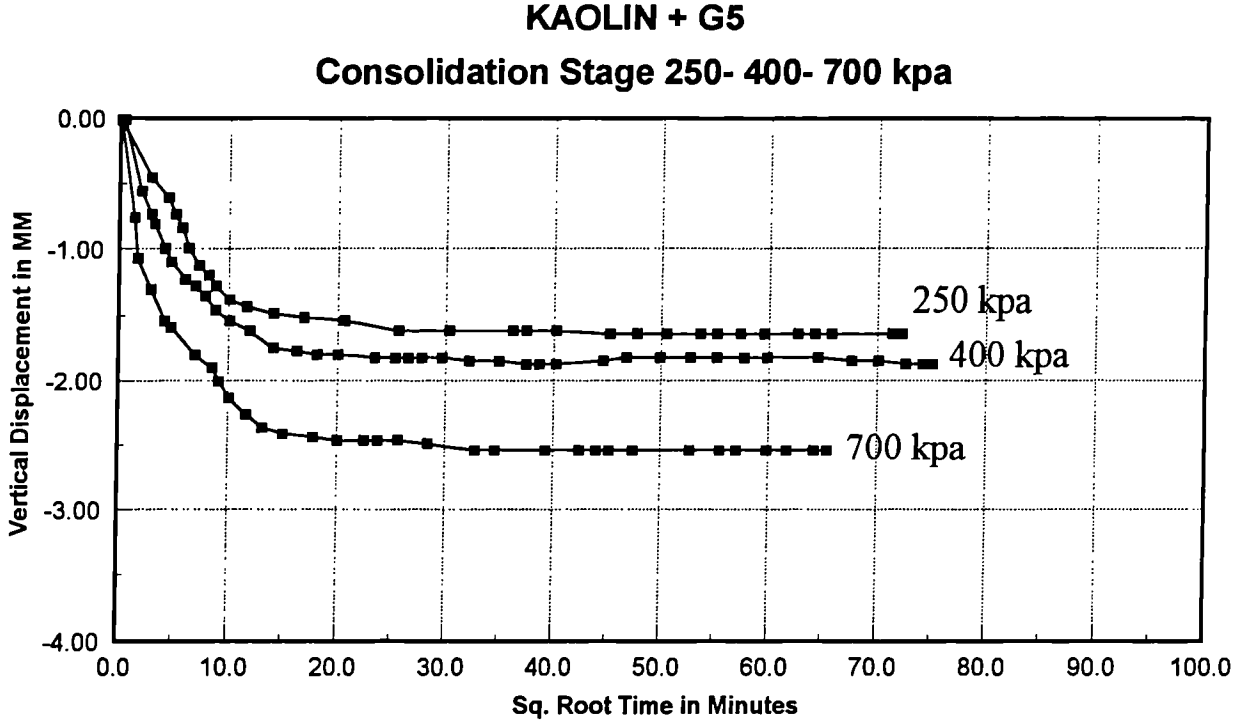

Fig. 67 Vertical displacemnet vs. sq. root time, Rowe cell consolidation test

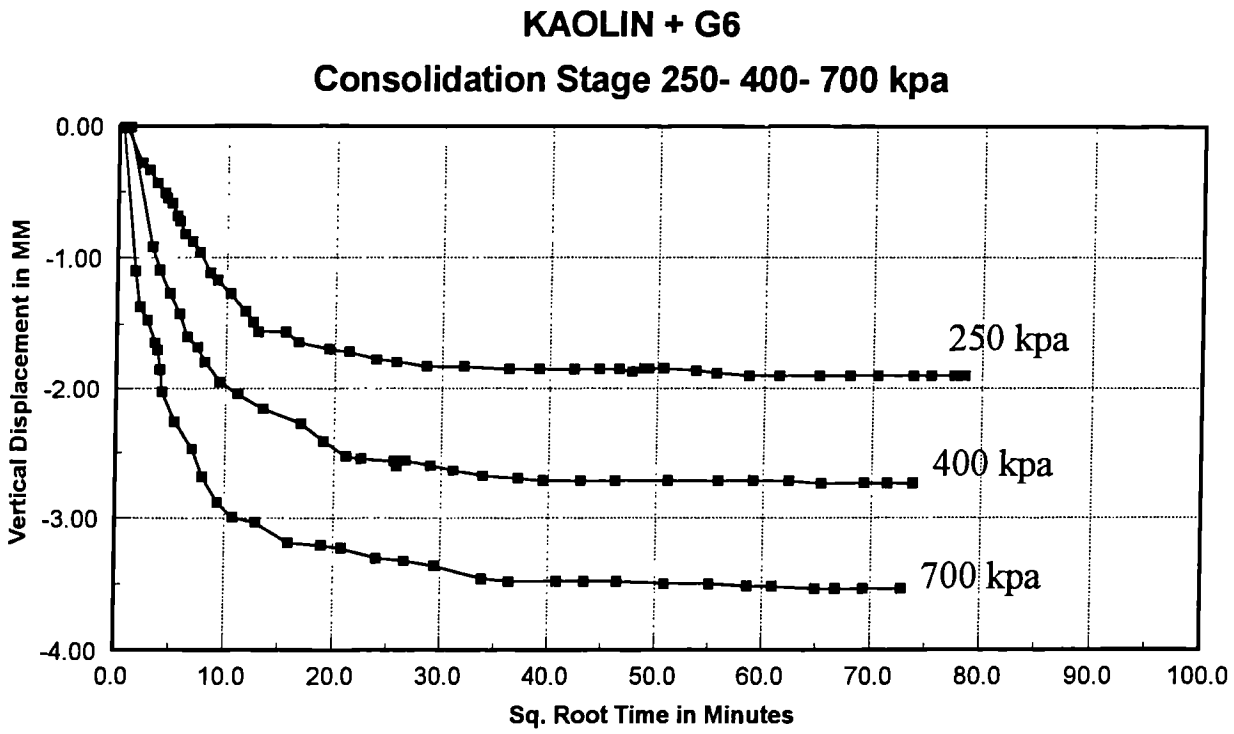

Fig. 68 Vertical displacement vs. sq root time, Rowe cell consolidation test

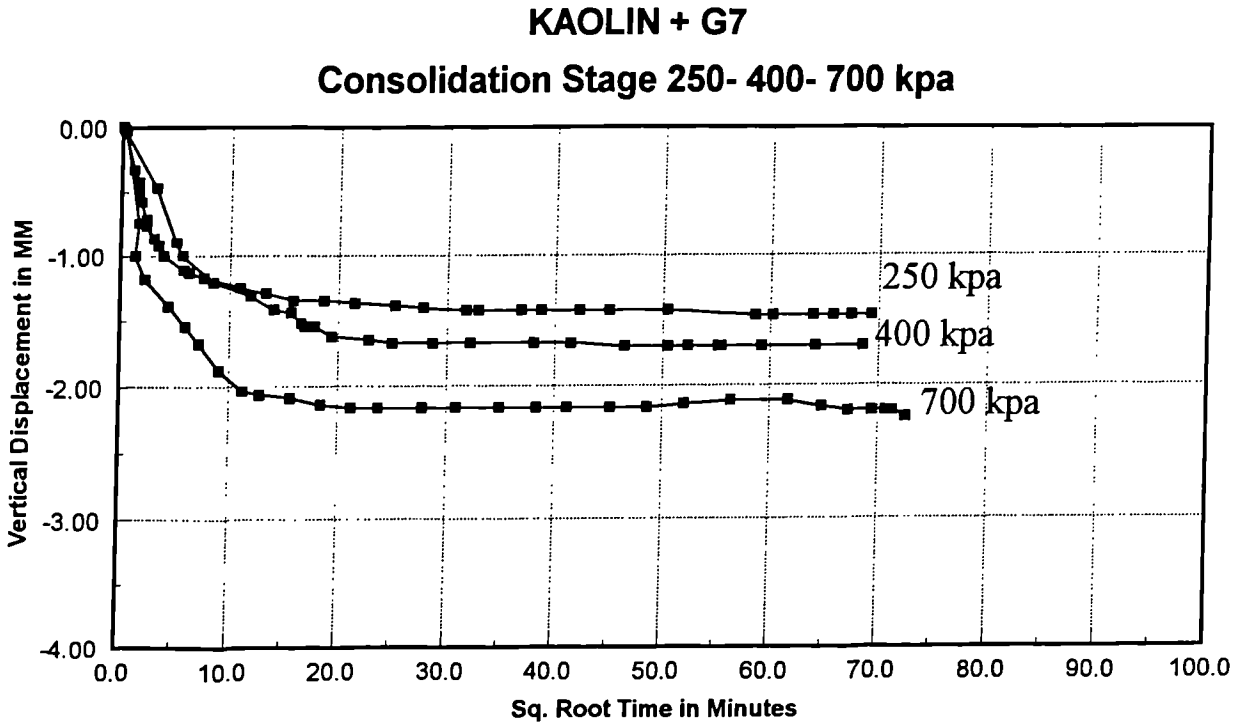

Fig. 69 Vertical displacement vs. sq. root time, Rowe cell consolidation test

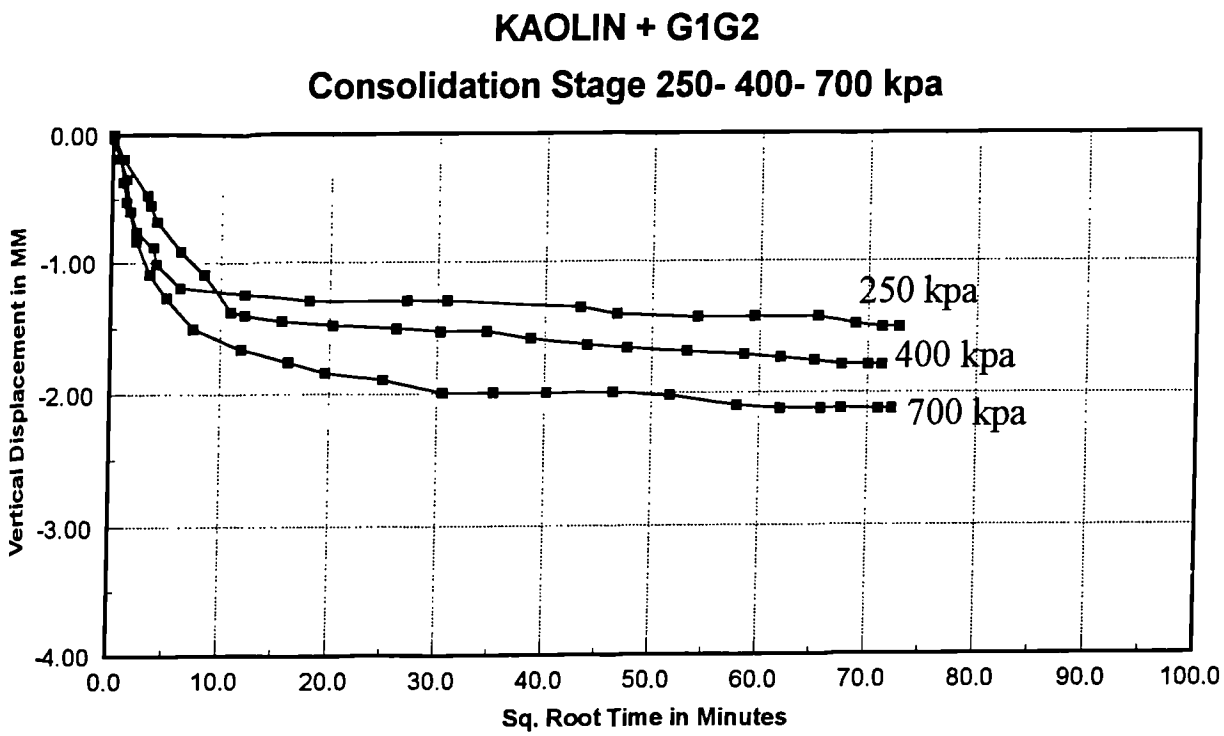

Fig. 70 Vertical displacement vs. sq. root time, Rowe cell consolidation test

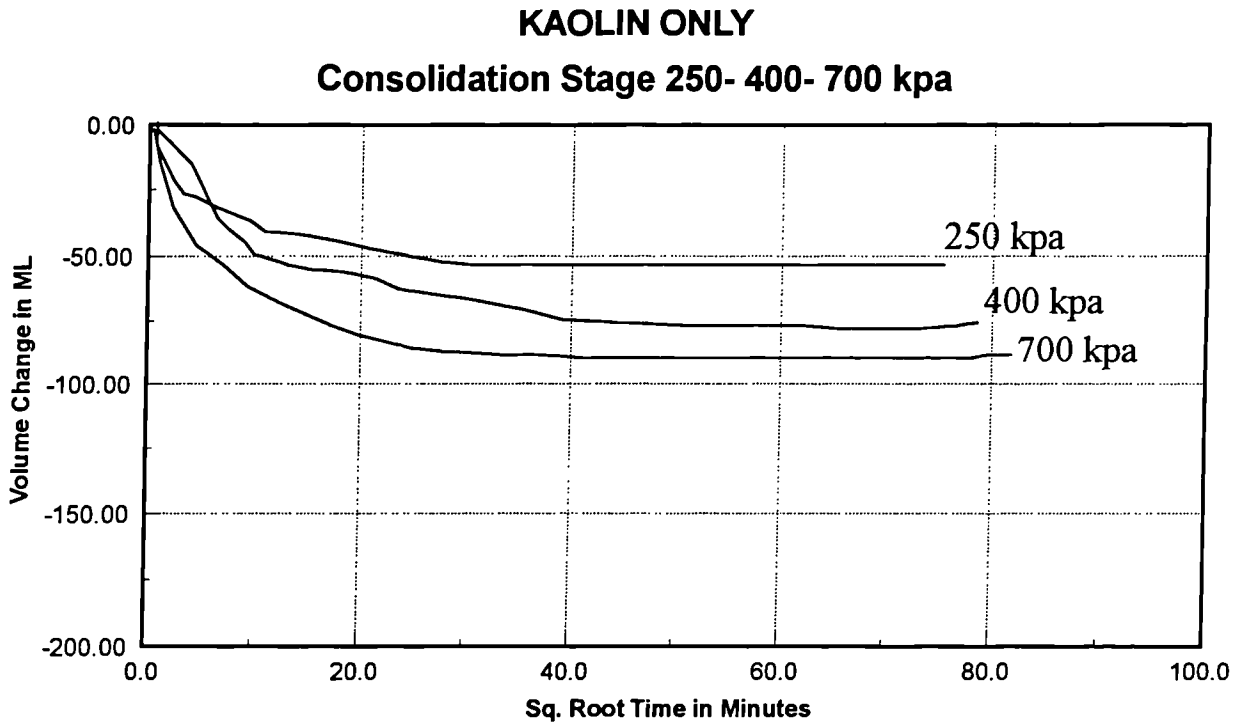

Fig. 71 Volume change vs. sq. root time, Rowe cell consolidation test

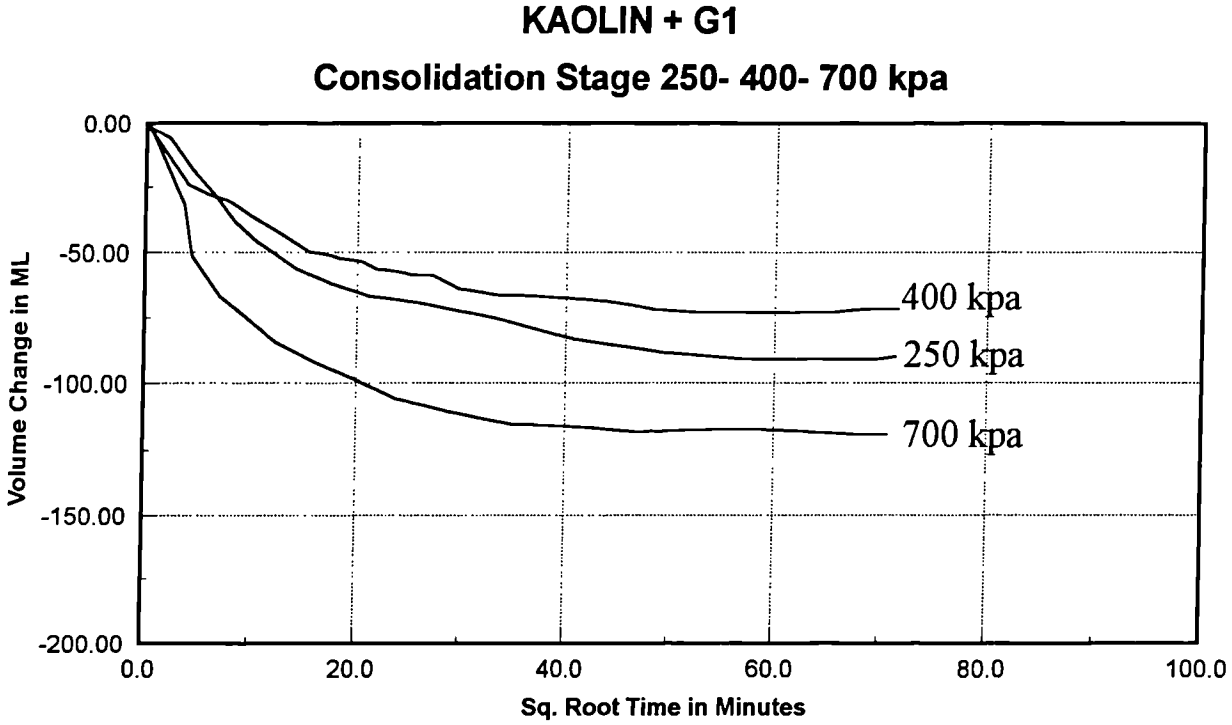

Fig. 72 Volume change vs. sq. root time, Rowe cell consolidation test

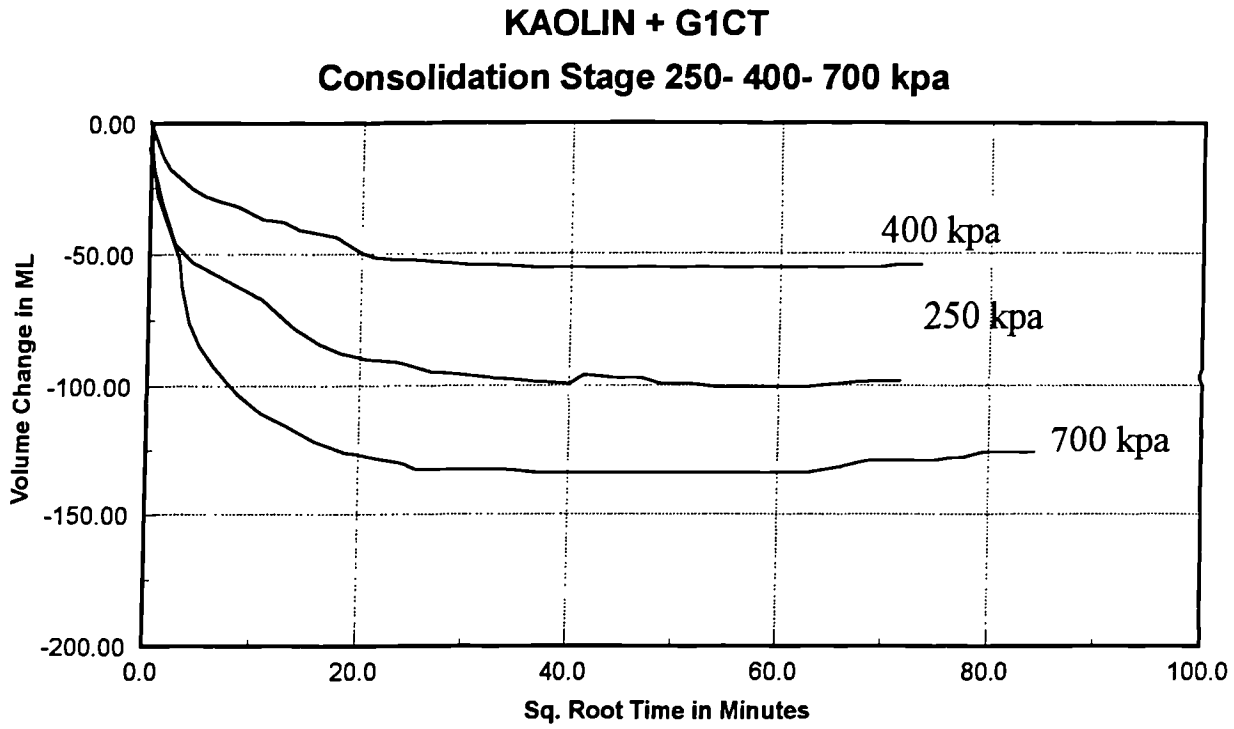

Fig. 73 Volume change vs. sq. root time, Rowe cell consolidation test

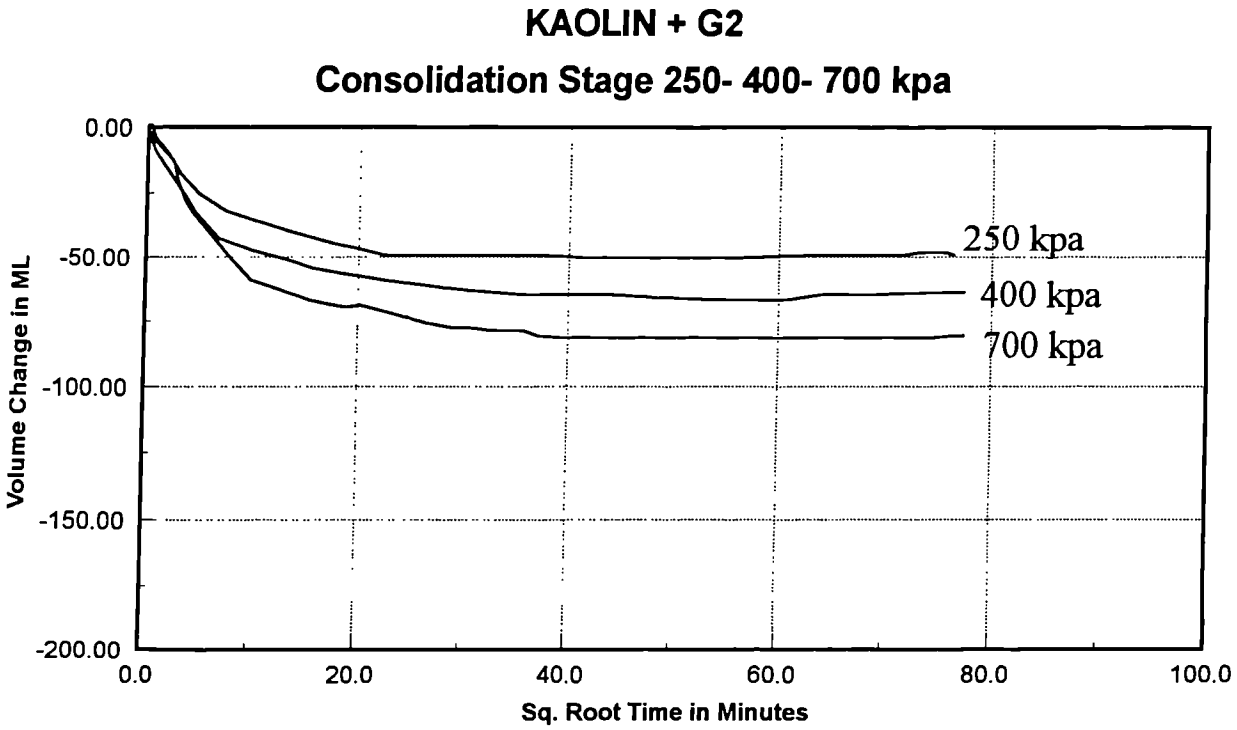

Fig. 74 Volume change vs. sq. root time, Rowe cell consolidation test

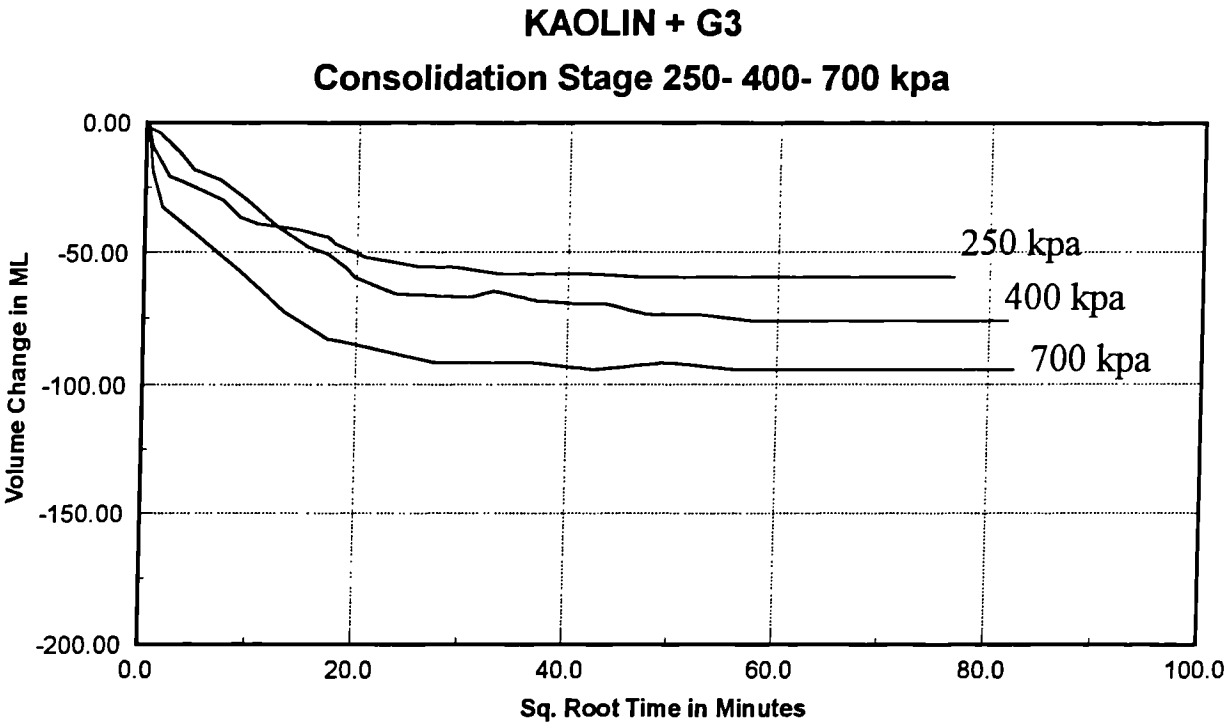

Fig. 75 Volume change vs. sq. root yime, Rowe cell consolidation test

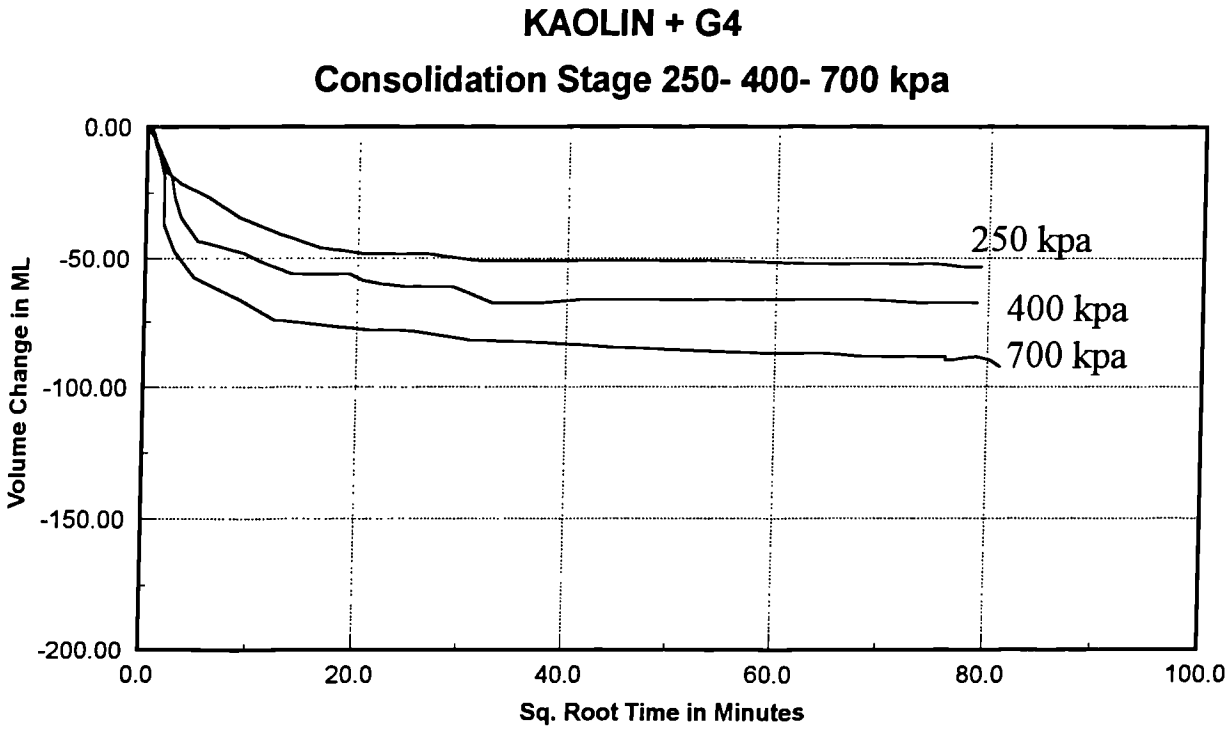

Fig. 76 Volume change vs. sq. root yime, Rowe cell consolidation test

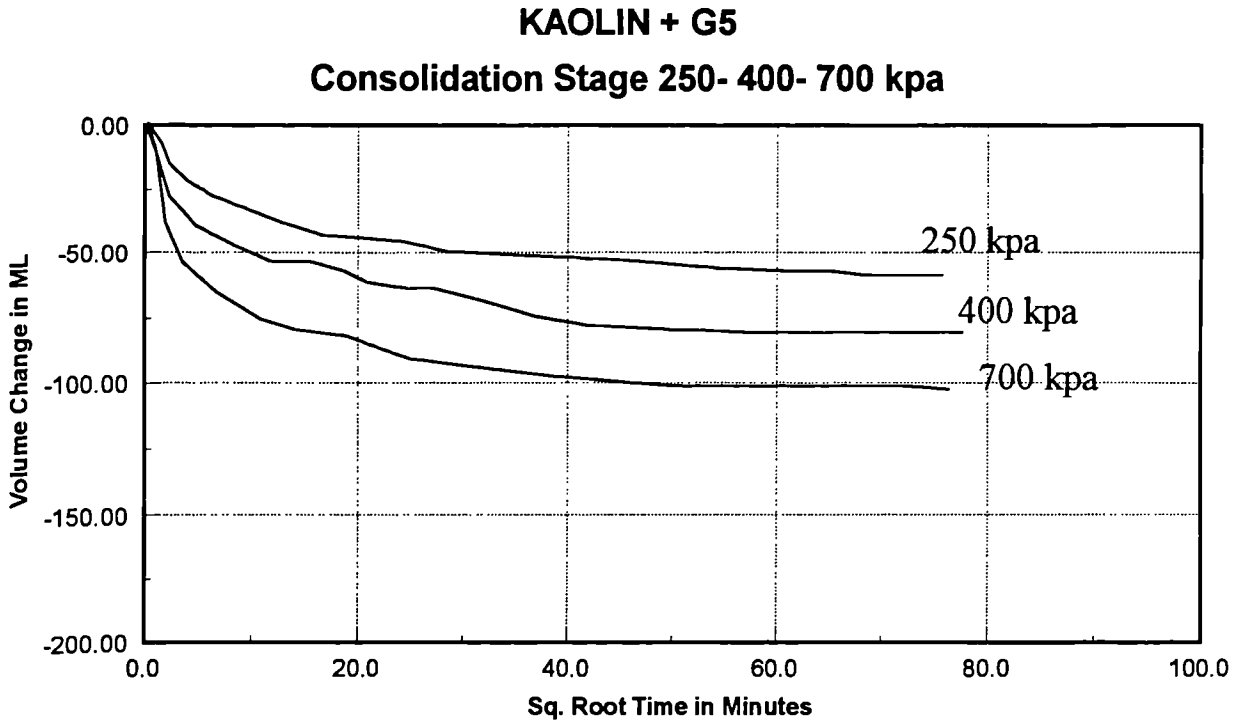

Fig. 77 Volume change vs. sq. root time, Rowe cell consolidation test

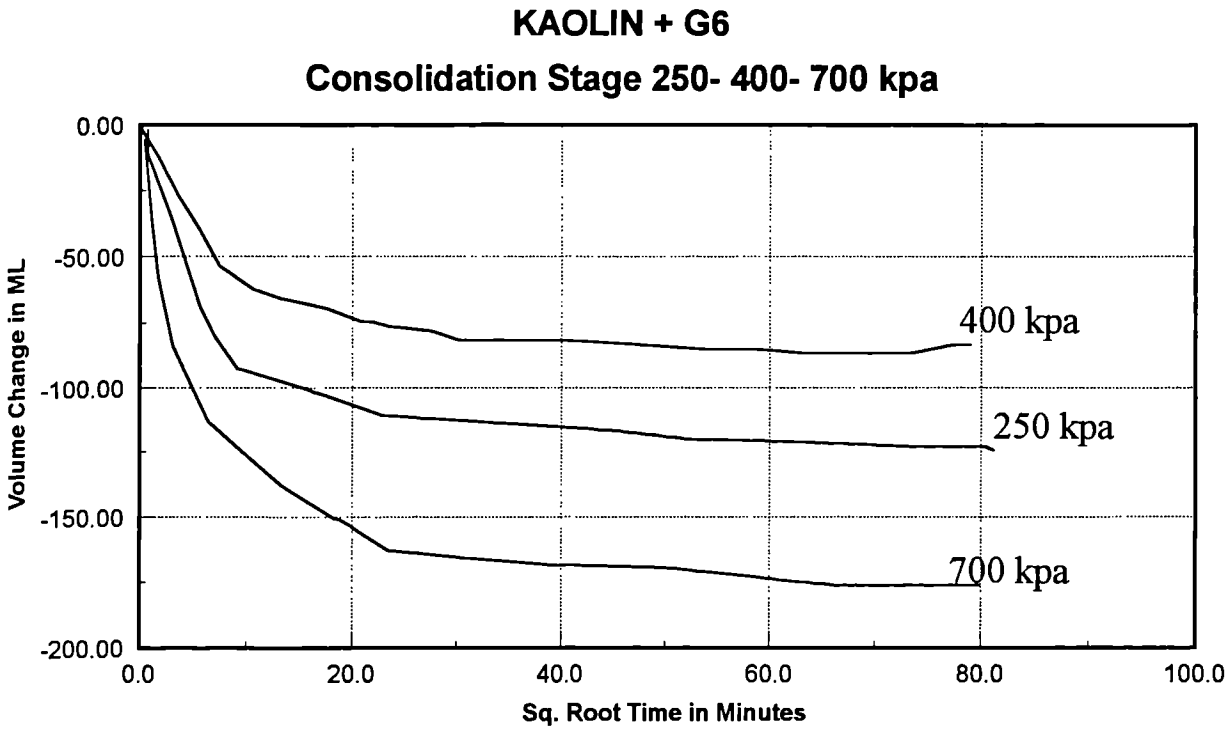

Fig. 78 Volume change vs. sq. root time, Rowe cell consolidation test

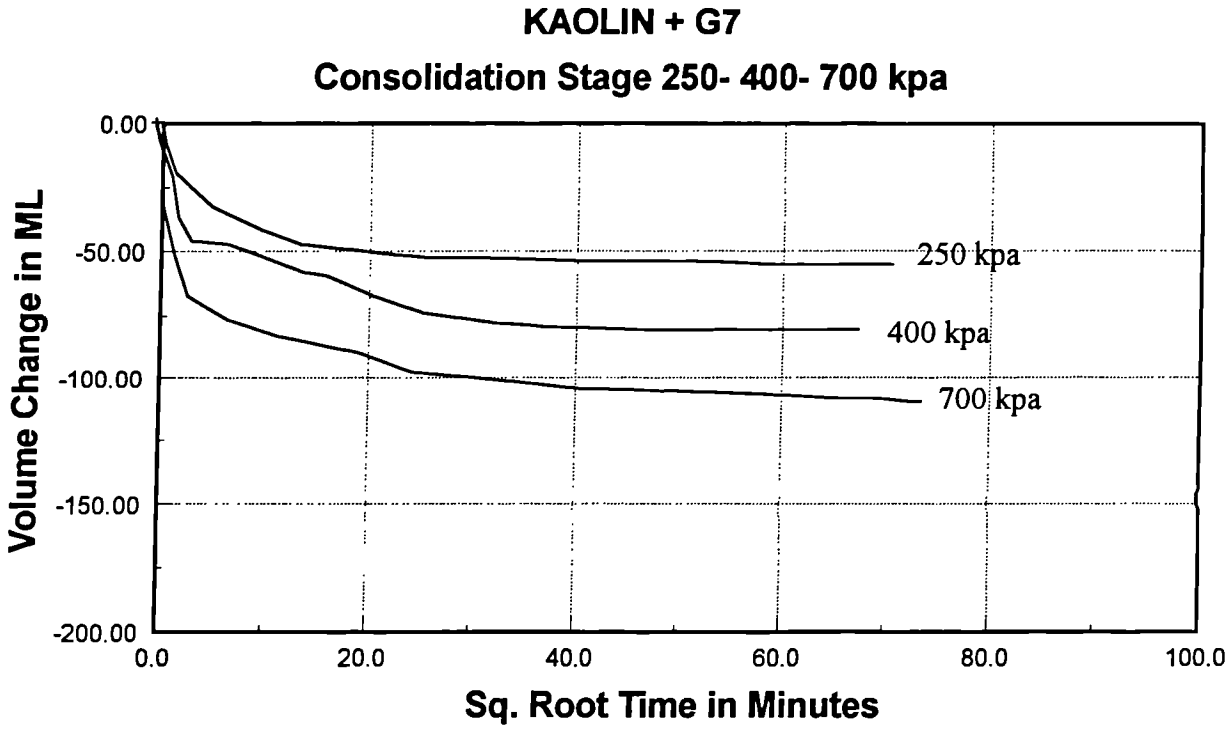

Fig. 79: Volume change vs. sq. root time, Rowe cell consolidation test

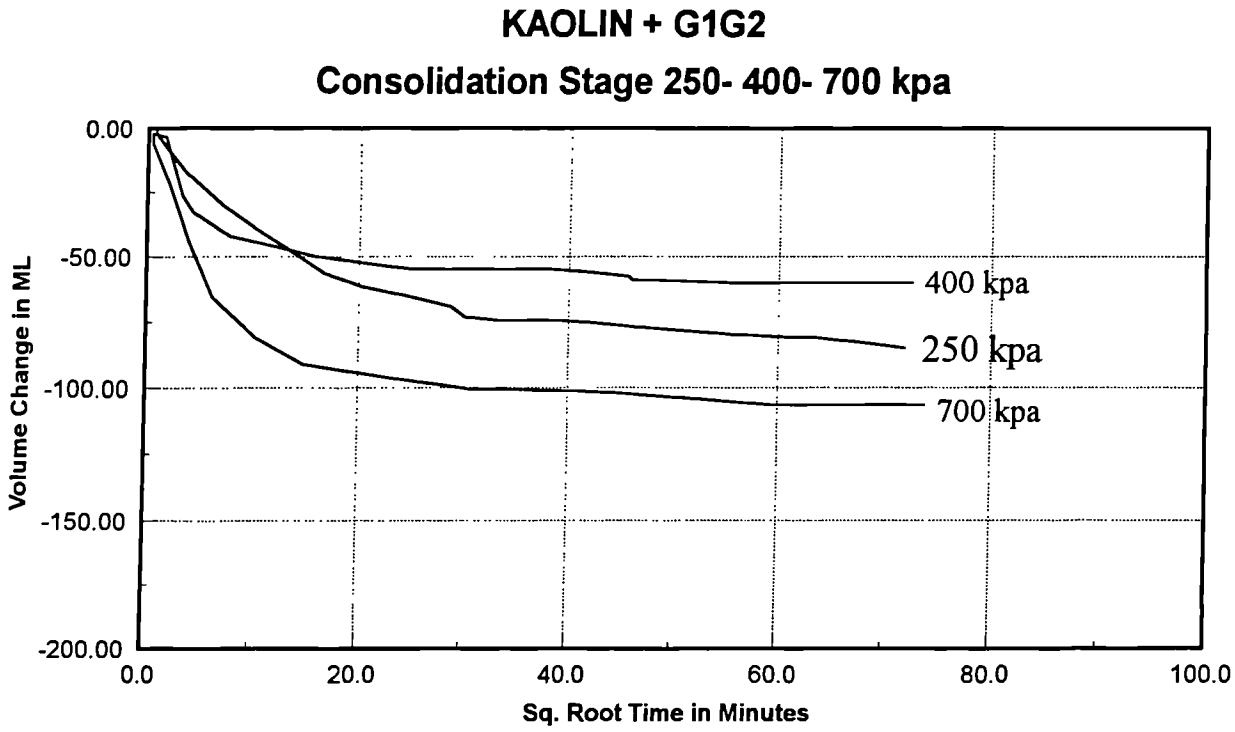

Fig. 80: Volume change vs. sq. root time, Rowe cell consolidation test

APPENDIX B

Related Text

B.1 HYPERBOLIC STRESS - STRAIN MODEL:

The hyperbolic model proposed by Kordner (1963) can be expressed as;

$$(\sigma_1 - \sigma_3) = \frac{\varepsilon}{a + b\varepsilon} \qquad (B.1)$$

where:
σ_1 and σ_3 = the major and minor principal stresses,
ε = the axial strain,
a and b = constant whose value may be determined experimentally.
Both of these constants a and b have readily visualised physical meanings; as shown in Fig. B.1, a is the reciprocal of the initial tangent modulus, E_i and b is the reciprocal of the asymptotic value of stress difference which the stress-strain curve approaches at infinite strain $(\sigma_1-\sigma_3)_{ult}$.

Kondner showed that the values of the coefficients a and b may be determined most readily if stress-strain data are plotted on transformed axes, as shown in Fig. B.2. When Equation B.1 is rewritten in the following form;

$$\frac{\varepsilon}{(\sigma_1 - \sigma_3)} = a + b\varepsilon \qquad (B.2)$$

It may be note that a and b equal respectively, the intercept and the slope of the resulting straight line. By plotting stress-strain data in the form shown in Fig. B.2, it is easy to determine the values of the parameters a and b corresponding to the best fit between a hyperbola (a straight line in Fig. B.2) and the test data.

When this is done it is commonly found that the asymptotic value of $(\sigma_1-\sigma_3)$ is larger than the compressive strength of the soil by a small amount. This would be expected, because the hyperbola remains below the asymptote at all finite values of strain. The asymptotic value may be related to the compressive strength, however, by means of a factor R_f as shown by;

$$(\sigma_1-\sigma_3)_f = R_f(\sigma_1-\sigma_3)_{ult} \qquad (B.3)$$

in which $(\sigma_1-\sigma_3)_f$ = the compressive strength, or stress difference at failure; $(\sigma_1-\sigma_3)_{ult}$ = the asymptotic value of stress difference; and R_f the failure ratio, which always has a value less than unity. For a number of different soils, the value of R_f as been found to be between 0.75 and 1.00, and to be essentially independent of confining pressure.
By expressing the parameters a and b in terms of the initial tangent modulus value and the compressive strength, Equation A.1, may be rewritten as;

$$(\sigma_1 - \sigma_3) = \frac{\varepsilon}{\frac{1}{E_i} - \frac{\varepsilon R_f}{(\sigma_1 - \sigma_3)_f}} \qquad (B.4)$$

This hyperbolic representation of stress-strain curves developed by Kondner et al., has been found to be a convenient and useful means of reprocessing the non linearity of soil stress-strain behaviour, and forms an important part of the stress-strain relationship.

(i) Stress-Dependency

Both the tangent modulus value and the compressive strength of soils have been found to vary with the confining pressure employed in the tests. Experimental studies by Janbu (1963), have shown that the relationship between initial tangent modulus and confining pressure may be expressed as;

$$E_i = KP_a\left(\frac{\sigma_3}{P_a}\right)^n \qquad (B.5)$$

where;
E_i = the initial tangent modulus,
σ_3 = the minor principal stress,
P_a = atmospheric pressure expressed in the same pressure units as E_i and σ_3,
K = a modulus number,
n = the exponent determining the rate of variation of E_i with $\sigma 3$, (both K and n are pure numbers).

Values of the parameters K and n may determined readily from the results of a triaxial tests by plotted the values of E_i against σ_3 on log-log scales and fitting a straight line to the data.
If it is assumed that failure will occur with no change in the value of σ_3, the relationship between compressive strength and confining pressure may be expressed conveniently in terms of the Mohr - Coulomb failure criterion as;

$$(\sigma_1 - \sigma_3)_f = \frac{2c\cos\phi + 2\sigma_3 \sin\phi}{1 - \sin\phi} \qquad (B.6)$$

in which c and ϕ = the Mohr - Coulomb strength parameters.

Equations B.5 and B.6, in combination with Equation B.4, provide a means of relating stress to strain and confining pressure by means of the five parameters K, n, c, ϕ, and Rf. Techniques for utilising this relationship in non-linear finite element method to predict the performance of reinforced soil walls are described by Jones (1988), and Jones and Heshmati (1993).

(ii) Tangent Modulus Values

The stress-strain relationship expressed by Equation B.4, may be employed very conveniently in incremental stress analyses because it is possible to determine the value of the tangent modulus corresponding to any point on the stress-strain curve. If the value of the minor principal stress is constant, the tangent modulus, Ft, may be expressed as;

$$E_t = \frac{\delta(\sigma_1 - \sigma_3)}{\delta_\varepsilon} \qquad (B.7)$$

Differentiation on Equation 4 leads t the following expression for tangent modulus;

$$E_t = \frac{\dfrac{1}{E_i}}{\dfrac{1}{E_i} + \dfrac{R_f \varepsilon}{(\sigma_1 - \sigma_3)_f}} \qquad (B.8)$$

Although this expression for the tangent modulus value could be employed in incremental stress analyses, it has one significant shortcoming: The value of the tangent modulus, Et, is related to both stress difference and strain [$(\sigma_1$-$\sigma_3)$ and ε], which may have different reference states. Although the reference state for stress difference [$(\sigma_1$-$\sigma_3) = 0$] can be specified exactly, the reference state for strain ($\varepsilon = 0$) is completely arbitrary. Thus, for example, the initial condition of a soil mass, before some external loading is applied, may rationally be referred to as the undeformed state, or state of zero strain. The same condition, however, could not be referred to as the state of zero stress difference if the mass contained non hydrostatic stresses as a result of body forces or any other influence. For the purpose of analysing the effects of a newly applied external

load, therefore, the initial condition could be chosen as the reference state for strain but not for stress difference. Therefore, the expression for tangent modulus may be made more generally useful if it is made independent of stress or independent of strain. Because the reference state for strain is chosen arbitrarily, and because stresses may be calculated more accurately than strains in many soil mechanics problems, it seems logical to eliminate strain and express the tangent modulus value in terms of stress only.

The strain, ε, may be eliminated from Equation B.8 by rewriting Equation B.4 as;

$$\varepsilon = \frac{(\sigma_1 - \sigma_3)}{E_i\left[1 - \frac{R_f(\sigma_1 - \sigma_3)}{(\sigma 1 - \sigma 3)_f}\right]} \qquad (B.9)$$

and substituting this expression for strain into Equation B.8. After simplifying the resulting expression, Et may be expressed as;

$$E_t = (1-R_f S)^2 \times E_i \qquad (B.10)$$

in which S = the stress level, or fraction of strength mobilised, given by;

$$S = \frac{(\sigma_1 - \sigma_3)}{(\sigma_1 - \sigma_3)_f} \qquad (B.11)$$

If the expressions for Ei, $(\sigma_1-\sigma_3)_f$, and S given by Equation B.6 and B.11 are substituted into Equation B.10, the tangent modulus value for any stress condition may be expressed as;

$$E_t = \left[1 - \frac{R_f(1-\sin\phi)(\sigma_1 - \sigma_3)}{2C\cos\phi + 2\sigma_3 \sin\phi}\right]^2 \times KP_a\left(\frac{\sigma_3}{P_a}\right)^n \qquad (B.12)$$

This expressions for tangent modulus may be employed very conveniently in incremental stress analyses, and constitutes the essential portion of the stress-strain relationship. It may be employed in either effective stress analyses or total stress analyses. For effective stress analyses, drained triaxial tests, with σ'_3 constant throughout, are used to determine

the values of the required parameters. For total stress analyses, undrained triaxial tests, with σ_3 constant throughout, are used to determine the parameter values.

The usefulness of equation 12 lies its simplicity with regard to factors;
i) because the tangent modulus is expressed in terms stresses only, it may be employed for analyses of the problems involving any arbitrary initial stress conditions without any additional complications.
ii) The parameters involved in this relationship may be determined readily from the result of laboratory tests.

(iii) Evaluation of Material Constants

To evaluate the constants in this model, only conventional triaxial compression test data will be required. A series of tests, conducted in the range of confining pressure of interest and with volume change measurements, will provide the necessary data basis for such evaluation.

The Mohr-Coulomb strength coefficients c and ϕ can be determined by any conventional procedure. Two methods are commonly used. The first methods involves plotting the Mohr circle of stresses at failure and measuring the intercept and angle of inclination of the linearized portion of the failure envelope over the stress range of interest. In the second method, the values at failure of $1/2(\sigma_1-\sigma_3)_f$ are plotted versus those of $1/2(\sigma_1+\sigma_3)_f$. The intercept, a, and the slope angle, α, of the best-fit line are used to calculate c and ϕ according to;

$$\phi = \sin^{-1}(\tan \alpha) \qquad (B.13)$$

and;

$$c = \frac{a}{\cos\phi} \qquad (B.14)$$

Two steps are involved in evaluating the modulus coefficients K and n, which prescribe the variation of the initial tangent modulus E_i with the confining pressure according to equation B.5. The first step is to determine E_i for each test, and is best executed by plotting $\varepsilon/(\sigma_1-\sigma_3)$ versus ε. The reciprocal of the intercept of the straight line (1/a) is equal to E_i, whereas the inverse slope of the line (1/b) is equal to $(\sigma_1-\sigma_3)_{ult}$, which defines the failure ratio in equation B.3. The second step is to plot E_i verses σ_3 from each test on a log-log scale, using the slope and the intercept of the data line to evaluate n and k in equation B.5.

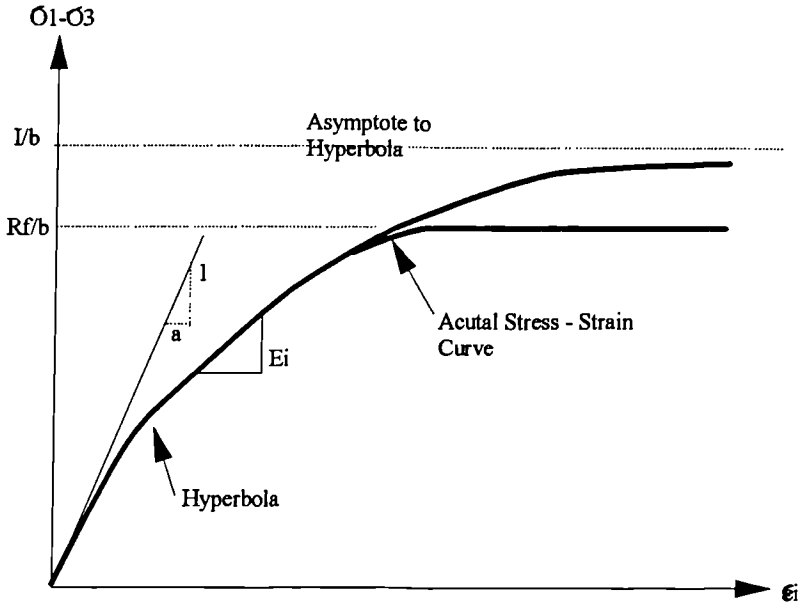

Fig. 8.1: Hyperbolic fit to stress-strain curve at constant Ó3

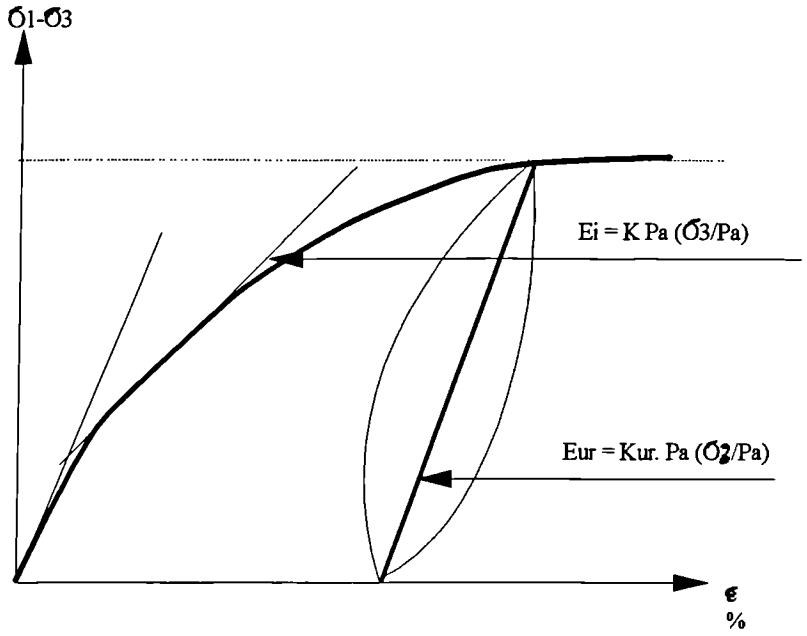

Hyperbolic Model

Fig. B.2: Hyperbolic Model

Fig. B.1 Fig. B.2	Hyperbolic Stress - Strain Model

APPENDIX C

Sample Calculations

C1. DETERMINATION OF TIME REQUIRED FOR THE RATE OF STRAIN TO FAILURE

The time to failure for both drained and undrained triaxial test are given by Head (1968). Factors for drained tests are derived from equations and data given by Bishop and Henkel (1962), and factors for undrained tests are in agreement with those derived by Blight (1963).

for drained test $t_f = 1.8 \times t_{100}$
for undrained test $t_f = 14 \times t_{100}$

t_{100} can be obtained from the plot of volume change versus root-time at the end of consolidation stage.
The rate of strain can be calculated using the relationship given by Head, (1986). volume 3, pp 956;

$$\text{Rate of Strain} = \frac{\varepsilon_f \% L}{100 \times t_f} mm / \min$$

Strain ε_f assumed = 10 %
$t_f = 1.8 \times \sqrt{t_{100}} = 1.8\ (36)^2 = 2333$ min
$\therefore$ rate = $10 \times 202 / 100 \times 2333 = 0.0086$ mm/minute

C2. COEFFICIENT OF CONSOLIDATION c_v m_v/YEAR

$$c_{vi} = \frac{\pi(D/1000)^2}{\lambda(t_{100}/(60 \times 24 \times 365.2))} m^2 / Year$$

$$c_{vi} = \frac{1.652 \times D^2}{\lambda t_{100}} m^2 / Year$$

Where;
D = the diameter in mm,
λ = a constant depending on drainage boundary condition and can be obtained from, Head (1986).
t_{100} is the time representing theoretical 100 % consolidation in minute.

D = 102.3 mm, and $\sqrt{t100} = 1521$ min

$$C_v = \frac{1.652 \times (102.3)^2}{80 \times 1521} = 0.14 m^2 / Year$$

$C_v = 0.14\ m^2$ / year

C3. COEFFICIENT OF VOLUME COMPRESSIBILITY,

The coefficient of volume compressibility for isotropic consolidation denoted here M_v is the change in volume per unit volume, ΔVc/Vs for a unit change of effective stress, Head (1986);

$$m_v = \frac{\Delta Vc}{Vs} / (\Delta \sigma')$$

$$m_v = \frac{\Delta Vc}{Vs} \times \frac{1000}{\Delta \sigma'} m^2 / MN$$

Note: The change in effective stress Δσ' is equal to the change of pore water pressure in the sample from start to the end of consolidation stage, since the cell confining pressure remains constant.

Example;

ΔV = 44.1 Cm^3

V = 1610 Cm^3

$$m_v = \frac{44.1}{1610} \times \frac{1000}{(315-201)}$$

$m_v = 0.44 m^2 / MN$

C4. COEFFICIENT OF PERMEABILITY, K

Value for the coefficient of permeability, K can be calculated from, Head (1982);

$K = C_v \times m_v \times 0.31 \times 10^{-9}$ m/s

Example:

C_v = 4.03 m2 / year

m_v = 0.44 m2 / mN

K = $0.44 \times 4.03 \times 0.31 \times 10^{-9}$ m/s

K = 0.55×10^{-9} m/s

C5. TO DETERMINE THE "m_v' S" IN THE ROWE CELL TESTS

The coefficient of volume compressibility Mv, derived from odometer consolidation test, is calculated by Head (1982). the change in height of sample at each stage given by Head, (1986).

$$m_v = \frac{1}{H0} Mv = \frac{1}{H_0} \times \frac{(H_0 - H_1)}{(\Delta\sigma')}$$

H_0- H_1 change in height = displacement change during the consolidation.

$\therefore$ H_0 = Height of sample at start of the consolidation. (Height at end of saturation stage) or other consolidation stage.

Example;

Sample K - Total pressure range 150 - 250 kpa

$$m_v = \frac{1}{86.5} \times \frac{(86.5 - 84.5)}{100}$$

$= 2.91 \times 10^{-4}$ m^2 / kN

$= 0.28$ m^2 / mN

C6. TO DETERMINE THE c_v, VALUES IN ROWE CELL TESTS

The Root time method was used in the determination of t_{90}. Since the radial as well as vertical consolidation took place in the sample the expressions given by Head, (1986).

$c_v = 0.131\ (Tv \times H^2) / t$ for vertical and,

$c_{ri} = 0.131\ (Tri \times H^2) / t$ for horizontal inward drainage,

c_v = Coefficient of consolidation - vertical drainage,

c_{ri} = Coefficient of consolidation - radial inward drainage,

H = Sample height,

D = Diameter of sample, 254 mm,

Tv, Tri = Theoretical time factor.

Sample K, Consolidation pressure 250 kpa Effective pressure is equal 150 kpa.

$t_{90} = 12.4$, $T_v = 0.848$ equivalent for t_{90} - vertical

$T_{ri} = 2.631$ equivalent for t_{90} - horizontal

$\therefore$ Assumed was that t_{90} vertical and t_{90} horizontal were equal for simplicity.

c_{ri} / cv = overall equivalent coefficient of consolidation which was referred to as just c_v.

$$c_v = \frac{0.131 \times Tv \times H^2}{t_{90}}$$

$$c_v = \frac{0.131 \times Tv \times D^2}{t_{90}}$$

$$\therefore c_v = \frac{0.131 \times Tv}{t_{90}}(H^2 + D^2)$$

Assumed a Tv factor of $\frac{(0.848 + 2.631)}{2} = 1.74$

Example;

Assumed a T_v factor of $\frac{(0.848 + 2.631)}{2} = 1.74$

$$c_v = \frac{0.131 \times Tv}{12.4} \times (0.0865 + 0.254)^2$$

cv = 0.76 Tv m^2 / Year

c_v = 1.32 m^2 / Year

C7. COEFFICIENT OF PERMEABILITY, K

K = $c_v \times m_v \times 0.31 \times 10^{-9}$ m/s

Example:

c_v = 8.3 m2 / year

m_v = 0.28 m2 / mN

K = $8.3 \times 0.28 \times 0.31 \times 10^{-9}$ m/s

K = $0.72\ 10^{-9}$ m/s

APPENDIX D

Publications

D. PUBLICATIONS

(i) List of papers already published;

1. **Heshmati, S., Jones, C.J.F.P., and Zakaria, N.Z, (1990)**
"Effect of Composite Non-woven Geotextile on the Consolidation and Shear Properties of Kaolin", First International Seminar on Soil Mechanics and Foundation Engineering of Iran, Tehran, Nov. 1990, Vol. 3. pp 864-870.

2. **Heshmati, S. (1991)**
"Prediction of the Behaviour of Two Test Walls by non-linear elastic analysis", Class A Prediction Symposium, Denver, Colorado, USA, August, 1991. pp 11.

3. **Jones, C. J. F. P., Heshmati, S. (1993)**
"The use of the Finite Element Method to the Performance of Reinforced Soil Walls", International Congress on Computational Methods in Engineering, Shiraz University, Shiraz, Iran..

4. **Jones, C. J. F. P., Heshmati, S. (1993)**
"The Action of Geotextile to Provide Combined Drainage and Reinforcement to the Cohesive Soil", Second International Seminar on Soil Mechanics and Foundation Engineering of Iran, Tehran.

(ii) List of potential publications;

5. **Jones, C. J. F. P., Heshmati, S.**
The Action of Geotextile to Provide Combined Drainage and Reinforcement to Cohesive Soils

6. **Jones, C. J. F. P., Heshmati, S.**
Problems of the combination of drainage and reinforcement geotextile to the cohesive soil and a proposed geocomposite drainage and reinforcement material

7. **Jones, C. J. F. P., Heshmati, S.**
Finite element analysis of reinforced cohesive soil using the unit cell concept

EFFECT OF A COMPOSITE NON-WOVEN GEOTEXTILE ON THE CONSOLIDATION AND SHEAR PROPERTIES OF KAOLIN

by

S. HESHMATI, Department of Civil Engineering
University of Newcastle upon Tyne, U.K.

and

C. J. F. P. JONES, Department of Civil Engineering
University of Newcastle upon Tyne, U.K.

and

N. Z. ZAKARIA, Department of Civil Engineering
University of Newcastle upon Tyne, U.K.

SUMMARY

The inclusion of a composite geotextile providing both drainage and reinforcing functions into test samples of kaolin, produces a marked increase in the shear strength characteristics of the clay material. The tests were conducted in such a manner that the separate effects of the drainage function of the geotextile and the reinforcing function could be identified. The results indicate that composite geotextiles promise significant technical and economic benefits when used with cohesive soils.

INTRODUCTION

The conventional method used to construct reinforced soil structures uses good quality frictional fill reinforced with tensile members, DTp (1978). In many parts of the world frictional fill is difficult to obtain at economic rates and consequently the use of reinforced soil in these areas is curtailed, even though a reinforced soil structure may offer a technically superior solution.

Reinforced soil structures need not be restricted to frictional fills, indeed the earliest examples of reinforced soil developed in Mesopatamia circa 2000 BC were constructed using reinforced clay blocks, whilst parts of the Great Wall of China contain examples of reinforced clay and gravel, Jones (1985). Recently, methods have been explored to design steep reinforced soil embankment structures using cohesive fill reinforced with geotextiles, Tatsuoka et al (1990).

Modern geotextiles are produced to provide four major functions classified as: separation, filtration, drainage and reinforcement. The cohesionless fills usually specified for reinforced soil structures are free draining and can be relied upon to provide stable conditions when reinforced. Cohesive soils are more complex and soil structures built with cohesive fills are susceptible to changes in moisture content. Drainage geotextiles can be used to improve the drainage of cohesive fills and the use of these materials frequently results in improved strength characteristics of these soils. This leads to the concept of composite geotextiles which combine

the function of drainage and reinforcement and to their use with cohesive soils.

A problem with composite geotextiles is lack of information and knowledge concerning the relative improvement of the physical properties of a cohesive soil related to the drainage elements of the geotextile and those to the reinforcement function. This paper provides preliminary results of fundamental studies of the behaviour of a cohesive soil (kaolin) containing an inclusion in the form of a geotextile which acts as both a drainage material and as reinforcement. The objective of the study is to identify the separate effects (improvement) on the shear strength properties of the kaolin provided by the drainage function and separately that provided by the reinforcing function of the geotextile.

EXPERIMENTAL WORK

In order to provide information relating to the relative importance of drainage and reinforcement of composite geotextiles, a number of consolidated undrained (Cu) and consolidated drained (Cd) triaxial compression tests were undertaken using 100mm diameter samples containing a single layer of geotextile placed at mid-height in the sample. Drainage from the sample was directed through the geotextile at the centre of the sample by providing additional drainage paths down the side of the sample but which were isolated from the kaolin, Wamaya (1989) and Zakaria (1990).

The separation of the reinforcement function and the drainage function of the geotextile was arranged by testing intact geotextile, and geotextile cut in a spiral. The intact geotextile provided both drainage and reinforcement, while the geotextile disk cut in the spiral before placing in the kaolin sample provided an intact drainage path but no reinforcing function. Unreinforced and undrained samples of kaolin were tested to provide base data and samples were tested at cell pressures of 100, 300 and 600 kPa.

The index properties of the kaolin samples used in all tests are shown in Table 1. The material properties of the composite geotextile are shown in Table 2.

RESULTS

The results of the tests on the consolidated undrained (Cu) samples, both reinforced and unreinforced, are shown in Table 3. The results of the consolidated drained tests (Cd) are shown in Table 4. A stress path plot for both drained and undrained tests are shown in Figure 1. In the consolidated undrained tests the geotextile acted as a drainage material only. In the consolidated drained tests the geotextile acted as a drainage material and as a composite drainage and reinforcing material.

The inclusion of the drainage geotextile in the fully consolidated undrained tests produced a reduction in the effective angle of internal friction (ϕ') [24.1→18.5°] but a major increase in cohesion (c') [7.4→44.4kPa]. In the fully consolidated drained test the geotextile acting as a drainage layer only had no effect on the internal friction but produced an increase in cohesion (c') [23.8→30.0kPa]. Adding the role of reinforcement to the same geotextile produced a slight reduction in the

internal friction (ϕ') [21.0→19.4] but again increased the cohesion (c') [30.0→37.6kPa].

The composite geotextile produced an overall increase in cohesion (c') of 58% in which 26% was due to the geotextile acting as a drainage material and 32% due to the reinforcement function.

CONCLUSIONS

The preliminary results of tests to determine the influence of composite drainage/reinforcement geotextile fabrics on improving the strength characteristics of cohesive soils indicate that it is possible to differentiate between the benefits produced by the drainage function and the benefits produced by the reinforcing element of the composite material. The degree of improvement offered by the particular geotextile tested suggests that geotextiles providing composite functions could be technically and economically very beneficial and could permit the use of cohesive fills in reinforced soil structures.

ACKNOWLEDGEMENTS

The authors wish to acknowledge the support of Netlon Limited who provided the composite geotextile material used in the tests.

REFERENCES

Department of Transport (1978) "Reinforced Earth Retaining Walls and Bridge Abutments for Embankments", Technical Memorandum (Bridges) BE3/78 (Revised 1987), H.M.S.O., London.

Jones, C. J. F. P. (1985) "Earth Reinforcement and Soil Structures", Butterworths, p. 192, (Revised reprint 1988), London.

Tatsuoka, F; Musata, O; Tateyama, M; Nakamura, K; Tamuta, Y; Ling, H.I.; Iwasaki, K, and Yamauchi, H. (1990) "Reinforcing steep clay slopes with a non-woven geotextile", B.G.S. International Reinforced Soil Conference, Paper No. 2/4, Glasgow, Scotland.

Wamaya, B.M. (1989) "Effects of a Geotextile on the drainage, consolidation and shear properties of Kaolin as a construction material in embankments" MSc Dissertation, University of Newcastle upon Tyne, England.

Zakaria, N.Z. (1990) "Effects of a Geotextile on the drainage and shear properties of Kaolin as a construction material in embankments" MSc Dissertation, University of Newcastle upon Tyne, England.

Table 1 : Index Properties of Kaolin
(After Wamaya 1989)

Index Property	
Plastic Limit, P.L %	35.5
Liquid Limit, L.L %	61.0
Plasticity Index, P.I %	25.5
Specific Gravity, S.G	2.63
Dry Density, ρd, kg/m^3	1.320

Table 2 : Index Properties of Geotextile

Description: Non-woven needle punched geotextile of Polypropylene fibres.	
Resistant to the chemicals naturally found in soils and water	
Weight (g/m^2)	500
Material thickness (mm) without any load with a load of 200 kPa	 5.5 2.0
Tensile strength Din 53857 Longitudinal (kN/m) Transverse (kN/m)	 8 10
Effective Opening Size (Dw) (mm)	0.15
Permeability (K) (m/S) at 2 kPa	1.0×10^{-2}
Transmissivity at 200 kPa (m^2/S)	3.0×10^{-6}
Roll Size (m)	3.9 x 100

Table 3 : Fully Consolidated Undrained (Triaxial test)
(after Wamaya 1989)

	Cell Pressure σ_3(kPa)	Deviator Stress $(\sigma_1-\sigma_3)$kPa	Strain At Failure E_f %
With Geotextile (drainage)	600	511	8.7
Without Geotextile	600	- (112.5)	(8.4)
With Geotextile (drainage)	300	330	8.2
Without Geotextile	300	290	8.4
With Geotextile (drainage)	150	199	7.4
Without Geotextile	150	171.3	12.8
	MOHR CIRLE ϕ/C	TOTAL STRESS PATH ϕ/C	EFF. STRESS PATH ϕ'/C'
With Geotextile			
Angle of Internal friction (degrees)	15°	14.4°	18.5°
Cohesion (kPa)	40	43.4	44.4
Without Geotextile			
Angle of Internal friction (degrees)	16°	16.3°	24.1°
Cohesion (kPa)	20	20.9	7.4

Table 4 : Fully Consolidated Drained

	Cell Pressure σ_3(KPA)	Deviator Stress $(\sigma_1-\sigma_3)$KPA	Strain At Failure E_f %
Without Geotextile	600	-	-
With Geotextile			
(drainage only)	600	-	
(drainage & reinforcement)	600	796	12.3
Without Geotextile	300	420	11.9
With Geotextile			
(drainage only)	300	427	11.2
(drainage & reinforcement)	300	416	11.4
Without Geotextile	150	248	11.6
With Geotextile			
(drainage only)	150	256	10.0
(drainage & reinforcement)	150	263	10.0

	MOHR Circle ϕ C	Effective Stress Path ϕ' C'
Without Geotextile		
Angle of Internal Friction (degrees)	21.3	21.0
Cohesion (kPa)	24.0	23.8
With Geotextile (drainage only)		
Angle of Internal Friction (degrees)	22.0	21.9
Cohesion (kPa)	31.0	30.0
With Geotextile (drainage & reinforcement)		
Angle of Internal Friction (degrees)	19.6	19.4
Cohesion (kPa)	37.5	37.6

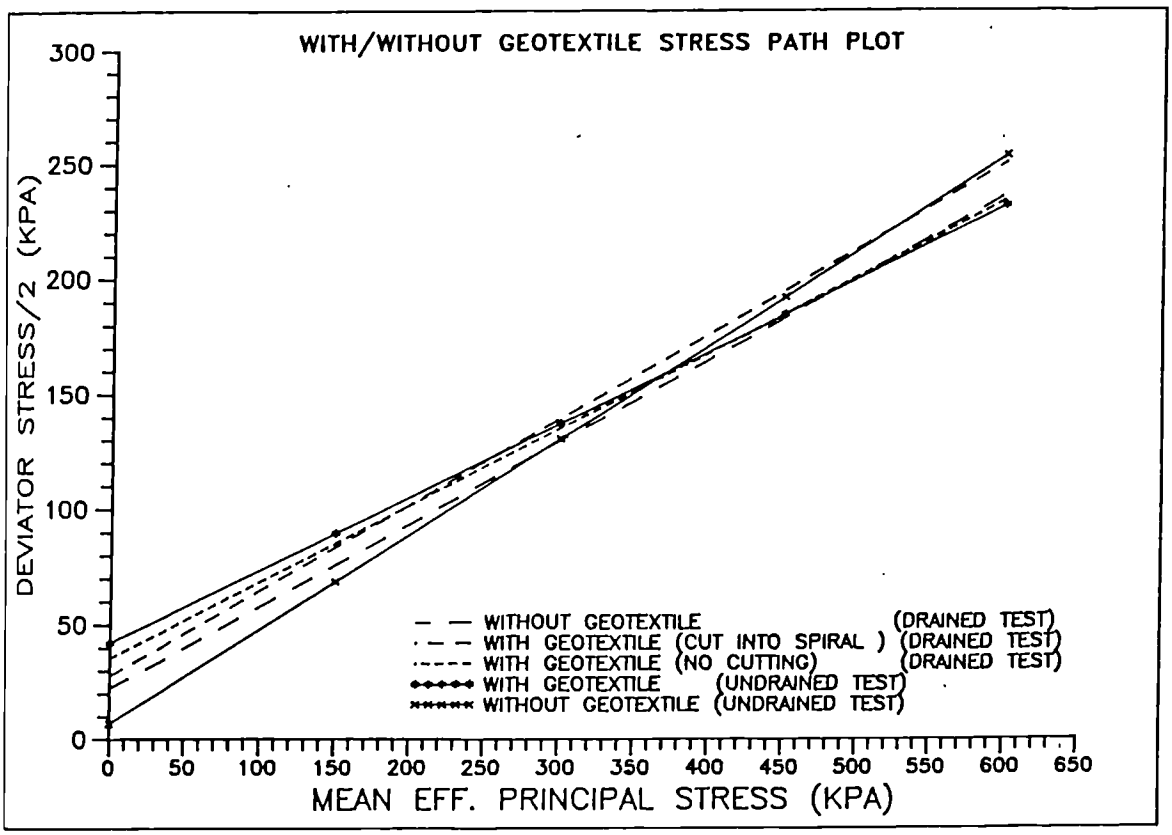

Figure 1 : Stress Path Plot for Samples with/without geotextile

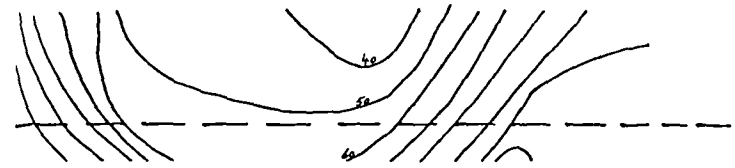

a.

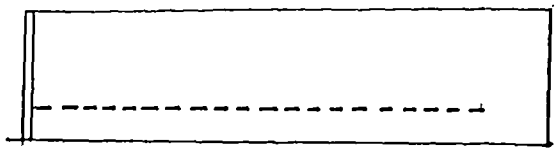

Step 1
1st Lift

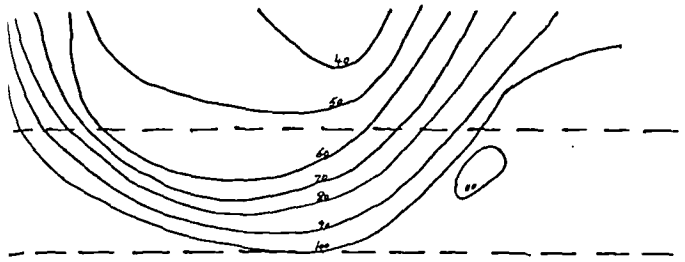

b.

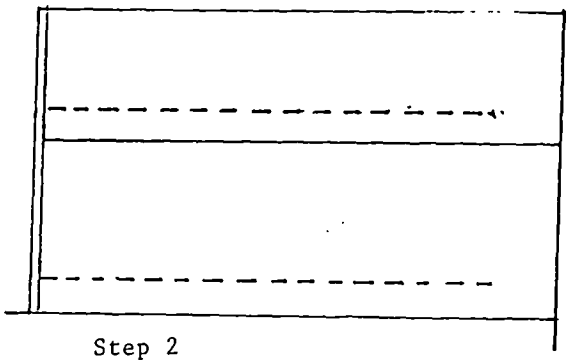

Step 2
2nd Lift

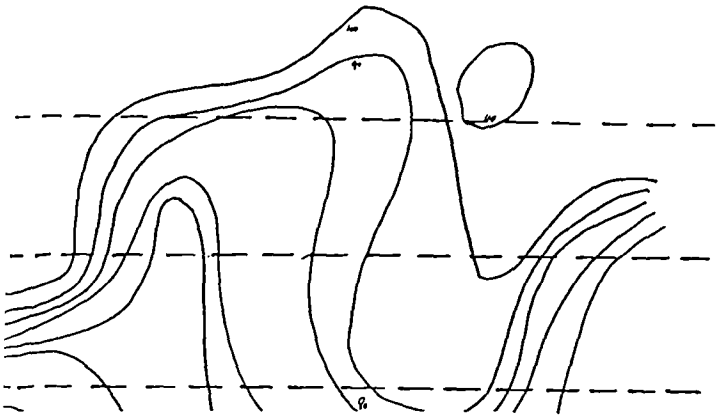

c.

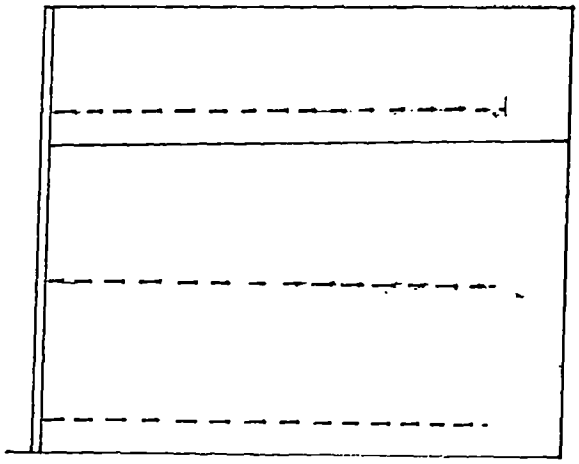

Step n
nth Lift

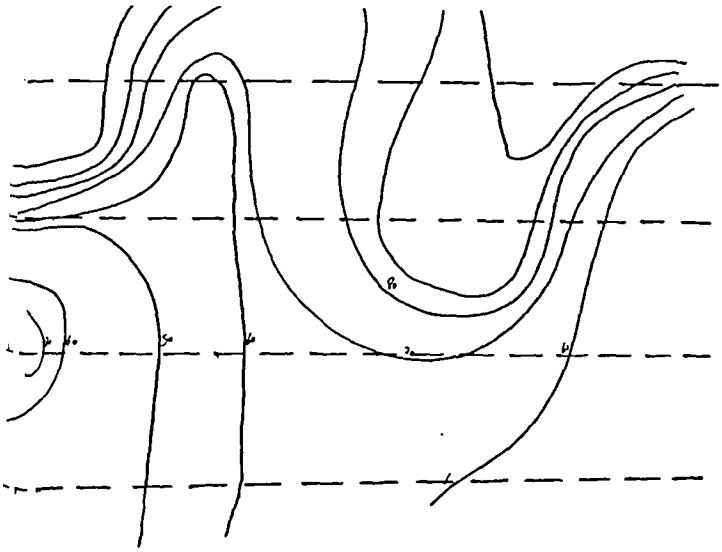

d.

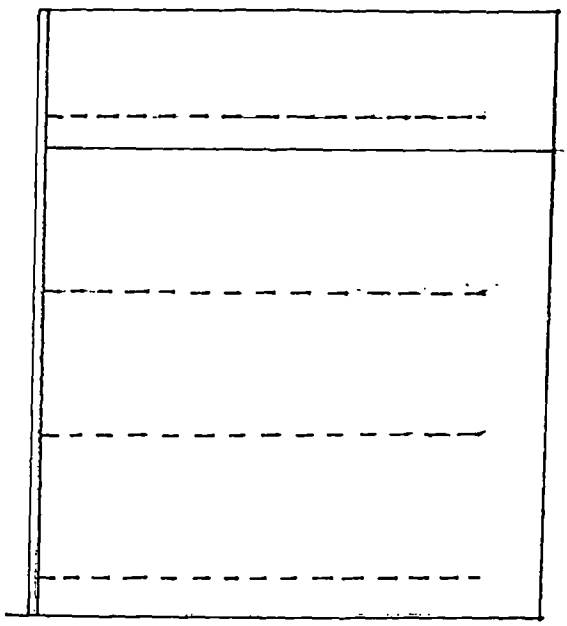

Step m
Final Lift

Step (m + 1) Surcharge Loading

Figure 1. Percentage mobilised shear stress distribution in the fill and back-fill

Figure 2. Construction sequence incremental loading

Plate 1 Predicted Wall Performance, with Granular Backfill, at End of Construction

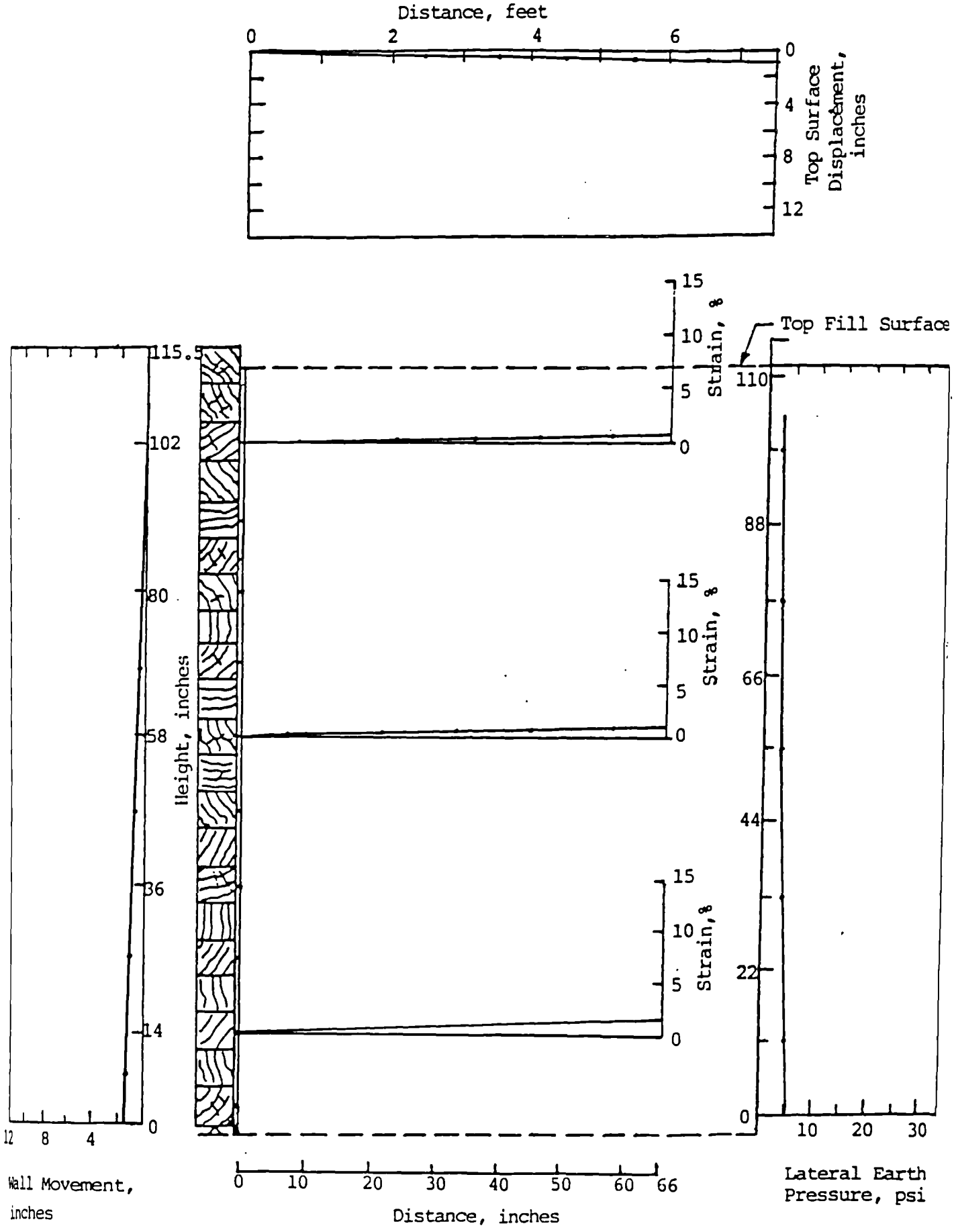

Plate 2 Predicted Wall Performance, with Granular Backfill, at 15 psi Surcharge Pressure

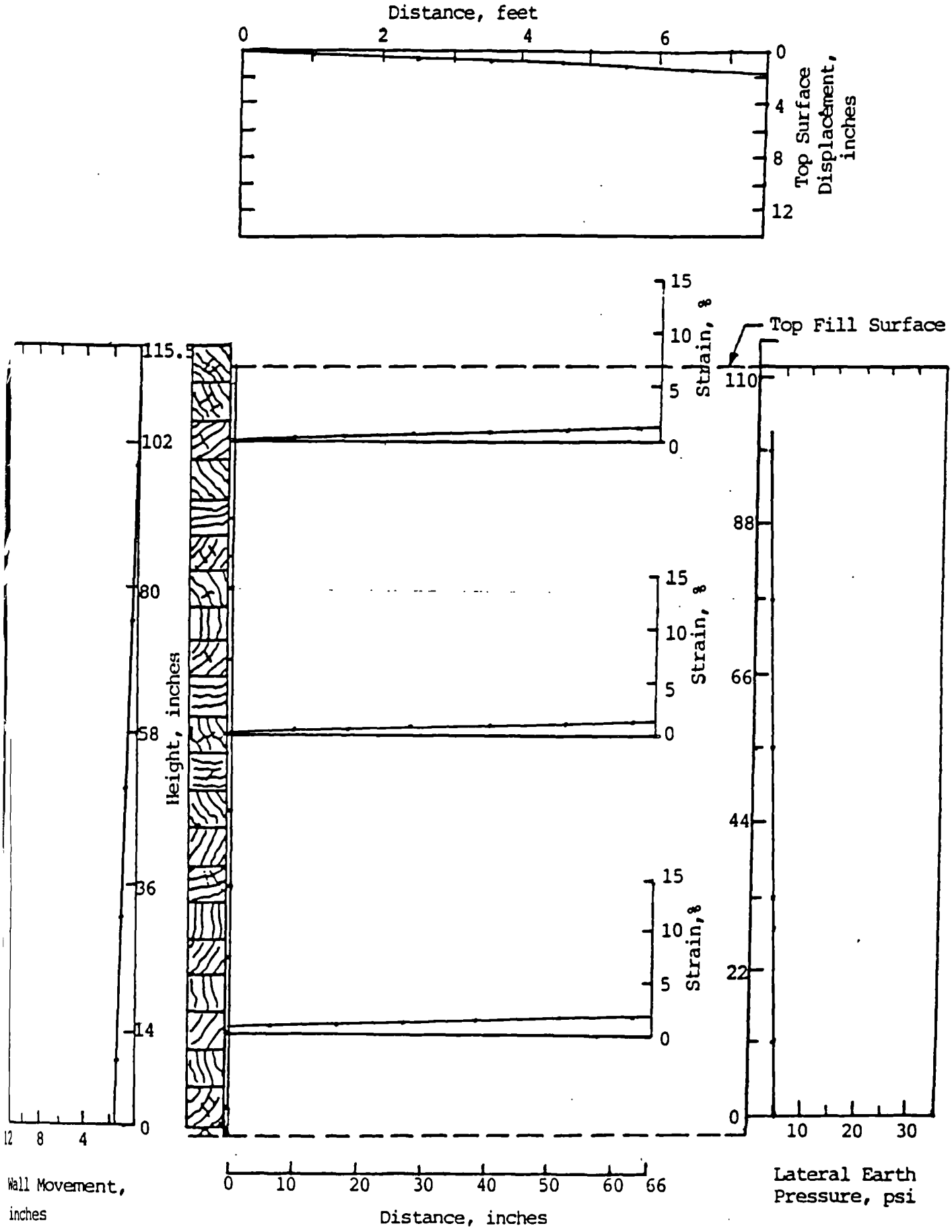

Plate 3 Predicted Wall Performance, with Granular Backfill, after 100-Hour Creep at 15 psi

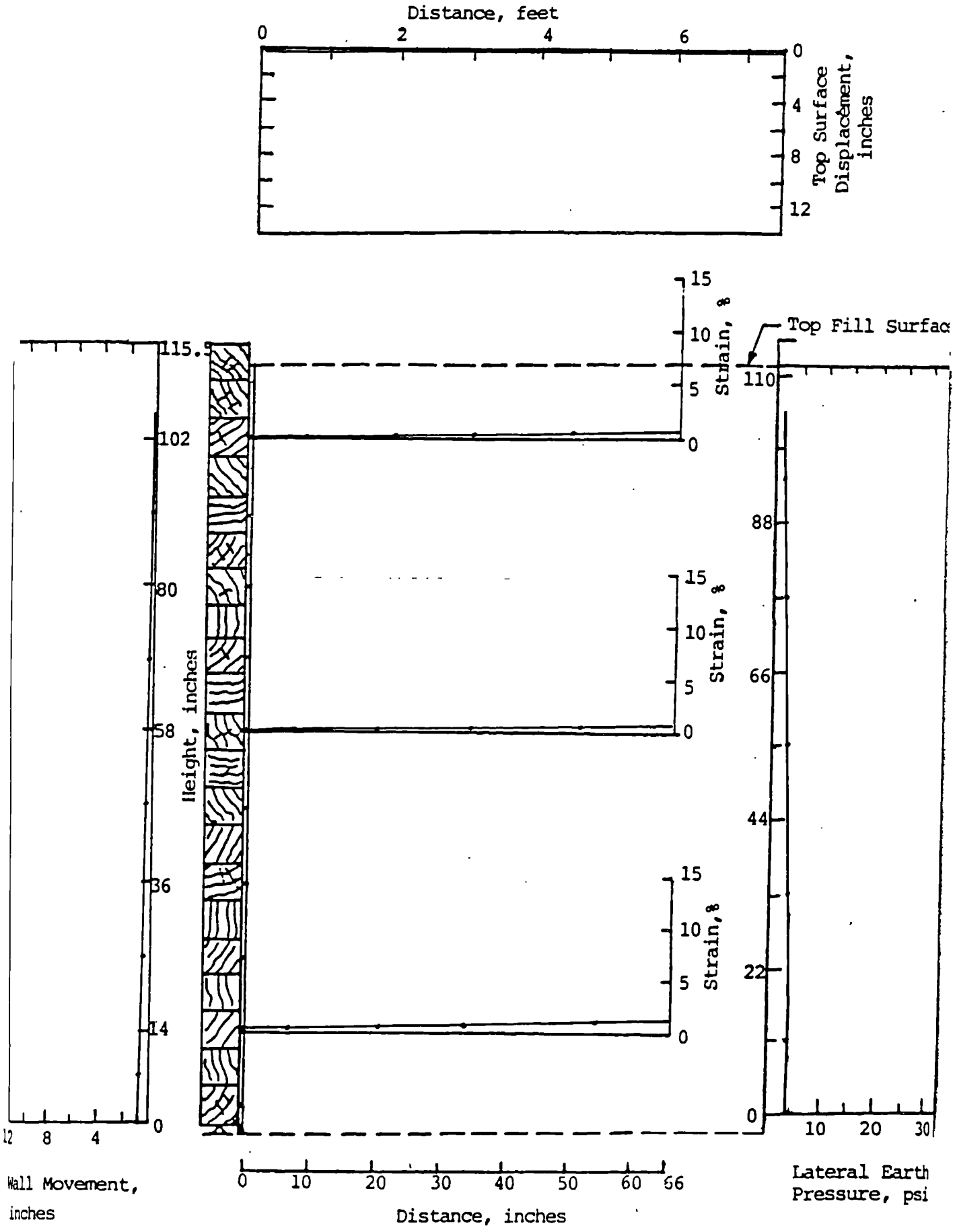

Plate 4 **Predicted Wall Performance, with Cohesive Backfill, at End of Construction**

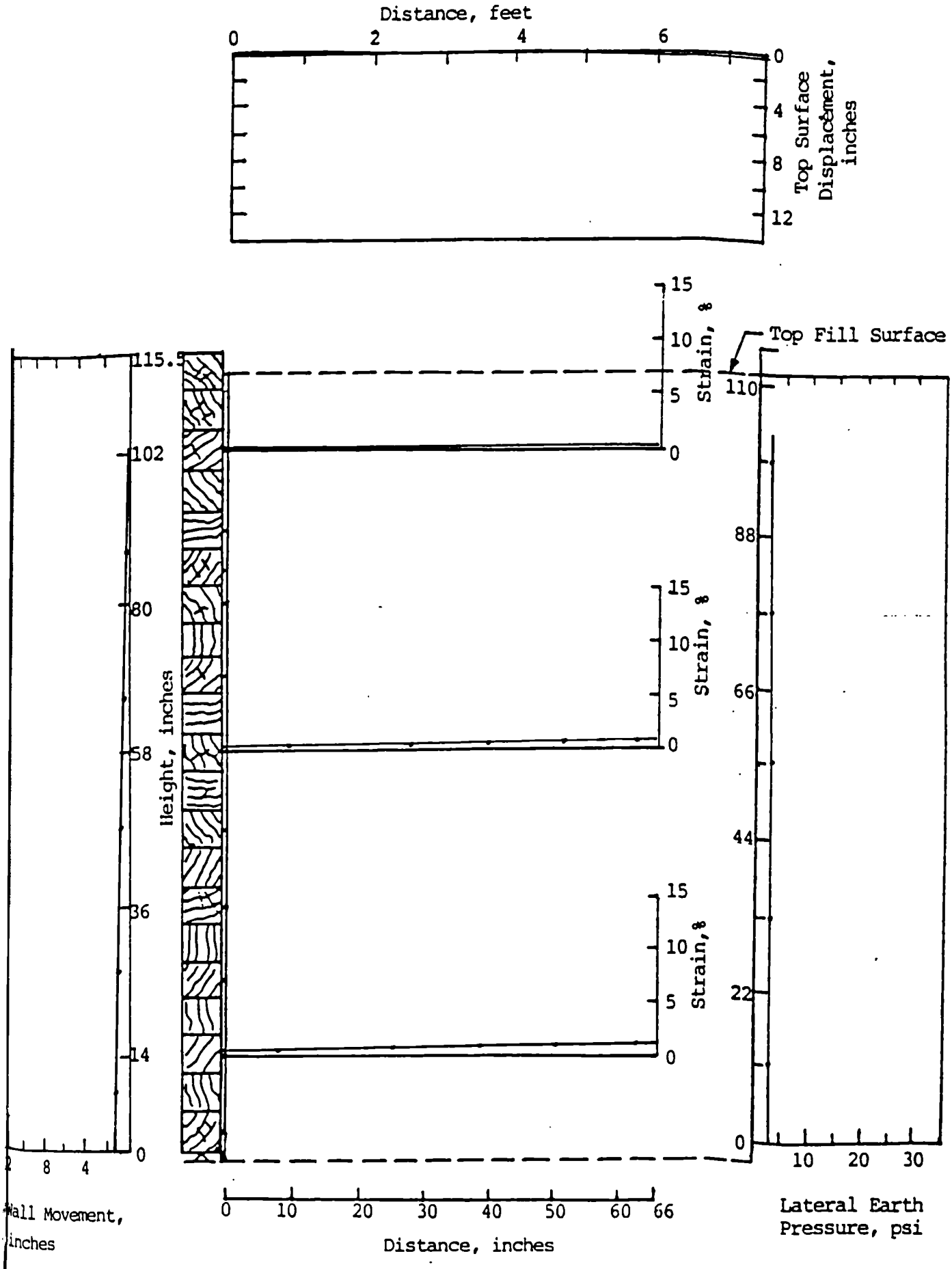

Plate 5 Predicted Wall Performance, with Cohesive Backfill, at 15 psi Surcharge Pressure

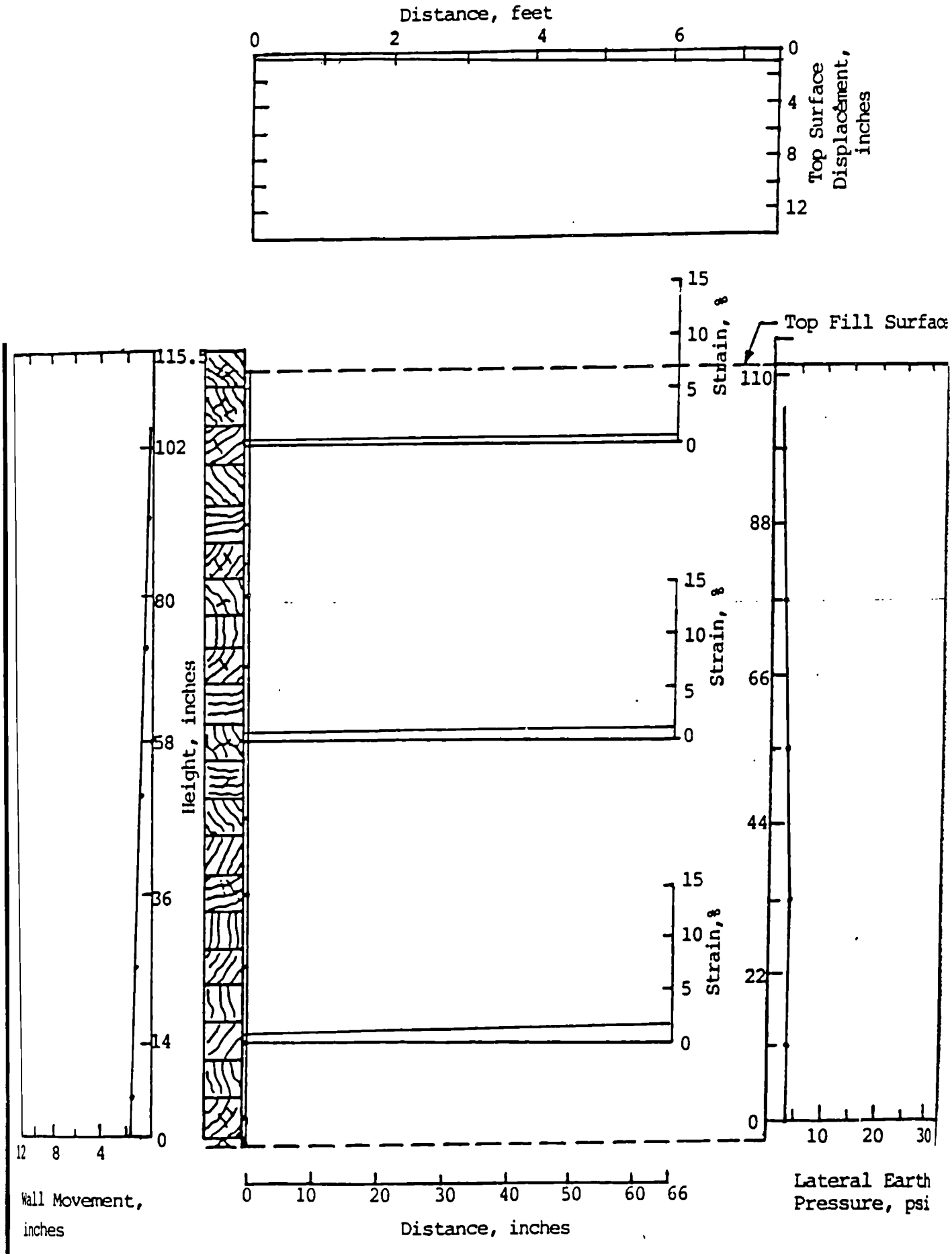

Plate 6 Predicted Wall Performance, with Cohesive Backfill, after 100-Hour Creep at 15 psi

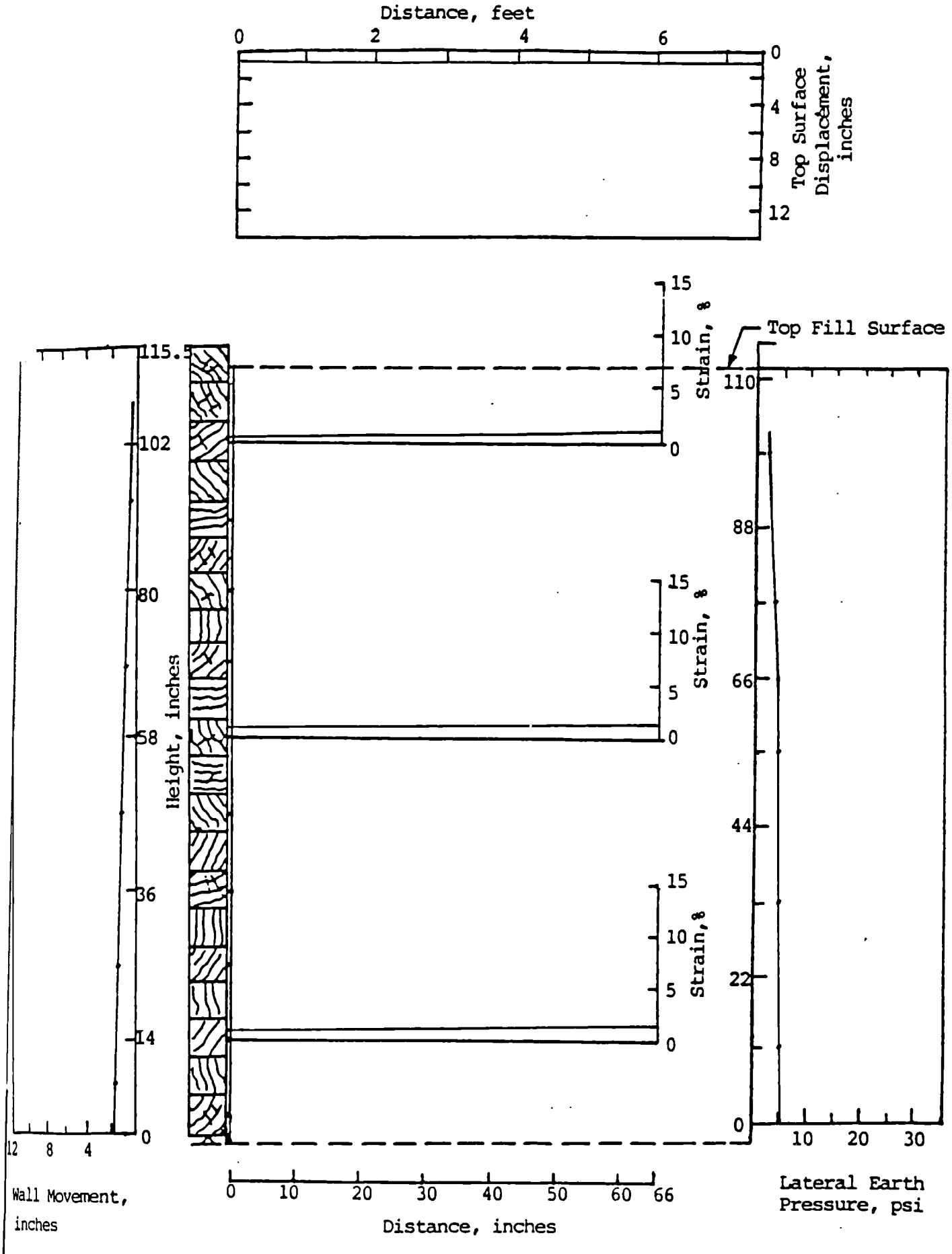

Plate 7 **Predicted Failure Condition, with Granular Backfill**

FAILURE CONDITION:

(a) Surcharge Pressure at Failure = 15.2 lb/in^2.
or,
Fill Height at Failure = _____ ft.

(b) Failure Mode: (description)

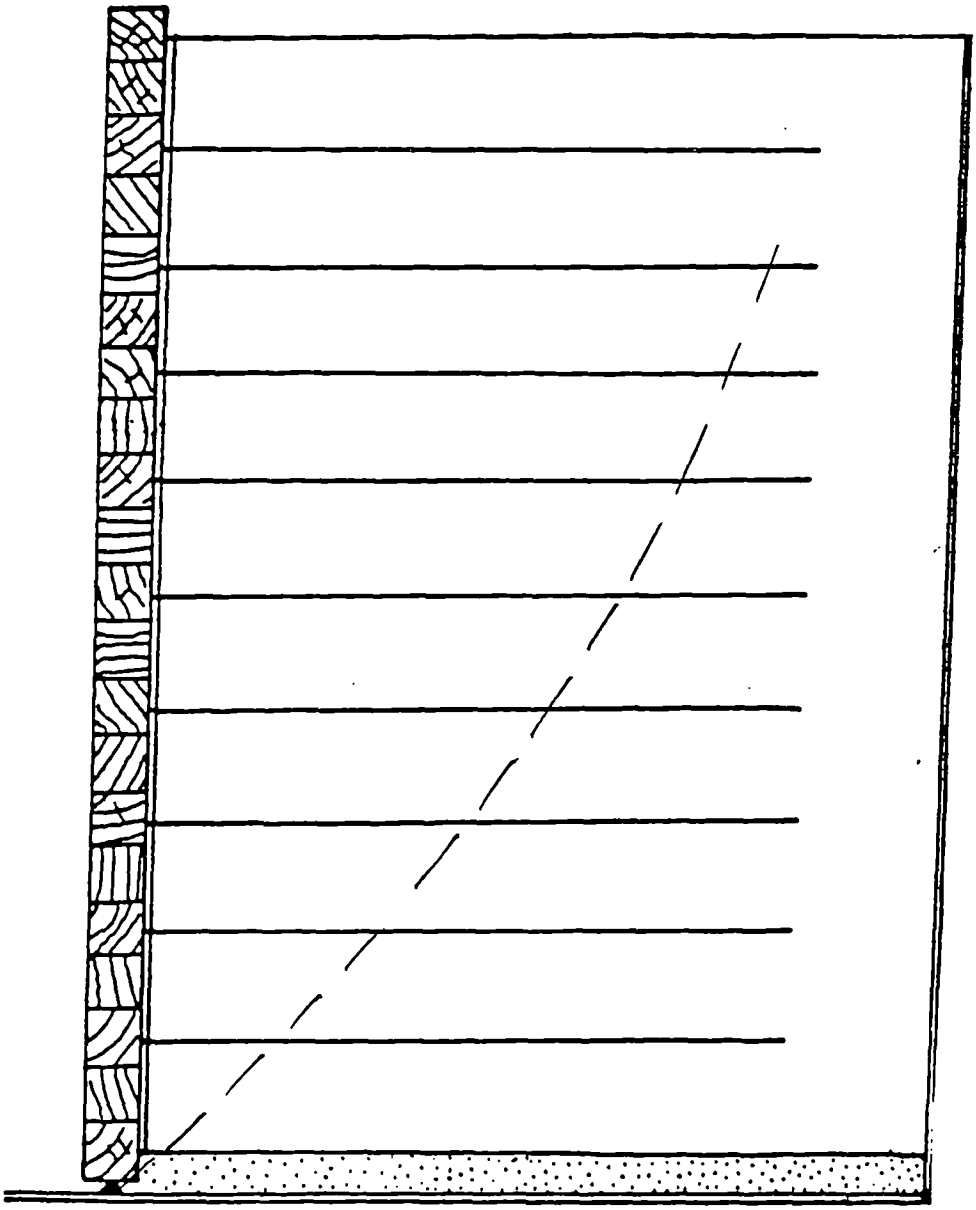

Plate 8 **Predicted Failure Condition, with Cohesive Backfill**

FAILURE CONDITION:

(a) Surcharge Pressure at Failure = 21.2 lb/in^2.
or,
Fill Height at Failure = _____ ft.

(b) Failure Mode: (description)

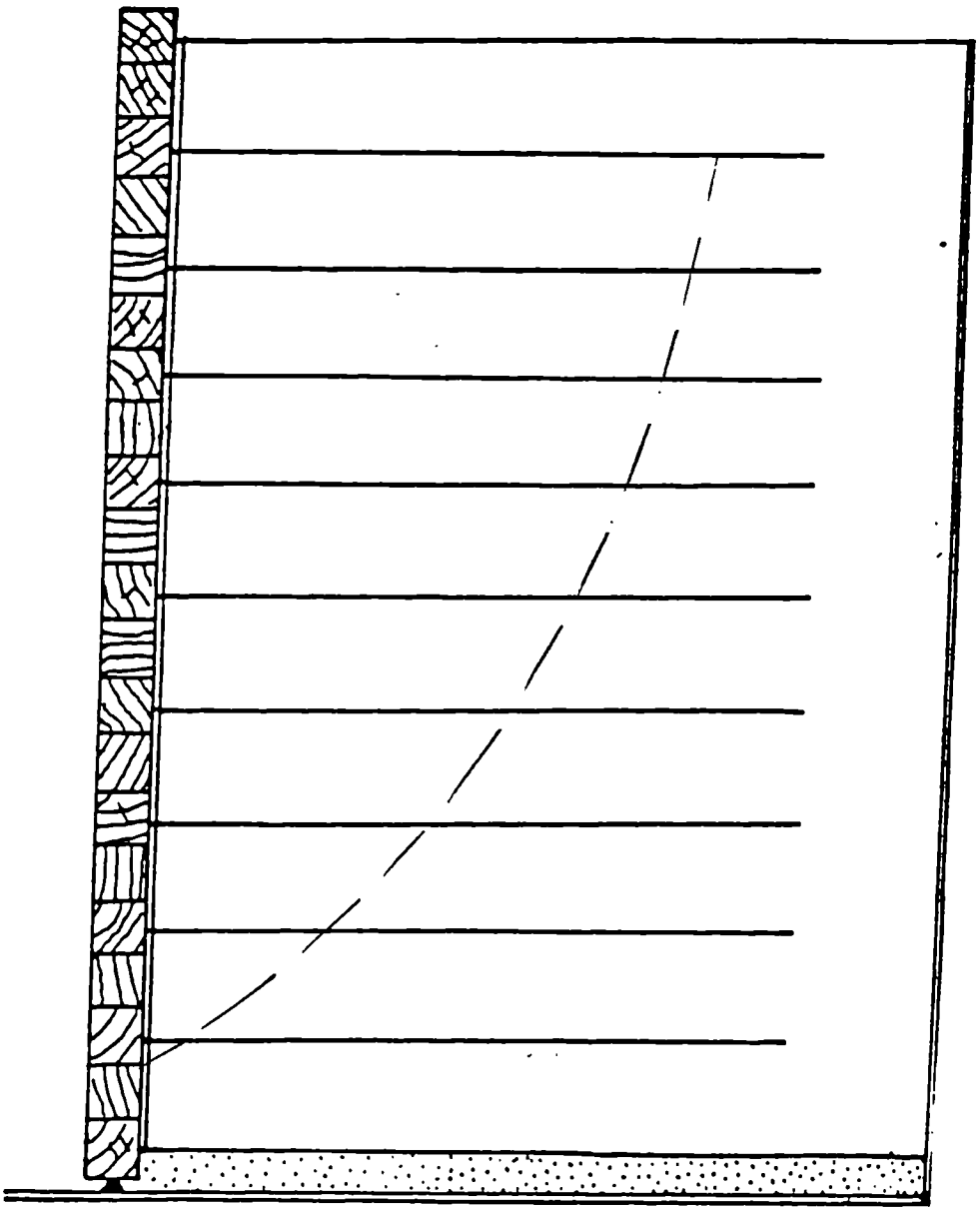

THE USE OF THE FINITE ELEMENT METHOD TO PREDICT THE PERFORMANCE OF REINFORCED SOIL WALLS

C. J. F. P. Jones and S. Heshmati
University of Newcastle upon Tyne, U.K.

The prediction of the behaviour of soil structures reinforced with geosynthetics has become a challenge to many engineers. In this paper, the finite element method (FELSTA) was used to analyses the two full scale retaining walls which had been constructed in the laboratory to identify the factors which influenced their behaviour. The walls were constructed as a focal point to the International Symposium on Geosynthetic-Reinforced Soil Retaining Walls held in Denver, Colorado, USA in 1991. Information on parameter selection and results are provided. The advantages of using the finite element method in the design and analysis of reinforced soil is discussed.

INTRODUCTION

Many full scale trials have been constructed in recent years to evaluate the performance of reinforced soil retaining walls and numerical modelling has proved to be a powerful technique in predicting behaviour at working conditions. However, calibration of the numerical model requires insight and understanding of the mechanics of reinforced soil and the correct selection of material parameters which are representative of the structure under consideration [1].

A range of finite element models and structure idealisations may be used. The structures are usually modelled in two dimensions (2D) but three dimensional modelling is required if the reinforcement is formed from discrete elements, or if the geometry of the structure cannot be assumed to be uniform. The latter could be the case with structures built across steep slopes or ravines or where the face of the structure is not planar.

In 1991 two large scale retaining wall model tests were performed at the University of Colorado and researchers all over the world challenged to predict their behaviour. This provided a good opportunity to study the performance of reinforced walls and to test the various computation methods available to designers. The overall objective of the Symposium was to improve the understanding of the behaviour of reinforced soil structures. The Colorado test walls were complimentary to the NATO Prediction Symposium held at the Royal Military College in Canada in 1987 [2]. At the NATO Symposium only one finite element analysis of the behaviour of the reinforced soil wall was attempted. Significantly this prediction was adjudged the winner of the prediction exercise. The finite element prediction in Canada was based upon the use of an established finite element system (FELSTA), [3] which had been developed specifically to correctly model the construction of aspects of civil engineering structures. Reinforced soil structures have been shown to be particularly sensitive to the influence of the construction process. This paper describes the use of the FELSTA finite element model to predict the behaviour of the two test walls built in Colorado.

THE COLORADO TRIAL WALL

The nature and form of the Colorado trial walls is described [4]. The configuration of the test walls and the loading facilities are shown in Figures 1 and 2. It is apparent in Figure 1 that the support of the loading (air bags) at the top of the structure provided a horizontal restraint to movement which is not usually found in practice. This restraint would make any prediction of the behaviour of the wall not based upon a finite element method very difficult to simulate.

MATERIAL PROPERTIES

The tested retaining walls contained several materials including the use of two backfill materials. The reinforcement was a non-woven geotextile of limited strength and the facing was of timber. The timber facing was representative of timber structures built by the Colorado Department of Transportation (CDOT). A unique element of the facing was that it was made up of timber bulks held together by plywood sheets nailed to the main members. This made the facing stiffer than usual in many reinforced soil structures built with elemental facings.

The selection of a geotextile reinforcement laid full width across the trial wall meant that a (2-D) dimensional analysis could be adopted without compromising the structural idealisation [1].

The selection of the material parameters was based upon carefully undertaken conventional laboratory studies of the materials used to form the structures. These tests were undertaken by the Symposium organisers and provided to all of the invited predictors. It is accepted that the accuracy of any prediction of the behaviour of the walls is dependent upon these tests and the degree to which they represent the actual conditions used in the construction of the test walls.

ANALYTICAL MODEL

The following conditions were assumed in respect of the idealisation of the trial walls:

2-dimensional

i Plane strain conditions would accurately reflect the wall behaviour.

ii The base of the wall was rigid.

iii The sides of the model walls were frictionless. (The organisers of the trial had gone to considerable lengths to reduce side wall friction in the trial structures to a minimum.)

iv The timber facing was assumed to be flexible with little inherent stiffness.

v The top and bottom layers of any overlapping reinforcement behaved similarly.

The finite element idealisation of the walls is shown in Fig. 3. A total of 215 high order quadrilateral elements were used to model the fill and facing with a further 86 line elements representing the reinforcement. The model used was the more linear elastic hyberbolic model just proposed [5] and modified [6].

In this model

$$(\sigma 1 - \sigma 3) = \frac{\varepsilon}{a + b} \qquad (1)$$

in which σ_1 and σ_3 = major and minor principle stresses, ε = axial strain, a + b = constants.

The asymptotic value of the soil at failure $(\sigma_1-\sigma_3)$ is greater than the ultimate compressive strength of the soil $(\sigma_1-\sigma_3)_{ult}$ but can be related to the ultimate value by the failure ratio R_f such that;

$$R_f = \frac{(\sigma_1 - \sigma_3)}{(\sigma_1 - \sigma_3)_{ult}} \tag{2}$$

By expressing the parameters a and b in terms of the initial tangulant modules value E_i and the compressive strength, equation 1 may be written as;

$$(\sigma 1 - \sigma 3) = \frac{E}{\frac{1}{E_i} + \frac{ER_f}{(\sigma 1 - \sigma 3)_f}} \tag{3}$$

Equation 3 may be used to model the non linearity of soil stress-strain behaviour.

$$\frac{E}{P_a} = \frac{K}{(\frac{\sigma_3}{P_a})^n} \tag{4}$$

in which P_a Atmopheric Pressure, K Primary Modules, n Modules exponent.

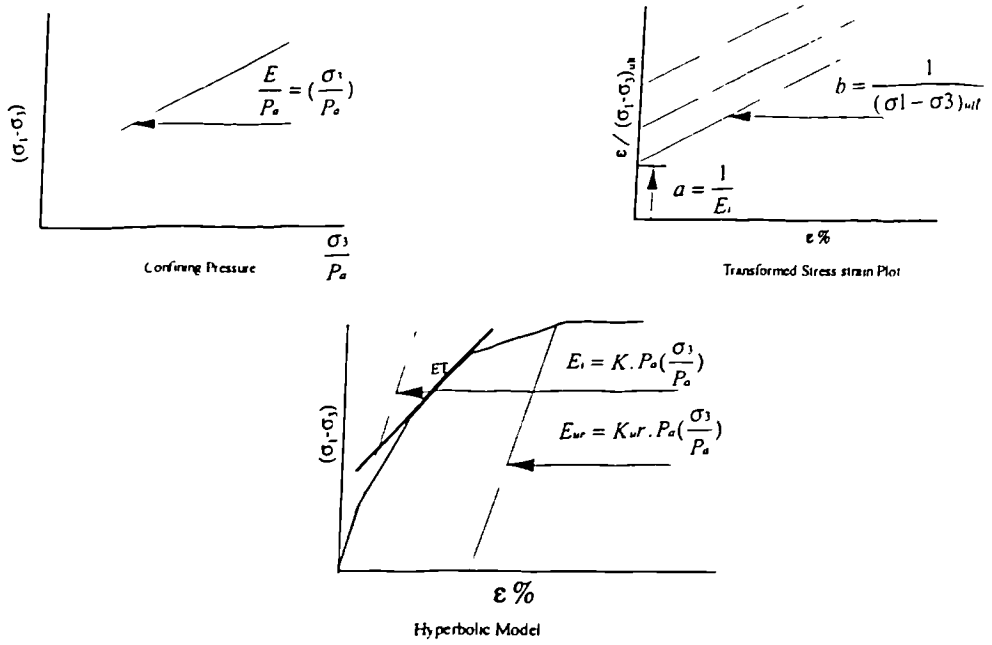

A constant Poison's ratio ν = 0.35 was used and no unloading-reloading was assumed. The parameters used in the model were generated from the information provided from the laboratory tests and included compaction stresses within the fill developed during stage construction, prestressing of the reinforcement, and the use of reinforcement whose stiffness varied with time. The facing elements were assumed to be elastic and a thin layer of compressible material was assumed between the incremental facing units. Modelling of the construction process and the loading procedures are shown in Figure 4. Figure 4 also provides details of the mobilised shear stress distribution within and behind the reinforced soil mass during construction. Details of the material parameters used in the FELSTA model of the Colorado walls are shown in Table I.

The results of predictions are shown in Figure 6, [7] which also shows the results from the trial walls. The prediction requirements were to estimate the following parameters for the walls,

a) At the end of construction the displacement of the top surface of the model.

   i) The lateral earth pressure behind the reinforced soil blocks.

   ii) The strain in the reinforcement along its length.

   iii) The involvement of the facing.

b) After 100 hours of reinforcement creep i)-iii) as above.

c) A prediction of the surcharge load to cause failure and the failure mode.

COMMENT ON THE COLORADO WALLS

Inspection of the Colorado test walls suggest that their behaviour is controlled by the construction technique. It can be assumed that the Colorado walls are a derivation of the old dry stone walls built during the Industrial Revolution and examples of this from the construction can still be seen in the gold mining towns of Colorado The failure mechanism of these structures, whereby the face distorts (bulges) outward until it becomes unstable is the same as that presumed to occur at collapse with the Denver trial walls, Fig 7. An important consideration with the Colorado walls is that stability is essentially a result of the shear strength of the soil fill; the reinforcement is of second order of importance and can therefore be 'weak'. However, once the mobilised shear strength of the soil reaches peak values the reinforcement becomes the primary stabilising influence. The Denver fabric wall tests showed that post peak shear strength deflections increased very rapidly indicating that the lightweight reinforcing fabric had insufficient strength to provide stability. From this observation it is possible to conclude that any finite element analysis of these walls should provide an indication of the percentage mobilised shear strength of the reinforced soil during the construction stages and in the serviceability condition. This would provide an indication of the reserve of strength in the system and can be used to determine the potential failure plane(s) and also a measure of the factor of safety.

CONCLUSIONS

The Colorado Symposium can be considered a success, in that a number of predictions of the behaviour of the walls agreed with the prototype behaviour. Nearly all the predictions were based on the finite element method and the following general conclusions can be made:

i) The finite element technique can be used to model the behaviour of reinforced soil structures up to failure.

ii) If the correct idealisation is made and the selection of parameter is accurate, very close agreement can be achieved between the performance of the model and the real structure.

iii) A finite element analysis represents a very large number of mathematical computations with the increase in computing power available to design offices, coupled with reduction in computing costs, the technique is a viable option to the designer to establish the behaviour at serviceability of any design.

iv) The finite element models do offer one advantage associated with the ultimate limit state as they can be used to identify potential failure planes, these can then be checked using limit equilibrium methods.

v) Prediction of the ultimate limit state condition using finite element models is difficult.

REFERENCES:

1. Jones, C.J.F.P. Predicting the behaviour of reinforced soil structures in theory and practice of Earth Reinforcement, Ed. Yamanouchi, Minra and Ochiiai, pp 534-540, Balkema, Rotterdam, 1988.

2. Jarrt, P. M., and McGowan, A., The application of polyamric Reinforced soil Retaining Structures, NATO AS, Serices Vol. 147, 1987.

3. FELSTA Finite element analysis programme, for plane stress-strain analysis of earth structures, including linear and nonlinear stress-strain material properties. Directorate of planning, Engineering & Transportation, Metropolitan County Council, West Yorkshire, England, 1977.

4. Wu, J. T. H., Predicting Performance of Geosynthetic-Reinforced Retaining Walls, Bulletin No. 1 and 2, Department of Civil Engineering, University of Colorado, Denver, USA, 1991.

5. Kondner, R. L., hyperbolic stress-strain response, cohesiv soils, Jour. Soil Mesh. and Foundation Div. ASCE, VOL. 85, pp 115-143, 1963.

6. Duncan, J.M. and Chang, C. Y. Non-liner analysis of stress and strain in soils. Jour. Soil Mesh. and Foundation Eng. ASCE,SM5, pp 1629-1653, 1970.

7. Heshmati, S. A finite element analysis for prediction of the performance of reinforced walls, International Symposium on Geosynthetic-Reinforced Retaining Walls, Denver, Colorado, USA, 1991.

Table 1 The parameters of Hyperbolic Model

Parameter	Description	Function	Granular Soil	Cohesive Soil CU Test	Cohesive Soil CD Test	Cohesive Soil CU Test	Cohesive Soil CD Test	Sand	Geotextile	Polymer	Wall
R	Failure Ratio	$\sigma-\sigma_3/E_i = R\ \sigma-\sigma_3$	0.70	0.70	0.75	0.70	0.75	-	-	-	-
ϕ	Friction Angle	-	38	15.1	26.5	15.1	26.5	-	-	-	-
C	Cohesion KN/m2	-	0	51	12.4	51	12.4	-	-	-	-
K	Primary Modulus	E_i/Confining Pre	10^3	75	53	75	53	-	-	-	-
P_a	Atmospheric Pressure	KN/m2	101.3	101.3	101.3	101.3	101.3	101.3	101.3	101.3	101.3
n	Modulus Exponent	E_i/KPa(3/Pa n	0.65	0.61	0.53	0.61	0.53	-	-	-	-
E_i	Initial Tangent	$a = 1/E_i$ KN	1531	1380	690	1380	690	-	-	-	-
$(\sigma_1-\sigma_3)_{ult}$	Asymptotic Deviator	$b = 1\ \sigma - \sigma_3$	2296	1104	749	1104	749	-	-	-	-
v	Poison Ratio	Constant	0.35	0.35	0.35	0.35	0.35	0.35	0.35	0.35	0.35
E	Young's Modulus	E = KN/m2	$0.35x10^6$	$0.34x10^4$	$0.1x10^5$	$0.34x10^4$	$0.1x10^5$	$0.35x10^5$	0.5	$0.23x10^2$	$0.2x10^5$

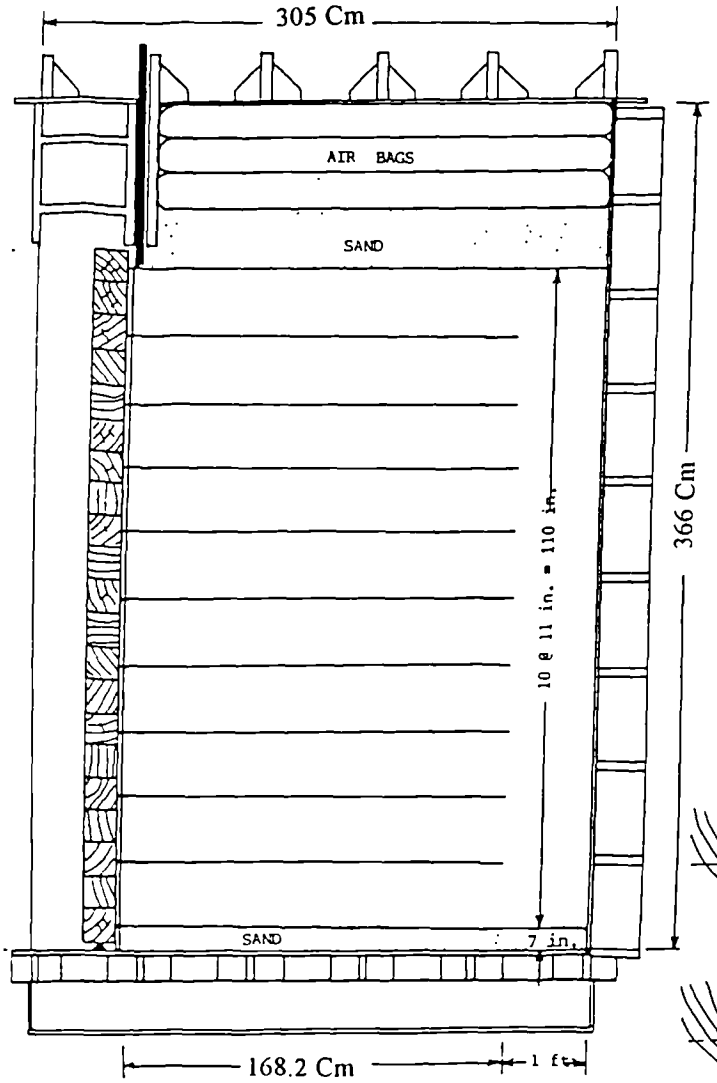

Figure 1: Configuration of the test wall loading facility

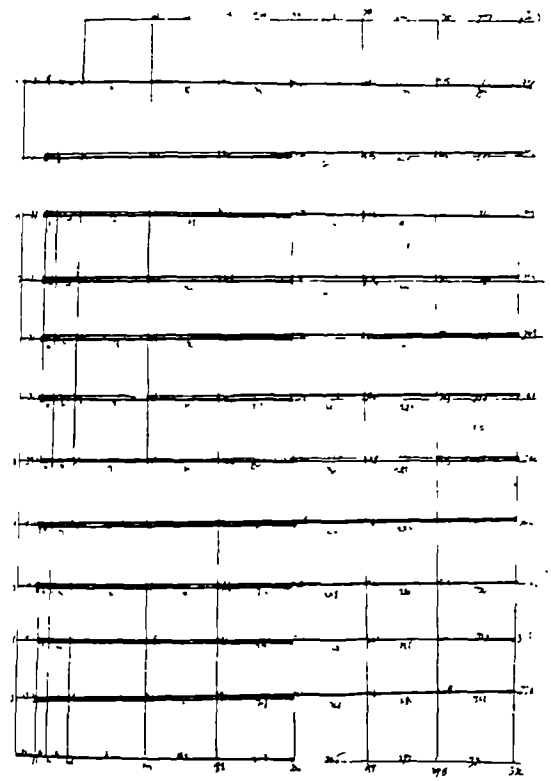

Figure 3: Finite element mesh model

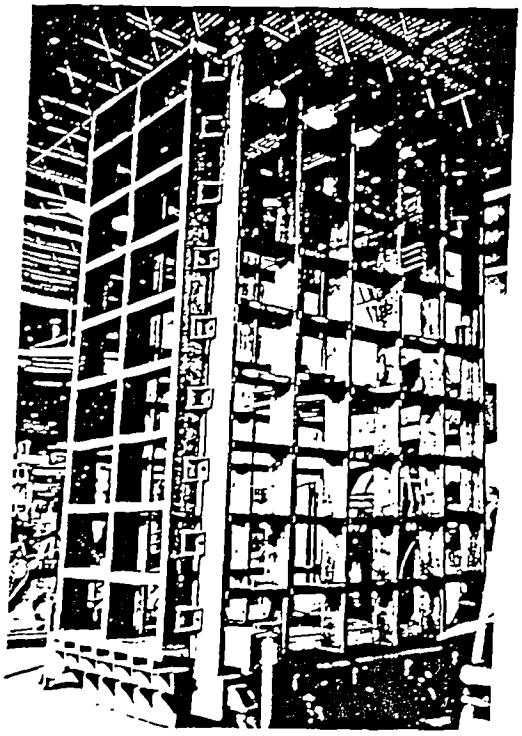

Figure 2: Structural steel support for the loading facility

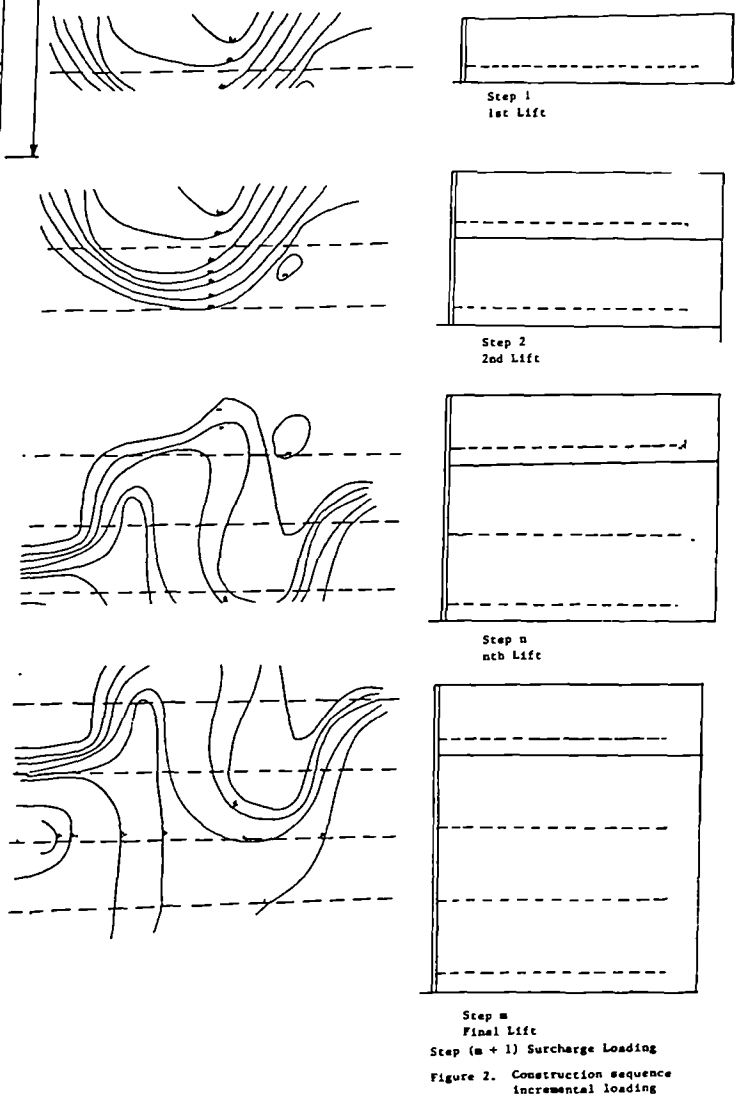

Figure 4: Construction sequence and loading procedures

Figure 5: Mobilised shear distribution within the reinforced soil

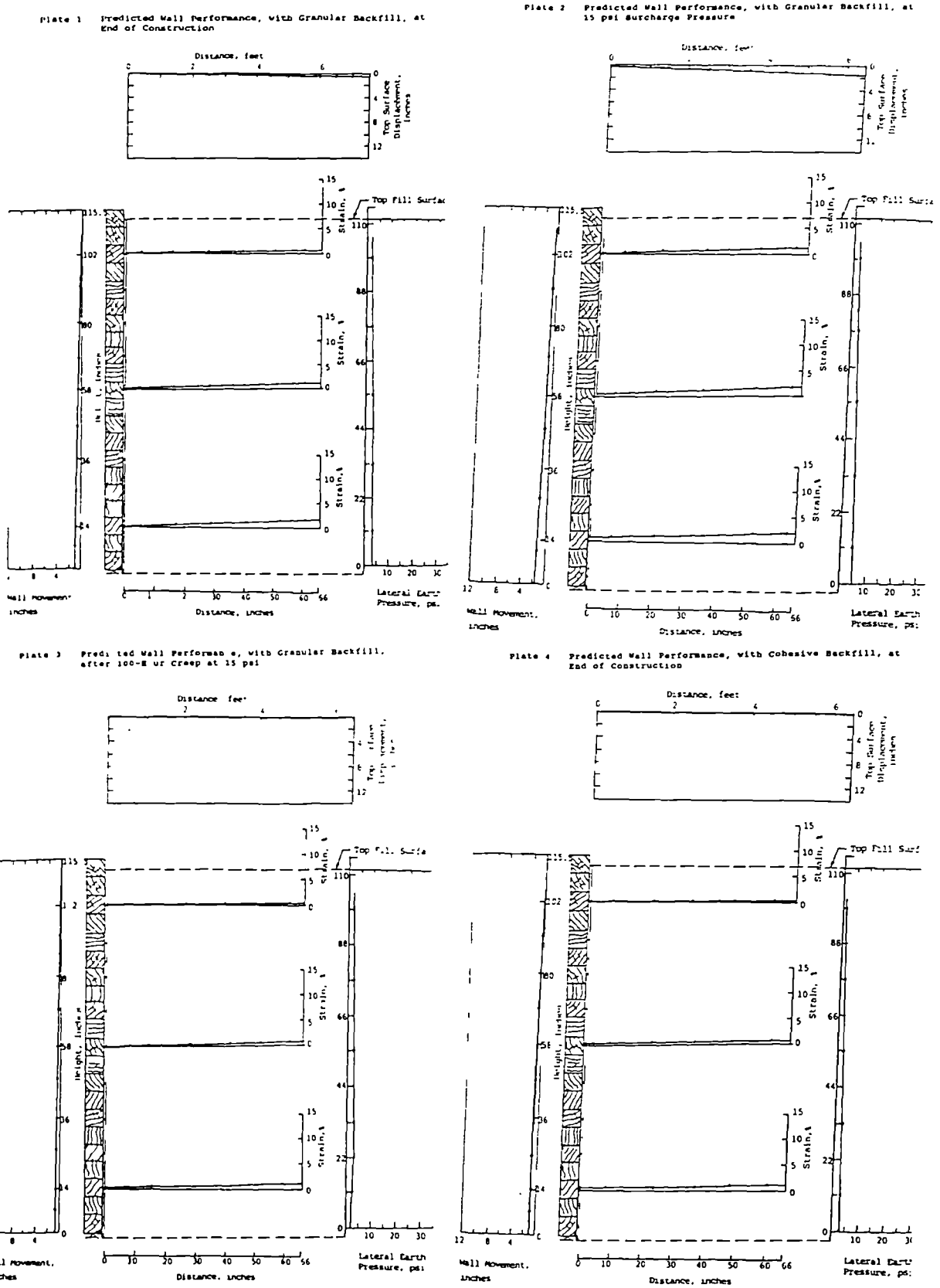

Figure 6. The result of predication

Plate 5 Predicted Wall Performance, with Cohesive Backfill, at 15 psi Surcharge Pressure

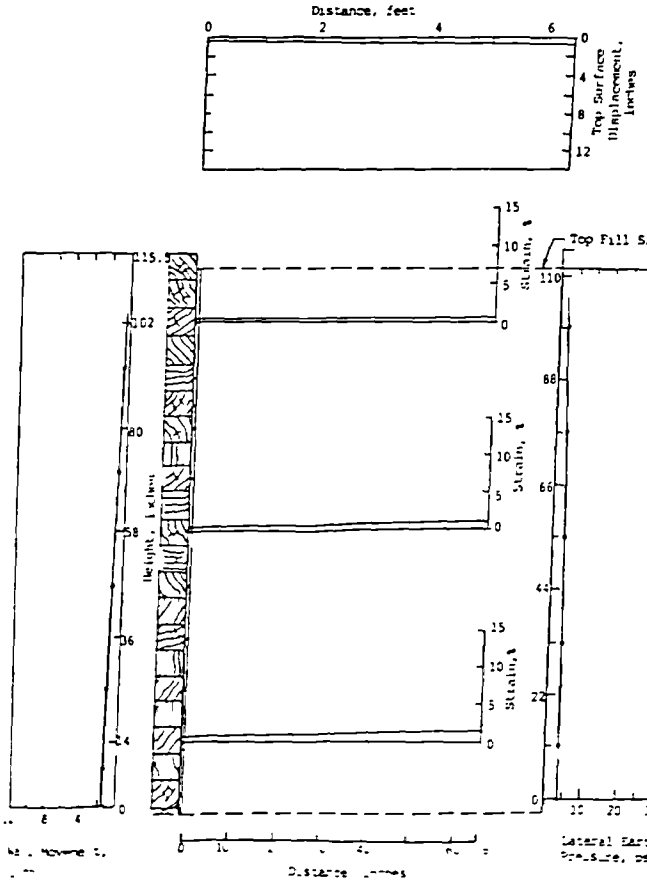

Plate 6 Predicted Wall Performance, with Cohesive Backfill, after 100-Hour Creep at 15 psi

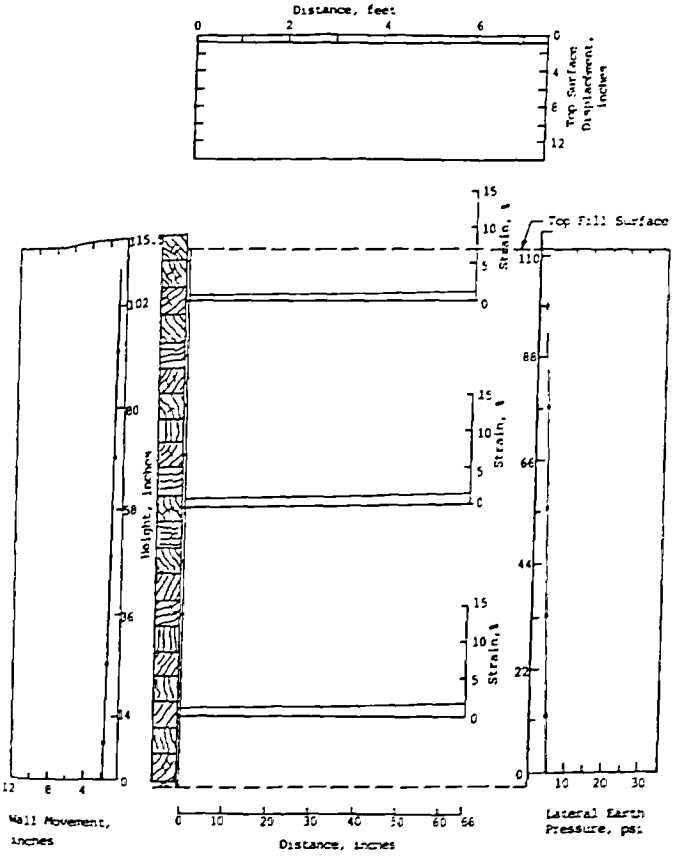

Plate 7 Predicted Failure Condition, with Granular Backfill

FAILURE CONDITION:

a Surcharge Pressure at Failure = 15.2 lb/in^2.
or
Fill Height at Failure = _____ ft.

b Failure Mode description

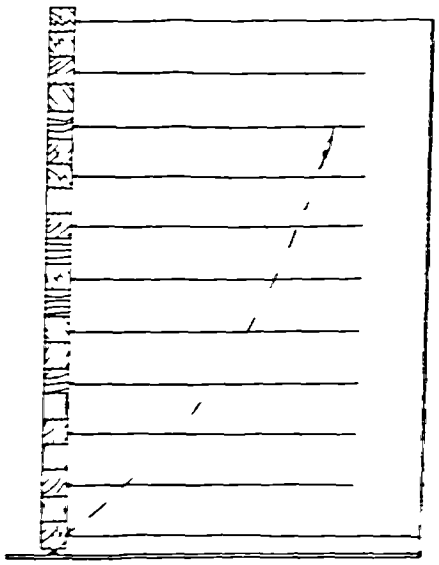

Plate 8 Predicted Failure Condition, with Cohesive Backfill

FAILURE CONDITION:

a) Surcharge Pressure at Failure = 21.7 lb/in^2.
or,
Fill Height at Failure = _____ ft.

b Failure Mode: (description)

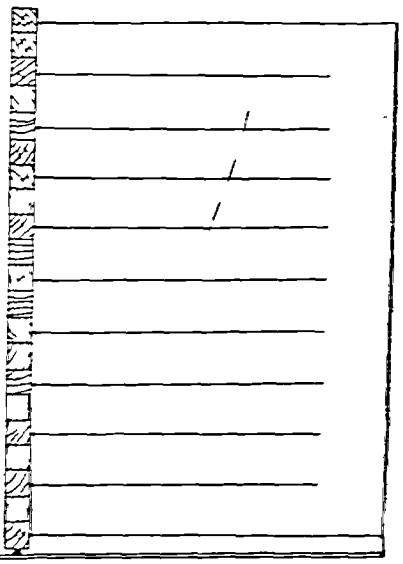

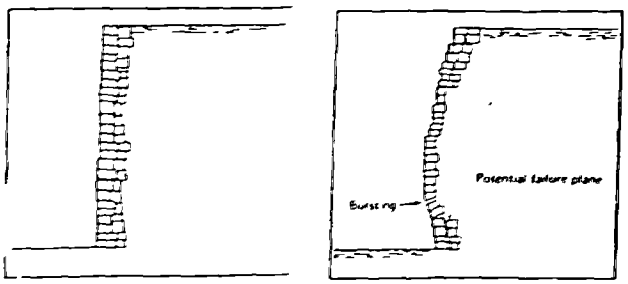

Figure 7. Nature and collapse mode of masonry retaining walls

THE ACTION OF GEOTEXTILE TO PROVIDE COMBINED DRAINAGE AND REINFORCEMENT TO COHESIVE SOIL

by

C.J.F.P. Jones and S. Heshmati
Department of Civil Engineering
University of Newcastle upon Tyne, U.K.

ABSTRACT

The inclusion of a composite geotextile providing both drainage and reinforcing function into a test sample of kaolin, produces a marked increase in the shear strength characteristics of the clay material. The tests were conducted in such a manner that the separate effects of the drainage function and the reinforcing function provided by a variety of geotextiles could be identified. The results show that composite geotextiles can offer significant technical, practical and economic benefits when used with cohesive soils.

INTRODUCTION

The conventional method used to construct reinforced soil structures uses good quality frictional fill, DTP (1978). In many parts of the word frictional fills are difficult to obtain at economic rates and consequently the use of reinforced soil in the these areas is curtailed.

In many cases poor quality on-site soils are available. If these could be shown to be adequate for reinforced fill the requirement for expensive imported cohesionless soil could be eliminated. Recent studies in Japan indicate that fine grained soils with water contents up to 130 per cent can be shown to be adequate as reinforced soil fill provided the correct type of reinforcement is selected, Tatsuoka (1992). The reinforcements which offer the potential of being suitable for use with fine grained soils are geogrids and geotextiles. In the case of geotextiles a dual role is possible with composite geotextiles providing both drainage and reinforcement. The economics and cost benefits of using geosynthetics in construction has been discussed by Jones (1992) and Wu (1992).

One of the earliest studies of the mechanism of soil reinforcement used the triaxial compression test. In this test a cylindrical soil-geosynthetic composite was sheared after isotropic consolidation, Yang (1972). The use of the triaxial test has been extended to cover reinforced clay, Ingold (1982), Tatsuoka et al (1986). A preliminary

study to determine the influence of composite drainage /reinforcement geotextile fabrics on improving the strength characteristics of cohesive soil (kaolin), under condition of both undrained and drained triaxial compression tests, has been undertaken by Heshmati et al (1989). The objective of these tests were to identify the separate roles of the geosynthetic in providing drainage and reinforcement. This paper extends this work showing how different geosynthetic composites provide different levels of improvement.

EXPERIMENTAL WORK

A number of consolidated undrained (CU) and consolidated drained (CD) triaxial compression tests have been undertaken using 100 mm diameter samples containing a single layer of different geotextiles placed at mid-height in the sample. The arrangement of the triaxial apparatus and the geotextile composite material used in the tests is shown in Figure 1. The range of geotextiles considered in the tests is shown in Figure 2 and the form and nature of the materials tested are shown in Table 1.

A major part of the experimental work was the deliberate separation of the reinforcement function provided by the geosynthetic materials identified as geogrids G2, G3, G4, and geotextile G5, and the drainage function provided by the materials Gl and G6. The action of geotextile G1 was limited to provide a drainage function only by cutting the intact material thereby destroying any reinforcement properties, (G1CT). Similarly the material G6 could be made to provide reinforcement properties only by removal of the outer filter membranes, (G7). G1 and G6 were used to provide both reinforcement and drainage functions, and Gl and G2 were combined together to provide both reinforced and drainage functions, G1G2.

Unreinforced samples of kaolin were tested to provide base data and samples were tested at cell pressures of 150, 300, 500 KPa. Samples were prepared in the laboratory in accordance with BS1377 (1990) by compacting 3.5 Kg of kaolin which had been mechanically mixed with 29 per cent water to obtain an optimum moisture content at 5 per cent voids.

The index properties of the kaolin samples used in all tests are shown in Table 2a. The material properties of the all geotextile materials are shown in Table 2b.

Both Consolidated Drained (CD) Triaxial tests and Consolidated Undrained (CU) Triaxial tests were undertaken using five stages, Head (1986);

i. Initial B - Test
ii. Saturation stage.
iii. B - Test stage
iv. Consolidation stage.
v. Shearing (compression) stage.

The first four stages were the same for both the drained (CD) and undrained (CU) tests. In the final stage for the CD tests the volume change valve was opened.

RESULTS AND DISCUSSION

Results of the consolidated undrained tests (CU) are shown in Tables 3. The results of the consolidated drained tests (CD) are shown in Tables 4. Examples of the samples after failure, are shown in Plate 1, whilst Plate 2 shows details of the samples which contained geosynthetic materials after test.

Graphs of the stress paths for the undrained tests (CU) and graphs of the stress path for the drained tests (CD) are shown in Figure 3.

In the consolidated undrained tests the non-woven geotextiles (G1, G1CT and G6) acted as drainage materials only. In the consolidated drained tests the non-woven geotextiles (G1, G1CT, G5 and G6) acted as drainage materials and also provided composite drainage and reinforcing functions.

It can be seen from the results that the inclusion of the drainage geotextiles in the fully consolidated undrained tests produced a **reduction** in the effective angle of internal friction (ϕ') [$K_{23.6°} \rightarrow G1_{20.1°}$], as did the cut geotextile [$K_{23.6°} \rightarrow G1CT_{20.6°}$], but a major **increase** in effective cohesion (c') [$K_{9.8} \rightarrow G1_{25.5}$], as did the cut geotextile [$K_{9.8} \rightarrow G1CT_{18.3}$].

In the fully consolidated drained tests the geotextiles acting as drainage layer only had no effect on the internal friction but produced an **increase** in effective cohesion (c') [$K_{18.5} \rightarrow G1_{31.5}$], as did the cut geotextile [$K_{18.5} \rightarrow G1CT_{25}$].

In the both the consolidated undrained and consolidated drained tests the geogrids (G2, and G7) acted as reinforcement which produced a **reduction** in the effective angle of internal friction (ϕ'); for the undrained tests [$K_{23.6°} \rightarrow G2_{20.4°} \rightarrow G7_{21.1°}$]; for the drained tests [$K_{23°} \rightarrow G2_{20.7°} \rightarrow G7_{20.5}$]. However, the presence of the reinforcement resulted in a major **increase** in effective cohesion (c') for the undrained tests [$K_{9.8} \rightarrow G2_{25} \rightarrow G7_{36}$], for the drained tests [$K_{18.5} \rightarrow G2_{43} \rightarrow G7_{44}$].

The results showed that the geogrids (G3 and G4) acting as reinforcement were not as effective as the materials (G2 and G7) probably due to the large apperture of the grid. G1G2 was thought to have the properties required to provide the dual action of drainage and reinforcement, but the results were not encouraging.

CONCLUSIONS

The comparison of the laboratory result of both consolidated undrained and consolidated drained triaxial compression tests with the requirements for fills for field use, indicates that properly selected geotextiles are perfectly capable of providing both drainage and reinforcement functions with cohesive soil. Geogrids alone can provide a reinforcing function to cohesive soil, the main criteria for success being the selection of the correct grid apperture.

In particular, the results of laboratory tests obtained in this study suggested that;

i. the use of geotextile composite materials could help provide better compaction of cohesive fills and more efficient drainage from the interior of the fill. Some geosynthetic material can also provide effective tensile reinforcement.
ii. some non-woven geotextiles function well as a drainage for cohesive soil, maintaining a high degree of suction (i.e. negative pore water pressure).
iii. the consolidated drained test is more reliable than the undrained test when studying geotextiles with good hydraulic conductivity.
iv. the size of a geogrid apperture determines the behaviour of the material when used as reinforcement for fine grained (cohesive) soils.

ACKNOWLEDGEMENT
The authors wish to acknowledge the support of Netlon Limited and Conwed Limited who provided the materials used in the tests.

REFERENCES:

Department of Transport (1978)
Reinforced Earth Retaining Walls and bridges Abutments for Embankments, Technical Memorandum (Bridges) BE3/78 (Revised 1987), H.M.S.O., London.

Ingold, T.S. and Miller, K.S. (1982)
"The behaviour of geotextile reinforced clay subjected to undrained loading", Proceeding of Second International Conference on Geotextiles, Las Vegas. pp. 593-597.

Jones, C.J.F.P. (1992)
"The Economic Construction of Reinforced Soil Structures", International Symposium on Recent Case History of Permanent Geosynthetic-Reinforced Soil Retaining Walls-Seiken Symposium, Tokyo, Japan.

Jones, C.J.F.P. and Hassan, C.A. (1992)
"Reinforced soil formed using synthetic polymeric anchors" In Earth Reinforcement Practice (Eds. Ochiai, Hayashi and Otani), Vol.1, pp.345-351, Balkema.

Head, K.H. (1986)
Manual of Soil Laboratory Testing, Vol. 3, Effective Stress Tests, Pentech Press, London.

Heshmati, S., Jones, C.J.F.P., and Zakaria, N.Z. (1989)
"Effect of composite non-woven geotextile on the consolidation and shear properties of Kaolin", First International Seminar on Soil Mechanics and Foundation Engineering of Iran, Tehran. pp. 864-870.

Ling, H. I. and Tatsuoka, F. (1992)
"Effects of anisotropic consolidation on the performance of soil-geosynthetic composite at plane strain compression", Geotechnical Engineering Laboratory Report, Institute of Industrial Science, University of Tokyo, Japan. pp. 165-168.

Tatsuoka, F., Ando, H., Iwasaki, K., Nakamura, K. (1986)
Performances of Clay Test Embankments Reinforced with a Non-Woven Geotextile, Third International Conference on Geotextiles, Vienna, Austria. 3B/5.

Tatsuoka, F. (1992)
"Permanent Geosynthetic-Reinforced Soil Retaining Walls for Railway Embankment In Japan", International Symposium on Recent Case Histories of Permanent Geosynthetic-Reinforced Soil Retaining Walls, Tokyo, Japan.

Wu, J.T.H., Barrett, R. and Chou, N.N.S. (1992)
"Developing Cost-Effective geosynthetic-Reinforced Soil Walls, Recent Efforts in Colorado U.S.A.", International Symposium on Recent Case History of Permanent Geosynthetic-Reinforced Soil Retaining Walls, Tokyo, Japan.

Yang, Z (1972)
"Strength and deformation characteristics of reinforced sand", Ph.D. Thesis, University of California at Los Angeles, 233 pp.

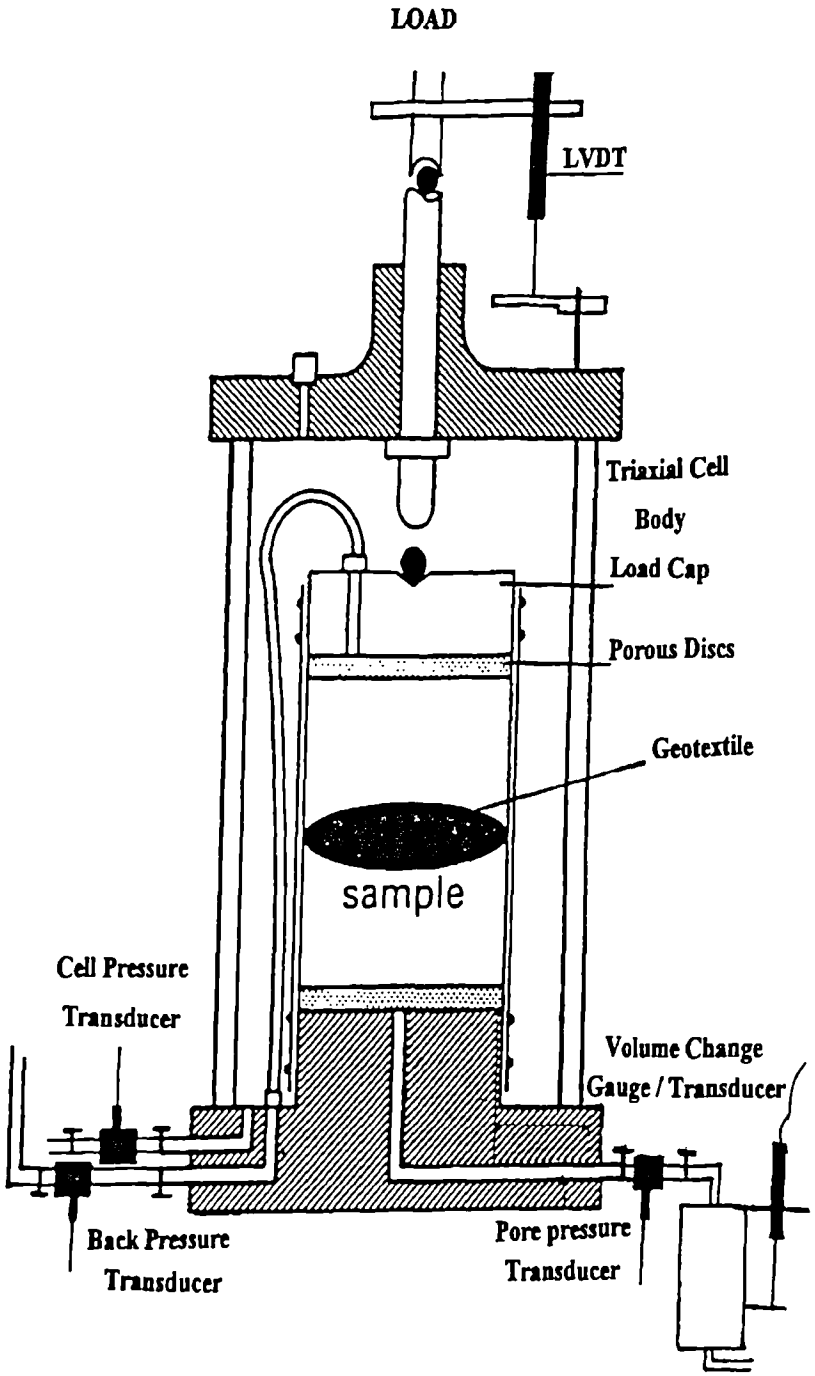

Fig. 1	Arrangement of apparatus and Geotextile specimen for Triaxial Tests

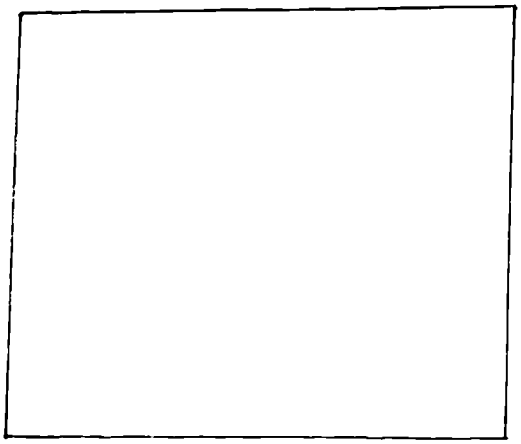

Kaolin

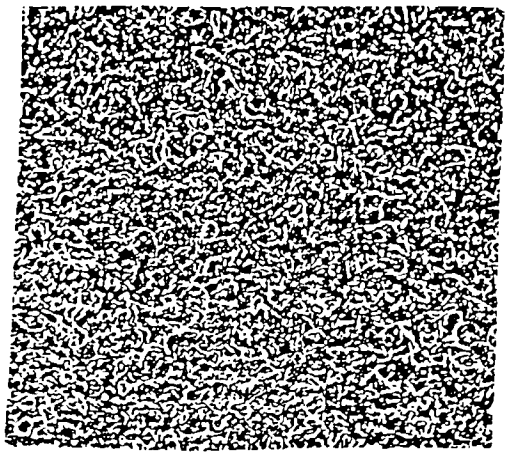

G1

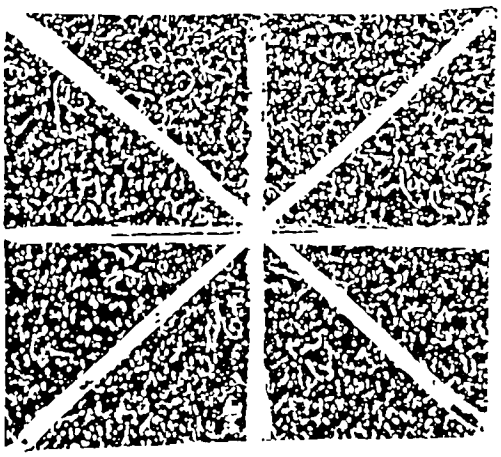

G1CT

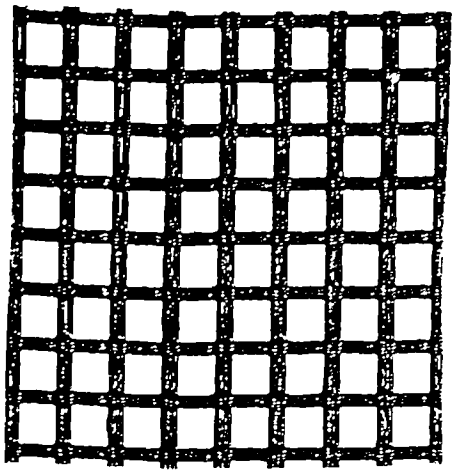

G2

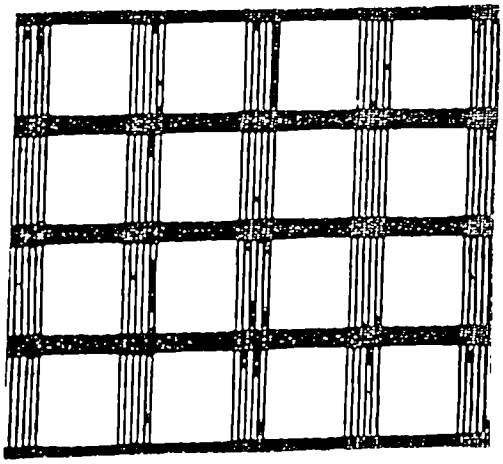

G3

Fig. 2	Type of Geotextiles used in the Triaxial Tests

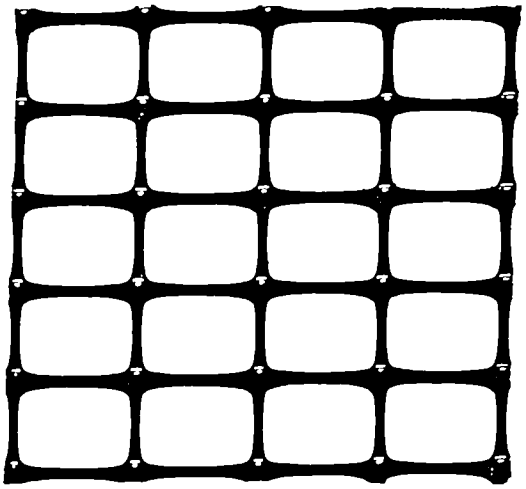

G4

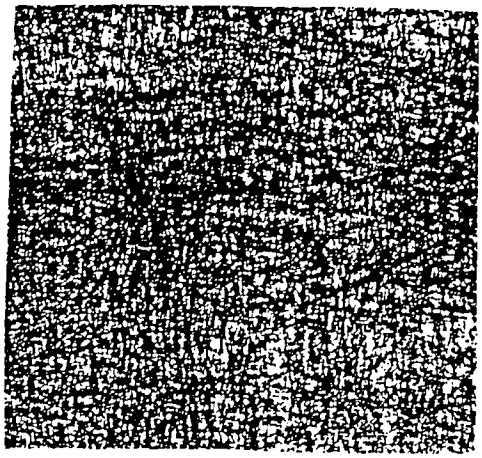

G5

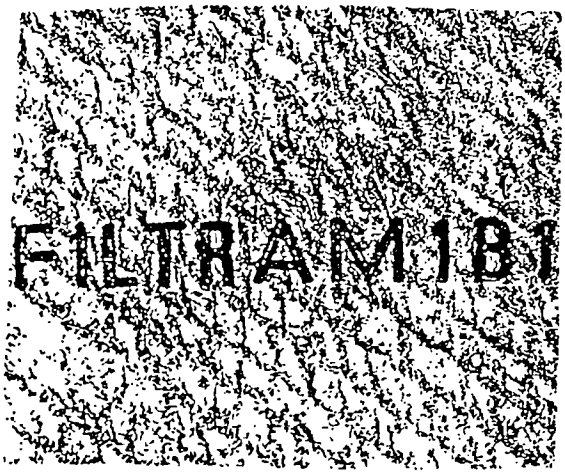

G6

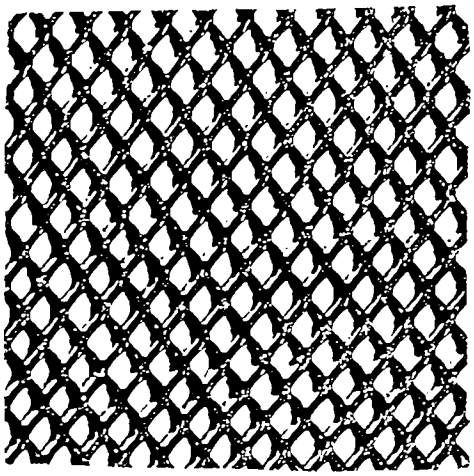

G7

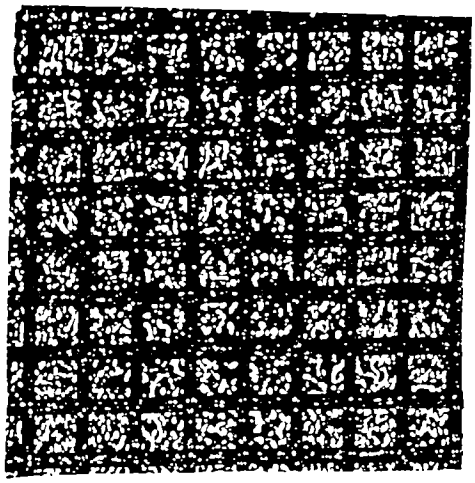

G1G2

Fig. 2 Continued .	Types of Geotextiles used in the Triaxial Tests

Table 1: Nature and Form of the Geotextile Materials Tested

Samples	Figures	Description
K		Kaolin only, China Clay, 0.002 mm Particle Size
K + G1	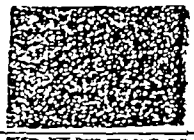	Kaolin with, Netlon 514R, non woven needle punched polypropylene fibres. (providing both drainage and reinforcement)
K + G1CT	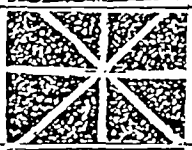	Kaolin with, Netlon 514R, non woven needle punched polypropylene fibres cut to equal wedges. (providing drainage)
K + G2	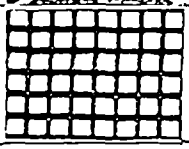	Kaolin with, Conwed Strata grid, geogrid, polyester 10x10 mm. (providing reinforcement)
K + G3		Kaolin with, Conwed 5033 geogrid, polyester, 25x25 mm. (providing reinforcement)
K + G4	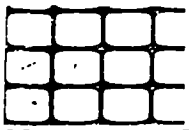	Kaolin with, Tensar SS1 geogrid, polypropylene, 28x38 mm. (providing reinforcement)
K + G5	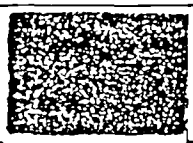	Kaolin with, non woven heat-bonded polypropylene geotextile.(providing reinforcement)
K + G6	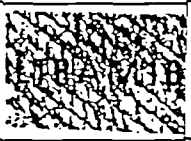	Kaolin with, Filtram 1B1, Netlon, Composite geotextile, mesh core spacer with filter on both side. (providing both drainage and reinforcement)
K + G7	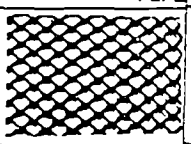	Kaolin with, Filtram 1B1, Netlon, mesh core, without filter on sides. (providing reinforcement)
K + G1G2	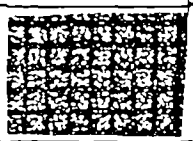	Kaolin with, Combined both G1 and G2 together. (providing both drainage and reinforcement)

Table 6.2a: Index Properties of Kaolin

Index Property	
Plastic Limit, P.L	35.05
Liquid Limit, L.L	61.00
Plasticity Index, P.I	25.05
Specific Gravity, G.S	2.63
Dry Density, ρ_d, Kg/m^3	1.32

Table 6.2b: Index Properties of Geotextiles

Material and Description	G1	G2	G3	G4	G5	G6	G7
Weight (g/m^2)	500	200	200	200	100	940	800
Material Thickness (mm) Without any Load With a Load of 200 KPA	 5.5 2.5	 1.6 1.5	 1.1 1.0	 0.8 -	 0.3 0.3	 - 6	 5
Tensile Strength Longitudinal (kn/m) Transverse (kn/m)	 8 10	 7.6 -	 5 -	 20 12.5	 3 -	 _	 12.5
Effective of Opening Size (mm)	0.15	0.99	2.5	2.8	0.3	0.1	1.6
Permeability (k) $\times 10^{-2}$ (m/s)	10× 10^{-2}	_	_	_	2× 10^{-2}	7.2× 10^{-2}	_
Transitivity at 200 KPA (m^2/s)	3× 10^{-6}	_	_	_	_	500	_
Roll Size (m)	3.9× 100	2× 100	2× 100	4× 50	_	3× 20	3× 20
Non woven Needle Punched Polypropylene Fibres	✓	_	_	_	_	_	_
Non woven Heat - Bonded Polypropylene Fibres	_	_	_	_	✓	_	_
Geogrid Type	-	✓	✓	✓	-	-	✓
Drainage Function	✓	-	-	-	-	✓	-
Reinforcement Function	-	✓	✓	✓	✓	-	✓
Drainage and Reinforcemnet	✓	-	-	-	-	✓	-

Table 3: Summary of Triaxial Test Result
Consolidated - Undrained Triaxial Compression Test (CU - Test)

Sample	Effective Cell Pressure KPA 150- 300- 500	Rate of Strain (mm/min)	Deviator Stress At Failure KPA $(\sigma'_1-\sigma'_3)_f$	$(\sigma'_1)_f$ KPA	Strain At Failure %	Shear Strength Parameter Cohesion - Angle of C'_{cu}	ϕ'_{cu}
K	150	0.035	140	235.5	10.5	9.8	23.6°
	300	0.028	220	393.4	9.5		
	500	0.030	308	566.4	9.0		
K + G1	150	0.074	215	357.7	10.7	25.5	20.1°
	300	0.028	283	611.5	8.0		
	500	0.040	325	795.3	10.7		
K + G1CT	150	0.048	170	317.9	8.6	18.3	20.6°
	300	0.074	340	575.6	10.7		
	500	0.077	418	637.4	11.0		
K + G2	150	0.054	130	218.9	7.2	25	20.4°
	300	0.090	170	345.7	9.4		
	500	0.11	350	709.5	7.8		
K + G3	150	0.041	162	281.4	10.5	16	21.7°
	300	0.11	262	453.7	8.2		
	500	0.033	358	634.5	8.8		
K + G4	150	0.041	145	248.2	8.2	16	20.5°
	300	0.053	250	402.7	10.5		
	500	0.059	391	715.8	11.5		
K + G5	150	0.055	175	276.5	9.2	18	19.3°
	300	0.079	240	418.7	8.7		
	500	0.078	390	632.3	11.5		
K + G6	150	0.067	210	306.4	6.5	39.5	18.9°
	300	0.028	331	221.7	9.5		
	500	0.030	392	674.5	9.0		
K + G7	150	0.033	229	364.9	8.2	36.1	21.2°
	300	0.057	282	465.5	9.8		
	500	0.047	388	703.1	10.7		
K + G1G2	150	0.035	160	262.5	8.5	16	20.5°
	300	0.035	270	453.7	8.2		
	500	0.037	407	718.1	9.0		

Table 4: Summary of Triaxial Test Result
Consolidated - Drained Triaxial Compression Test (CD - Test)

Sample	Effective Cell Pressure KPA 150 - 300 - 500	Deviator Stress At Failure KPA $(\sigma'_1-\sigma'_3)_f$	Strain At Failure ε_f %	Shear Strength Parameter Cohesion - C'_d	Angle of Internal Friction ϕ'_d
K	150 300 500	118 220 330	11.7 9.8 9.2	18.5	23.0°
K + G1	150 300 500	262 420 798	10.2 11.0 11.9	31.5	22.5°
K + G1CT	150 300 500	260 396 623	9.5 11.0 9.0	25	22.5°
K + G2	150 300 500	377 462 650	8.0 10.0 10.0	43.0	20.7°
K + G3	150 300 500	239 362 710	9.5 12.4 10.0	23.0	22.2°
K + G4	150 300 500	220 424 602	7.7 8.7 8.7	27.0	21.1°
K + G5	150 300 500	230 419 580	9.7 11.5 12.0	29.5	18.7°
K + G6	150 300 500	245 282 372	9.6 8.0 7.6	41.5	18.6°
K + G7	150 300 500	280 400 610	9.5 11.0 11.0	44.0	20.5°
K + G1G2	150 300 500	238 418 579	6.5 8.0 8.0	30.0	18.9°

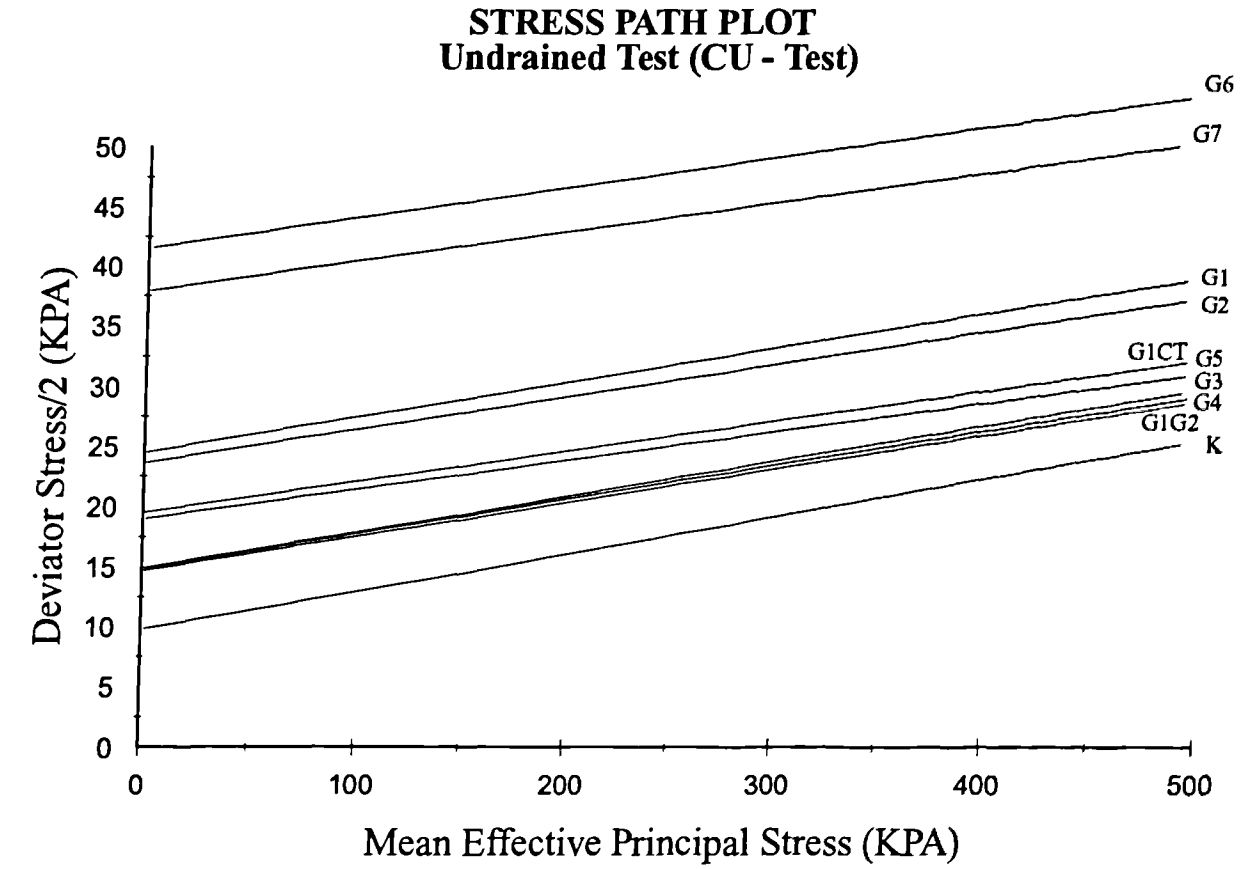

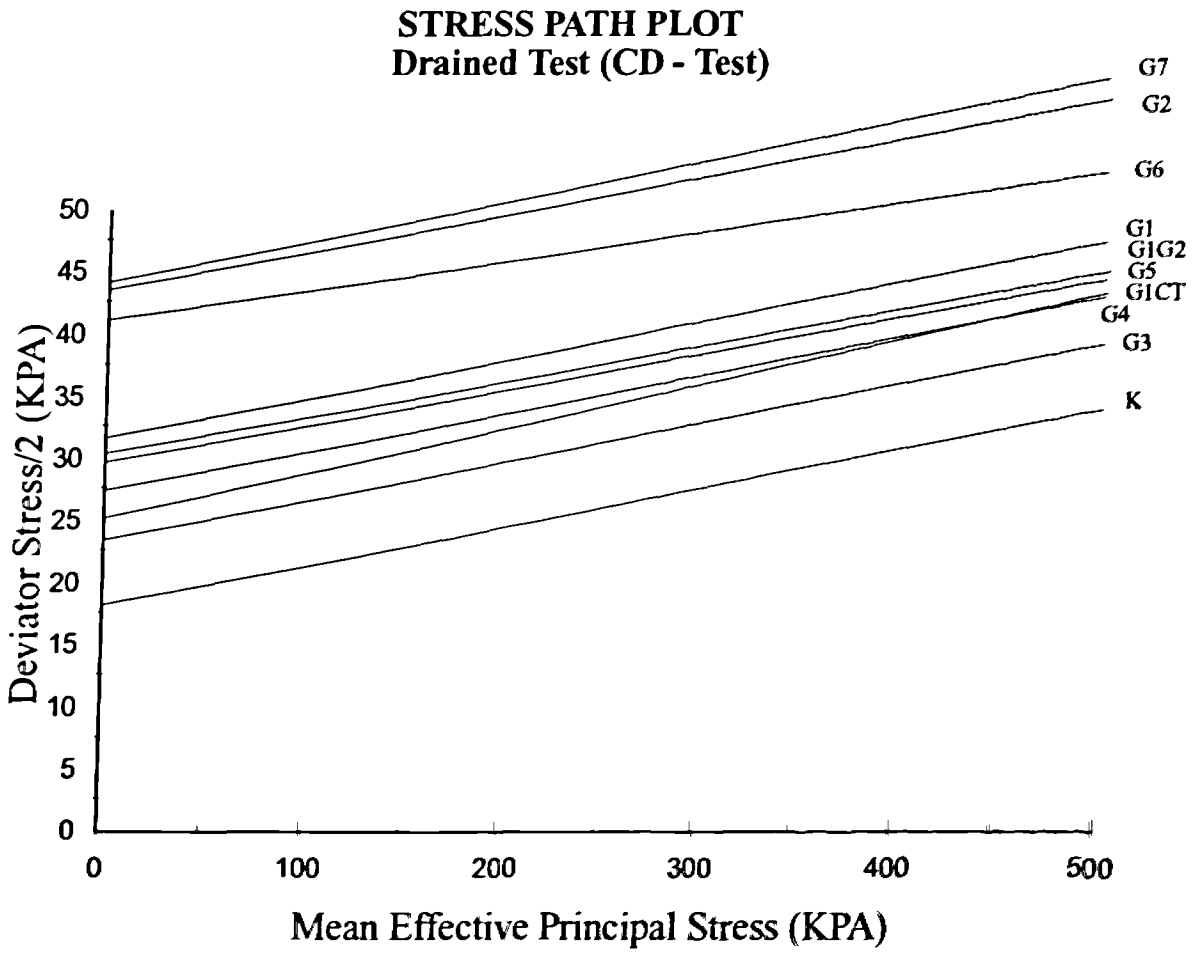

Fig. 3: Stress Path for Undrained and Drained Tests